I. STUDIES IN THE CHEMISTRY OF SODIUM DITHIONITE

II. A pH STUDY OF THE α-CHYMOTRYPSIN CATALYSED HYDROLYSIS OF METHYL HIPPURATE

Thesis by

Thomas Pascoe Gordon

In Partial Fulfillment of the Requirements

For the Degree of

Doctor of Philosophy

California Institute of Technology

Pasadena, California

1959

ACKNOWLEDGEMENTS

I am happy to acknowledge my indebtedness to Professor Carl Niemann, who directed this research and guided my last three years at the Institute. His constant interest, friendliness, and patience will always remain a high example to me.

I am likewise indebted to Professor William Corcoran. He stimulated me to attack the dithionite chemistry problem, and whatever progress we have made has resulted in large measure from his philosophy of sticking with a problem until it is done, and done well.

The first section of this thesis is submitted jointly with Robert G. Rinker. The dithionite studies reported here constitute more than a two man effort. It is largely due to Bob's incessant labor that the work was completed.

To the California Institute, I am indebted financially for Institute Scholarships and Research and Teaching Assistantships during my first four years here, and to the E. I. Dupont Co., for the Dupont Teaching Fellowship this past year.

I am particularly indebted to Roy Sakaida for his considerable help with the dithionite thermal decomposition studies, and to Henry Dearman for his experimental help and thought in the EPR experiments.

Professors Norman Davidson, Ernest Swift, Edward King, Harden McConnell, Fred Anson, and Don Yost have been extremely helpful in the course of the dithionite research. Their

wise counsel is much appreciated.

My colleagues in 262 Crellin and Chemical Engineering have provided a friendly and stimulating atmosphere in which to work. Their interest and friendship have made my years at Caltech happy as well as intellectually profitable ones.

Finally, I gratefully acknowledge the assistance of my wife, Nancy, who shared my problems, and typed many of the pages that follow.

ABSTRACT

I. The kinetics of the air oxidation of sodium dithionite in alkaline solution suggest the transfer of an electron from SO_2^- radical-ions, which are in equilibrium with $S_2O_4^=$ ions, to molecular oxygen in the rate determining step.

Electron paramagnetic resonance experiments confirm the presence of SO_2^- radical-ions in equilibrium with $S_2O_4^=$ ions in solution.

Electrolytic reduction of sulfurous acid solutions at constant potential in the range -0.7v to -0.9v produces dithionite at constant current efficiency.

Thermal decomposition of dithionite solutions occurs slowly at first, apparently by a free radical mechanism, and then rapidly, indicating a degenerate chain-branching mechanism.

II. The results of a pH study of the α-chymotrypsin catalysed hydrolysis of methyl hippurate at three different added salt concentrations are consistent with the postulation of ionizing groups at the active site of the enzyme with pK_a values 6.9 ± 0.1 and 8.6 ± 0.1. Important interactions of added salt and hydrogen ion concentrations are not indicated.

Hippuric acid and L-tryptophan are shown to be competitive inhibitors.

The development of a negative charge at or near the active site of the enzyme above pH 8 is confirmed.

TABLE OF CONTENTS

SECTION I

STUDIES IN THE CHEMISTRY OF SODIUM DITHIONITE

GENERAL INTRODUCTION

CHEMISTRY OF SODIUM DITHIONITE

Sodium dithionite, $Na_2S_2O_4$, is a powerful reducing agent that has considerable usage in vat dyeing, bleaching, and in the manufacture of various chemicals. The first step in the process most generally used in the United States for the production of dithionite involves the reduction of liquid sulfur dioxide with zinc dust slurried in water. A continuous reactor is used. The reaction mixture is circulated through a tubular cooler at 35°C and zinc is continually removed. The filtered liquor is converted to the sodium salt by addition of caustic soda at 25°C. Filtration of the slurry removes the zinc hydroxide. To the filtrate is added sodium sulfide for removal of heavy metals. The final solution, containing 20% by weight of sodium dithionite, is then salted out with sodium chloride and alcohol. Partial dehydration of the dithionite crystals is accomplished with direct steam at 65°C, and final drying is done under vacuum at 85°C.

As early as 1850, dithionite (also called hydrosulfite or hyposulfite) was prepared by Schonbein (1) from the action of zinc dust on an aqueous solution of sodium bisulfite. In 1869, Schutzenberger (2) crystallized sodium dithionite and found its composition to be $Na_2S_2O_4$.

An important contribution to the knowledge of the properties and reactions of dithionite was made by Jellinek (3) in

1911. He prepared pure anhydrous sodium dithionite by heating a saturated solution of the impure salt to 60°C and then salting it out with NaCl and a small amount of NaOH. At a lower temperature, the hydrate, $Na_2S_2O_4 \cdot 2H_2O$, was salted out but was much less stable. Also, he found that the solubility of sodium dithionite dihydrate in water at 20°C was 21.8 gm/100 gm of water and that the temperature-solubility curve between 1°C and 20°C was a straight line. Freezing-point and conductance measurements gave good evidence in favor of the doubled formula $Na_2S_2O_4$. From careful measurements of the equivalent conductance of $Na_2S_2O_4$ solutions, Jellinek (4) determined the degrees of ionization in a 0.125 molar solution to be 0.697, 0.698 and 0.700 at 0, 18.3 and 25°C, respectively. A comparison with freezing point data showed that the value of the degree of ionization calculated from the freezing point was always greater for the sodium salts than that derived from the conductivity data. For the potassium salts, however, the degree of ionization was the same whether calculated from freezing-point or conductivity data. Jellinek explained the peculiarity by concluding that intermediate ions such as $NaS_2O_4^-$ were present in the sodium dithionite solutions but not in the potassium dithionite solutions. From conductance data for dithionous acid and the acid salt, the first and second ionization constants were calculated to give $K_1 = 0.45$ and $K_2 = 0.0035$ in a 0.1 molar solution of dithionite.

PART 1. AIR OXIDATION STUDIES

INTRODUCTION

Probably the earliest air-oxidation study of dithionite was conducted by Meyer (5) in 1903. He studied the oxidation of sodium dithionite by observing the oxygen uptake in shaken flasks containing aqueous dithionite solution. His results showed that the products of reaction were sulfite and sulfate. He proposed the primary reaction to be:

$$H_2S_2O_4 + H_2O + O_2 = H_2SO_4 + H_2SO_3 \qquad (1)$$

Also, he found that a competing reaction was

$$2H_2S_2O_4 + 2H_2O + O_2 = 4H_2SO_3 \qquad (2)$$

From the over-all reaction rates, he computed first-order rate constants but found that they drifted over a wide range.

Bassett and Durrant (6) in 1927 studied the reaction between dithionite and molecular oxygen but without any meaningful results. Their explanation of the oxidation mechanism was based upon arguments which will be summarized in the introduction to Thermal Decomposition Studies.

Nicloux (7) in 1933 was interested in determining the over-all stoichiometry of the reaction between dithionite and oxidizing agents of varying strengths. With a comparatively weak oxidizing agent such as silver ion, the dithionite was oxidized to sulfite. With molecular oxygen, an equimolar

mixture of sulfite and sulfate was formed. Finally, with a very strong oxidizing agent, sulfate was the only product. No experimental details were given.

The results of Lynn (8) suggested that the atmospheric oxidation of $Na_2S_2O_4$ proceeded according to a first-order mechanism with respect to dithionite and that the rate increased with temperature. He stated that the over-all stoichiometry was described by the equation:

$$Na_2S_2O_4 + O_2 + H_2O = NaHSO_4 + NaHSO_3 \qquad (3)$$

An examination of his data at 50°C showed that the oxidation rate increased with an increase in air flow. As a result, the reaction rate was dependent upon the diffusion rate of oxygen, which was not carefully controlled. Therefore, his results are only approximate. In the presence of 0.1 molar sodium bisulfite, the oxidation rate was extremely high, but in the presence of 0.1 molar sodium hydroxide the rate was inhibited, and the reaction proceeded smoothly.

SUMMARY

A study of the air-oxidation of sodium dithionite was conducted in aqueous solutions which were 0.1 molar in sodium hydroxide. The concentration of the dithionite was measured as a function of time at 30, 40, 50 and 60°C. Initial concentrations varied from 5×10^{-3} to 20×10^{-3} molar.

Air was bubbled into the reacting mixture through a glass frit at a rate of 2500 to 3000 cc/min, and the volume ratio of air flow per minute to reactor contents ranged from five to six. With stirring at a rate of 1100 rpm, the mixture was homogeneous and sufficiently turbulent to allow good contact between the air and liquid so that diffusion from gas to liquid and within the liquid was not a rate-determining factor.

Analyses of the end products showed the presence of sulfite, sulfate and thiosulfate. The sulfite and sulfate, usually found in a molar ratio of three to one, were the principal products and were considered to be the end products of the primary oxidation. The thiosulfate, however, was found only in relatively small quantities and was considered to be a product of a secondary reaction, namely, the thermal decomposition of dithionite. This reaction accounted for about 10% of the overall dithionite decomposition at 30°C.

An analysis of the rate data showed that the oxidation was one-half order with respect to dithionite and first order with respect to molecular oxygen. The specific rate constant

k_c was determined by integrating the rate expression at constant oxygen concentration for a half-order reaction to give:

$$k_c = \frac{2}{\theta} [C_o^{1/2} - C^{1/2}] \qquad (4)$$

For each initial concentration, C_o, the rate constant was calculated as a function of time θ from the unsmoothed oxidation data. Since it was found that k_c drifted slightly with time, its value at zero time was determined by extrapolation. Most of the drift was attributed to the effects of thermal decomposition since analysis showed the presence of thermal decomposition products, thiosulfate and sulfite, at the end of the reaction. Experiments involving increases in ionic strength by factors of three and five showed no effect on the rate of the reaction.

At each temperature, the average value of k_c at zero time was divided by the saturation concentration of oxygen in the solution to give k_c°. The rate expression is given as follows:

$$r_{observed} = k_c^{\circ}[S_2O_4^{=}]^{1/2} [O_2] \qquad (5)$$

k_c° at 30°C was found to be 0.151 $(moles/liter)^{-1/2}sec^{-1}$. A plot of log k_c° vs $1/T$ °K was used to obtain the Arrhenius activation energy of 9.3 kcal/mole. The frequency factor, A, was found to be 7×10^5 $(moles/liter)^{-1/2}sec^{-1}$. The observed half-order dependence on dithionite concentration and first

order dependence on molecular oxygen concentration suggested the following mechanism:

$$S_2O_4^{=} \rightleftharpoons 2SO_2^{-} \qquad (6)$$

$$SO_2^{-} + O_2 \longrightarrow \text{products} \qquad (7)$$

The equilibrium between the SO_2^{-} and $S_2O_4^{=}$ species was assumed to be the initial step in the mechanism of the oxidation. The second step was rate-determining, and consisted of an electron transfer or bimolecular combination reaction between SO_2^{-} and molecular oxygen.

APPARATUS

Reactor and Auxiliary Components

The air oxidation of the sodium dithionite was carried out in a glass reactor with a volume of approximately 600 cc (see Figure 1). Air was bubbled at a rate of 2500 to 3000 cc/min into the reaction mixture near the bottom of the reactor through a medium-coarse glass frit which could be inserted or removed through a standard-taper opening on the reactor. During the reaction, the frit was always immersed in the liquid contents.

Before the air entered the frit, it was passed first through an alundum-stone trap to remove suspended solids and aerosols; next through a molecular-sieve dryer; and finally through a temperature-conditioning coil. The air flow was measured by means of a wet-gas meter placed on the downstream side of the reactor.

Mixing was accomplished by means of a glass stirrer having two impellers. The stirrer was supported and sealed through a mercury-in-glass bearing. Stirring speeds could be varied up to 1100 revolutions per minute.

The reactor and temperature-conditioning coil were thermostated in a 28-liter water bath, which maintained the temperature within $\pm$ 0.02°C. Heaters in the water bath were energized by an electronic-relay circuit which in turn received its signal from a mercury-expansion switch immersed in the water.

Samples were taken from the reactor through an opening in the top. A syringe needle or pipette was inserted into the reacting mixture, and the sample was then removed.

Nitrogen Purification Train

Commercial-grade nitrogen was the source of supply for the oxygen-free atmosphere required in preparing the sample of fresh sodium dithionite to be charged to the reactor. The nitrogen contained approximately 0.01% oxygen by volume. That amount proved excessive. Hence, most of the oxygen was removed by passing the nitrogen through two scrubbing towers in series. Each contained 0.2 molar chromous chloride solution in 1.0 normal hydrochloric acid. Acid and water vapors were subsequently removed by passing the nitrogen through a 0.1 molar sodium hydroxide solution and then through a calcium chloride dryer.

EXPERIMENTAL PROCEDURE

Concentration of Dithionite as a Function of Time

Chemically pure sodium dithionite (Baker Chemical Company, Batch No. 3712, Lot No. JTB6113) was the starting point for the source of dithionite ions. In preparing the dithionite for a typical run, approximately 25 gm of the powder were placed in an oxygen-free flask into which a stream of oxygen-free nitrogen had been passed for several minutes. Then, approximately 100 cc of distilled water, free of oxygen and carbon dioxide, were injected into the flask through a serum-bottle cap. The mixture was heated to 60°C with constant agitation until a saturated solution was obtained. With great care to avoid contact with oxygen, a 60 cc sample of the saturated solution was withdrawn with a syringe and injected into a side-armed test-tube already filled with nitrogen. The tube with its contents was then cooled to 0°C in an ice bath while maintaining the pressure of the nitrogen constant at slightly above one atmosphere. At the lower temperature the liquid became supersaturated with sodium dithionite; and with sufficient agitation, crystals of $Na_2S_2O_4 \cdot 2H_2O$ were formed. Again, with great care, practically all the liquid was removed from the tube leaving the white crystals settled at the bottom. Approximately 4 cc of distilled water at 0°C and free of carbon dioxide and oxygen were injected into the tube to wash the crystals.

This process was repeated once again to obtain reasonably pure crystals. The final saturated solution with a volume of approximately 20 cc was used to supply the reactor with an initial concentration of dithionite.

Before injection of the dithionite, the reactor was filled with 505.0 cc of 0.1 molar sodium hydroxide solution. The reactor was then immersed in the water bath and allowed to reach steady conditions of temperature, stirring rate, and air flow. The time of initial air flow was noted in order to account for evaporation losses from the reactor. At steady conditions, 5.00 to 15.00 cc of the saturated dithionite solution, depending upon the initial concentration desired, were injected into the reactor. Since the delivery times of large syringes are of the order of several seconds the time at which half of the sample was injected was taken as the initial time of the reaction.

Without delay, 1.00 or 2.00 cc samples were removed from the reactor with a calibrated syringe and injected into 150 cc flasks containing a mixture of 50 cc of 0.1 molar potassium hydroxide and 15 cc of methyl alcohol. Also, the flasks contained a nitrogen atmosphere which was maintained during titration. The titration flasks were stirred magnetically. The time at which half of a sample from the reactor had been injected into a titration flask was recorded as the injection time.

The concentration of dithionite in the titration flasks

was determined by titration with a standardized aqueous solution of methylene blue having a concentration in the range of 9.0×10^{-4} to 9.3×10^{-4} molar.

Usually, the total time required to obtain a sample and titrate it was 40 sec. At the maximum temperature of 60°C and at the minimum initial concentration of 5×10^{-3} molar, the time of reaction was a minimum. Under these conditions, at least five titrations were accomplished before the end of the reaction.

As soon as all the dithionite had been oxidized, the air-flow was stopped, and the time was noted. The reactor was removed from the water bath, and the volume of its contents was measured. A material balance coupled with the knowledge of the air-flow rate and the assumption that the exit air was saturated with water vapor, made it possible to calculate the loss of water by evaporation prior to and during the reaction.

In the analysis of the dithionite samples, the methylene blue was reduced quantitatively on an equimolar basis from an intense blue color to an almost colorless leuco-form. It was found, in agreement with Lynn's work (8), that the leuco-form was relatively insoluble in water at room temperature; and unless it was dissolved, it apparently absorbed unreacted methylene blue during the titration. This resulted in a lowered over-all rate of reaction because of the time required for the dithionite to diffuse to the solid surface before

reaction could occur. The purpose of the addition of the methyl alcohol in the titration flasks was to dissolve the solid leuco-compound and hence speed up the titrations. When titrated quickly, any thiosulfate and sulfite present in a sample did not interfere in the reaction between dithionite and methylene blue for the temperature range 0 - 30°C. The end-point was sharp and was rapidly attained at room temperature.

Standardization of the methylene blue was done according to the method of Welcher (9) and Kolthoff (10). Briefly, the methylene blue was titrated into a standard water-solution of 0.005 molar picrolonic acid which was buffered at a pH of about 6. Periodic removal of the dark green product, methylene blue picrolonate, from the water phase was necessary in order to detect the end-point. This was accomplished by extraction of the methylene blue picrolonate with chloroform. Neither the picrolonic acid nor the methylene blue was soluble in the chloroform. Near the end-point, only 2 or 3 drops of methylene blue were titrated into the acid between successive extractions with chloroform. The end-point occurred when a blue color persisted in the water phase after addition of one drop of methylene blue, but with no color in the chloroform phase. When carefully applied, this method gave results accurate to $\pm$ 0.5% compared with the classical iodine-precipitation method (11).

Solubility of Dithionite at 0°C

A solution of sodium dithionite saturated at 0°C was prepared as described in the previous section. The saturation concentration of the dithionite, however, far exceeded the desired value for titrations with reasonable volumes of methylene blue. Therefore, 5.00 cc of the saturated solution were injected through a serum-bottle cap into a 1-liter vessel which contained 500.0 cc of 0.1 molar sodium hydroxide maintained under a nitrogen atmosphere and at a temperature of 0°C. Several 2.00 cc samples of the resulting solution were titrated with methylene blue under conditions similar to those stated in the previous section. From these results, the solubility of the dithionite at 0°C was calculated.

End-Products of the Dithionite Oxidation Reaction

A knowledge of the types and quantities of the oxidation products of dithionite was important in determining a mechanism for the reaction. For the qualitative tests, a decomposed sample of dithionite was prepared by adding 0.20 gm of the purified powder to 100 cc of 0.1 molar sodium hydroxide solution through which air was bubbled until a negative test for dithionite was obtained. A sample of the reaction mixture was acidified with hydrochloric acid to a pH of about 2, followed by addition of lead acetate. A white precipitate resulted which indicated the absence of sulfide from the mixture. Had sulfide been present in the absence of appreciable amounts of chloride ion, it would have appeared as the black

precipitate of lead sulfide. Another sample, when mixed with potassium triiodide at a pH of about 5, decolorized the iodine, indicating the presence of thiosulfate and/or sulfite. Still another sample at that pH was treated with barium chloride to remove sulfite and sulfate, if present, as barium sulfite and barium sulfate. The white precipitate was filtered, and the filtrate was titrated with potassium triiodide to give a positive test for thiosulfate. Treatment of the precipitate with strong hydrochloric acid resulted in the evolution of sulfur dioxide to give a positive test for sulfite. The fact that a portion of the precipitate was unattacked by an excess of acid showed the presence of sulfate as barium sulfate.

The procedure for the quantitative analysis was based upon the results of the qualitative findings. The principal ions of interest were sulfite, sulfate, and thiosulfate. Any complexes of these ions or the presence of other ions were considered highly unlikely or in concentrations too low to be detected.

Samples for quantitative analysis were taken from two sources, both of which were different from the source used in the qualitative analysis. The first source was contained in a flask which originally was charged with 500 cc of 0.1 molar sodium hydroxide at 30°C and with 7 cc of saturated dithionite solution. Oxygen entered the liquid bulk only by molecular diffusion through the surface of the liquid. This

mixture was checked for completion of dithionite oxidation before other components were studied. The second source was contained in the reactor following a usual run at 30°C as described previously.

In both cases, the method of analysis for end-products was the same. Four separate analyses were made on four separate samples from each source. These were as follows:

1. Iodometric titration to determine the sum of the concentration of thiosulfate and sulfite.
2. Iodometric titration to determine only the concentration of thiosulfate.
3. Barium chloride titration to determine the sum of the concentration of sulfite and sulfate.
4. Barium chloride titration to determine only the concentration of sulfate.

In the iodometric analysis for the sum of the sulfite and thiosulfate, a 10 to 25 cc sample was buffered with a solution which was 0.4 molar in sodium acetate and 0.4 molar in acetic acid. Usually, a volume of the buffer solution equal to the volume of the sample was added to give a constant pH of about 5. Using a starch end-point, the solution was titrated with a standardized solution of approximately 0.01 normal triiodide. In case of excess addition of triiodide back-titration was done with a standard thiosulfate solution which was approximately 0.01 normal in thiosulfate.

In the iodometric analysis for only the thiosulfate ion,

a 10 to 25 cc sample was buffered to a pH of about 5. To this was added a volume of 37 wt % formaldehyde in water equal to about half the volume of the the sample. The purpose of the formaldehyde was to form a complex with the bisulfite according to the reaction:

$$\begin{matrix} H \\ \diagdown \\ \quad C = O \\ \diagup \\ H \end{matrix} + HSO_3Na \longrightarrow CH_2(OH)SO_3Na \qquad (8)$$

The mixture was stirred for fifteen minutes at room temperature to allow sufficient time for the complexing to occur. The unreacted thiosulfate was then determined with the standard triiodide solution.

The use of barium chloride in a titration method to determine sulfate was suggested in the literature by Fritz and Freeland (12). This method depends upon a color change in the indicator Alizarin Red-S which acts as an adsorption indicator in the presence of a barium sulfate precipitate. In solution the alizarin anion was yellow; but on the surface of suspended barium sulfate and in the presence of excess barium ion, the alizarin complexed with the barium ion to give a red color to the suspended solid. In using the procedure outlined by Fritz and Freeland, however, the method was limited to concentrations of sulfate greater than 20×10^{-3} molar. It was necessary, then, to modify the procedure in applying it to concentrations of sulfate down to 4×10^{-3}

molar. After several tests, it was noted that the limitation in the amount of sulfate detectable was mainly due to the relative concentration of the precipitate on which the alizarin could absorb. Too small a quantity of precipitate, although colored red with complexed alizarin, could not overshadow the yellow color of the alizarin in solution. Therefore, by adding a quantity of semi-colloidal barium sulfate suspended in methyl alcohol to the titration mixture, it was possible to detect the end-point with an accuracy of 1 or 2%. A further improvement in detecting the end-point was to pass an intense light beam through the suspension during the titration. This aided in bringing out color changes more sharply.

To determine the sum of the sulfite and sulfate concentration by the above method, it was first necessary to oxidize the sulfite to sulfate by means of the triiodide ion. The amount of triiodide needed was determined by a starch end-point; but there was some uncertainty as to the effects of the starch on the subsequent sulfate titration. Therefore, it was decided to avoid using the starch by first running a blank to determine the exact triiodide requirement and then adding the same amount in the absence of starch to a fresh sample buffered at a pH of about 5 as specified above. Following the oxidation of the sulfite, the buffered solution was acidified to a pH of about 3.5 with 20% acetic acid. The volume of acetic acid required was about equal to the volume of the original sample. Then methyl alcohol containing a

semi-colloidal suspension of barium sulfate was added in an optimal amount equal to 38% by volume of the final mixture. With constant stirring, 90% of the estimated 0.1 molar barium chloride requirement was rapidly added and was followed by the addition of 3 to 5 drops of 0.020 % alizarium-red solution. The final titration was performed slowly with an interval of 3 to 5 sec between drops of barium chloride solution.

Finally, in determining the concentration of sulfate alone, the sulfite was complexed by addition of formaldehyde. The subsequent barium chloride titration was not affected adversely by the presence of the formaldehyde.

All the standard solutions used in the foregoing analyses were prepared and standardized according to the procedures outlined by Swift (13).

RESULTS

Kinetic Analysis

Tables 1-4 list the experimental and derived data for the air-oxidation of dithionite. Graphical presentations of the data are shown in Figures 2-5, in which concentrations of dithionite in moles per liter are plotted against time in seconds. Initial concentrations of dithionite ranged from 5×10^{-3} to 20×10^{-3} moles/liter. The rate of change of concentration was rapid in the initial stages but fell off continuously and rapidly as the concentration decreased.

In the determination of the order of the reaction with respect to dithionite, the oxygen concentration was held constant for a given temperature. Only for those experiments in which the order with respect to oxygen was to be determined was the oxygen concentration varied. Pure oxygen was used at atmospheric pressure instead of air to give a fivefold increase in oxygen concentration. If Henry's Law is assumed to apply, the concentration ratio in solution between oxygen dissolved from pure oxygen and oxygen dissolved from air would be 4.76. For the equipment used, this method of varying the oxygen partial pressure in the gas phase at a constant total pressure of one atmosphere was preferred to the method in which the total pressure on the system would have been increased.

It was found experimentally that the initial rate of the

reaction was increased by a factor of 5 when pure oxygen was substituted for air, all other conditions remaining the same. Hence the reaction was believed to be first order with respect to molecular oxygen.

The first step in analyzing the data was to determine initial concentrations and the corresponding initial rates. Several procedures were available for determining the initial concentrations. Experimentally, solubility tests were performed on the dithionite to determine its concentration at 0°C in the saturated solutions which were injected into the reactor for any given decomposition run. From a knowledge of the solubility and the initial quantity of water in the reactor, the initial concentration could be calculated.

A direct extrapolation of the concentration-vs-time curves back to zero time was the second method and a fairly reasonable one since sampling from the reactor was begun 30 to 50 sec after the injection. The total time for decomposition varied from 120 to 530 sec over the temperature and initial concentration range studied.

Of the two procedures, the direct extrapolation method was used. Although the solubility of dithionite at 0°C was fairly well established by the procedure described in the experimental section, the use of this value in calculating the initial concentrations in the reactor depended upon exact reproducibility of injection samples for each run.

The initial rates were determined by plotting slopes of

concentrations vs time curves as a function of time for each initial concentration. A series of these curves is shown in Figure 6 for runs at 50°C. An extrapolation to zero time produced the initial rates. These compared satisfactorily with the values obtained by drawing tangents to the concentration vs time curves at zero time.

From a knowledge of the initial rates and concentrations, the order n of the reaction with respect to dithionite was obtained. The relationship used in this determination and applied at time zero was the following:

$$-\frac{dc}{d\theta} = k_c[C]^n \qquad (9)$$

in which C is the concentration of dithionite in moles per liter; θ is the time in seconds; and k_c is the specific reaction rate constant which includes the constant concentration of oxygen.

A plot of log $\left(\frac{dc}{d\theta}\right)_o$ vs log C_o is shown in Figure 7 for runs at 30, 40, 50 and 60°C. The slopes of the best straight lines through the points at each temperature were calculated to be 0.50 ± 0.04 which was near enough to 0.5 to indicate that the reaction was one-half order with respect to dithionite. The purpose of obtaining n for conditions at zero time was to eliminate any possible effects of reaction products or side reactions in masking the true order of the reaction. More explanation of these effects is given in a later discussion on product analysis.

The integrated form of Equation 9 was used to obtain values of k_c as a function of time, and the unsmoothed data provided the numerical information to solve for k_c. Integration of Equation 9 gives:

$$k_c = \frac{2}{9} [C_o^{1/2} - C^{1/2}] \qquad (4)$$

It was found that k_c calculated from Equation 4 drifted slightly as a function of time when calculated over 50% completion of reaction, but the variation was smooth and linear. A typical plot for data at 30°C is shown in Figure 8. The curves for k_c, when extrapolated to time zero, seemed to converge to a range of values well within experimental accuracy. Hence greater credence was placed upon an average value of k_c at time zero than for any other time. The fact that the values for k_c varied smoothly provided a satisfactory argument in favor of using unsmoothed data in the calculations. The calculated values of k_c as a function of temperature are shown in Figures 8-11. Since these values included the concentration of oxygen, which is a function of temperature itself, the dependence of k_c on oxygen concentration was eliminated by dividing k_c by the saturation concentration of oxygen in water, and hence in the dilute solutions used here, in moles per liter at that temperature (14). The new k's, independent of concentration and designated as k_c^o, are also shown in Figures 8-11.

The overall activation energy and frequency factor were obtained from the Arrhenius Equation relating the rate constant to temperature. A form of the Arrhenius Equation was used in which the dependence of the frequency factor on temperature was omitted. The range of temperatures studied was sufficiently narrow to make this simplification justified. The form of the equation used is:

$$k = Ae^{-\frac{\Delta E}{RT}} \qquad (10)$$

A plot of log k_c° vs 1/T °K is shown in Figure 12. The slope of the best straight line through the points gave a value for the activation energy, ΔE, of 9.3 kcal/mole. The intercept, at 1/T equals zero, gave a value of 7×10^5 (moles/liter)$^{-1/2}$ sec^{-1} for the frequency factor A.

Product Analyses

Table 10 lists the experimental results for the end-product analyses. For the reactions conducted in the flasks, the molal ratio of sulfite to sulfate was found to be 2.3. In the case of the analyses of the end products in the reactor, the ratio was more nearly 3.0. Such a large difference between the two ratios was due primarily to the difference in reaction time. Whereas the flask-reactions required approximately 29 hr for completion, the reactor runs were completed in about 300 sec. During the relatively long time in the flasks, the oxidation of sulfite to sulfate was undoubtedly

significant. In comparison to the rate of dithionite oxidation, and under identical conditions, the sulfite oxidation without catalysis was shown to be quite slow (see Figure 15 and Table 9). This was also shown to be true when at the completion of a dithionite oxidation the air flow was allowed to continue for 10 to 15 minutes without a significant change in the sulfite-sulfate ratio. There was no real assurance, however, that in the presence of dithionite ions or transient intermediates the sulfite oxidation was not catalyzed. Indeed, the oxidation of sulfite to sulfate by molecular oxygen has been shown to be catalyzed by free radicals (15). The presence of appreciable amounts of sulfate in the reaction products suggests that catalysis was occurring. The observed ratio of sulfite to sulfate of 3 to 1 sets an upper limit of 25% conversion of sulfite to sulfate by catalyzed air oxidation.

As shown in Table 10, thiosulfate in small but measurable quantities was also among the products. There seemed to be no explanation of its formation unless it were assumed that a secondary reaction involving thermal decomposition was occurring simultaneously with the air oxidation. As the product of a secondary reaction, it accounted for nearly 10% of the dithionite disappearance for a temperature of 30°C. This is based upon the stoichiometry of the thermal decomposition in which the two major products are sulfite and thiosulfate. Probably the secondary reaction was the greatest single factor contributing to the drift in the rate constant k_c.

The stability of thiosulfate in the basic solution and in the presence of molecular oxygen was established by the absence of sulfide and tetrathionate in the end-products, and also by the fact that the thiosulfate concentration in the flask reactions remained constant up to 100 hours after the depletion of the dithionite. Further evidence for the very slow oxidation of thiosulfate was obtained when a 0.028 molar solution was subjected to the same conditions of temperature, stirring and air flow in the reactor that existed for dithionite oxidations. No significant oxidation was measured for times up to 15 min (see Figure 15 and Table 9).

Diffusion Effects

As stated in the experimental procedure, the rate of air or oxygen discharge through the frit into the reacting mixture was varied from 2500 to 3000 cc/min. Preliminary tests showed, however, that an air rate of only 1200 cc/min was sufficiently high to oxidize the dithionite independently of the air rate. Hence, reproducibility of tests was not affected by variable air rates greater than 1200 cc/min. The rate of stirring (approximately 1100 rpm) in the reactor was rapid enough to maintain an isothermal, homogeneous mixture. A stirring rate of only 800 rpm, coupled with an air rate of 1200 cc/min gave the same results within experimental error as a stirring rate of 1100 rpm and an air rate of 2500 cc/min, all other conditions being the same (see Figure 13 and Table 7).

Figure 13 also shows concentrations of dithionite as a function of time for the same initial concentration at 60°C and a stirring speed of 800 rpm but with different air rates. As the air rate was increased up to 1200 cc/min, the curves moved closer to an asymptotic curve which established the lower limits of operation. The fact that the curves of Figure 13 differed indicated that diffusion of oxygen to a point in the system was a controlling factor in the rate of oxidation for air rates less than the asymptotic value of 1200 cc/min. In the kinetic experiments, the greatest demand for oxygen occurred at the highest temperature, which was 60°C, and at the maximum initial concentration of dithionite, which was approximately 20 x 10^{-3} molar. The tests represented by Figure 13 were performed at nearly the extreme demand conditions, as noted above, except that the initial concentration was only 12 x 10^{-3} molar. The experimental data for the kinetic runs at concentrations higher than 12 x 10^{-3} molar were consistent with data obtained for runs below this concentration. Thus, it was assumed that for the air rates and stirring speeds used throughout the experimental work the diffusion of oxygen was not a controlling factor.

Ionic Strength Effects

Figure 14 shows that the rate of the reaction did not change upon increasing the concentration of NaOH, and hence the ionic strength, by factors of three and five. The result shown in Figure 14 for an experiment conducted in 0.01 molar

NaOH appears anomalous. It is almost certain that the different course of reaction resulted from thermal decomposition when generated hydrogen ion neutralized the added NaOH.

pH and Metal Ion Effects

The pH of the dithionite solutions changed approximately from 13 to 12.8 for the highest initial concentration of 20×10^{-3} molar. This indicated that hydrogen ion was generated as one of the products of reaction. No detailed study of the pH variation was made for the air oxidation of dithionite.

No careful study was made to determine the effects of metal ions on the oxidation of dithionite. It was observed, however, in a qualitative way, that mercury in minute quantities caused the reaction to become erratic. A reasonable suggestion is that the mercury reacted to form complexes such as $Hg(SO_3)_2^{=}$.

Solubility Studies

Table 11 lists the experimentally determined solubility of sodium dithionite in water at 0°C. The average value of 11 determinations was found to be 13.20 gms/100 gms of water with a standard deviation of 1.08 gms/100 gms of water or about 8%. Yost (16) lists a value of 12.85 gms/100 gms of water at 1°C, and Rao and Patel (17) list 11.86 gms/100 ml of solution at 0°C. These authors do not give any error limits.

DISCUSSION OF RESULTS

Reaction Mechanisms

A mechanism which satisfied the established order of reaction with respect to dithionite and oxygen and in which the initial step was dissociation of dithionite is as follows:

$$S_2O_4^{=} \rightleftharpoons 2SO_2^{-} \qquad (6)$$

$$SO_2^{-} + O_2 \longrightarrow \text{Products} \qquad (7)$$

Since the first step is a quickly-established equilibrium, the second step is rate determining. Thus, the observed reaction rate is

$$r_{observed} = k_2[SO_2^{-}][O_2] \qquad (11)$$

where

$r_{observed}$ = reaction rate in moles per liter per second.
k_2 = rate constant in moles-liters-seconds units.
$[SO_2^{-}]$ = concentration of SO_2^{-} in moles per liter.
$[O_2]$ = concentration of O_2 in moles per liter.

The equilibrium constant for the first step may be written

$$K_c = \frac{[SO_2^{-}]^2}{[S_2O_4^{=}]} \qquad (12)$$

where K_c has the units of moles per liter

A substitution of the concentration of SO_2^- from the equilibrium-constant expression into the rate expression gives

$$r_{observed} = k_2 K_c^{1/2} [S_2O_4^=]^{1/2} [O_2] \qquad (13)$$

The experimentally determined rate constant, k_c^o, is related to k_2 and K_c by

$$k_c^o = k_2 K_c^{1/2} \qquad (14)$$

The variation of k_c^o with temperature permitted the calculation of the Arrhenius activation energy of 9.3 kcal/mole and the frequency factor of 7.5×10^5 $(\text{moles/liter})^{-1/2}\text{sec}^{-1}$. It will be shown later that the rate determining step probably involves an electron transfer to form O_2^- and SO_2. The observed activation energy of 9.3 kcal/mole seems high for such an electron transfer. Uri (18) has correlated data for a number of exothermic electron transfer reactions, and found typical activation energies to lie between 0 and 5 kcal/mole. The observed value of 9.3 kcal/mole, however, includes a contribution from the equilibrium step. Using approximate values of frequency factors from Frost and Pearson (19), order-of-magnitude calculations can be made for the limiting contributions of the equilibrium and rate-

determining steps to the observed activation energy. The calculations are as follows:

$$k_c^{\circ} = k_2 K_c^{1/2} \text{ where } K_c = \frac{k_1}{k_{-1}} \tag{14}$$

$$A_c^{\circ} e^{-\frac{\Delta E_c^{\circ}}{RT}} = A_2 e^{-\frac{\Delta E_2}{RT}} \left[\frac{A_1 e^{-\frac{\Delta E_1}{RT}}}{A_{-1} e^{-\frac{\Delta E_{-1}}{RT}}} \right]^{1/2} \tag{15}$$

$$\ln A_c^{\circ} - \frac{\Delta E_c^{\circ}}{RT} = \ln A_2 - \frac{\Delta E_2}{RT} + \frac{1}{2} \ln \frac{A_1}{A_{-1}} - \frac{1}{2} \frac{(\Delta E_1 - \Delta E_{-1})}{RT} \tag{16}$$

$$\Delta E_c^{\circ} - RT \left[\ln \frac{A_c^{\circ}}{A_2} - \frac{1}{2} \ln \frac{A_1}{A_{-1}} \right] = \Delta E_2 + \frac{1}{2} (\Delta E_1 - \Delta E_{-1}) \tag{17}$$

Frost and Pearson suggest 10^6 to 10^7 $(\text{moles/liter})^{-1/2}\text{sec}^{-1}$ for A_2, 10^{13}sec^{-1} for A_1, and 10^5 to 10^6 $(\text{moles/liter})^{-1/2}\text{sec}^{-1}$ for A_{-1}. Substituting 9.3 kcal/mole for ΔE_c° and 7×10^5 $(\text{moles/liter})^{-1/2}\text{sec}^{-1}$ for A_c° gives:

$$\Delta E_2 + \frac{1}{2} (\Delta E_1 - \Delta E_{-1}) = 15 \text{ kcal/mole} \tag{18}$$

Thus the above order-of-magnitude calculations place mathematical limits on ΔE_2 and $(\Delta E_1 - \Delta E_{-1})$ as follows:

$$0 \leq \Delta E_2 \leq 15 \text{ kcal/mole}$$

$$0 \leq \Delta E_1 - \Delta E_{-1} \leq 30 \text{ kcal/mole} \qquad (19)$$

If one goes further and assumes a value of ΔE_2 median in the range 0 - 5 kcal/mole, namely 3 kcal/mole, the equations above can be used to calculate K_c and k_2. K_c is found to be 8×10^{-11} moles/liter and k_2 is therefore 2×10^4 $(\text{moles/liter})^{-1}$ sec^{-1}. These values are, at best, order-of-magnitude estimates.

The order of reaction of the air oxidation studies with respect to dithionite and molecular oxygen determines the composition of the transition state in the rate-determining step. That is, the activated complex must consist of one molecule of SO_2^- and one molecule of O_2. Further information about the geometry of the activated complex or the products which result from its decomposition cannot be inferred with certainty from the observed data. Knowledge of the composition of the transition state and the composition of the end products does, however, place a reasonable limit on the number of mechanisms which might be proposed for the intermediate steps. Two possibilities are suggested immediately for the rate determining step:

$$SO_2^- + O_2 \longrightarrow \text{complex A} \xrightarrow{K_2} SO_4^- \qquad (20)$$

$$SO_2^- + O_2 \longrightarrow \text{complex B} \xrightarrow{K_2} SO_2 + O_2^- \qquad (21)$$

It is not inconceivable that both of these mechanisms could occur. Both free radical intermediates SO_4^- and O_2^- have ample precedent in the literature (18). End product analysis does, however, exclude the mechanism given in Equation 20 from being the only mechanism by which the activated complex is decomposed. Subsequent steps would almost certainly be of the type

$$SO_4^- + SO_2^- \longrightarrow SO_4^= + SO_2 \qquad (22)$$

which would lead to a sulfite-to-sulfate ratio of unity in the reaction products. The mechanism given by Equation 21 leads to a series of free-radical intermediates of hydrogen peroxide. The following series of reactions may be written as a suggestion:

$$S_2O_4^{=} \rightleftharpoons 2SO_2^{-}$$

$$SO_2^{-} + O_2 \xrightarrow{k_2} \text{complex B} \xrightarrow{k_3} SO_2 + O_2^{-}$$

$$SO_2^{-} + O_2^{-} \xrightarrow{k_4} SO_2 + O_2^{=}$$

$$O_2^{=} + H_2O \xrightarrow{k_5} HO_2^{-} + OH^{-}$$

$$HO_2^{-} + SO_3^{=} \xrightarrow{k_6} SO_4^{=} + OH^{-} \qquad (23)$$

$$HO_2^{-} + SO_2^{-} \xrightarrow{k_7} SO_3^{=} + OH$$

$$OH + SO_2^{-} \xrightarrow{k_8} SO_2 + OH^{-}$$

$$SO_2 + OH^{-} \xrightarrow{k_9} SO_3^{=} + H^{+}$$

$$\tfrac{1}{2} SO_3^{=} + \tfrac{1}{4} O_2 \xrightarrow{k_{10}} \tfrac{1}{2} SO_4^{=}$$

Certainly there is nothing unique about this suggested series of reactions. It does lead to the observed overall stoichiometry and by suitable choice of kinetic constants could be shown to be kinetically consistent. In common-sense terms, the peroxide intermediates which are formed on a mole for mole basis by the decomposition of dithionite can react either with sulfite molecules already formed to form sulfate or with

SO_2^- radical ions to form more sulfite and regenerate peroxide intermediates. Since the concentration of sulfite ions in solution greatly exceeds that of SO_2^- ions after the first second of the reaction, the preponderance of sulfite rather than sulfate in the products requires that $k_7 >> k_6$ in the above scheme. A steady state concentration of intermediates need not be postulated in this hypothetical analysis.

CONCLUSIONS

The chemistry of reactions of sulfur-oxygen species in aqueous solution is sufficiently complex to inject a certain amount of ambiguity into the interpretation of nearly all practicable experiments. Such is the case for the work described herein. A true and unambiguous understanding would require considerably more experimentation and methods that are far more subtle than the ones used in the present experiments.

As shown earlier, only a very specific investigation was conducted. The study of the effects of other variables such as the addition of certain ionic species, both anionic and cationic, was omitted entirely. Undoubtedly, a study in this direction would contribute to the understanding of this complex problem.

A brief summary of the major results obtained in the study of the air-oxidation of dithionite is given as follows:

1. The reaction was one-half order with respect to dithionite.
2. The reaction was first order with respect to molecular oxygen.
3. The activation energy based on the Arrhenius Equation for the specific rate-constant of reaction was 9.3 kcal/mole. The frequency factor A, was found to be 7×10^{-5} $(\text{moles/liter})^{-1/2}\text{sec}^{-1}$. The rate of reaction is given by the expression

$$r = k_c^{o}[S_2O_4]^{1/2}[O_2].$$

4. The rate of sulfite oxidation to sulfate was low compared to the oxidation rate of dithionite.
5. The small pH change from 13 to approximately 12.8 indicated the generation of hydrogen ion in the reaction. This result agrees with the observed overall stoichiometry that there is a net increase in acidic sulfur anions.
6. The ratio of sulfite to sulfate in the reacted mixture was 3 to 1 on a mole basis.

A mechanism which satisfied the established order with respect to dithionite and oxygen and in which the initial step was dissociation of dithionite is proposed as follows:

$$S_2O_4^{=} \rightleftharpoons 2SO_2^{-} \qquad (6)$$

$$SO_2^{-} + O_2 \longrightarrow \text{products} \qquad (7)$$

Since the first step is an instantaneous equilibrium process, the second step must be rate determining. Hence the measured rate must have a direct relationship to the second step. The kinetic expression becomes:

$$r = k_2[SO_2^{-}][O_2] \qquad (11)$$

From the first step, the equilibrium constant can be

written as:

$$K_c = \frac{[SO_2^-]^2}{[S_2O_4^=]} \tag{12}$$

A substitution of the concentration of SO_2^- from the equilibrium expression into the rate expression gives:

$$r = k_2 K_c^{1/2} [S_2O_4^=]^{1/2}[O_2] \tag{13}$$

Unfortunately, the value of K_c was indeterminate since the concentration of SO_2^- was experimentally inaccessible.

The rate constant k_c^o, which was calculated directly from the data, is related to k_2 by:

$$k_c^o = k_2 K_c^{1/2} \tag{14}$$

Thus the derived rate expression, which is equivalent to the experimental rate expression, is given as follows:

$$r = k_c^o [S_2O_4^=]^{1/2}[O_2] \tag{24}$$

The temperature variation of k_c^o is given by

$$k_c^o = 7 \times 10^5 \, e^{-\frac{9300}{RT}} \ (\text{moles/liter})^{-1/2}\text{sec}^{-1} \tag{25}$$

Values of k_c^o are listed in Figures 8-11.

The observed order of reaction with respect to dithionite and molecular oxygen and the stoichiometry of the reaction products suggest that hydrogen-peroxide-type intermediates are involved in steps subsequent to the rate-determining step. A hypothetical mechanism can be described to account for the observed kinetic and stoichiometric facts.

PART 2. DITHIONITE STRUCTURE STUDIES

INTRODUCTION

Perhaps the earliest attempt to elucidate the structure of sodium dithionite by purely physical methods was made by Klemm (20) in 1937. He determined by gross magnetic susceptibility measurements that the anhydrous salt of sodium dithionite is diamagnetic.

It was of some interest, therefore, when Van der Heijde (21) in 1953 found that the exchange rate of S^{35} between dithionite and sulfur dioxide in neutral or acid solution was almost instantaneous, indicating the ready cleavage of the S-S dithionite bond. The exchange reactions were stopped by the addition of a large excess of formaldehyde, which complexed the dithionite and bisulfite ions according to the following equations:

$$Na_2S_2O_4 + 2CH_2O + H_2O \longrightarrow CH_2(OH)SO_2Na + CH_2(OH)SO_3Na \quad (1)$$

$$NaHSO_3 + CH_2O \longrightarrow CH_2(OH)SO_3Na \quad (2)$$

No exchange occurred, however, between SO_2 and trithionate ($S_3O_6^{=}$) which presumably has a normal S-S bond.

The first crystal structure studies of sodium dithionite were reported by Dunitz (22) in 1956. He found that the dithionite anion, in the crystal structure of sodium dithionite, consists of two SO_2^- units, joined by an unusually long S-S

bond which is 2.389 Å in length. By assuming the usual S-S single-bond distance of 2.08 Å, application of Pauling's (23) relationship $-\Delta R_{(n)} = 0.353 \log n$ between bond number, n, and the bond-type correction, $\Delta R_{(n)}$, relative to a single bond, predicts 0.36 for the bond strength. In the crystal, the dithionite anion has an eclipsed configuration with the planes of opposite SO_2^- groups inclined at 30° to one another. From these observations, Dunitz concluded that there should be ready cleavage of the S-S bond in dithionite.

An electron-paramagnetic-resonance (EPR) investigation by Hodgson, Neaves, and Parker (24) showed that anhydrous crystals of dithionite at the temperature of liquid oxygen gave weak electron-spin resonance. They reported a spectroscopic splitting factor of 2.01 ± 0.01 and a peak width of 12 ± 3 gauss. By treating the crystals with a small amount of degassed water or ethyl alcohol but not enough to dissolve them, the radical-ion content increased. When enough water was added to dissolve the crystals at room temperature and the mixture was frozen in liquid oxygen, no resonance could be detected. Upon evaporation of part of the water to re-form the crystals, a radical-ion signal was again observed. The radical-ions disappeared only very slowly when air was admitted. Hodgson, et al., estimated that approximately 0.01% of the dithionite ions was dissociated into SO_2^- radical-ions. They further stated that it was not clear whether the radical-ions were present only in the crystals or whether they were also present in the aqueous solution.

SUMMARY

A study of the electron-paramagnetic-resonance (EPR) properties of saturated dithionite solutions, which were stabilized at room temperature with sodium hydroxide, showed the presence of the SO_2^- radical-ion. On the EPR trace, the sharp resonance peak of this paramagnetic ion gave a peak width at half-height of 1.3 gauss and a spectroscopic splitting factor of 2.0051 at a klystron frequency of 9.453×10^9/sec and a magnetic-field strength of 3365 gauss. Observations on dithionite solutions of various dilutions showed that the SO_2^- concentration varied as the square root of the dithionite concentration so that the equilibrium relationship may be written as:

$$K_c = \frac{[SO_2^-]^2}{[S_2O_4^{=}]} \qquad (3)$$

Dry sodium dithionite powder was also observed to exhibit paramagnetism. This phenomenon is explicable in terms of minute amounts of $NaSO_2$ radicals occluded in dithionite powder.

Sodium formaldehyde sulfoxylate solutions were likewise shown to exhibit paramagnetism when adjusted to pH 6 or lower. The acidified solutions appeared to contain free radicals identical with those detected in dithionite solutions.

APPARATUS AND PROCEDURE

Chemically pure sodium dithionite (Baker Chemical Company, batch No. 3712, lot JTB 6113) was further purified by three fractional crystallizations from oxygen-free aqueous solutions at 0°C. The crystallization procedure was the same as that described in Air Oxidation Studies. The purified crystalline product was then used to make a saturated, oxygen-free alkaline solution at 0°C which was 0.5 molar in sodium hydroxide to inhibit thermal decomposition of the dithionite at room temperature.

Pyrex sample tubes with outside diameters of 1 mm and lengths of 76 mm were filled with the solution and sealed at both ends. Another set of sealed tubes of the same dimensions was prepared by filling with a tenfold and a hundredfold dilution of the saturated dithionite. A third set was prepared by filling with a completely oxidized sample of the saturated dithionite solution. Finally, a fourth set was prepared by filling with an acidified sample of a saturated thiosulfate solution, to provide a source of colloidal sulfur.

Each of the sealed tubes was analyzed in an EPR apparatus which had a cavity diameter slightly greater than 5 mm and a length of approximately 23 mm. During the EPR measurements, some difficulty was experienced in obtaining cavity resonance because of the dipole heating of the water molecules.

A calibration tube was made up from 0.1 molar manganous

chloride in order to compare the known values of the splitting factor and the gauss separation between resonance peaks for the free electron of the manganous ion with the resonance trace of the dithionite samples. In the calibration runs, the instrument settings for the sweep rate of the magnetic field were kept the same as those used for the dithionite.

In the experiments with dry $Na_2S_2O_4$ powder, the purified material was dried at 100°C in a vacuum over P_2O_5 for several days before sampling. The finely-divided, dry powder was loaded into a pyrex tube in a desiccator.

Eastman Kodak sodium formaldehyde sulfoxylate, m.p. 65°C, was recrystallized from water-methanol and dried at 50°C in a vacuum. The dry powder, saturated solutions in pure water, 1 molar NaOH, and 1 molar HCl were examined for paramagnetism.

RESULTS

The results of the EPR studies are shown in Figures 16 and 17. An arbitrary signal voltage which was a first-derivative function of the phase-sensitive detection system of the EPR apparatus is plotted against magnetic field strength in Figure 16a. Since the klystron frequency of the apparatus was held constant, the magnetic field strength was varied over the range in which resonance was expected to occur. The rate of magnetic scanning in relationship to chart speed on the graphic recorder fixed the time constant from which the magnetic field strength at resonance and the resonance peak width were calculated. The scale factor for conversion of instrument readings to corresponding field-strength values was obtained from a calibration using the resonance peaks of manganous ions which have a peak to peak distance of 98 gauss.

Only the three samples which contained oxygen-free stabilized dithionite of different dilutions showed paramagnetism. Sharp resonance occurred at 3.365 kilogauss with a fixed klystron frequency of 9.453×10^9 cycles/sec. The width of the single resonance peak for each sample was approximately 1.3 gauss at half-peak height, and the spectroscopic splitting factor g was found to be 2.0051 based upon a comparison with the free-electron g-value of 2.0023 for manganous ion in aqueous solution.

Figure 17 shows the absorption peaks of the three dithionite concentrations studied. An estimate of the area ratios of the absorption peaks for the saturated solution, the tenfold dilution and the hundredfold dilution was 10 to 3 to 1, respectively. This indicated that the SO_2^- concentration varied as the square root of the dithionite concentration, so that they are related by the expression:

$$K_c = \frac{[SO_2^-]^2}{[S_2O_4^=]} \qquad (3)$$

No absolute concentration of the SO_2^- was determined from these few tests, but the limiting concentration of the paramagnetic species which could be detected in the 5 mm cavity was estimated to be 2×10^{-6} molar or 10^{-9} moles.

In agreement with Hodgson et al. (24), dry $Na_2S_2O_4$ powder was also observed to exhibit paramagnetism. The width of the single resonance peak, measured at half-peak height, was 5 gauss. Ultraviolet irradiation of the dry powder for several hours did not increase the paramagnetism in an experiment carried out at room temperature.

Sodium formaldehyde sulfoxylate crystals did not exhibit paramagnetism. Saturated aqueous solutions in pure water or 1 molar NaOH gave the same result. The acidified solution, however, either at pH 5-6 or pH 1, gave a sharp resonance peak whose width and g-value are indistinguishable from that obtained from dithionite solutions. Figure 16b shows

the resonance absorption obtained from the acidified sodium formaldehyde sulfoxylate solution and from the solid $Na_2S_2O_4$ powder when both samples were placed in the cavity. Two peaks, superimposed upon one another, can be distinguished. The narrower, inner peak corresponds to the liquid sample and the outside peak shows the resonance absorption in the solid. Likewise, Figure 16c shows the superposition of the same solid sample on the aqueous dithionite resonance absorption. Within the limits of experimental detection, the peak widths and g-factors of these free radicals are identical.

DISCUSSION AND CONCLUSIONS

The observation that the SO_2^- free radical exhibits a single resonance absorption is consonant with the fact that no nuclear spins are present in the molecule, and therefore one would expect no hyperfine splitting.

The close proximity of the observed g-value to that of a free electron indicates that spin-orbit interactions are probably small. Since the EPR studies were conducted at only one frequency, however, it cannot be concluded that there is no orbital contribution to the paramagnetism.

The narrow peak observed for the aqueous SO_2^- indicates that the rate of combination-dissociation between the dimer dithionite and the monomer SO_2^- ions must be low compared with the free electron relaxation time of 10^{-9} seconds. Moreover, the fact that the absorption peak width changed only slightly upon dilution by 100-fold suggests that exchange narrowing is not a significant process in this instance.

The observed paramagnetism of dry dithionite powder is somewhat surprising since aqueous solution results require the interpretation that the undissociated dithionite dimer be diamagnetic. Crystal structure studies (22) indicate that dithionite is not dissociated in the crystal. Although a completely unambiguous explanation of this phenomenon cannot be given at this time, it seems likely that extremely small amounts of SO_2^- or $NaSO_2$ are occluded or trapped in the

crystals. Certainly the similarity of g-value and narrow line width suggests that again an SO_2^- radical ion is involved. Since extremely small concentrations of SO_2^- would be required to give the observed resonance, i.e., about one part in 100,000, crystal structure studies would not detect these occlusions.

The observed paramagnetism of acidic solutions of sodium formaldehyde sulfoxylate is also surprising since the unprotonated complex is diamagnetic in neutral and basic solutions. Evidently protonation of the ionized complex causes cleavage of the carbon-sulfur bond with liberation of the radical-ion SO_2^-. Thus:

$$CH_2(OH)SO_2^- + H^+ \longrightarrow SO_2^- + ? \qquad (4)$$

That the free radical obtained upon acidification is SO_2^- has not been definitely established. The only evidence offered in support of the thesis that it is SO_2^- is the fact that sodium formaldehyde sulfoxylate is formed from formaldehyde and dithionite in basic solution:

$$S_2O_4^= + CH_2O + H_2O \longrightarrow CH_2(OH)SO_2^- + SO_3^= + H^+ \qquad (5)$$

and similarities in the resonance absorptions shown in Figures 16b and c. Heretofore three investigators (6,21,25) believed that acidification of the complex liberated the anion

of sulfoxylic acid and regenerated formaldehyde.

$$CH_2(OH)SO_2^- + H^+ \longrightarrow CH_2O + SO_2^= + 2H^+ \qquad (6)$$

The fact that this is not the case explains the instability of pyridine nucleotide complexes (25,26,27,28), which are similar to formaldehyde complexes, with dithionite and sulfoxylate in acidic media. Also explicable is the rapid decomposition of neutral and acidic solutions of formaldehyde sulfoxylate complex with metal ions known to catalyze free radical decompositions (6).

The unambiguous demonstration that appreciable concentrations of SO_2^- ion exist in equilibrium with $S_2O_4^=$ in solutions of sodium dithionite supports the mechanism proposed for the air oxidation of dithionite solutions. SO_2^- radical-ions are confirmed to be real intermediates in the air oxidation mechanism. Moreover, the limit of sensitivity of the detection apparatus and the results of the dilution experiments enable one to make order-of-magnitude calculations of the equilibrium constant, K_c. The concentrations of dithionite corresponding to the adsorption curves in Figure 17 are 7.4×10^{-1}, 7.4×10^{-2} and 7.4×10^{-3} molar in decreasing order. Estimating that one more tenfold dilution of dithionite to 7.4×10^{-4} molar would decrease the SO_2^- concentration to the limit of detection of the apparatus, i.e., 2×10^{-6} molar, permits a rough calculation of K_c to be made:

$$K_c \approx \frac{(2 \times 10^{-6})^2}{7.4 \times 10^{-4}} \approx 5 \times 10^{-9} \text{ moles/liter} \qquad (7)$$

This order-of-magnitude calculation is in reasonable agreement with the order-of-magnitude calculation of 8×10^{-11} moles/liter based upon air oxidation studies.

PART 3. ELECTROLYTIC STUDIES

INTRODUCTION

The electrolytic synthesis and electrochemical properties of sodium dithionite were first investigated nearly a hundred years ago by Schutzenberger (2), one of the pioneers in dithionite chemistry. Schutzenberger reduced a solution of sodium bisulfite electrolytically and obtained a crystalline solid which proved to have powerful reducing properties. He assigned the molecular formula $NaHSO_2$ to the substance.

Nearly half a century later, Jellinek (29) used electrochemical methods to investigate the equilibrium

$$H_2 + 2HSO_3^- \rightleftharpoons S_2O_4^{=} + 2H_2O \qquad (1)$$

Determination of the emf corresponding to the electrode reaction

$$S_2O_4^{=} + 2H_2O \rightleftharpoons 2HSO_3^- + 2H^+ + 2e^- \qquad (2)$$

enabled him to calculate the heat of reaction for the equilibrium process. He reported the following, for equilibrium at 21°C:

$$S_2O_4^{=} + 2H_2O \rightleftharpoons 2HSO_3^- + H_2 \quad \Delta H = -15{,}300 \text{ cal} \qquad (3)$$

In a later article (30) Jellinek stated that the electrolytic reduction of $NaHSO_3$ to $Na_2S_2O_4$ gave decreasing yields of dithionite during electrolysis. He concluded that this decrease in yield resulted from thermal decomposition of the dithionite formed according to the equation:

$$2Na_2S_2O_4 + H_2O \longrightarrow Na_2S_2O_3 + 2NaHSO_3 \qquad (4)$$

He discounted the possibility that the dithionite itself could be reduced to thiosulfate in the electrolytic reduction.

The first precise electrochemical work reported in the literature was by Gossman (31) in 1930. Studying the reduction of sulfur dioxide in aqueous solutions at the dropping mercury electrode, Gossman postulated that $H_2S_2O_4$ was formed by reduction of SO_2 in strongly acidic media. At a cathode potential of -0.2v vs S.C.E. in 1 molar HCl, 2 moles of electrons were believed to be transferred to 2 moles of aqueous SO_2 yielding $H_2S_2O_4$, which he incorrectly believed to be stable in strongly acidic media. Thus:

$$2SO_2 + 2H^+ + 2e^- \longrightarrow H_2S_2O_4 \qquad (5)$$

At pH 6, two smaller cathodic waves were observed. He postulated that the dithionite was unstable at pH 6 and decomposed thus:

$$H_2S_2O_4 \longrightarrow H_2SO_2 + SO_2 \qquad (6)$$

The second cathodic wave he ascribed to the reduction of the liberated SO_2. Above pH 7 no cathodic waves were observed at potentials less than that required to reduce sodium ion at the mercury electrode.

Kolthoff and Miller (32) in 1941 repeated Gossman's work and obtained the same experimental data. Their interpretation of the data, however, was quite different. They stated that the reduction of sulfur dioxide in 1 molar HCl is a two electron transfer process, instead of the one electron transfer process postulated by Gossman. Thus:

$$SO_2 + 2H^+ + 2e^- \longrightarrow H_2SO_2 \qquad (7)$$

Sulfoxylic acid, not dithionous acid, was stated to be the reduction product. They reasoned that the diffusion coefficient for SO_2 calculated from the data and the use of Ilkovic's equation for one and two electron transfer reactions agreed with the previously known diffusion coefficient of oxygen under similar conditions only in the case of the two electron transfer. In order to explain the two cathodic waves at pH 6, they reverted to a one-electron transfer reaction which is followed by a dimerization reaction and subsequent reduction of the dimer to thiosulfate. Thus:

$$HSO_3^- + 2H^+ + e^- \longrightarrow HSO_2 + H_2O \qquad (8)$$

$$2HSO_2 \longrightarrow H_2S_2O_4 \longrightarrow S_2O_4^{=} + 2H^+ \qquad (9)$$

$$2H^+ + S_2O_4^{=} + 2e^- \longrightarrow S_2O_3^{=} + H_2O \qquad (10)$$

No analyses of reduction products were reported.

In a series of articles published between 1949 and 1953 Patel and Rao (17) described investigations of the feasibility of producing sodium dithionite electrolytically on a commercial basis. The effects of a great number of reaction conditions were systematically studied in an attempt to maximize the yield of sodium dithionite. The cathodic potential used in all cases, however, was sufficiently negative to reduce sodium ion; hence the reducing agent was actually sodium-mercury amalgam. Using a reactor maintained at 5°C and pH 5 to 5.5 with a HSO_3^- concentration of 30% by weight (maintained by constant SO_2 gas feed), dithionite concentrations of 20% by weight could be obtained with 91% current efficiency. Under optimal conditions, a current density of $2.0 - 2.6 \times 10^{-2}$ amps/sq cm was maintained between a rapidly stirred mercury cathode, which contained 0.13% Zn, and a carbon rod anode.

The present investigation of the electrochemical synthesis and properties of sodium dithionite was designed to seek answers

to several problems left unsolved by the investigations described above. Knowledge of the fact that SO_2^- radical ions exist in aqueous solution in equilibrium with undissociated dithionite suggested that the cathodic waves obtained by Gossmen and Kolthoff and Miller corresponded to reduction of SO_2 to SO_2^- by a one electron transfer reaction:

$$SO_2 + 1e^- \longrightarrow SO_2^- \qquad (11)$$

Identification of the reduction product by its ability to reduce methylene blue and the paramagnetism of its solutions would confirm the suggestion that dithionite is formed. Furthermore, a study of the efficiency of the reduction process and the stability of the dithionite formed would be of interest.

Since the completion of the work described in the following sections, two important studies have been reported in the literature.

Munemori (33) reported the coulometric titration of dyestuffs with electrolytically generated dithionite. Electrolyses of solutions 0.01 molar in bisulfite ion between pH 3 and 5 with cathode potential -0.63v vs S.C.E. and constant currents between 3.1 and 5.0 milliamps produced dithionite at essentially 100% current efficiency.

Cermak (34,35) reported extensive studies of the polarographic properties of dithionite solutions. His experiments included the effects of pH, concentration and reaction tempera-

ture. His results are in agreement with the existence of SO_2^- radical-ions in aqueous solutions of dithionite. In order to explain the anodic and cathodic kinetically-controlled waves obtained, it was necessary to postulate the dissociation of the dimer $S_2O_4^=$ to monomer SO_2^- ions. Two anodic waves corresponding to the oxidation of SO_2^- to SO_2 and $S_2O_4^=$ to $S_2O_5^=$ were postulated. Two cathodic waves corresponding to the reduction of SO_2 to SO_2^- and SO_2^- to $SO_2^=$ were also postulated. The heights of the kinetically-controlled waves enabled him to calculate the ratio of the forward rate constant of the $S_2O_4^=$ dissociation to the square root of the equilibrium constant for the reaction

$$S_2O_4^= \underset{k_{-1}}{\overset{k_1}{\rightleftharpoons}} 2SO_2^- \qquad (12)$$

where $K_c = \frac{k_1}{k_{-1}}$

The value of $\frac{k_1}{\sqrt{K_c}}$ at 40°C was given as 6×10^{-3} (moles/liter)$^{-\frac{1}{2}}$ sec^{-1}. Separate evaluation of the rate constants or equilibrium constant was not possible from this work.

SUMMARY

Dithionite ion has been established as the reduction product in the electrolysis of aqueous bisulfite solutions of pH 5-5.3 at cathode potentials of -0.60 to -0.98v vs S.C.E. That the reduction is a one-electron transfer process by which SO_2^- ions are formed from aqueous sulfur dioxide at the cathode seems likely, although the possibility of two electron transfer has not been excluded.

APPARATUS AND PROCEDURE

A simple electrolysis cell consisting of a 600 ml Berzelius beaker with a tight-fitting Plexiglas lid was immersed in an ice bath. The cathode consisted of a pool of clean mercury 7 mm deep and 49 sq cm in area. The cathode was connected to a terminal on the Plexiglas lid by a platinum wire shielded from the electrolyte by glass tubing. The cathodic pool was not stirred. The anode consisted of a platinum electrode, with surface area 1 sq cm, placed in an anode compartment. The anode compartment consisted of a fine-mesh gas-dispersion frit mounted on the end of a length of 1 cm glass tubing fixed to the Plexiglas lid. Fresh electrolyte solution was added to the compartment at intervals in order to maintain a positive pressure differential between the anode compartment and the bulk of the electrolyte solution. A Heathkit Model PS-3 power supply was used to drive the cathode potential negative and measure the current in milliamperes. A Leeds and Northrup Model 7664 pH meter measured the potential of the cathode with respect to a saturated calomel electrode immersed in the electrolyte solution and fixed to the Plexiglas lid. The electrolyte solution was stirred at a rapid and constant speed with a glass paddle-stirrer.

The electrolyte solution was prepared by saturating 250 ml of distilled water with reagent grade sodium bisulfite and by adding reagent grade sodium acetate and water, as needed, to

produce a saturated solution at the desired pH of 5.0-5.3.

One-or two-cc samples were withdrawn from the electrolyte by a pipette at suitable time intervals and titrated with standardized methylene blue as described in Air Oxidation Studies.

A total of three experiments were conducted at constant currents of 100, 150, and 200 milliamperes. The cathode potential varied between -0.67 and -0.98 v. At the conclusion of the 200 milliampere experiment the electrolysis was allowed to proceed for several hours. The electrolysis was then stopped, the solution made alkaline by the addition of 1 molar NaOH solution, and pure crystalline NaCl added to salt out a white precipitate. This white precipitate was collected by centrifugation and quickly loaded, as a wet paste, into a pyrex tube for examination by EPR.

RESULTS AND CONCLUSIONS

Figure 18 and Table 12 present the data obtained from the three electrolysis experiments. Evidently dithionite can be generated at constant current efficiency of about 75% under the conditions studied. The rather low current efficiency obtained probably results, at least in part, from the fact that the cathode was not stirred.

Electron paramagnetic resonance absorption similar in all respects to the one shown in Figure 16a was obtained from the sample of precipitated reduction product. This confirms the identity of SO_2^-, and hence $S_2O_4^=$, as the reduction product.

The question of whether the reduction is a one or two electron transfer, however, has not been unambiguously solved. The two possibilities are

$$SO_2 + 1e^- \longrightarrow SO_2^- \qquad (11)$$

and

$$SO_2 + 2e^- \longrightarrow SO_2^= \qquad (13)$$

The identification of SO_2^- as the reduction product is not sufficient to distinguish between these two mechanisms. It is possible that $SO_2^=$, if generated, could react with aqueous SO_2 to yield $S_2O_4^=$ and hence SO_2^-. Thus:

$$SO_2^{=} + SO_2 \longrightarrow S_2O_4^{=} \rightleftharpoons 2SO_2^{-} \qquad (14)$$

Since it has been demonstrated by EPR that sodium formaldehyde sulfoxylate, heretofore believed (6,21,25) to be a source of $SO_2^{=}$ ions, liberates SO_2^{-} in solution of pH 6 or less, the reaction written above cannot be tested using sodium formaldehyde sulfoxylate as the source of $SO_2^{=}$ ions. An experiment using another source has not been attempted.

The polarographic studies of aqueous SO_2 solutions (31, 32,34,35) as interpreted by Cermak indicate that $SO_2^{=}$ is not formed by the reduction of SO_2^{-} ions until a cathode potential of -1.23v is reached. This seems to be an entirely reasonable interpretation of the polarographic waves observed, although it is not a unique one.

Use of the Cermak relation $k_1/\sqrt{K_c} = 6 \times 10^3$ (moles/liter)$^{\frac{1}{2}}$ sec^{-1} together with order-of-magnitude calculations of the equilibrium constant, K_c, from air oxidation and EPR studies enables one to obtain order-of-magnitude values for k_1 and k_{-1}. The values of K_c estimated from air oxidation and EPR studies are 8×10^{-11} and 5×10^{-9} moles/liter respectively. If one uses a logarithmic average value, namely 6×10^{-10} moles/liter and solves for k_1 and k_{-1} in equation 12 using the Cermak relation, k_1, and k_{-1} are found to be 2×10^{-7} sec^{-1} and 3×10^2 (moles/liter)$^{-1}$ sec^{-1}, respectively. The bimolecular rate constant, k_{-1}, seems rather low, although the approximate nature of these calculations does not justify any further conclusions which might be drawn.

PART 4. THERMAL DECOMPOSITION STUDIES

INTRODUCTION

The first careful study of the thermal decomposition of sodium dithionite solutions was reported by Jellinek (36) in 1919. Examining the decomposition reaction in neutral and sodium-bisulfite-containing solutions, he found that dithionite decomposed almost quantitatively in accordance with the equation:

$$2Na_2S_2O_4 + H_2O \longrightarrow 2NaHSO_3 + Na_2S_2O_3 \qquad (1)$$

In reactions carried out at constant temperature, the rate constant was found to be proportional to the square of the initial bisulfite concentration. The variation in rate constant with temperature, at constant initial bisulfite concentration, was in a manner predicted by the Arrhenius equation.

Bassett and Durrant (6) in 1927 reviewed all of the literature pertaining to the interrelationships of the sulfur acids and attempted a correlation with the results of extensive experimental work of their own. In order to explain the complexity of products of dithionite reactions, they postulated that dithionite exists in three isomeric forms. Each isomer was believed to decompose in a way such that all of the observed reaction products could be explained by one or more of the mechanisms. Although Bassett and Durrant's work is of

considerable value as a compilation of experimental observations of dithionite reactions, subsequent work has invalidated their interpretation of these reactions.

Lynn (8) carried out the most extensive investigation of the thermal decomposition reaction reported to date. He found that an aqueous solution of purified sodium dithionite at 60°C decomposed slowly at first, and then, after a certain elapsed time, decomposed very rapidly. This behavior suggested to him a degenerate chain-branching mechanism. He assumed the stoichiometry of the reaction to be that described by Equation 1 above. He observed that the hydrogen ion concentration increased in a manner which was almost a mirror image of the decreasing dithionite concentration. At low pH, the dithionite decomposed in a few seconds. In addition, the presence of colloidal sulfur accelerated to a lesser extent the onset of the rapid decomposition reaction.

Lynn also studied the effects of added salts on the reaction rate. The addition of sodium hydroxide or sodium sulfite was observed to inhibit the onset of the rapid decomposition reaction. Addition of sodium chloride catalyzed this reaction, presumably by a Bronsted positive-salt effect. Sodium thiosulfate, likewise, accelerated the onset of the rapid decomposition reaction. Sodium bisulfite, however, had a different effect. At concentrations less than the initial dithionite concentration its effect was similar to that of sodium thiosulfate, but when greater, it changed the course

of the reaction entirely. The reaction became apparently first order in both bisulfite and dithionite concentrations. Moreover, when thiosulfate was added to this mixture, the reaction became apparently first order in thiosulfate as well as in bisulfite and dithionite. The third order rate constant, however, was found to be an undetermined function of hydrogen ion and initial dithionite concentrations.

Superimposed on this complex reaction system, Lynn found that the observed rate was periodic with time, i.e. periodically increased and decreased as the reaction proceeded. In order to explain this curious phenomenon, he postulated the presence of an unknown product species having properties similar to dithionite. In addition, there was a significant lack of reproducibility in many of the experiments reported. This was believed to result from the presence of differing amounts of suspended sulfur particles in the initial dithionite solutions.

SUMMARY

A study of the thermal decomposition of sodium dithionite was conducted in buffered and unbuffered media in the pH range 4.0 to 7.0. The concentration of the dithionite was measured as a function of time at 60, 70, and 80°C. Initial concentrations varied from 5.5 to 11.5 x 10^{-3} molar. The pH of the unbuffered systems was measured as a function of time with a Beckman Model G pH meter. The reaction was observed to consist of an induction period in which the decomposition was slow, followed by a decay period, in which the concentration of dithionite rapidly decreased to zero. Apparent periodic increases and decreases in dithionite concentration during the induction period were observed and could not be explained solely on the basis of experimental error. One possible explanation of this unusual phenomenon is the formation of unstable intermediate(s) possessing reducing potentials comparable to dithionite with respect to methylene blue. The amplitude of the apparent oscillations in dithionite concentration decreased with increasing temperature, suggesting that the concentration of the hypothetical reactive intermediate(s) likewise decreased with increasing temperature. Absence of oscillations in solutions of pH greater than 7 suggests that the hypothetical intermediate(s) either are not formed or are unstable in alkaline solution.

During the induction period, the reaction was observed

to be 1/2 order with respect to H^+ and 3/2 order with respect to dithionite, giving a rate expression of the following form:

$$r_{induction} = k_c[H^+]^{1/2}[S_2O_4^{=}]^{3/2}$$

The variation of k_c with temperature gives a straight line on an Arrhenius equation plot. The activation energy ΔE was found to be 12 kcal/mole and the frequency factor A was found to be 1.3×10^8 $(moles/liter)^{-1}sec^{-1}$.

The anions $SO_3^{=}$, HSO_3^{-}, $SO_4^{=}$, and $S_2O_3^{=}$ had no specific effects in buffered reactions. Colloidal sulfur catalyzed the reaction by decreasing the length of the induction period.

The rapid increase in the rate of dithionite decomposition during the decay period followed an exponential relationship with time. This fact together with the catalysis by colloidal sulfur suggests that an autocatalytic or a degenerate branching chain mechanism is occurring.

APPARATUS

In general, the apparatus for the thermal decomposition studies was the same as that described in Air Oxidation Studies. The only change was to eliminate the presence of oxygen from the reaction system. This was accomplished by partially diverting the oxygen-free nitrogen from the scrubbing system previously described into the reactor. It is important to note that the nitrogen was not allowed to pass through the reactor in a steady stream. The pressure of the nitrogen above the reaction mixture was maintained slightly above atmospheric and was controlled manually by occasionally adjusting a by-pass valve upstream from the reactor. A water-filled manometer which was connected directly to the exit line indicated the pressure.

EXPERIMENTAL PROCEDURE

The preparation of the recrystallized dithionite was accomplished in the same manner as described in the experimental procedure of the Air Oxidation Studies. Also, by the same procedure, the saturated solution of dithionite was subsequently prepared from the crystals and used to supply the initial concentration to the reactor.

The volume of the liquid mixture in the reactor was approximately 500 cc. The composition of the solution before addition of the saturated dithionite varied according to the desired hydrogen-ion concentration. The majority of tests were performed in water that had been triply distilled. Other tests were performed in buffered solutions wherein the pH was varied from 4.0 to 7.0. The buffering agents were mixtures of KH_2PO_4 and NaOH or $KHC_8H_4O_4$ and NaOH in proportions commensurate with the desired pH. In Appendix I, the compositions of the buffer solutions are described in detail.

Experiments at 60, 70 and 80°C were conducted with the unbuffered systems in order to determine the effect of temperature on the rate of decomposition. The buffered systems were studied only at 60°C since, in this case, the effect of a controlled pH was of primary importance. At each temperature and for both the buffered and unbuffered systems, the initial concentration of dithionite was varied from 5.5 to 11.5 x 10^{-3} molar.

In the unbuffered systems, no products of reaction such as HSO_3^-, $S_2O_3^=$, $SO_3^=$, S, and H^+ were added to the system in order to determine their specific catalytic effects. This work had been done previously by Lynn (8). To the buffered reactions, however, HSO_3^-, $S_2O_3^=$, $SO_4^=$, and $SO_3^=$ were added in concentrations ranging from one-half to three halves of the stoichiometric quantities according to the reaction:

$$2S_2O_4^= + H_2O \longrightarrow S_2O_3^= + 2HSO_3^- \qquad (2)$$

These anion additions were always made while the decomposition experiments were in progress. The purpose of their addition was to determine their catalytic effects in the presence of controlled H^+ ion.

By conducting successive tests in the reactor without removing the contents of the previous runs, the catalytic effects of the product species $S_2O_3^=$ and sulfur were determined. Usually, three dithionite solutions were decomposed in each experiment, and in all cases the systems were buffered at a pH of 5.00. After the first decomposition which was begun with fresh solution, and after each successive decomposition, enough buffer solution was added to restore the volume of the reactor contents to 500 cc. Also, the initial dithionite concentrations which varied from 5.5 to 6.0 x 10^{-3} molar, originated from the same saturated solution. A pH measurement was taken at the beginning and end of each decomposition

in order to insure that sufficient buffer was present.

Great care was taken to prevent oxygen contamination. When transferring samples from the reactor to the titration flasks, for example, the sampling syringe was flushed with nitrogen several times prior to removing a sample from the reactor. As a further precaution to prevent contamination, the syringe was rinsed several times with oxygen-free distilled water after taking each sample.

Reactant and Product Analysis

The concentration of $S_2O_4^{=}$ was estimated by titration with methylene blue as described in the experimental procedure of the Air Oxidation Studies. The sample flasks which received a measured volume of the reaction mixture were initially filled with 50 cc of 0.1 molar KOH and 30 cc of CH_3OH. Titration of the samples with methylene blue was done immediately in order to minimize the errors due to slight oxygen contamination or further thermal decomposition. Occasionally, titrations were performed at approximately 5°C to check for any significant effects of temperature upon the results. No effect was noted, so that titrations at room temperature were done with confidence.

In order to determine the relative concentrations of the end-products, an unbuffered reaction at 30°C was carried out in a sealed vessel with an initial dithionite concentration of 7.32×10^{-3} molar. The completion of reaction was determined

by titration of a 10 cc sample with methylene blue. The concentration of the product $S_2O_3^=$ was estimated by iodometric titrations of samples from the sealed vessel. The sampling flasks were initially filled with 10 cc of formaldehyde, 30 cc of distilled water, and 20 cc of acetate buffer with a pH of about 5. The purpose of the formaldehyde was to complex the HSO_3^- by the reaction,

$$CH_2O + NaHSO_3 \longrightarrow CH_2(OH)SO_3Na \qquad (3)$$

This reaction was allowed 20 minutes for completion. In the complexed form, the HSO_3^- was unaffected by I_3^- so that the concentration of $S_2O_3^=$ alone could be determined.

The HSO_3^- ion was analyzed by an iodometric oxidation in which the excess iodine was titrated with a standardized 0.01 normal $S_2O_3^=$ solution. The sampling flasks were initially filled with 50 cc of standardized 0.01 normal iodine solution and 25 cc of acetate buffer with a pH of about 5. The resulting sum of the concentrations of $S_2O_3^=$ and HSO_3^- allowed the concentration of HSO_3^- to be calculated by difference.

Hydrogen Ion Concentration

The pH of the reacting mixtures was measured with a standard Beckman Model G pH meter, which was connected to electrodes inserted into the reactor through standard-taper glass fittings. pH readings were taken approximately every 100 seconds. In this way, depending upon the duration of reaction, between

twenty and forty measurements of pH were obtained for each run.

With the buffered systems, the pH was measured only before and after reaction to insure that the hydrogen ion concentration had been held constant.

RESULTS

Unbuffered Reactions--General

The experimental data on the concentration of dithionite as a function of time for the unbuffered systems are presented in Tables 13-15 and Figures 19-21. The general trend of the curves as shown in the figures is in substantial agreement with Lynn's results. The decomposition began with an induction period in which the dithionite concentration decreased slowly. In most cases, this was followed by an abrupt and rapid decrease in the concentration.

In Table 13 and Figures 19a, b, c, which present experimental results of the decomposition at 60°C, it is noted that the total time of reaction was a function of initial dithionite concentration. Also, independently of the initial concentration, the curves show marked oscillations which have amplitude variations as high as ± 15%, with the average being closer to ± 5%.

The data at 70°C, which are plotted in Figure 20 and listed in Table 14, show a similar dependence of total time of reaction on initial concentration. The amplitude of the oscillations, however, is considerably less than at 60°C and varies as high as ± 6% with an average variation of ± 2%.

In Figure 21 and Table 15, the amplitude of the oscillations at 80°C is practically negligible. The maximum variation is only ± 1.5% with an average variation of less than ± 0.5%.

Variation of pH in Unbuffered Reactions

As stated under Apparatus and Procedure, the pH of unbuffered decompositions was measured continually during many of the tests. Typical plots of H^+ concentration vs time for 60 and 70°C are shown in Figures 22 and 23. The data for the plots are listed in Table 17. For comparison, the dithionite concentrations as a function of time are also plotted in the same figures. The curves show that the H^+ concentration varies almost as the mirror image of the dithionite concentration. Particularly interesting is the fact that the H^+ curves oscillate. There appears, however, to be no simple relationship in frequency or amplitude between the oscillations of the dithionite curves and the H^+ curves.

Buffered Reactions--General

The experimental data on the concentration of dithionite as a function of time for the buffered systems are presented in Table 16 and Figures 25a,b. With the exception of the results at a pH of 7.00, the curves for concentration vs time are practically the same as those obtained for the unbuffered systems. Again there is an induction period followed by a rapid decrease in dithionite concentration giving rise to curves which are convex. Also, the characteristic oscillations which were present in the unbuffered systems were found to exist for the buffered reactions. At a pH of 7.00, the concentration of dithionite decreased so slowly that the rapid decomposition period was not reached during the time in which

the reaction was studied. Significant oscillations were still present.

Effect of pH on Buffered Reactions

It was found experimentally that the induction time and likewise the total time of reaction decreased with increasing H^+ concentration. As presented in Table 19 and Figure 24 for the pH range of 4.80 to 6.00 and at an initial dithionite concentration of 11.0×10^{-3} molar, the time of the induction period was inversely proportional to the first power of the H^+ concentration, i.e.

$$\theta_I \propto \frac{1}{C_b} \qquad (4)$$

where θ_I is the time of the induction period and C_b is the concentration of H^+ in the buffered solution. At a pH lower than 4.5, the decomposition was very rapid and could not be studied with the analytical methods used.

Effect of Additives on the Buffered Reactions

The addition of HSO_3^-, $S_2O_3^=$, $SO_4^=$ and $SO_3^=$ had no measurable effect on the rate of dithionite decomposition. This is presented in Table 20 and Figures 27a,b in which the concentration of dithionite is plotted vs time at a pH of 7.00. On the plots are shown the concentrations of the additives and the time of their injection into the reactor.

The addition of air to the decomposition reaction at pH of 7.00 also had no measurable effect on the rate. This is

shown on Figure 27a.

In Table 21 and Figures 28a,b are presented the results of two identical experiments. As stated under Experimental Procedure, for each experiment three successive decomposition reactions were conducted wherein the reactor contents consisted of the products of the previous tests. The figures show the dithionite concentration as a function of time. The rate of reaction showed a marked increase in each successive test, and this indicated that a product, probably sulfur, catalyzed the decomposition. It is interesting to note that the curves for the two experiments are almost identical even with respect to the oscillations.

Product Analysis

The end-products of the thermal decomposition reaction were found to consist mainly of thiosulfate and bisulfite in an approximate molar ratio of 1 to 2, respectively. A typical analysis is listed in Table 22 for an experiment at 30°C. From a knowledge of the initial dithionite concentration, a sulfur material balance indicated that other products such as free sulfur were present but in low concentrations. The analysis listed in Table 22 does not represent the only product distribution to be expected in every dithionite decomposition experiment. The relative amount of sulfur in the products apparently depends on conditions of acidity, temperature and catalysis.

Appearance of Sulfur in Buffered and Unbuffered Reactions

The formation of sulfur as one of the products of dithionite decomposition was not measured quantitatively in this investigation. Its formation, however, was definitely established by visual inspection. As the reaction proceeded toward completion it was found that the reactor contents acquired a slight milky appearance which sometimes disappeared and reformed several times before the end of the induction period. At the onset of the rapid decrease in dithionite concentration, the milky appearance reached a maximum opacity. This phenomenon was considered to be the formation of solid particles of sulfur which either coalesced to form colorless macromolecules or reacted with other species in the solution. The appearance of sulfur was found in both unbuffered and buffered reactions at a pH less than or equal to 7.0. At a pH greater than 7.0, no sulfur was found by visual inspection.

Order of Reaction with Respect to the Concentration of Dithionite for the Induction Period

The dependence of the rate during the induction period upon the concentration of dithionite was obtained from the results of the unbuffered systems. For each temperature, the initial rates were plotted vs the initial concentrations on logarithmic paper and the slope of the best line through the points gave the order of the reaction with respect to dithionite. This calculation was based on the rate expression,

$$-\frac{d[S_2O_4^{=}]_o}{d\theta} = k[S_2O_4^{=}]_o^n \qquad (5)$$

and the results are presented in Table 23 and Figure 29. A value of n = 1.5 ± 0.2 was obtained for the order of reaction with respect to dithionite. The use of Equation 5 assumes that the initial rate is a function only of the initial concentration of dithionite. This would be correct if all other independent variables such as temperature and the concentrations of other reactants were held constant. All of the experiments were performed under conditions of constant temperature. Most of the experiments were performed in unbuffered systems in which the H^+ was not controlled. Measurements of the H^+ concentration were taken, however, and since it was found that the initial H^+ concentration did not vary by more than a factor of 2, the error introduced by using Equation 5 was not significant. This conclusion was in agreement with the results of tests in buffered solutions, which were designed primarily to determine the order of reaction with respect to H^+. Thus at a pH of 5.00 and at a temperature of 60°C, decomposition experiments were conducted for several initial concentrations of dithionite. The order of reaction with respect to dithionite was obtained in the same way as noted above and was found to be 1.6. These results are presented in Table 24 and Figure 30.

Order of Reaction with Respect to the Concentration of H^+ for the Induction Period

The dependence of the rate during the induction period upon the concentration of H^+ was obtained from the buffered reactions. The initial rate was determined at each value of pH for the same initial concentration of dithionite (11.0×10^{-3} molar).

The rate of dithionite decomposition was found to increase in proportion to the square root of the H^+ concentration. These results are presented in Table 19 and Figure 31. The fact that the rate of reaction varied as the square root of the H^+ concentration explains why the initial rate of dithionite decomposition in unbuffered systems was reasonably insensitive to a twofold variation in H^+ concentration.

Rate Expression for the Induction Period

The 3/2 order dependence of rate upon the concentration of dithionite and the 1/2 order dependence upon the concentration of H^+ were combined to give a rate expression for the induction period. The relationship is given as follows:

$$r_{induction} = k_c[S_2O_4^{=}]^{3/2}[H^+]^{1/2} \qquad (6)$$

for which the values of k_c as a function of temperature are given in Table 25. The temperature dependence of k_c is given by the Arrhenius equation, $k = Ae^{-\Delta E/RT}$ in which the value of ΔE and A were obtained from a plot of log k_c vs 1/T given

in Figure 32. Therefore, the equation for k_c is:

$$k_c = 1.3 \times 10^8 \, e^{-\frac{12,000}{RT}} \quad (\text{moles/liter})^{-1}\text{sec}^{-1} \qquad (7)$$

It is important to note here that since the thermal decomposition of dithionite was complicated by the oscillatory nature of the reaction, there was considerable uncertainty both in the initial concentration of dithionite and in the initial reaction velocity. Since the order of reaction is contingent upon these parameters the established order of reaction with respect to both the H^+ and $S_2O_4^=$ is an approximation which is good to only $\pm$ 15%.

Rate Expression for the Decay Period

The convex nature of the concentration-time relationship for dithionite and the apparent catalytic effect of sulfur suggested that either an autocatalytic or degenerate branching chain process might be occurring. Both of these processes can be described by an exponential relationship between rate and time (37). A brief discussion of the application of these theories to the present data is given under DISCUSSION OF RESULTS AND CONCLUSIONS.

From the exponential law that

$$-\frac{dC}{d\Theta} = Ae^{B\Theta} \qquad (8)$$

the algebraic relationship between the concentration of di-

thionite C and time θ is found by integration to be

$$C_o - C = \frac{A}{B}(e^{B\theta} - 1) \qquad (9)$$

For degenerate, branching-chain reactions the term $(e^{B\theta} - 1)$ can be approximated by $e^{B\theta}$ since this term becomes very large after branching begins. Hence, with the above simplification, the logarithm of Equation 9 gives

$$\log(C_o - C) = \log \frac{A}{B} + \frac{B}{2.303}\theta \; . \qquad (9a)$$

By plotting $(C_o - C)$ vs θ on a semi-logarithmic scale, series of straight lines for the decay period were obtained for the data at 60, 70 and 80°C. The plots are presented in Table 26 and Figures 33-35; and as shown, the curves were non-linear for the induction period as would be expected. Also, the non-linearity near the end of reaction was not surprising since in this region the accuracy of analysis was a limiting factor. The fact that the lines at a given temperature are not parallel and do not have a common intercept, by extrapolation, indicates that both constants A and B are a function of initial dithionite concentration. The observed increase in slope with increase in temperature shows that B is also a function of temperature. Inspection of the curves indicates that these functional relationships are complex.

DISCUSSION OF RESULTS AND CONCLUSIONS

Oscillations in Dithionite Concentration vs Time Curves

Lynn (8) was unable to explain the oscillations which occurred during the decomposition of dithionite. The present experimental investigation of the thermal decomposition was undertaken primarily to determine the validity of these oscillations. No amount of care in removing sources of error or contamination succeeded in eliminating them. It may be pointed out that reproducibility of the oscillations was not in general obtained in the unbuffered systems (See Figures 19a,b). Oscillation reproducibility was, however, found to be more prevalent among the buffered systems than in the unbuffered systems. An example of this reproducibility is presented in Table 21 and Figures 28a,b for a pH of 5.00.

The amplitude of the oscillations was in many experiments too large to be explained solely on the basis of experimental error. The magnitude of these errors is discussed briefly as follows:

1. The calibrated syringe which was used to remove samples from the reactor had a capacity of 2 cc and was found to give reproducibility with a precision of $\pm$ 0.2%.
2. Further reaction of the sample after injection into a sample flask at 25°C was considered negligible since the flask contained 0.1 molar NaOH under a

nitrogen atmosphere. Furthermore, the sample experienced a 70 to 1 dilution. Titrations at 5°C did not affect the oscillations. Simultaneous samples which were titrated at different times, one immediately and one approximately 10 min later, did not show any measurable differences. Therefore, errors introduced by further reaction in the sample flasks were considered to be less than the titration error.

3. The concentrations of methylene blue solutions were selected to give differences in burette readings up to 40 cc for each dithionite sample titrated. The color of methylene blue is so intense that a drop of 0.0001 molar solution gives a clearly discernible blue color in 150 ml of water. For all the titrations in the present investigation, however, methylene blue with a concentration of about 0.001 molar was used. Rapid titrations could be carried out to $\pm$ 0.05 cc or an average error of $\pm$ 0.5%.

4. The ultimate products of the decomposition, $NaHSO_3$, $Na_2S_2O_3$, and varying amounts of sulfur did not reduce methylene blue under the conditions described in the experimental procedure. In fact, concentrations of $S_2O_3^{=}$, $SO_3^{=}$ and $S^{=}$ in quantities greater than one hundred times the concentration of $S_2O_4^{=}$ did not interfere. Lynn (8) stated that a very accurate but time-consuming chromate test for $S_2O_4^{=}$ gave results that compared closely with the methylene blue approach.

5. Perhaps the most unpredictable source of error was contamination by oxygen. In spite of the many precautions, this possibility cannot be ruled out, and it would be expected to cause errors in a completely random way. As described previously, however, there was some degree of reproducibility in the oscillations under certain conditions. Hence if the oscillations were caused entirely by oxygen contamination, it would be difficult to explain their semi-reproducibility. Also as stated previously, small amounts of air appeared to have no measurable effects on the systems buffered at a pH of 7.00. Yet these systems displayed oscillations in the curves of dithionite concentration vs time. Another argument opposed to oxygen contamination as the sole cause of the oscillations is the fact that the amplitude of the oscillations decreased with increase in temperature, as shown in Figures 19-21. This result is the converse of what would be expected on the basis of oxygen effects.

Therefore, excluding the small random error of oxygen contamination, the overall error in the analysis for $S_2O_4^{=}$ was $\pm$ 1%. This value is on the average much lower than the per cent changes in concentration of $S_2O_4^{=}$ as a result of the oscillations.

Several other factors related to the oscillation problem should be mentioned here. Significantly, there were no oscillations in the air-oxidation experiments. Yet the same method

of analysis for dithionite was used with both systems. Secondly, the H^+ concentrations of unbuffered systems not shown here, but similar in all respects to the H^+ concentration shown in Figure 22, were analyzed by use of pH electrodes without disturbing the system through removal of samples. Still, oscillations were present in the H^+ concentration as a function of time.

The above arguments would rule out experimental errors and oxygen contamination as the only cause of the oscillations. The fact that oscillations were semi-reproducible under certain conditions suggests that a series of reactions involving unstable intermediates of reducing potential comparable to dithionite was responsible for this unusual phenomenon.

Effect of Oxygen on the Thermal Decomposition of Dithionite

In the unbuffered decomposition of dithionite, the addition of small volumes of air (2 - 5 cc) during the reaction caused erratic changes in the concentration of dithionite. Several such additions of air usually shortened the induction period of the decomposition. This effect of the oxygen was apparently related to the effect of hydrogen ion concentration because in the buffered decomposition of dithionite at a pH of 7.00, erratic changes in concentration by addition of acid did not appear. It is likely that in both cases the oxygen reacted with species in solution such as SO_2^- or HSO_3^- by a chain mechanism to form anions of greater acidity. The increase of hydrogen ion had an imperceptible effect on the buffered

system, but in the unbuffered system increased the H^+ concentration. Indeed, the marked decrease in pH is illustrated by Figure 24, in which the concentration of H^+ vs time is shown for the decomposition of dithionite after several additions of air. That small amounts of oxygen caused relatively large changes in the H^+ ion concentrations suggests a chain or catalytic reaction which is inhibited in solutions of pH 7 or greater. Others (15,37,38) have found, for example, that HSO_3^- ion, which is present in the products of dithionite decomposition, reacts with O_2 by a chain mechanism in which oxygen is one of the chain initiators.

Catalytic Effects of Additives

The results of the present investigation show that the anions $SO_3^=$, $SO_4^=$, HSO_3^-, and $S_2O_3^=$ have no catalytic effect on the thermal decomposition of dithionite under conditions of controlled pH. These results are in disagreement with Lynn's work. He found that both HSO_3^- and $S_2O_3^=$ catalyzed the decomposition, but his investigations were conducted without careful control of the H^+ concentration.

In agreement with Lynn, it was found that sulfur does catalyze the decomposition by shortening the induction period in either buffered or unbuffered solutions. A discussion of the mechanism of the catalysis is presented below under The Decay Period.

Sensitivity of Reaction to H^+

The thermal decomposition of dithionite was found to be very sensitive to changes in H^+ concentration. At a pH greater than 7 the rate of decomposition was very low. In highly alkaline solutions from which air was rigorously excluded, reaction times were observed to be of the order of several hundred hours. At a pH lower than 4.8 the rate of decomposition was extremely rapid and could not be studied by the methods used in this work. In fact, at a pH of 4.0 the acidity was high enough for detectable concentrations of H_2S to be observed in the gas phase above the reacted mixture. H_2S formation would be expected from the acid decomposition of thiosulfate, which is a product of the dithionite decomposition reaction. The fact that H^+ also has a large effect on the decomposition of thiosulfate has been carefully studied by La Mer (40). A mechanism given by Davis (41) explains the experimental results of La Mer. His proposed mechanism consists of a series of nucleophilic substitution reactions between protonated anions. Briefly, this mechanism is as follows:

$$S_2O_3^{=} + H^+ \rightleftharpoons HS_2O_3^-$$

$$HS_2O_3^- + S_2O_3^{=} \rightleftharpoons HS_3O_3^- + SO_3^{=} \qquad (10)$$

(etc. until molecule contains 9 sulfur atoms)

$$HS_9O_3^- \rightleftharpoons S_8 + HSO_3^-$$

With increasing acidity, the products of the individual reactions in the above mechanism can produce sulfur having less than eight atoms per molecule, i.e.

$$HS_3O_3^- \xrightleftharpoons{H^+} S_2 + HSO_3^- \qquad (11)$$

This could possibly explain the various forms of sulfur that probably exist during the decomposition of dithionite.

Similarity of $S_2O_3^=$ and $S_2O_4^=$ Decomposition

It is interesting to note that the rate of S_8 formation during the initial decomposition of thiosulfate was found by LaMer (40) to follow the rate expression:

$$\frac{dS_8}{d\theta} = k[H^+]^{1/2}[S_2O_3^=]^{3/2} \qquad (12)$$

This expression is the same type found for the initial rate of dithionite disappearance with the exception that $S_2O_3^=$ is replaced by $S_2O_4^=$. The fact that addition of thiosulfate has been shown to have no effect on dithionite decomposition in buffered systems excludes the possibility, on mass action principles, that $S_2O_4^=$ is in equilibrium with $S_2O_3^=$, whose decomposition is the rate controlling factor as described by the equation above. Moreover, a dithionite decomposition mechanism parallel to the thiosulfate decomposition mechanism proposed by Davis seems unlikely since no sulfate is found in

the reaction products. One must conclude, therefore, on the basis of information gathered to date, that the similarity in rate expressions is fortuitous.

Mechanism of the Induction Period

In the past, dithionite has been postulated to dissociate into $SO_2^{=} + SO_2$ (6), $SO + SO_3^{=}$ (42), and $SO^{-} + SO_3^{-}$ (39) by various investigators attempting to explain the thermal decomposition and solution reactions of dithionite. There has been no experimental confirmation of any of these dissociation reactions, or of the presence of these intermediates in dithionite solutions, reported to date. Moreover, unsymmetrical dissociation reactions of the types suggested do not lead in a straightforward way to the observed 3/2 order of the reaction with respect to dithionite.

The reality of the symmetrical dissociation of dithionite into SO_2^{-} radical-ions has been confirmed by air oxidation kinetics, EPR spectra, and polarographic studies. The observed sensitivity of the thermal decomposition reaction to changes in hydrogen-ion concentration suggests that protonated forms of the ions SO_2^{-} or $S_2O_4^{=}$ are involved in the rate-determining step. Two alternative mechanisms are suggested for the rate-determining step:

$$HS_2O_4^{-} + SO_2^{-} \longrightarrow HSO_3 + S_2O_3^{=}$$

and (13)

$$S_2O_4^{=} + HSO_2 \longrightarrow HSO_3 + S_2O_3^{=}$$

Either mechanism would be followed by the faster reactions:

$$HSO_3 + HSO_2 \longrightarrow HSO_3^- + SO_2 + H^+ \qquad (14)$$

$$SO_2 + H_2O \longrightarrow HSO_3^- + H^+ \qquad (15)$$

If one makes the assumption that HSO_2 is a much weaker acid than $HS_2O_4^-$, for which Jellinek (4) established an ionization constant of 3.25×10^{-3} at 25°C by conductance measurements, then most of the experimental facts about the decomposition reaction can be explained in terms of either or both the above mechanisms. The observed rate of reaction would be 3/2 order with respect to dithionite concentration. In the pH interval 5 to 6.5 the reaction would appear 1/2 order with respect to hydrogen ion. Below pH 4.5 the rate of reaction would be extremely rapid, indicating greater than 1/2-order dependence. In neutral or alkaline solutions the rate of decomposition would be extremely low and would appear insensitive to changes in hydrogen ion concentration. The only products of the primary decomposition reaction would be sulfite and thiosulfate, and in the observed stoichiometric ratio. Finally, the acidity of the reaction medium would increase during the reaction because of the ionization of the sulfurous acid formed.

It is impossible, on the basis of established experimental facts, to distinguish between the alternative mechanisms sug-

gested. Unfortunately the positive salt effect reported by Lynn is not sufficiently well documented by facts, and this evidence cannot be used in favor of the first mechanism suggested. Both mechanisms are incomplete to the extent that periodic increases in dithionite concentration with time cannot be explained. Therefore, these mechanisms are offered merely as suggestions.

The Decay Period

The concentration vs time curves shown in Figures 19-21 for the unbuffered systems and in Figures 25a,b for the buffered systems suggest that chain reactions are involved and, in particular, the degenerate branching type. According to theory (37), during the induction period, only a primary chain exists. As the chain progresses, it generates a stable intermediate which later reacts to form new active centers. These centers cause branching of the primary chain; or if it has already disappeared as is often the case, the active centers form new primary chains with branching. It is often difficult to distinguish between degenerate branching chain reactions and autocatalyzed reactions in which the catalyst is formed during the progress of reaction. Although in the case of the degenerate chain reactions the induction period always exists, there may or may not be an induction period in autocatalysis. In both cases, following the induction period, there is usually a rapid decrease in the concentration of the primary reactant resulting in a convex curvature of the

concentration vs time function. Attempts to resolve the problem as to which type of reaction, if either, occurred during the dithionite decomposition were not too successful. Some discussion of the experimental results from the point of view of these theories is presented here.

Sulfur, either as a polymer S_8 or as a colloid $(S_8)_x$ was the only species under conditions of controlled pH, temperature, and initial dithionite concentration, that caused a decrease in the time of the induction period and hence the time of the overall reaction. This effect might be explained by several possible mechanisms:

1. Polymeric sulfur which is formed as a product may combine with one of its predecessor ions to form a reactive complex. After a series of decomposition steps, the sulfur is regenerated. An example of this type of chain-branching intermediate is $S_x \cdot SO_3^{=}$ or $S_x \cdot S_2O_3^{=}$.
2. Colloidal or polymeric sulfur may act autocatalytically as an adsorption catalyst which accelerates the rate-determining step of the thermal decomposition reaction.
3. The several forms of sulfur that might exist in the solution could each have a specific effect on the reaction rate. Thus in the form of a monomer, the sulfur could suppress the equilibrium step in which it is formed, i.e. $HS_2O_3^- \overset{H^+}{\rightleftharpoons} S + HSO_3^-$. Eventually,

the monomer may polymerize to S_8 and then to colloidal sulfur. These higher aggregates can adsorb the monomer sulfur and thus accelerate the overall decomposition autocatalytically.

Conclusions

The thermal decomposition of sodium dithionite solutions in buffered and unbuffered media in the pH range of 4.0 to 7.0 was observed to consist of an induction period in which the decomposition was slow, followed by a decay period, in which the concentration of dithionite rapidly decreased to zero. Apparent periodic increases and decreases in dithionite concentration during the induction period were observed and could not be explained solely on the basis of experimental error. One possible explanation of this unusual phenomenon is the formation of unstable intermediate(s) possessing reducing potentials comparable to dithionite with respect to methylene blue. The amplitude of the apparent oscillations in dithionite concentration decreased with increasing temperature, suggesting that the concentration of the hypothetical reactive intermediate(s) likewise decreased with increasing temperature. Absence of oscillations in solutions of pH greater than 7 suggests that the hypothetical intermediate(s) either are not formed or are unstable in alkaline solution.

During the induction period, the reaction was observed to be 1/2 order with respect to H^+ and 3/2 order with respect to dithionite, giving a rate expression of the following form:

$$r_{induction} = k_c[H^+]^{1/2}[S_2O_4^{=}]^{3/2} \qquad (6)$$

The variation of k_c with temperature gives a straight line on an Arrhenius equation plot. The activation energy ΔE was found to be 12 kcal/mole and the frequency factor A was found to be 1.3×10^8 $(moles/liter)^{-1}sec^{-1}$.

The anions $SO_3^{=}$, HSO_3^{-}, $SO_4^{=}$, and $S_2O_3^{=}$ had no specific effects in the buffered systems. Colloidal sulfur catalyzed the reaction by decreasing the length of the induction period.

The rapid increase in the rate of dithionite decomposition during the decay period followed an exponential relationship with time. This fact together with the catalysis by colloidal sulfur suggests that an autocatalytic or a degenerate branching chain mechanism is occurring.

REFERENCES

1. Schonbein, J. prakt. Chem., 61, 193 (1852).
2. Schutzenberger, P., Compt. Rend., 69, 196 (1869).
3. Jellinek, K., Zeit. Anorg. Chem., 70, 93 (1911).
4. Jellinek, K., Zeit. physik. Chem., 76, 257 (1911).
5. Meyer, J., Zeit. Anorg. Chem., 34, 43 (1903).
6. Bassett, H., and Durrant, R. G., J. Chem. Soc., 2, 1401 (1927).
7. Nicloux, M., Compt. Rend., 196, 616 (1933).
8. Lynn, S., Ph.D. Thesis, Calif. Inst. (1954).
9. Welcher, F. J., "Organic Analytical Reagents," D. Van Nostrand Co., New York (1948).
10. Kolthoff, I. M., and Cohn, G., J. Biol. Chem., 148, 711 (1943).
11. Rosin, J., "Reagent Chemicals," D. Van Nostrand, New York (1937).
12. Fritz, J. S., and Freland, M. Q., Anal. Chem., 26, 1593 (1954).
13. Swift, E., "Systematic Quantitative Analysis," Prentice-Hall, New York (1939).
14. Lange, N. A., "Handbook of Chemistry," 7th ed., Handbook Publishers, Inc., Sandusky, Ohio (1949).
15. Alyea, H. N., and Backstrom, H. L. J., J. Am. Chem. Soc., 51, 90 (1929).
16. Yost, D. M., and Russell, H., "Systematic Inorganic Chemistry," Prentice-Hall, Inc., New York (1944).
17. Rao, M. R. A., and Patel, C. C., Proc. Nat. Inst. Sc. India, 19, 211 (1953).
18. Uri, N., Chem. Revs., 50, 375 (1952).
19. Frost, A. A., and Pearson, R. G., "Kinetics and Mechanism," Wiley, New York (1953).

20. Klemm, L., Zeit. Anorg. Chem., 231, 136 (1937).

21. Van der Heijde, H. B., Rec. Trav. Chim. Pays-Bas, 72, 95 (1953).

22. Dunitz, J. D., Acta Chryst., 9, 579 (1956).

23. Pauling, L., J. Am. Chem. Soc., 69, 542 (1947).

24. Hodgson, W. G., Neaves, A., and Parker, C. A., Nature, 178, 489 (1956).

25. Yarmolinsky, M. B., and Colowick, S. P., Biochim. Biophys. Acta, 20, 177 (1956).

26. Karrer, P., and Benz, F., Helv. Chem. Acta, 19, 1028 (1936).

27. Schlenk, F., Hellström, H., and von Euler, H., Ber. 71, 1471 (1938).

28. Kosower, E. M., personal communication.

29. Jellinek, K., Zeit. Elektrochem., 17, 157 (1911).

30. Jellinek, K., Zeit. Elektrochem., 17, 245 (1911).

31. Gossman, B., Coll. Czech. Chem. Commun., 2, 185 (1930).

32. Kolthoff, I. M., and Miller, C. S., J. Am. Chem. Soc., 63, 2818 (1941).

33. Munemori, M., Talenta, 1, 110 (1958).

34. Cermak, V., Chemicke Zvesti, 8, 714 (1954).

35. Cermak, V., Coll. Czech. Chem. Commun, 23, 1471 (1958).

36. Jellinek, K., and Jellinek, E., Zeit. physik Chem., 93, 325 (1919).

37. Semenoff, N., "Chemical Kinetics and Chain Reactions," Oxford Clarendon Press (1935).

38. Haber, and Franck, Naturw., 19, 450 (1931).

39. Fujinawa, K., J. of Ind. Chem., Japan, 54, 160 (1951).

40. Dinegar, R. H., Smellie, R. H., and La Mer, V. K., J. Am. Chem. Soc., 73, 2050 (1951).

41. Davis, R. E., J. Am. Chem. Soc., 80, 3565 (1958).

42. Von Deines, O., and Elstner, G., Zeit. Anorg. Allgem. Chem., 191, 340 (1930).

LIST OF FIGURES

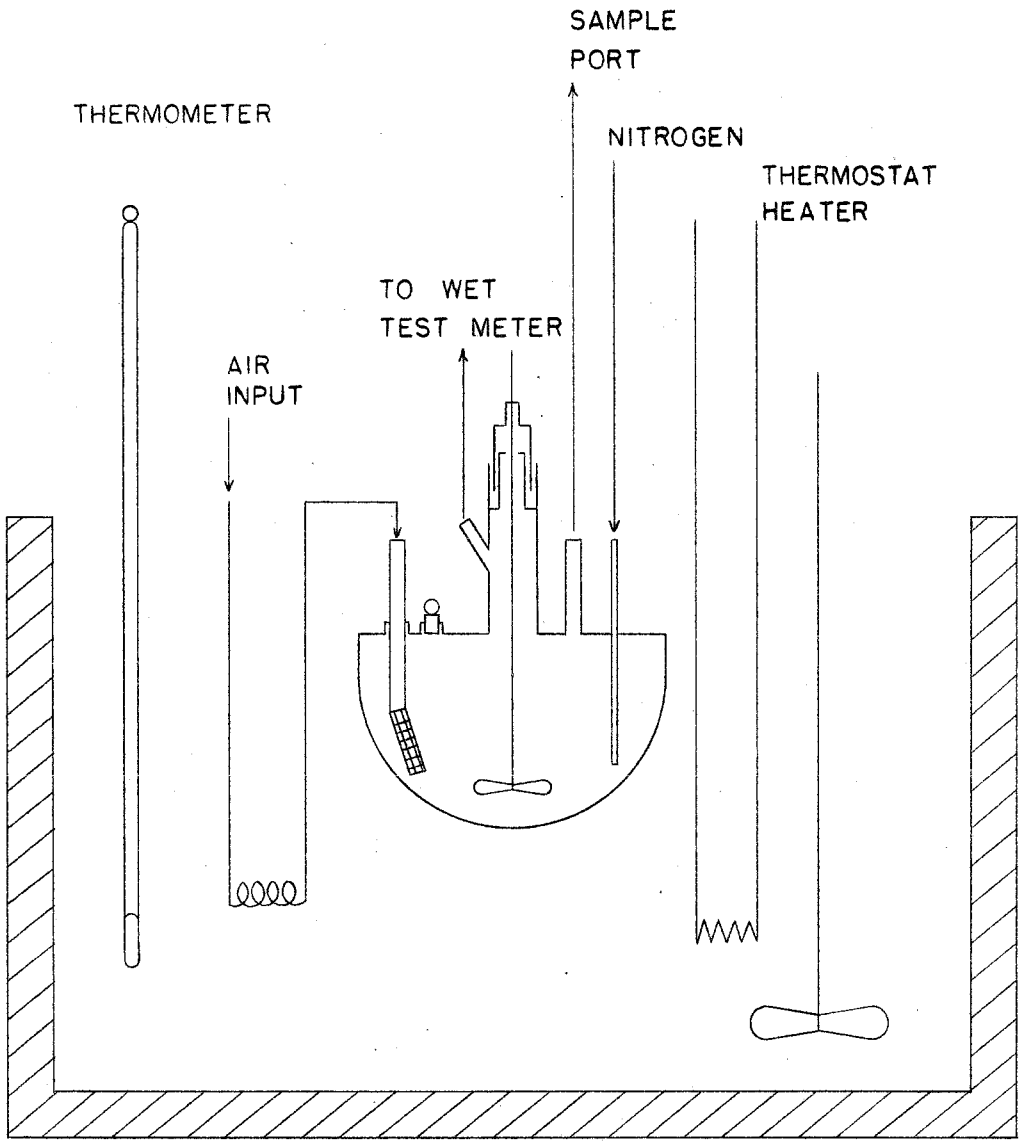

Figure 1--Diagram of Apparatus

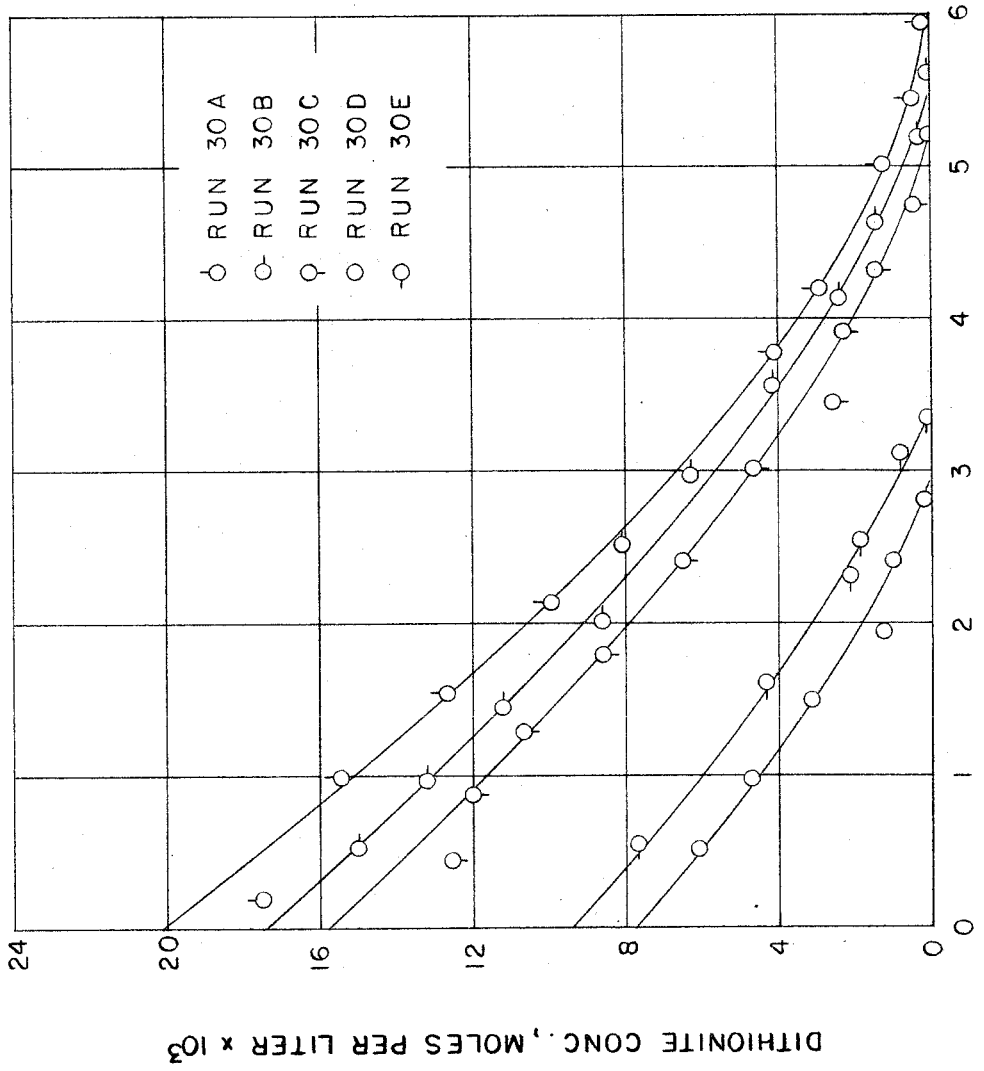

Figure 2--Air Oxidation Studies. Dithionite Concentration vs Time at 30°C

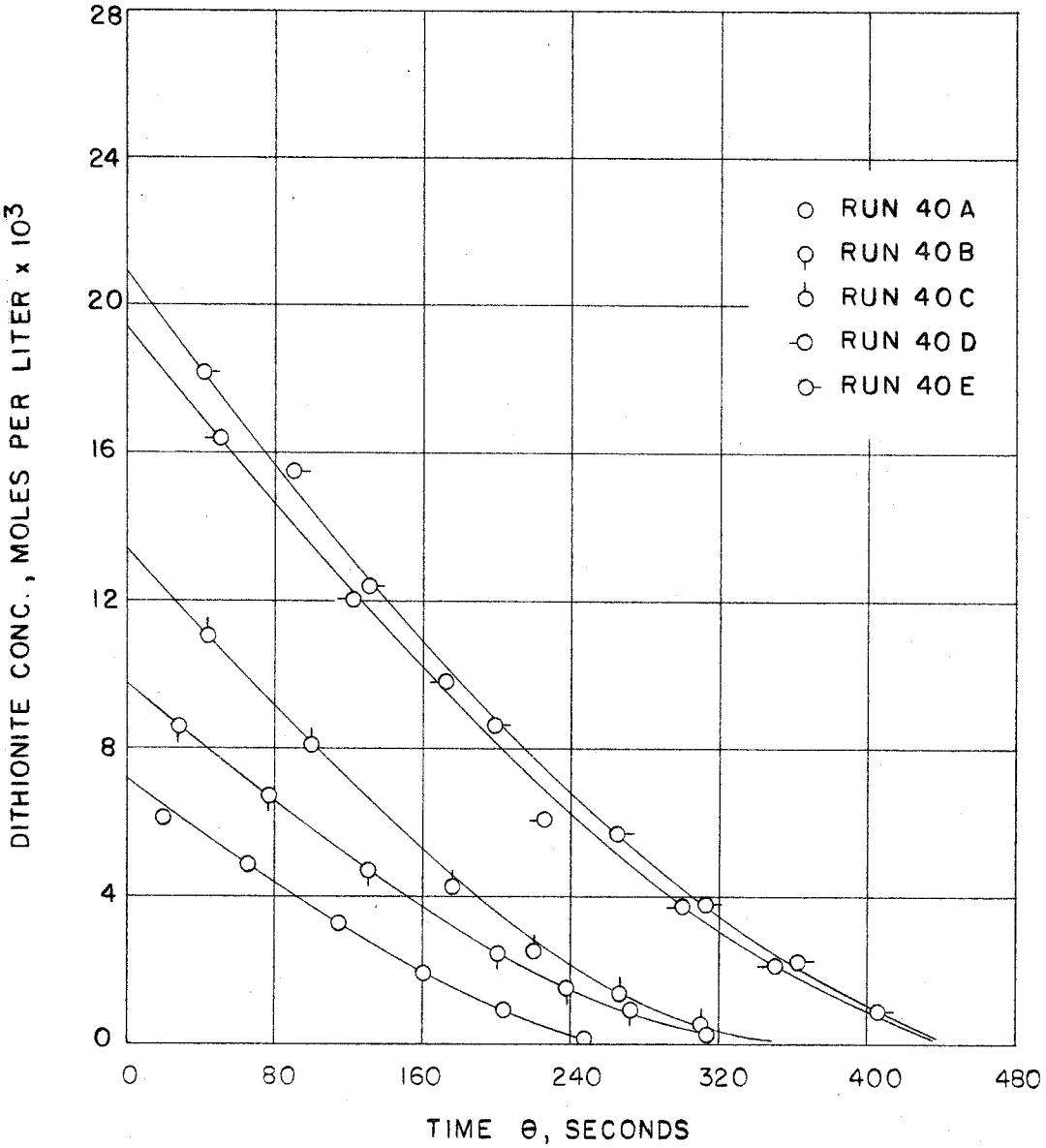

Figure 3--Air Oxidation Studies. Dithionite Concentration vs Time at 40°C

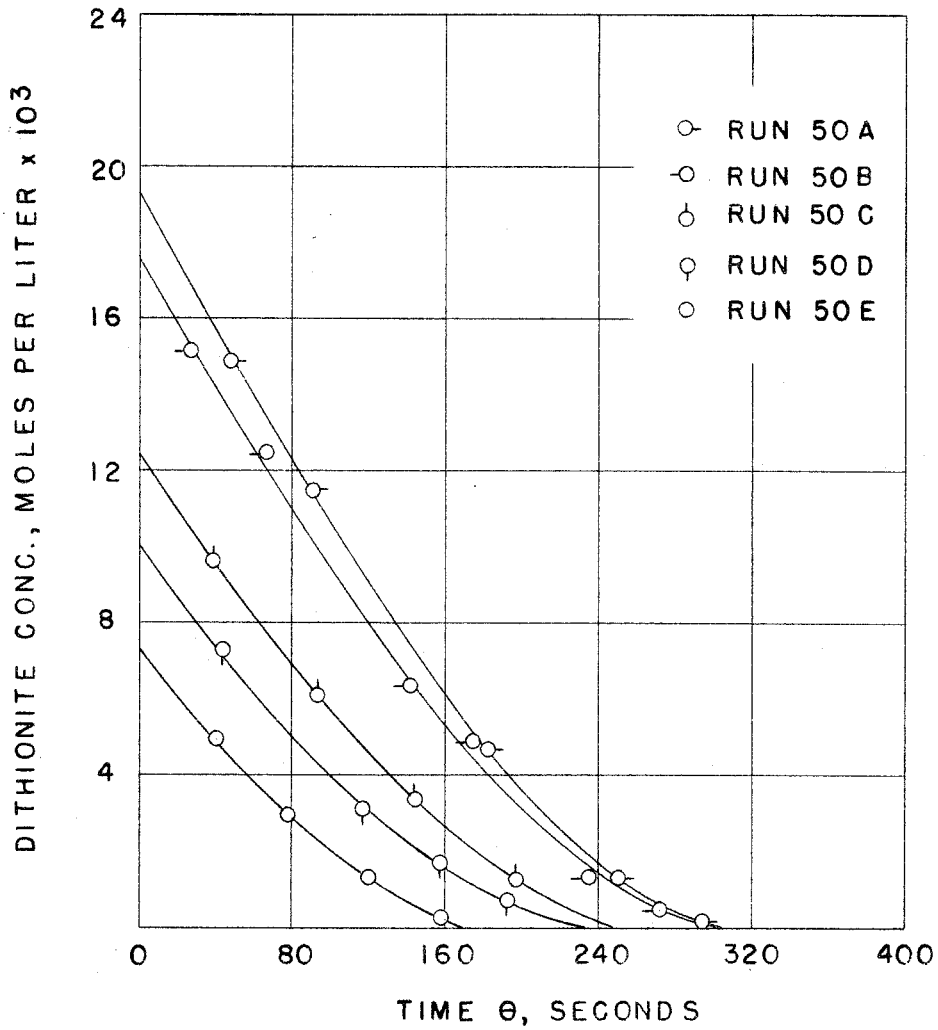

Figure 4--Air Oxidation Studies. Dithionite Concentration vs Time at 50°C

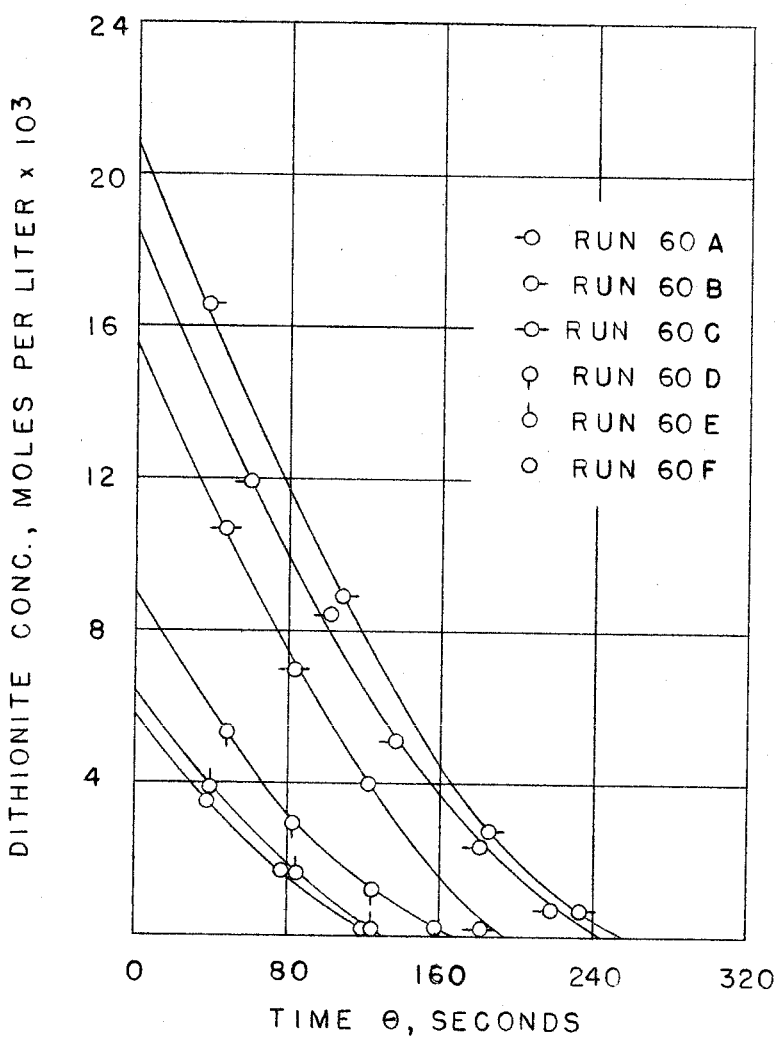

Figure 5--Air Oxidation Studies. Dithionite Concentration vs Time at 60°C

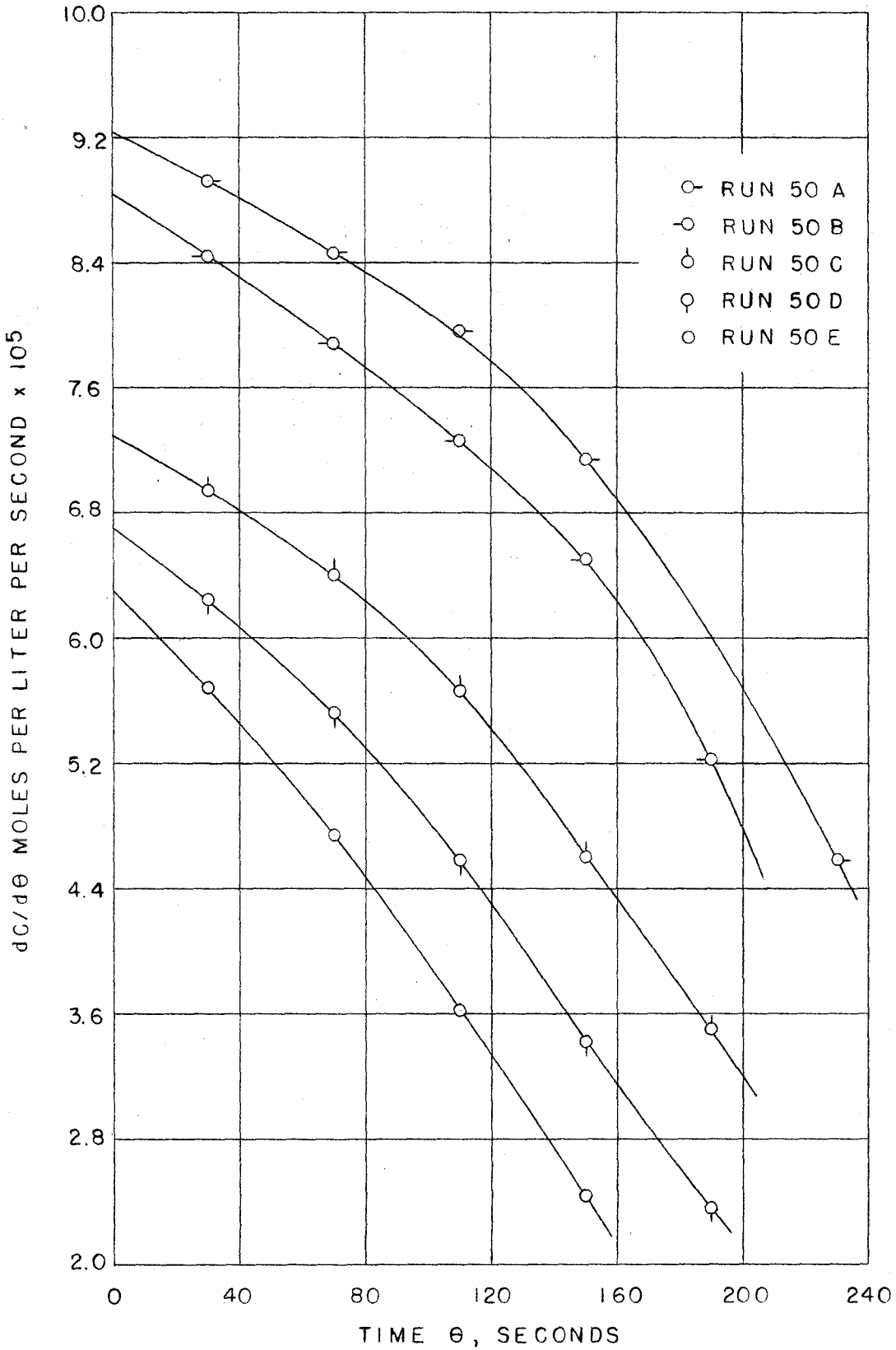

Figure 6--Air Oxidation Studies. Determination of Initial Rates. ($dC/d\theta$) vs Time at 50°C

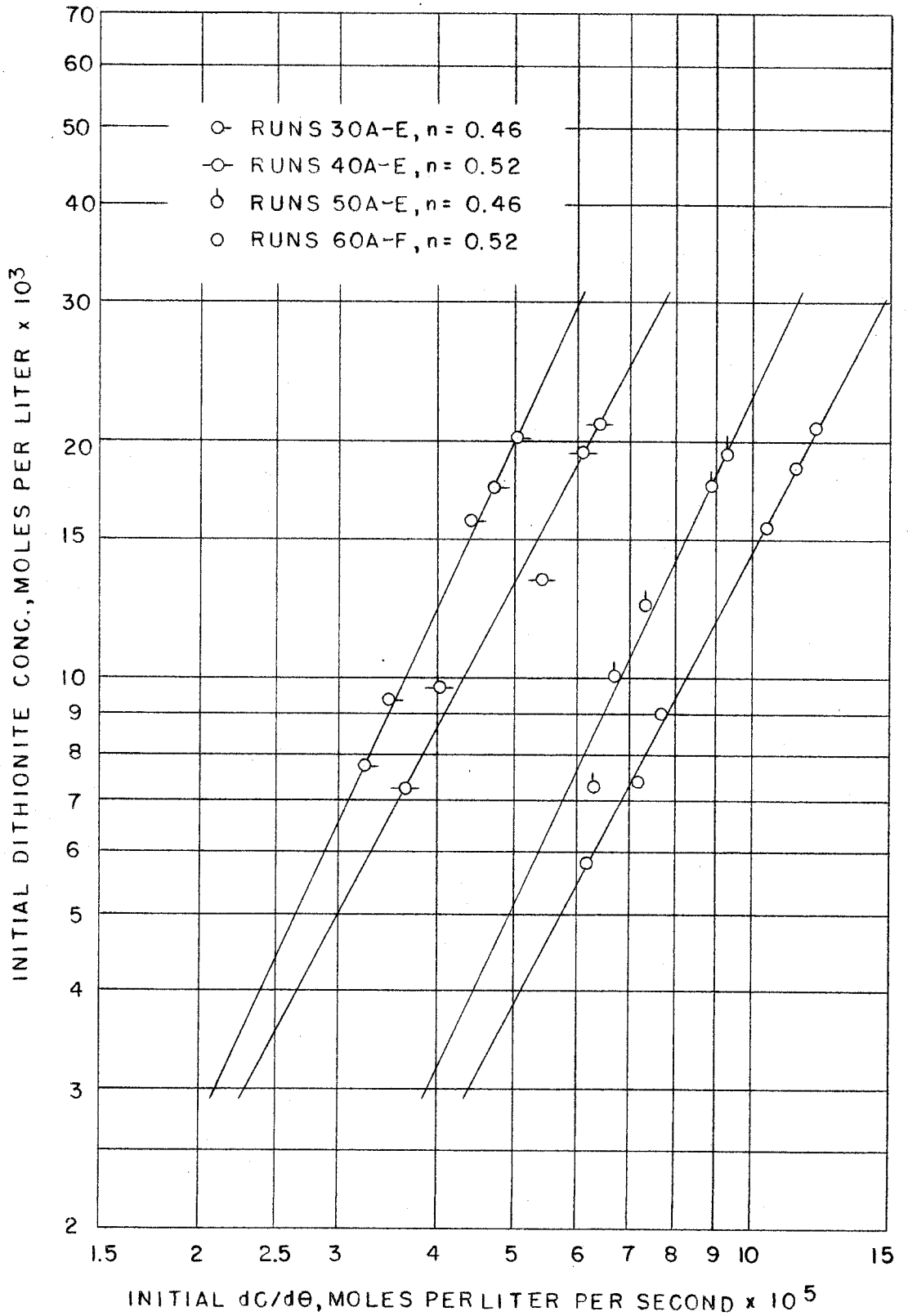

Figure 7--Air Oxidation Studies. Determination of n. Log $(dC/d\theta)_o$ vs Log C_o at 30, 40, 50, and 60°C

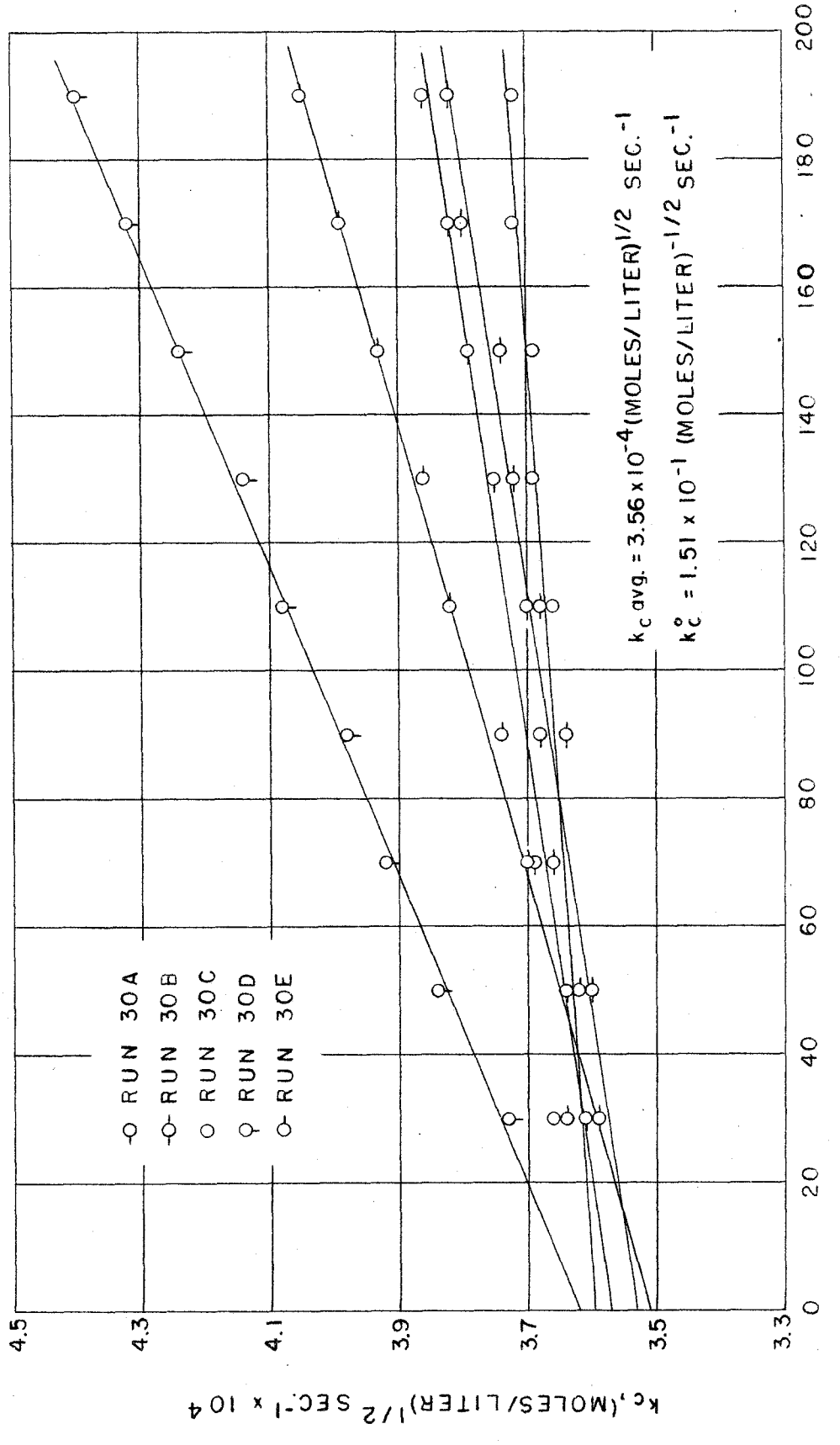

Figure 8--Air Oxidation Studies. Determination of k_c°. k_c vs Time at 30°C

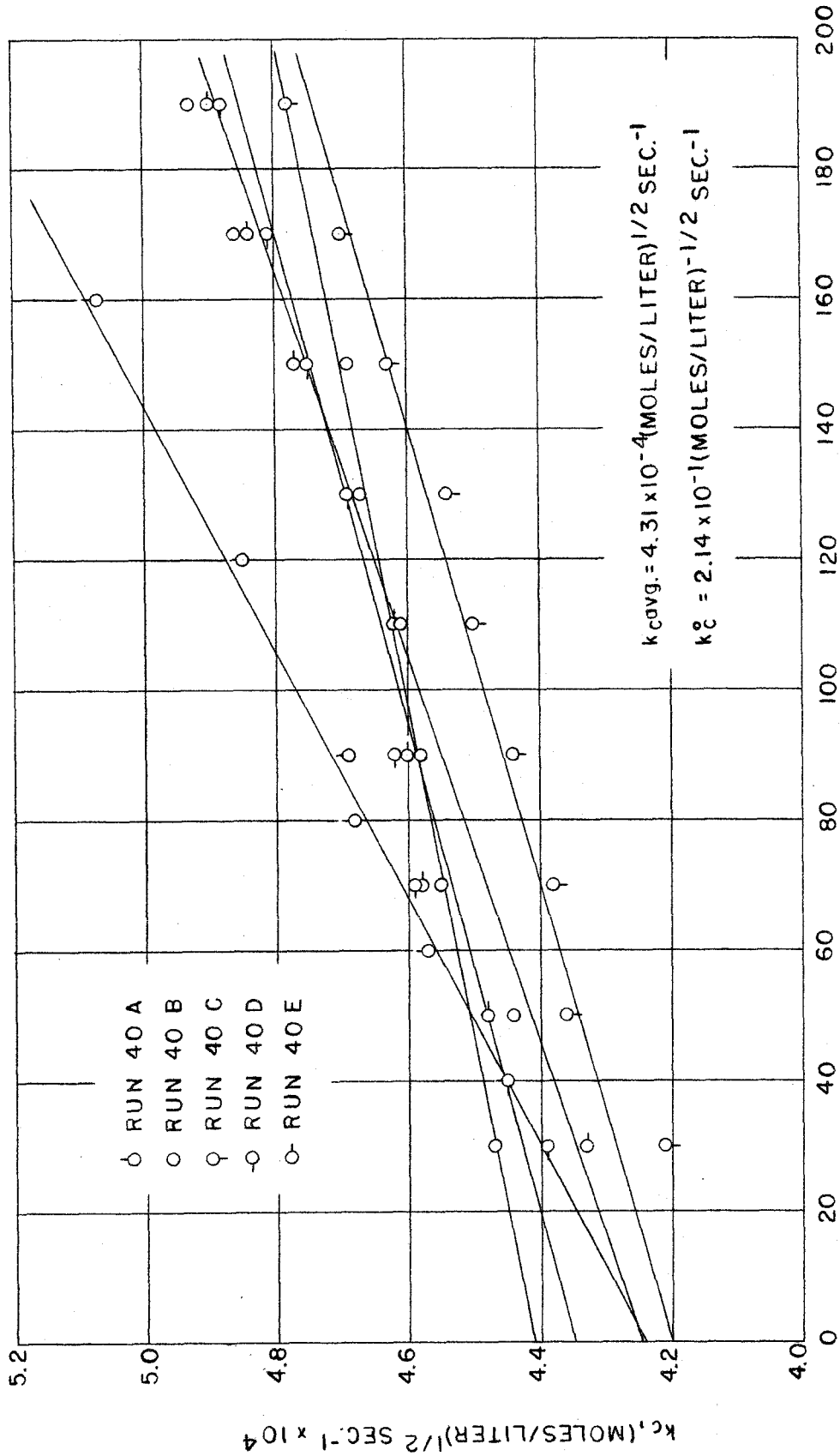

Figure 9--Air Oxidation Studies. Determination of k_c^o. k_c vs Time at 40°C

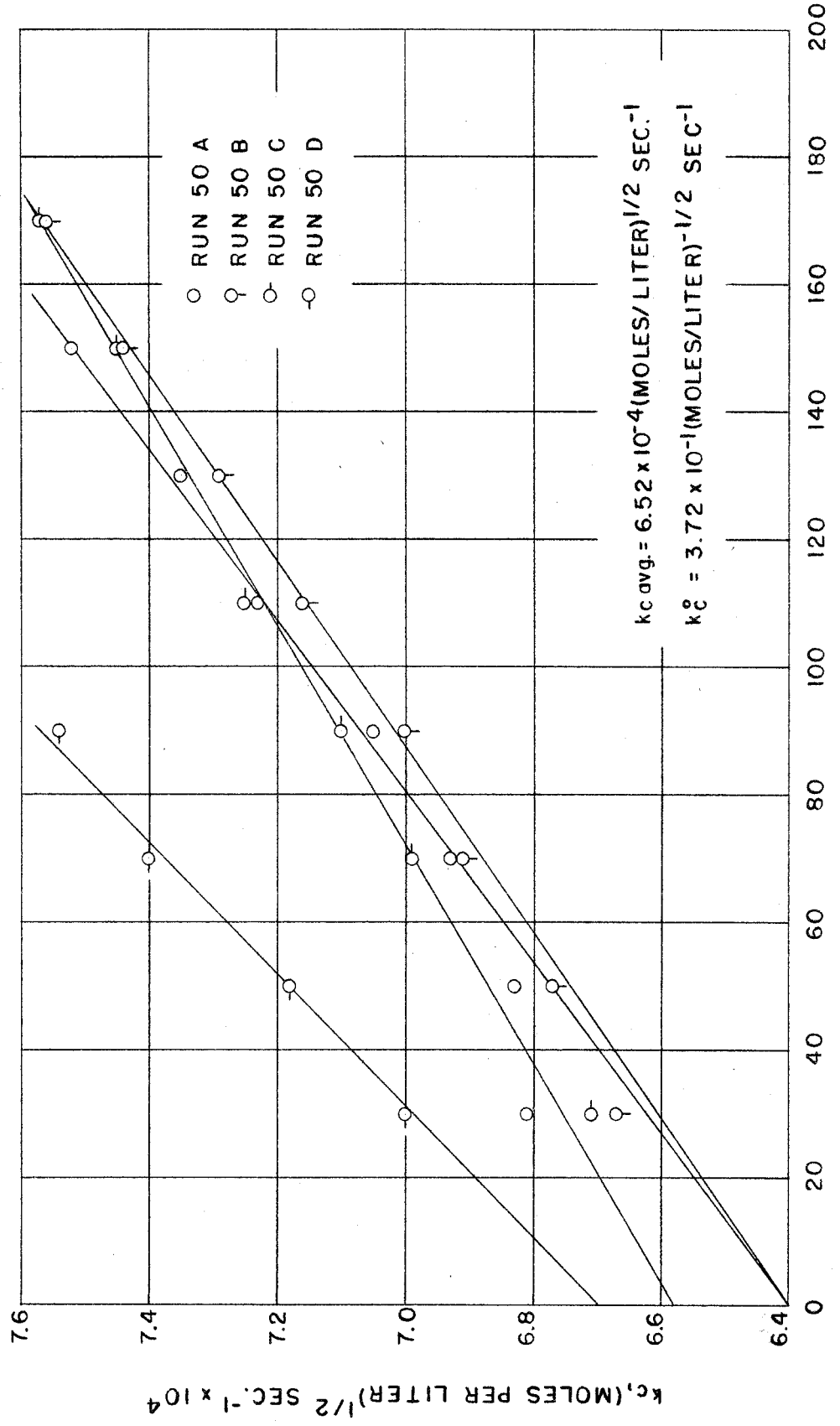

Figure 10--Air Oxidation Studies. Determination of k_c^o. k_c vs Time at 50°C

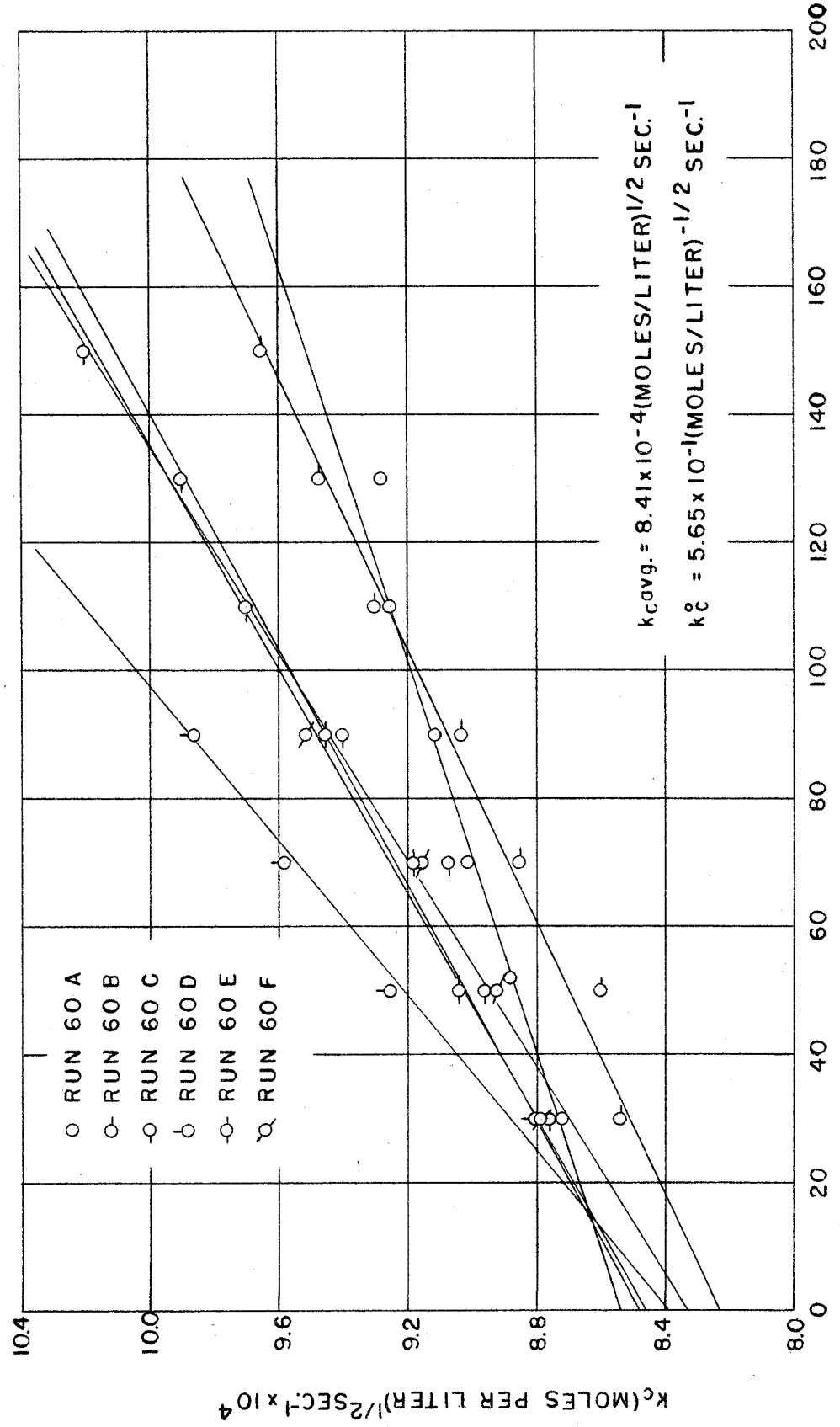

Figure 11--Air Oxidation Studies. Determination of k_c^o. k_c vs Time at 60°C

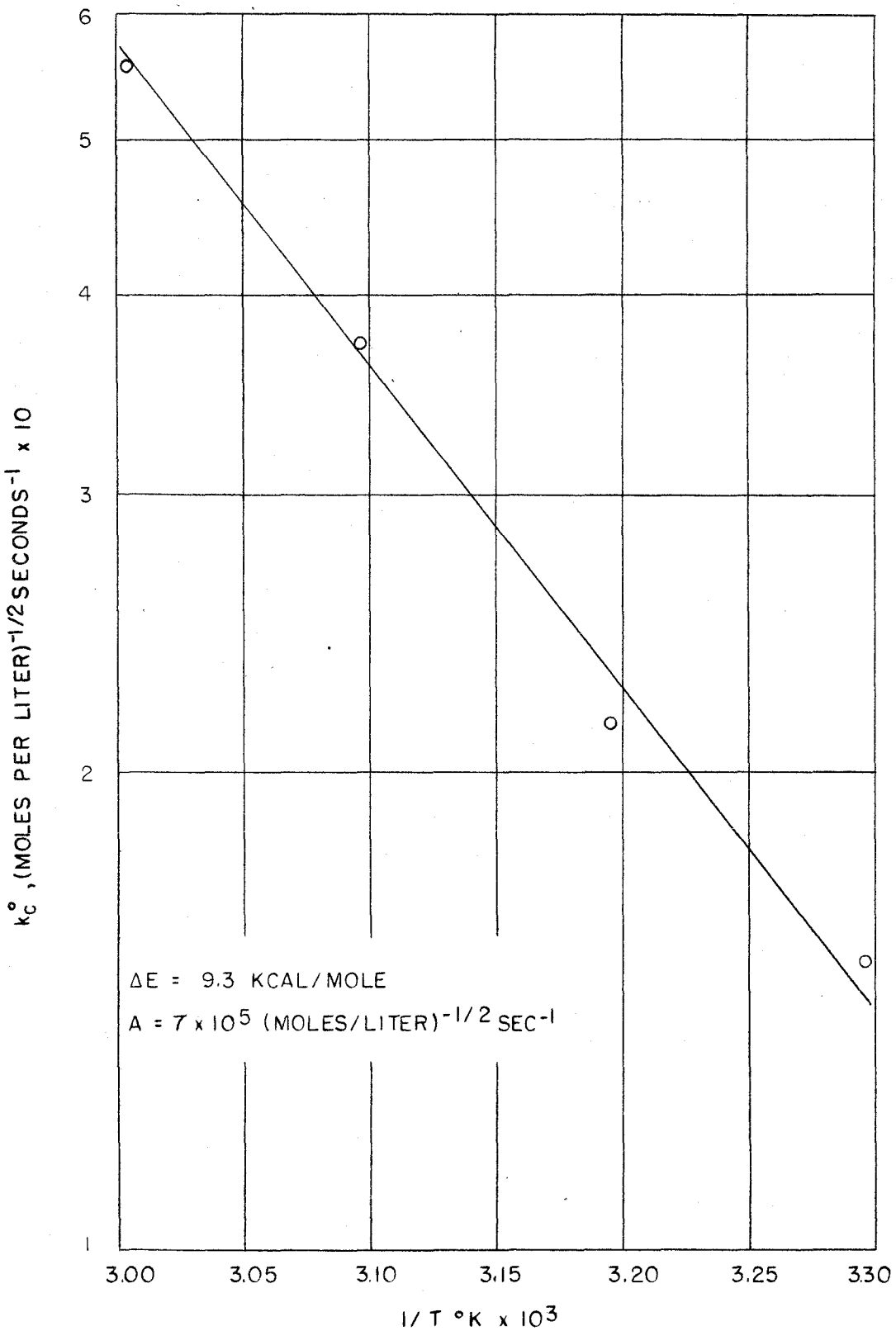

Figure 12--Air Oxidation Studies. Arrhenius plot. Log k_c° vs $1/T°K$

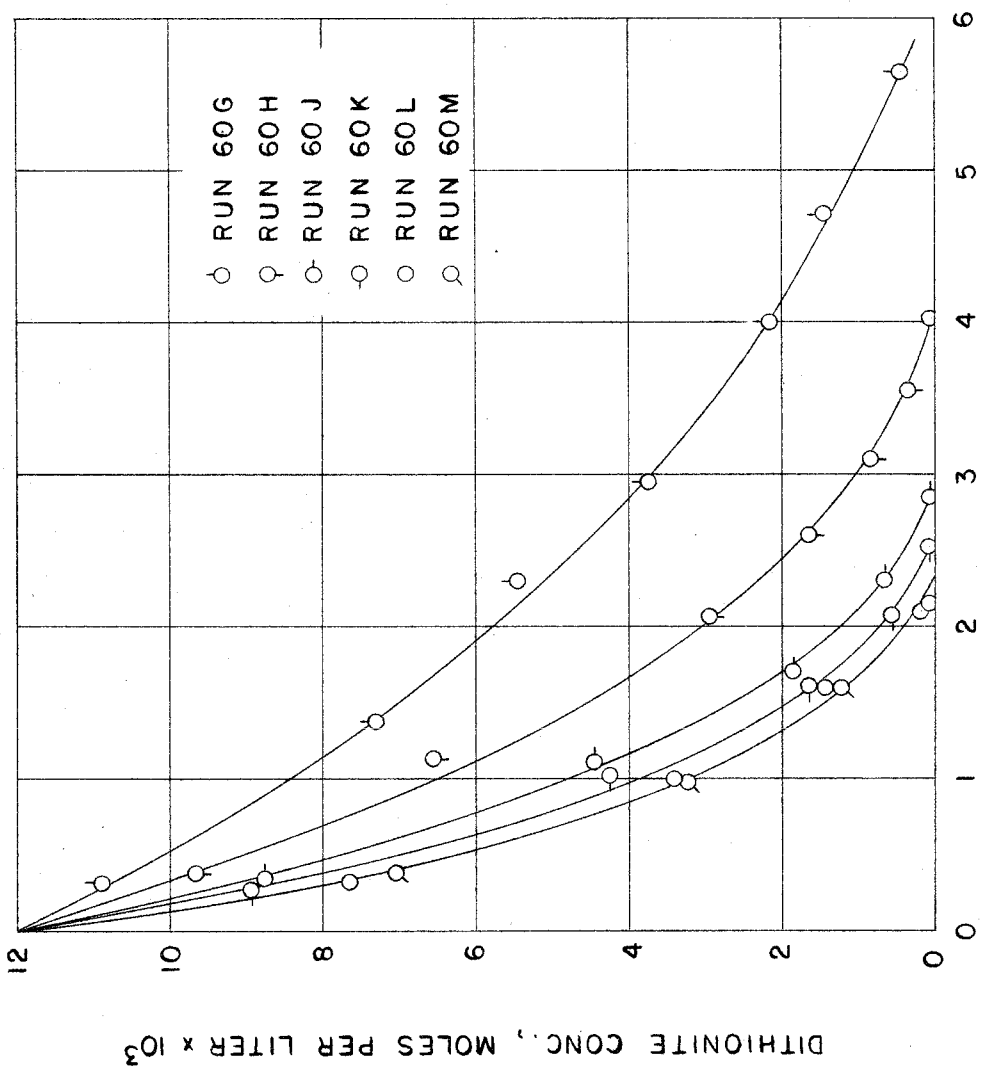

Figure 13--Air Oxidation Studies. Effects of Stirring Rate and Air Flow. Dithionite Concentration vs Time

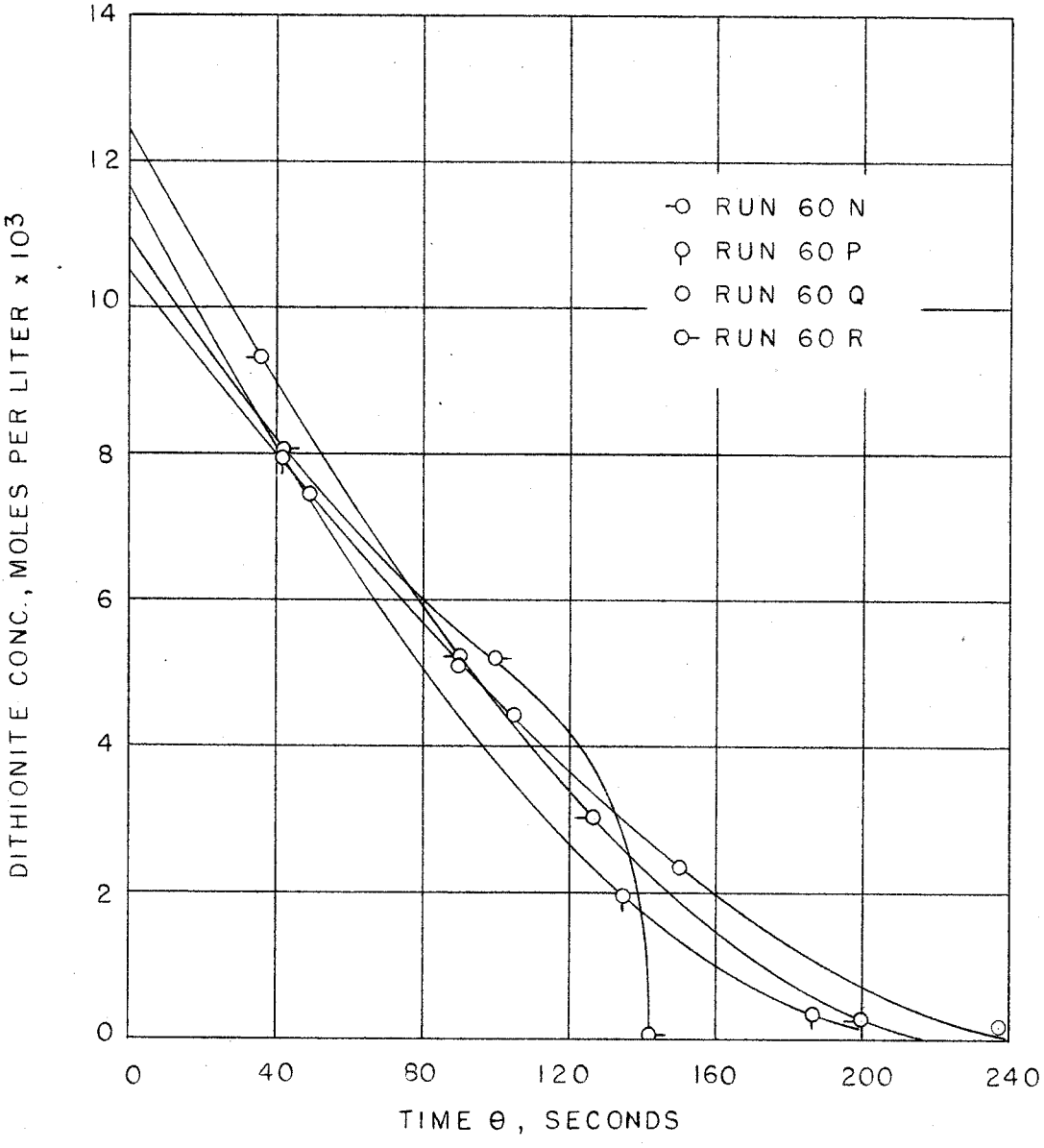

Figure 14--Air Oxidation Studies. Effects of Ionic Strength. Dithionite Concentration vs Time

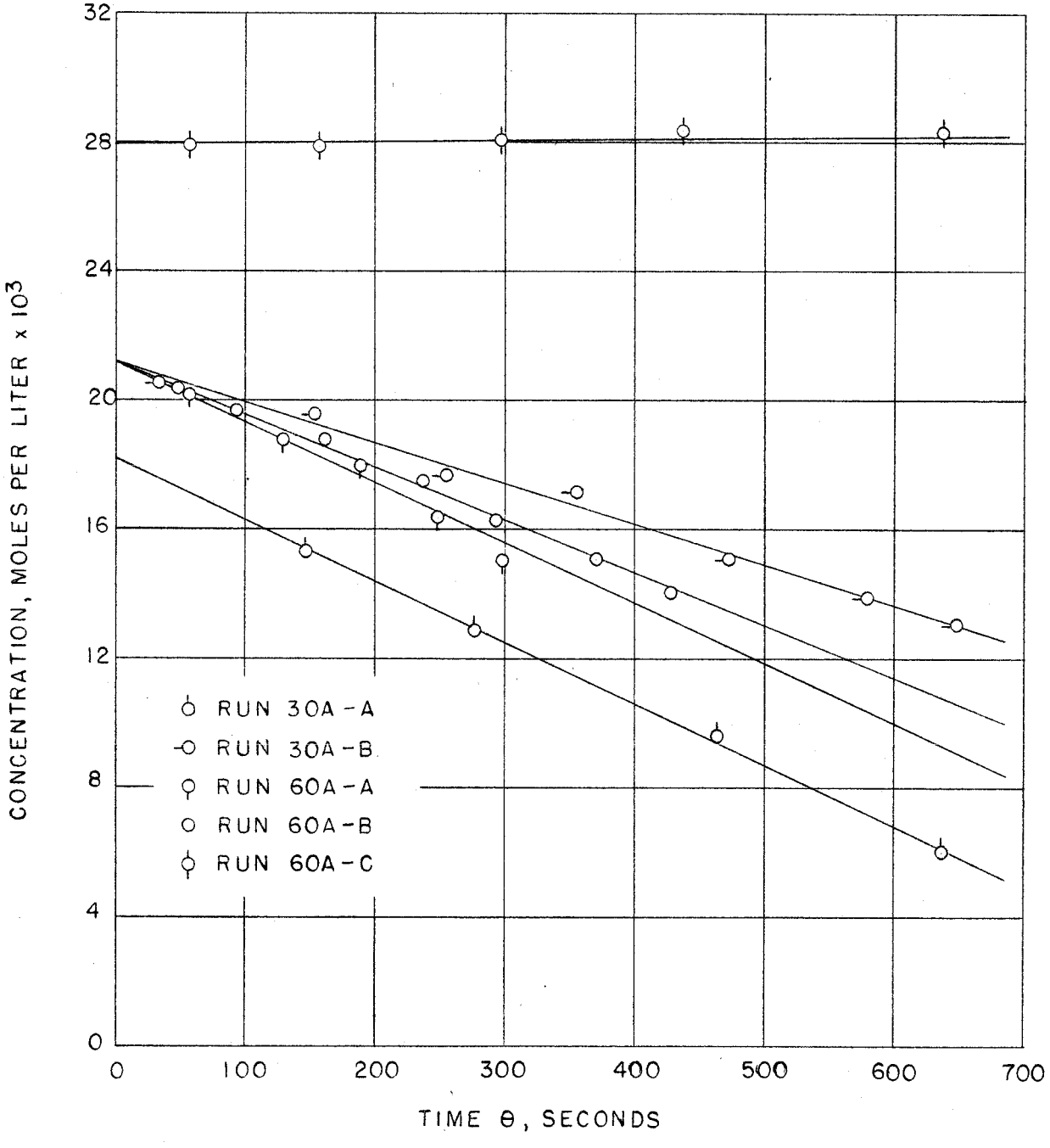

Figure 15--Air Oxidation Studies. Sulfite and Thiosulfate Concentration vs Time

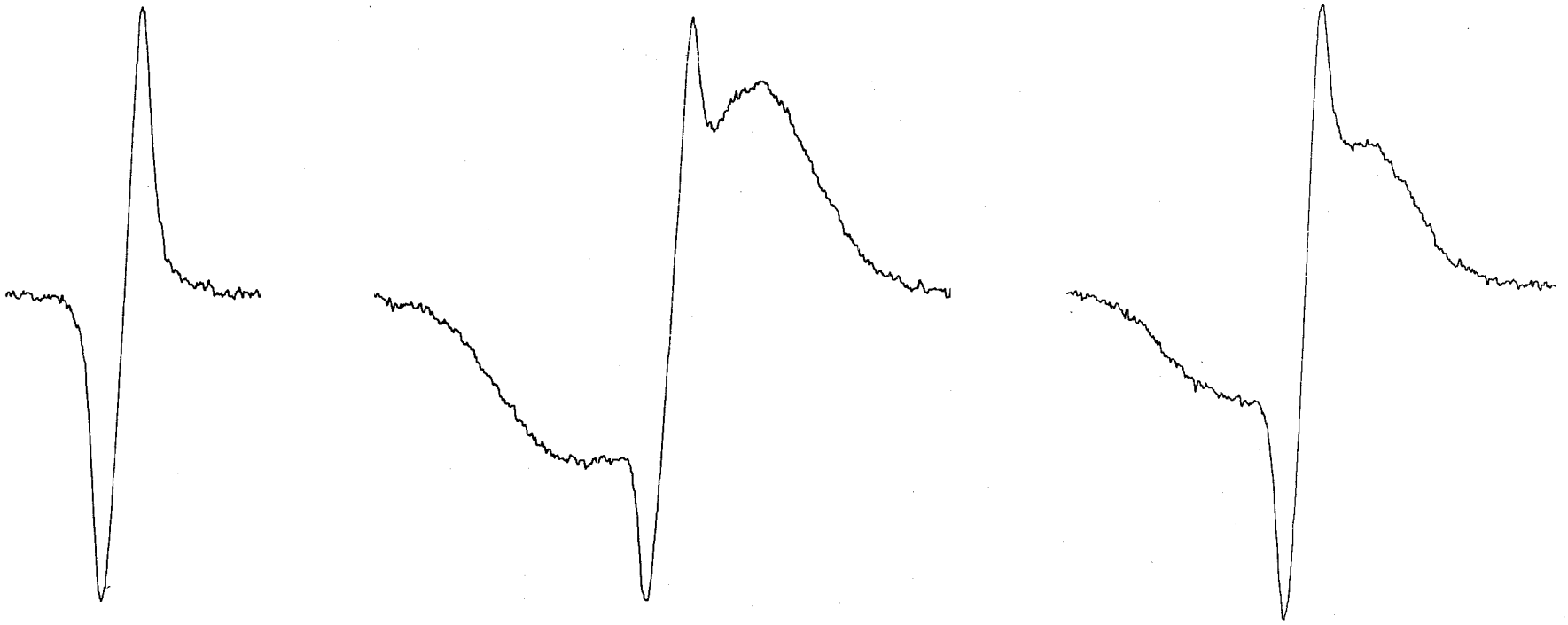

A - EPR of Aqueous Dithionite

B - EPR of Acidified Sulfoxylate and Solid Dithionite

C - EPR of Aqueous Dithionite and Solid Dithionite

Figure 16--Dithionite Structure Studies.

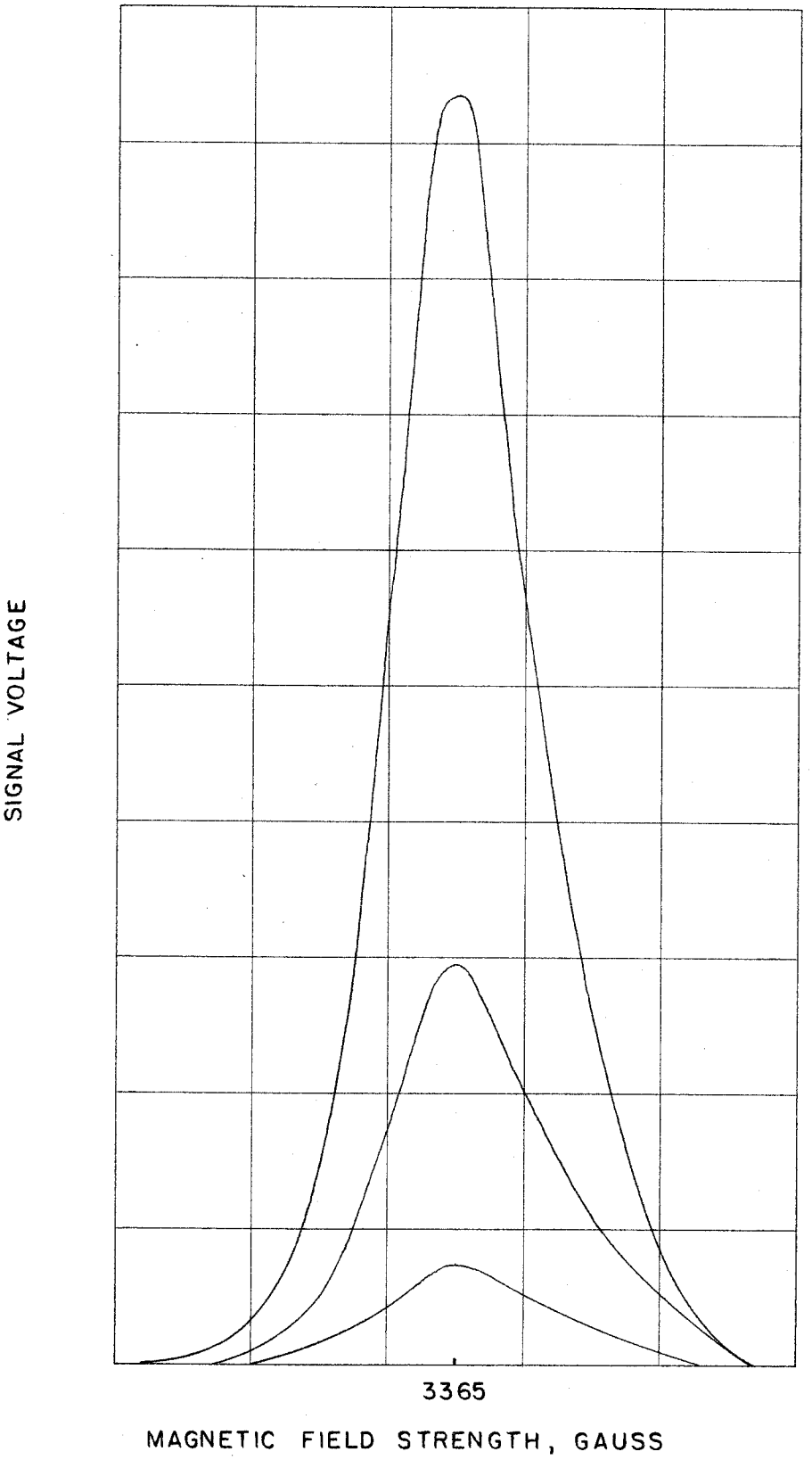

Figure 17--Dithionite Structure Studies. EPR Absorption Peaks for Diluted Dithionite Solutions

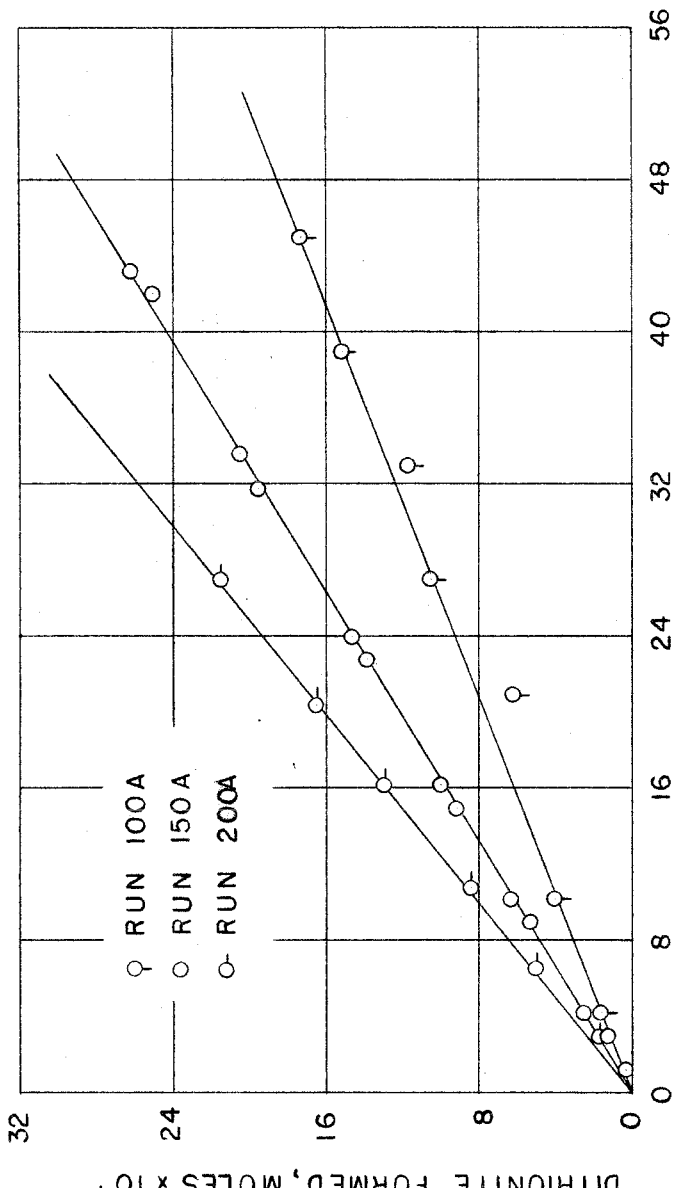

Figure 18--Electrolytic Studies. Electrolytic Generation of Dithionite. Dithionite Formed vs Time at 100, 150, and 200 ma

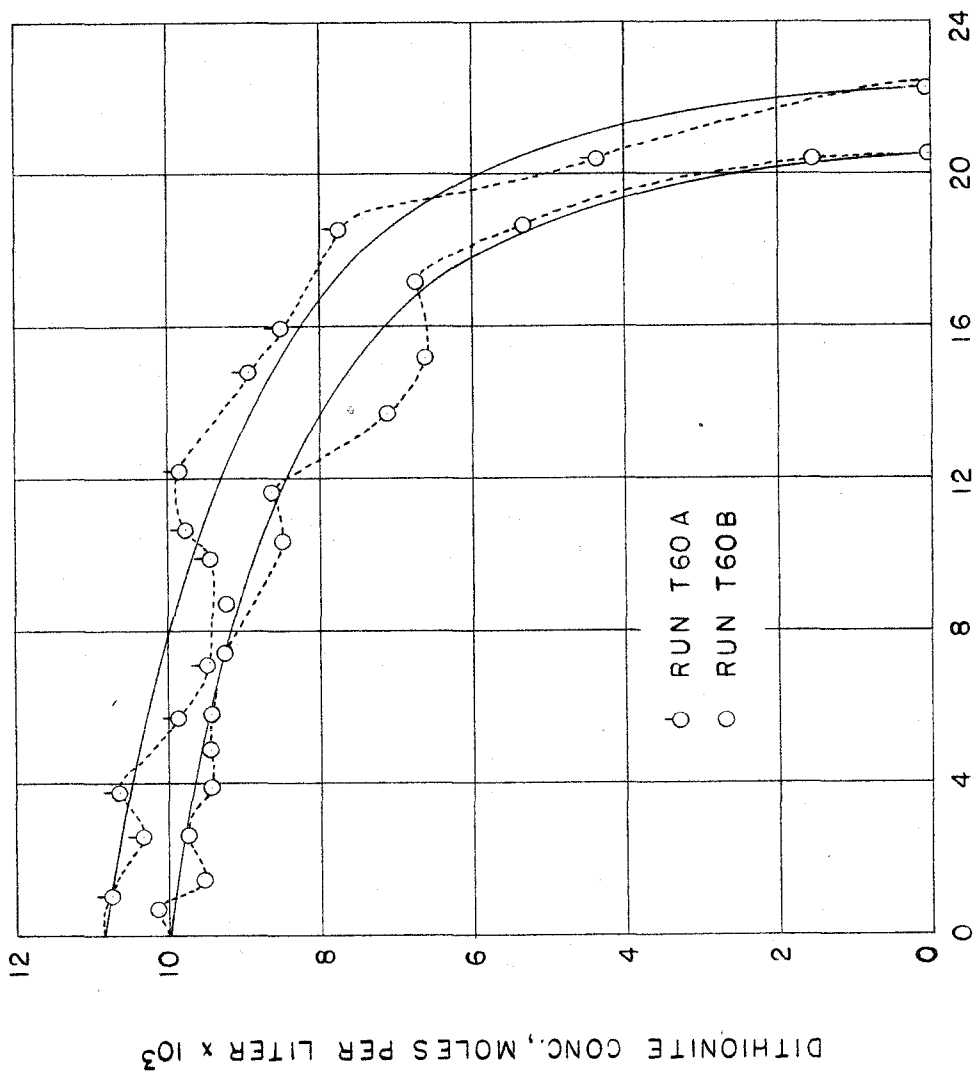

Figure 19a--Thermal Decomposition Studies. Dithionite Concentration vs Time at 60°C

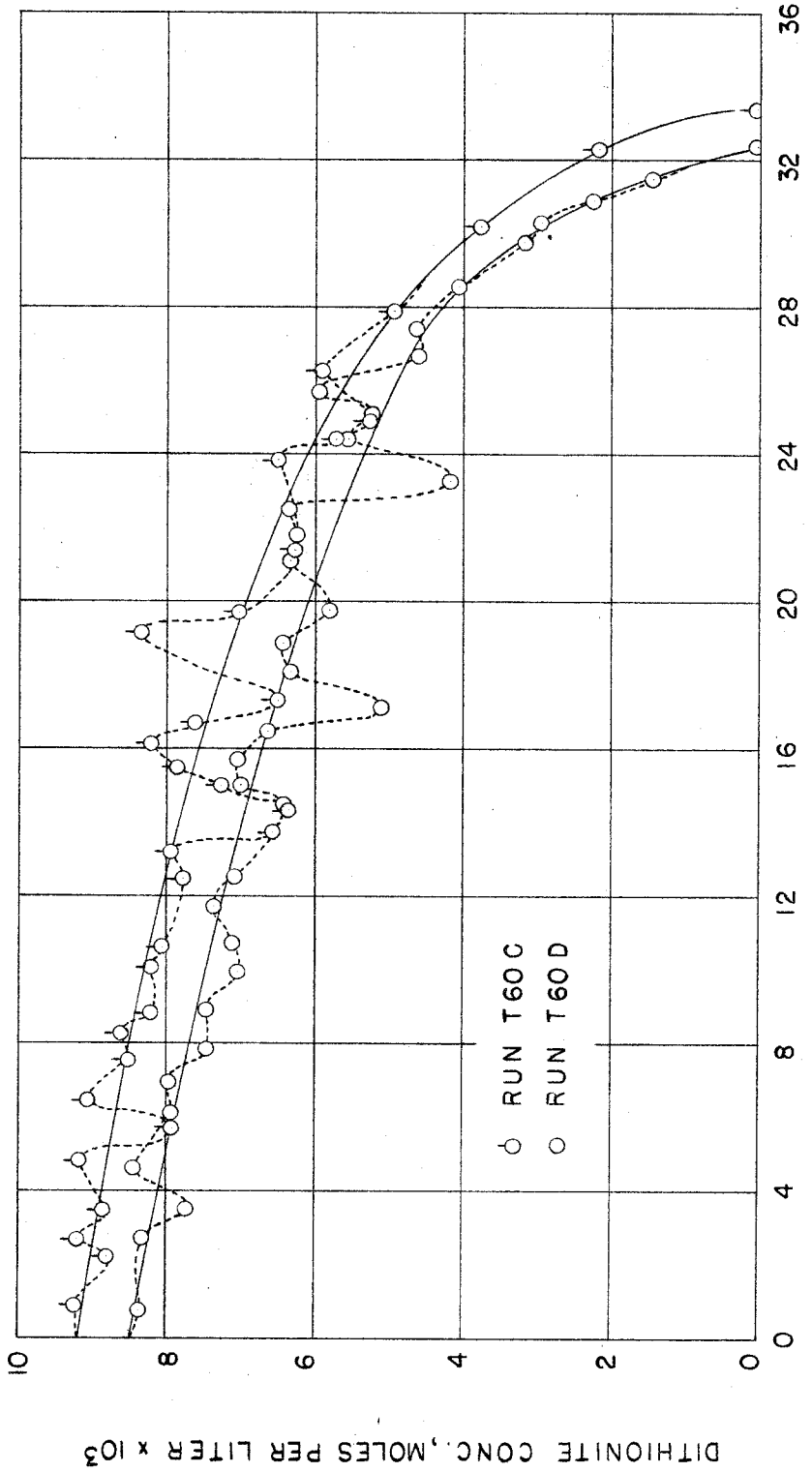

Figure 19b--Thermal Decomposition Studies. Dithionite Concentration vs Time at 60°C

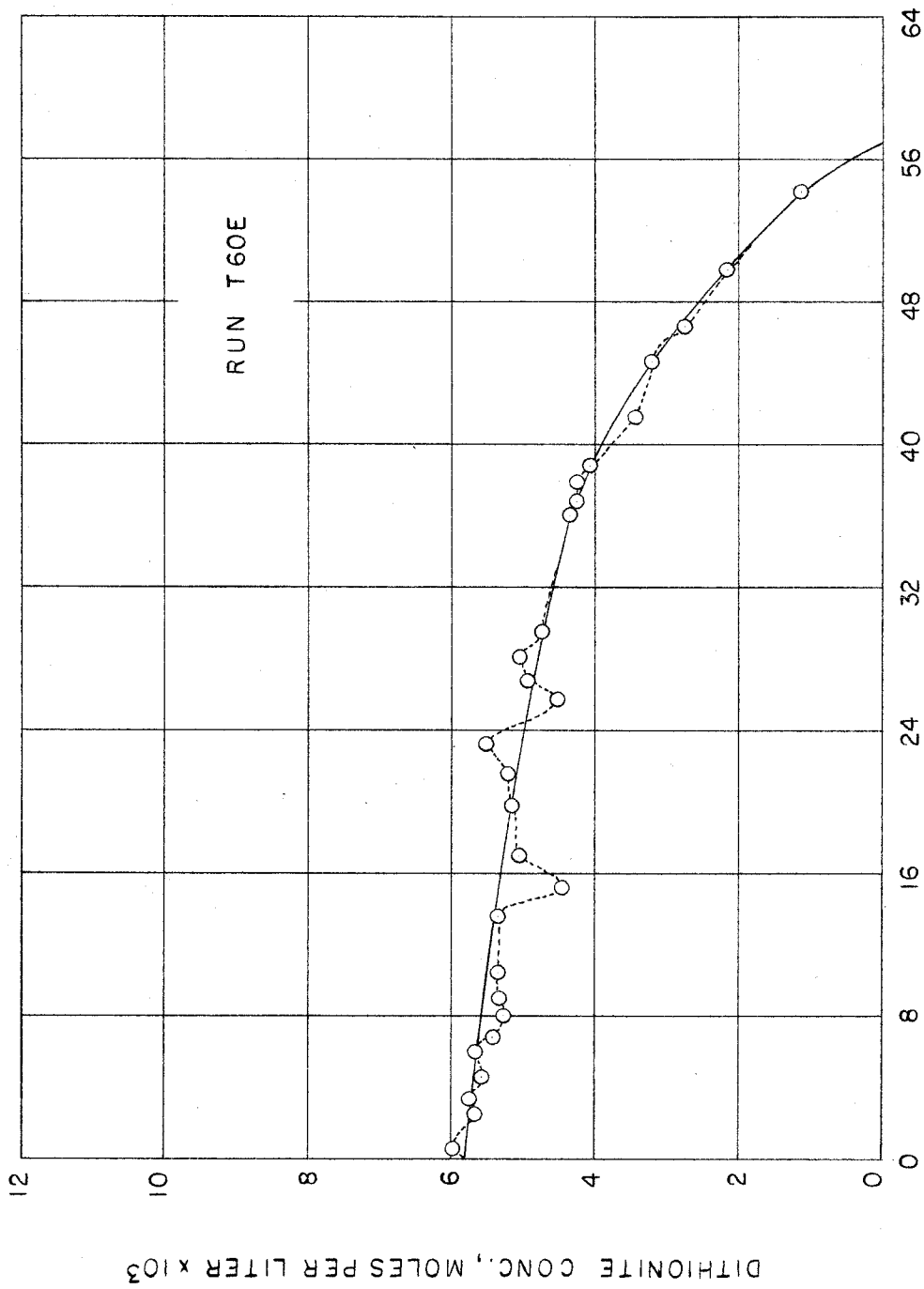

Figure 19c--Thermal Decomposition Studies. Dithionite Concentration vs Time at 60°C

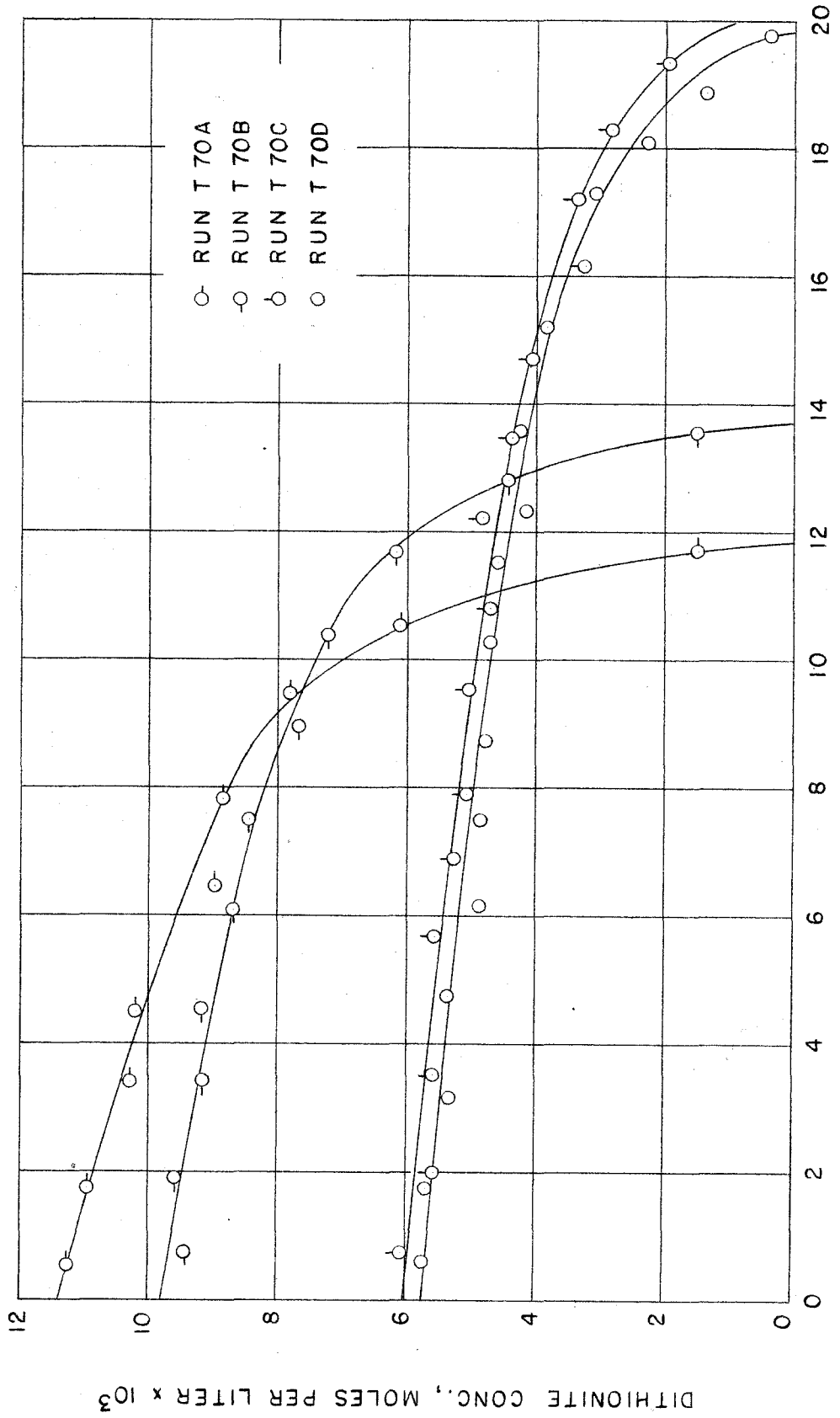

Figure 20--Thermal Decomposition Studies. Dithionite Concentration vs Time at 70°C

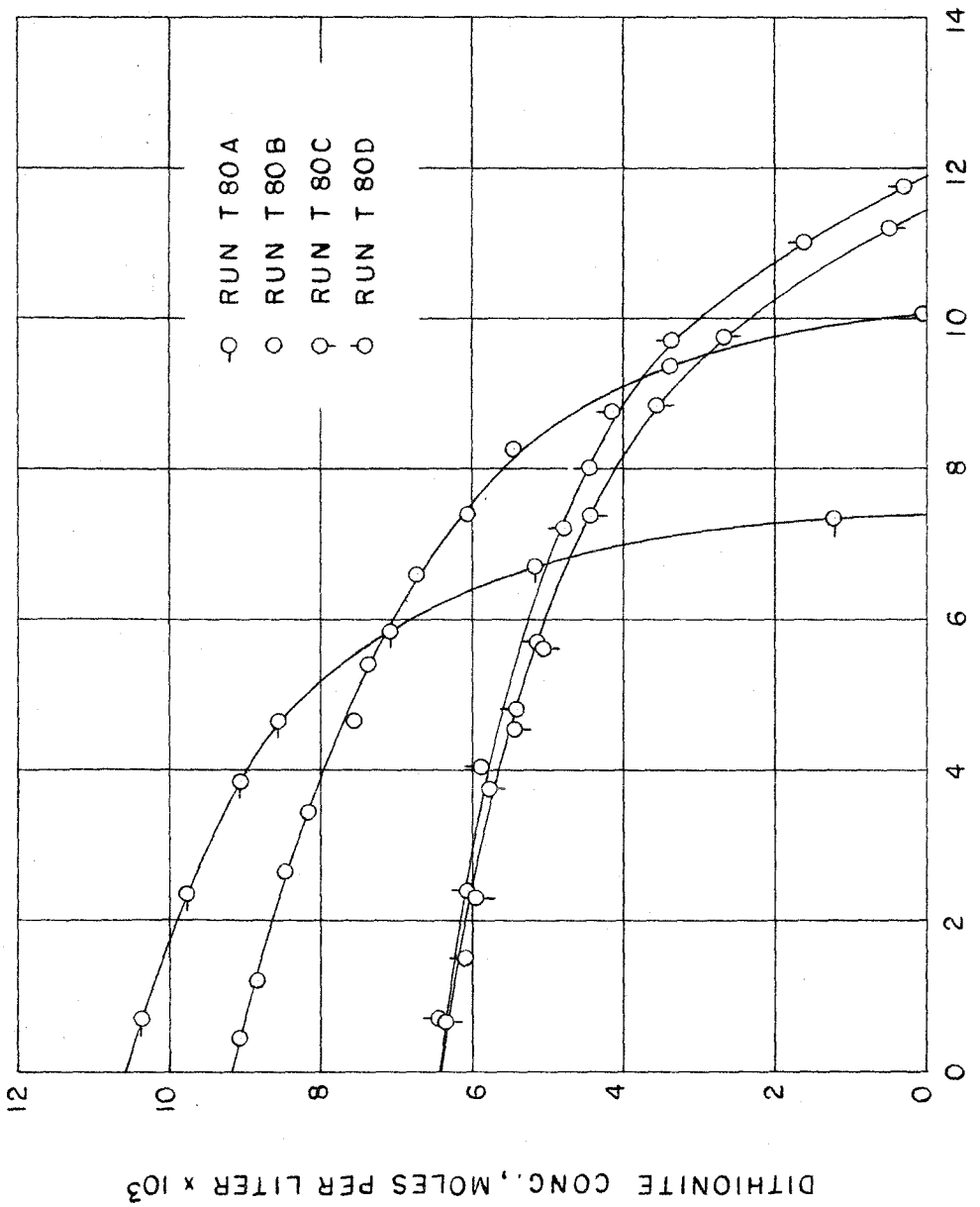

Figure 21--Thermal Decomposition Studies. Dithionite Concentration vs Time at 80°C

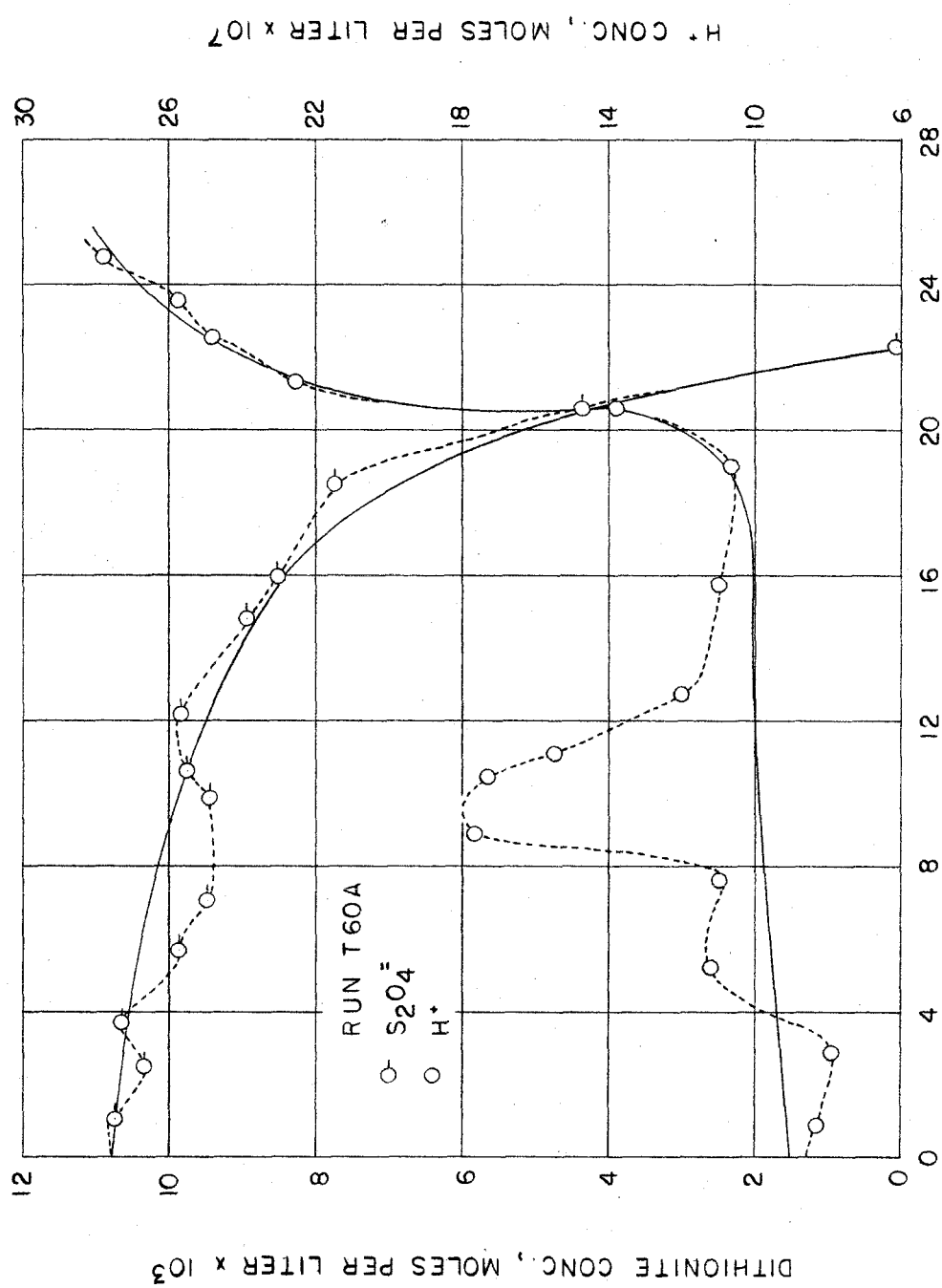

Figure 22--Thermal Decomposition Studies. H^+ and Dithionite Concentration vs Time at 60°C

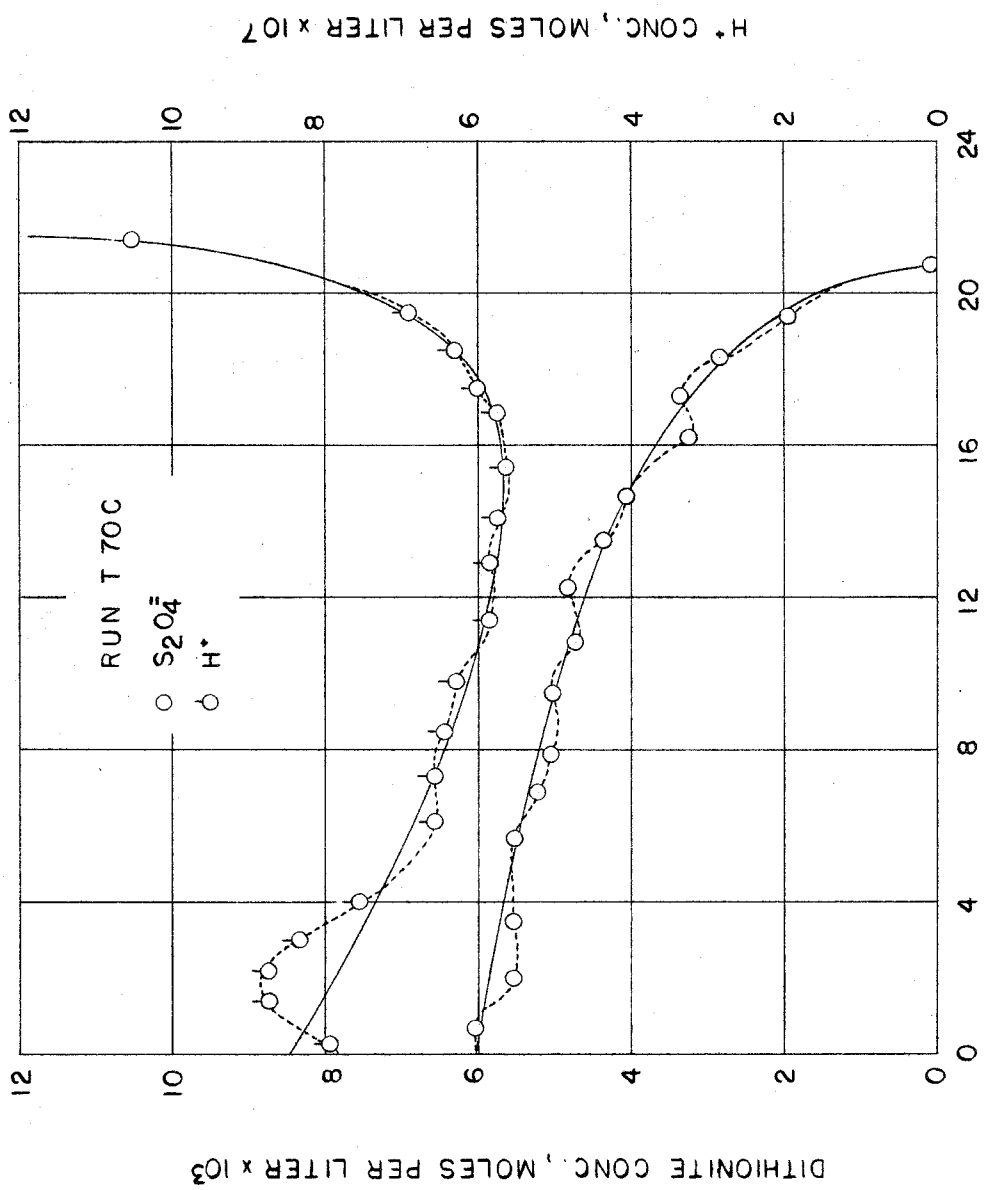

Figure 23--Thermal Decomposition Studies. H^+ and Dithionite Concentration vs Time at 70°C

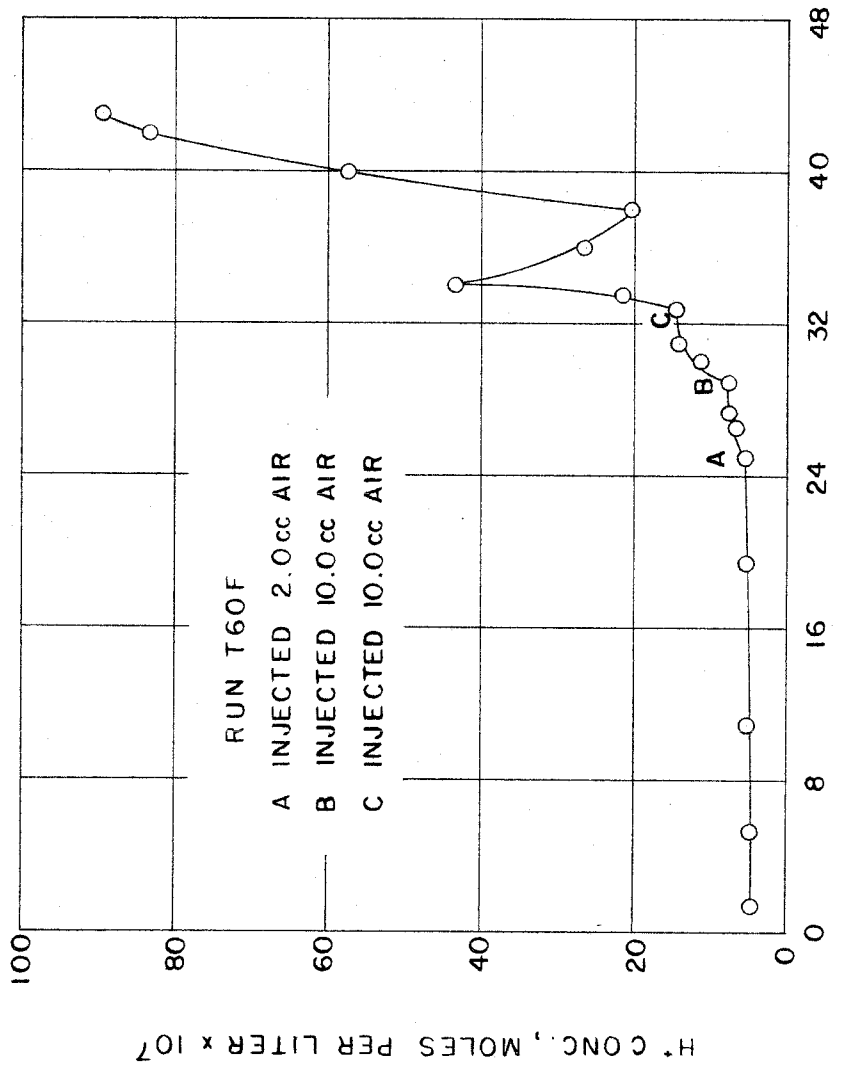

Figure 24--Thermal Decomposition Studies. O_2 Effects on H^+. H^+ Concentration vs Time at 60°C

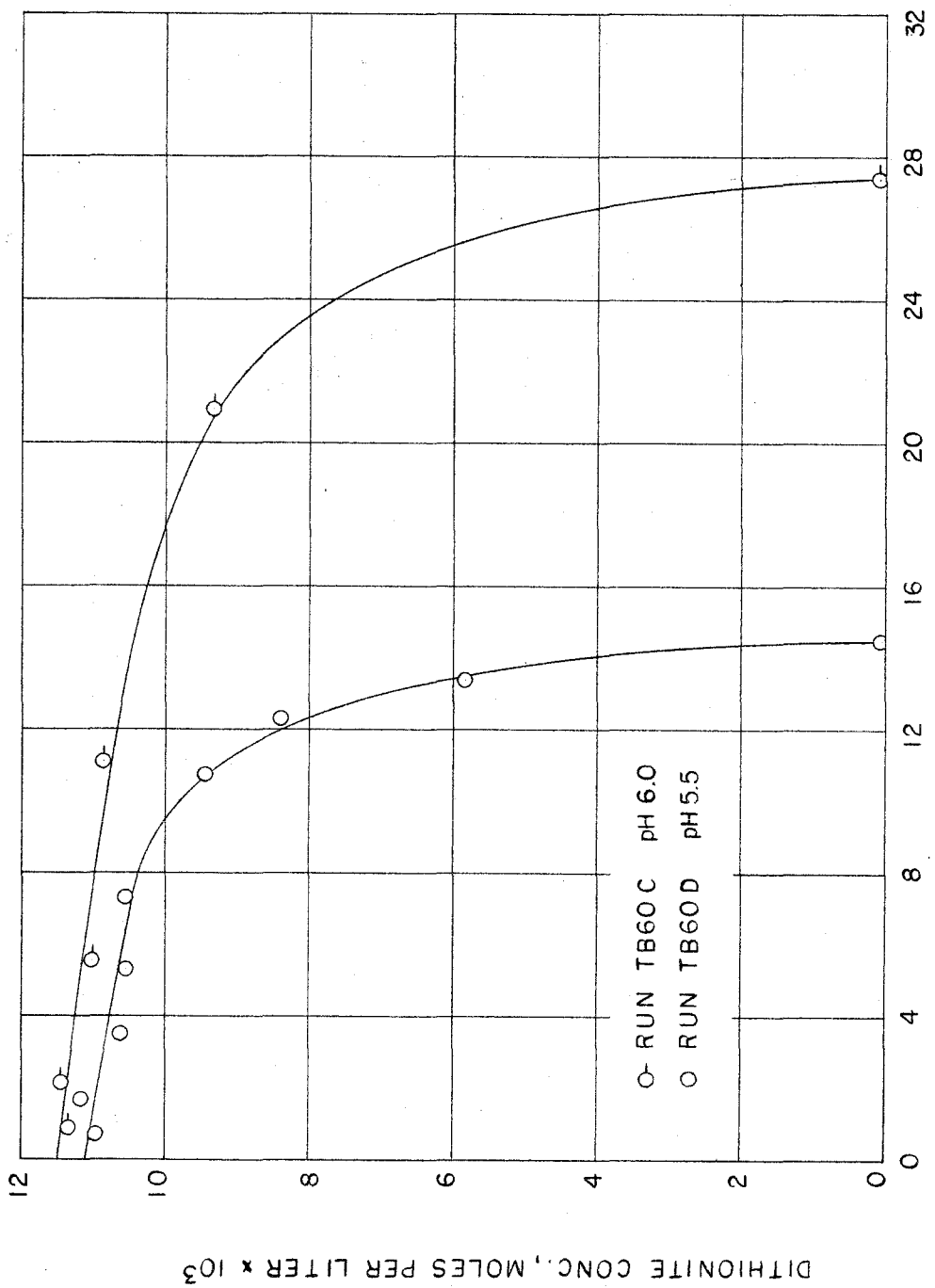

Figure 25a--Thermal Decomposition Studies. Dithionite Concentration vs Time at 60°C in Buffered Systems

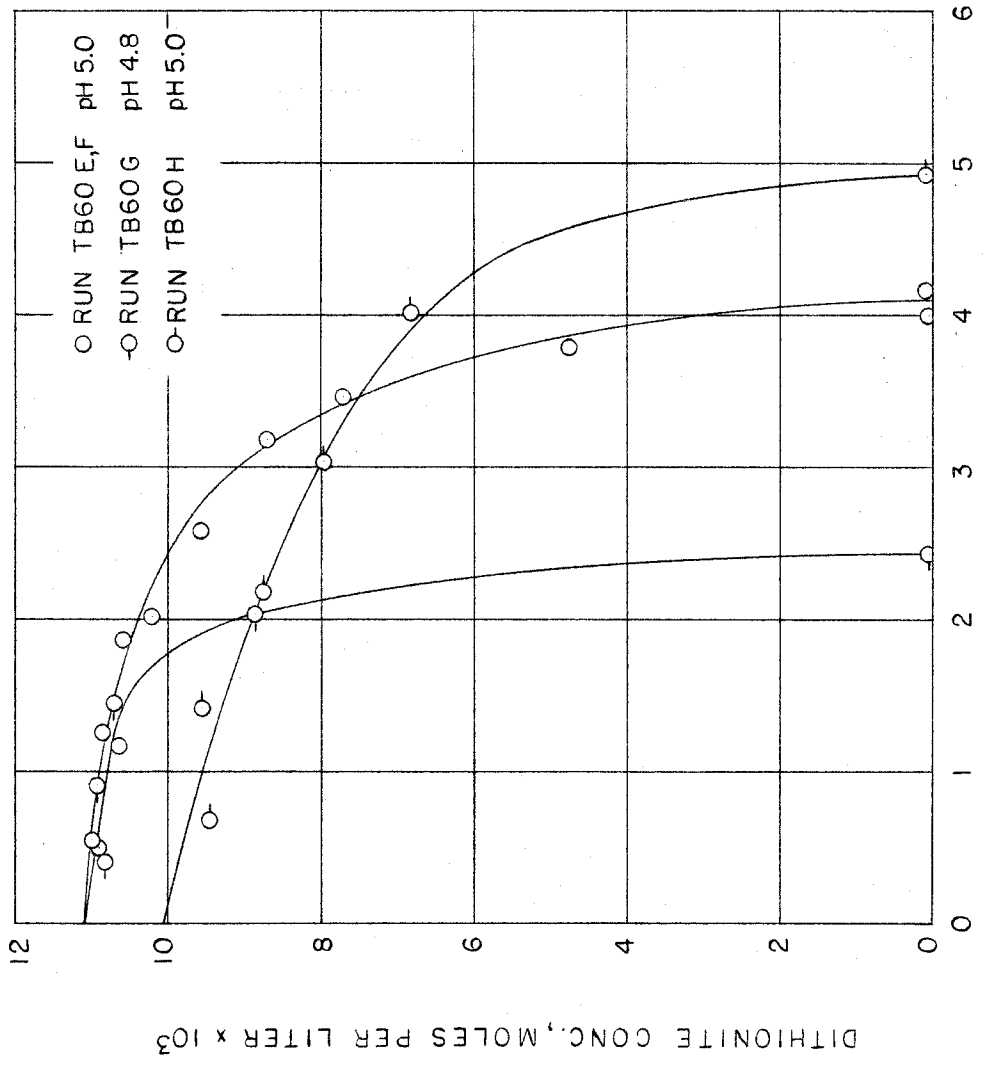

Figure 25b--Thermal Decomposition Studies. Dithionite Concentration vs Time at 60°C in Buffered Systems

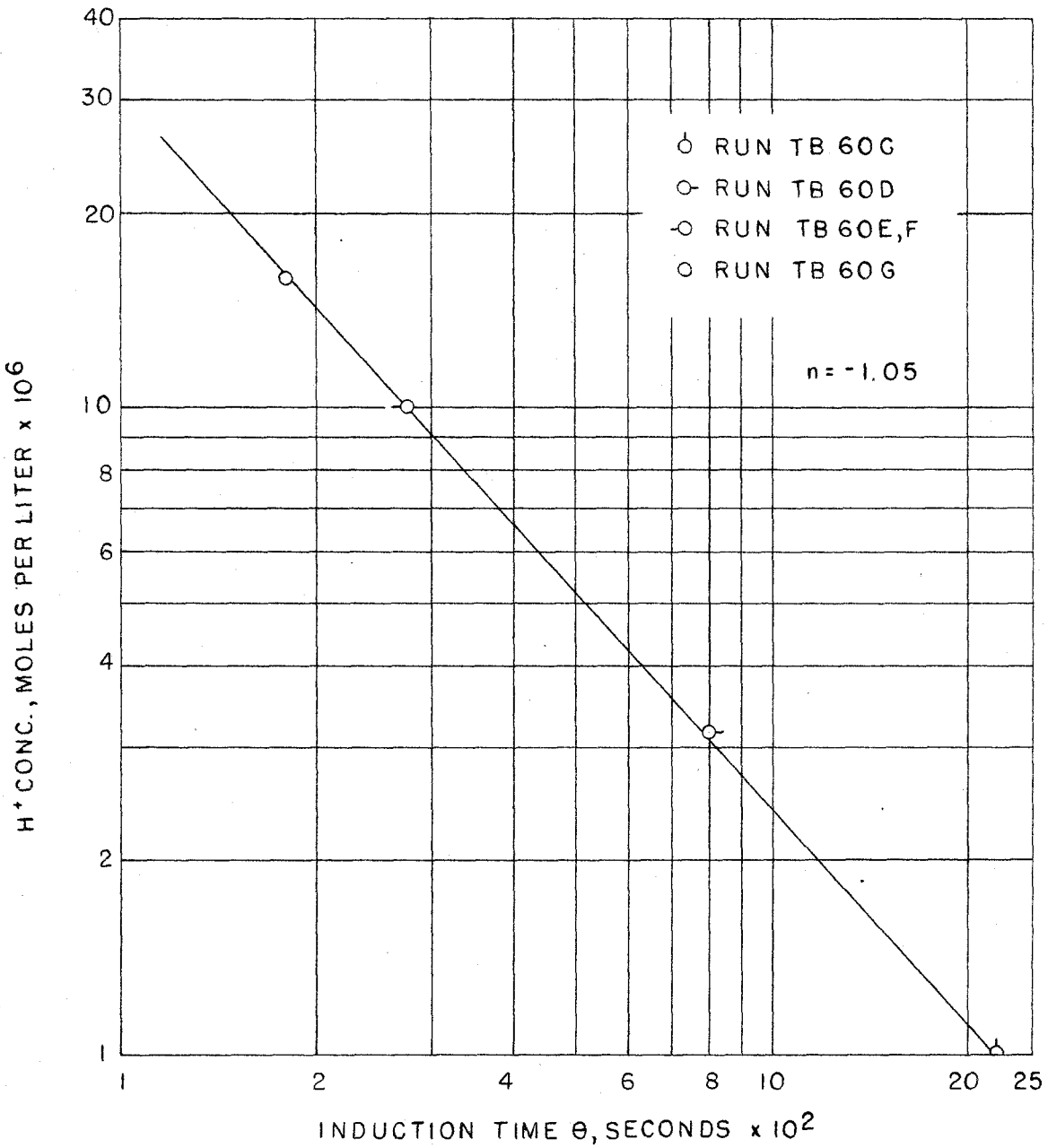

Figure 26--Thermal Decomposition Studies. Log of Induction Time vs Log of H^+ Concentration

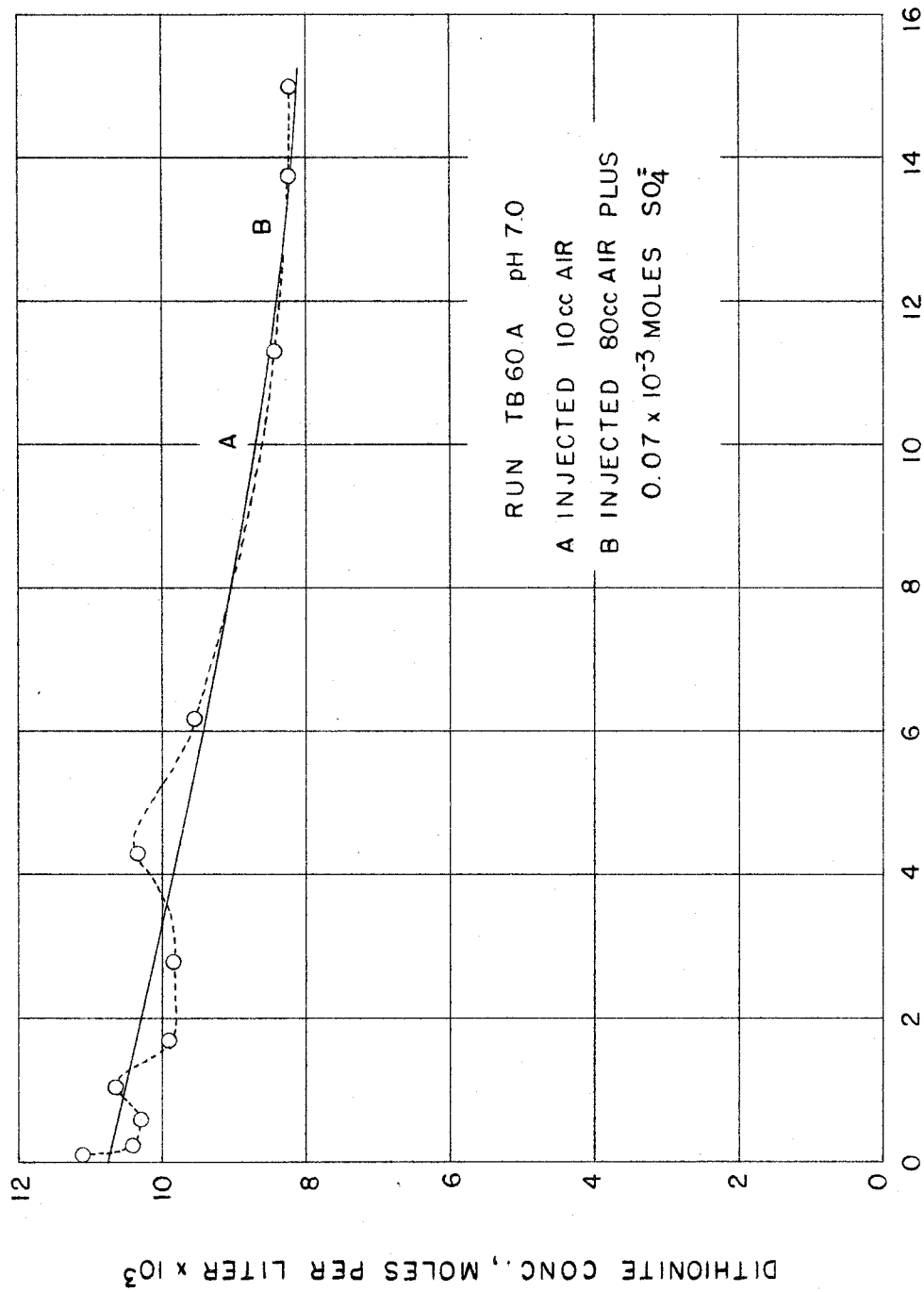

Figure 27a--Thermal Decomposition Studies. Effects of Air and $SO_4^=$. Dithionite Concentration vs Time at 60°C in System Buffered at pH 7

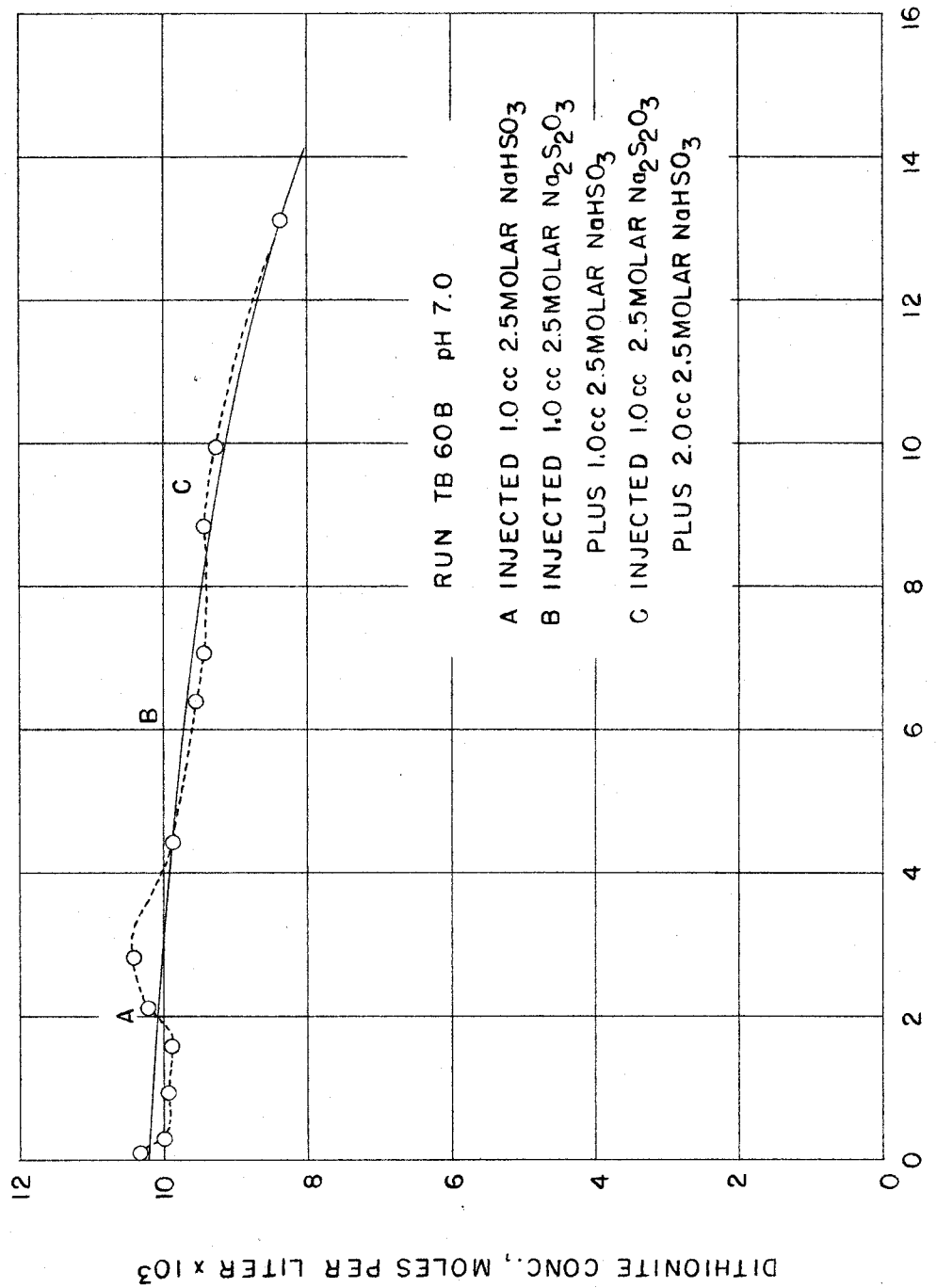

Figure 27b--Thermal Decomposition Studies. Effects of $S_2O_3^=$ and HSO_3^-. Dithionite Concentration vs Time at 60°C in System Buffered at pH 7

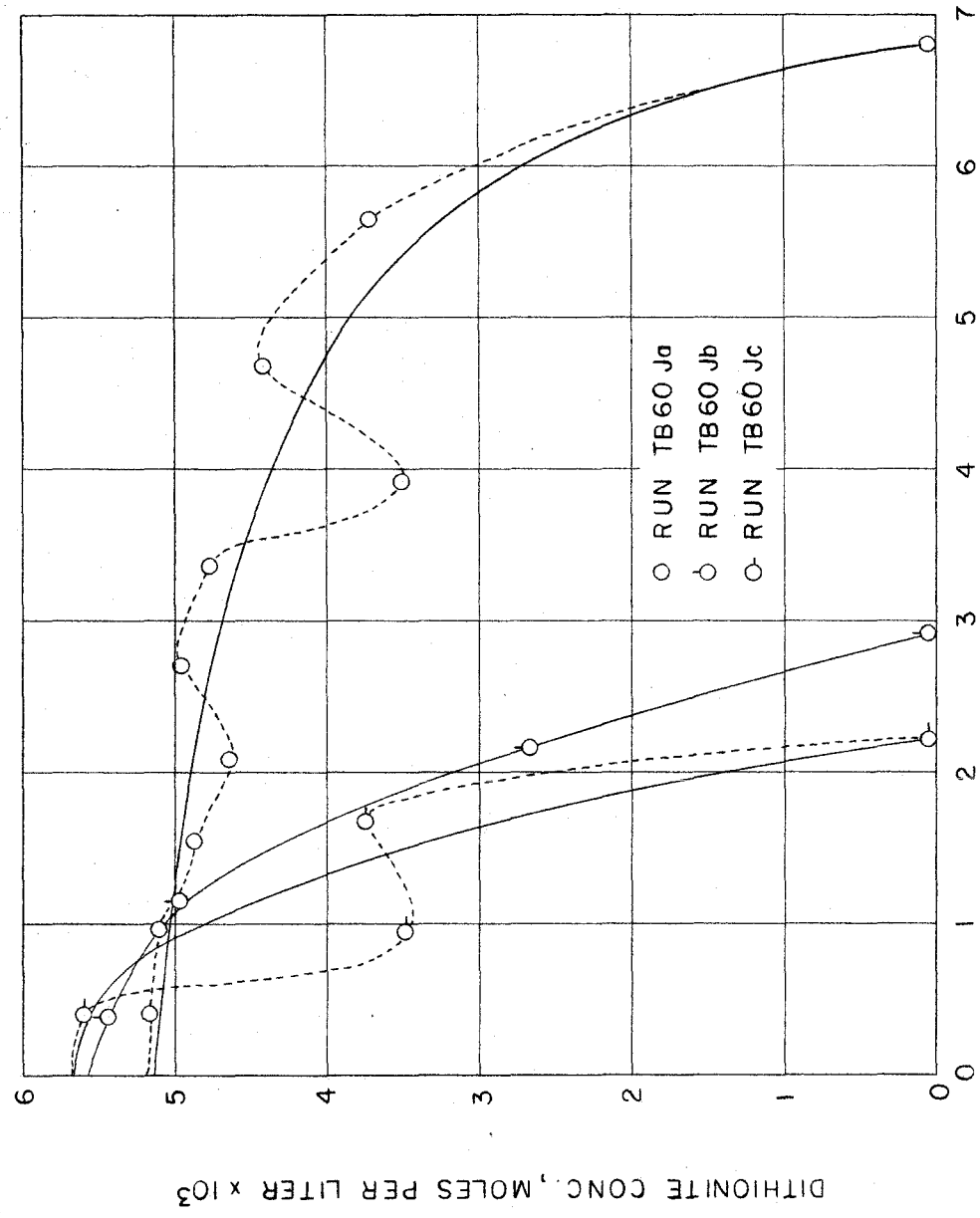

Figure 28a--Thermal Decomposition Studies. Effects of End Products. Dithionite Concentration vs Time at 60°C in System Buffered at pH 5

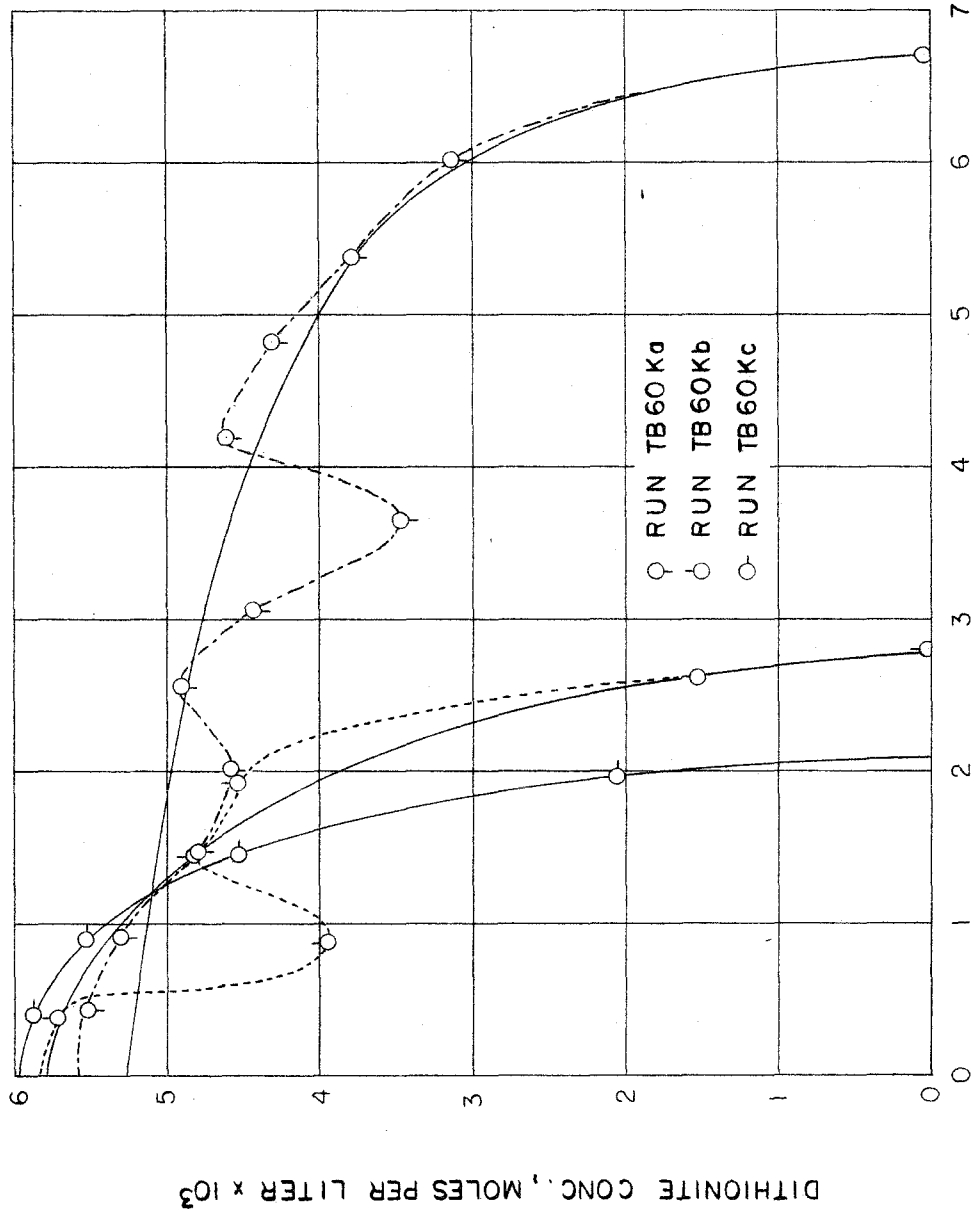

Figure 28b--Thermal Decomposition Studies. Effects of End Products. Dithionite Concentration vs Time at 60°C in System Buffered at pH 5

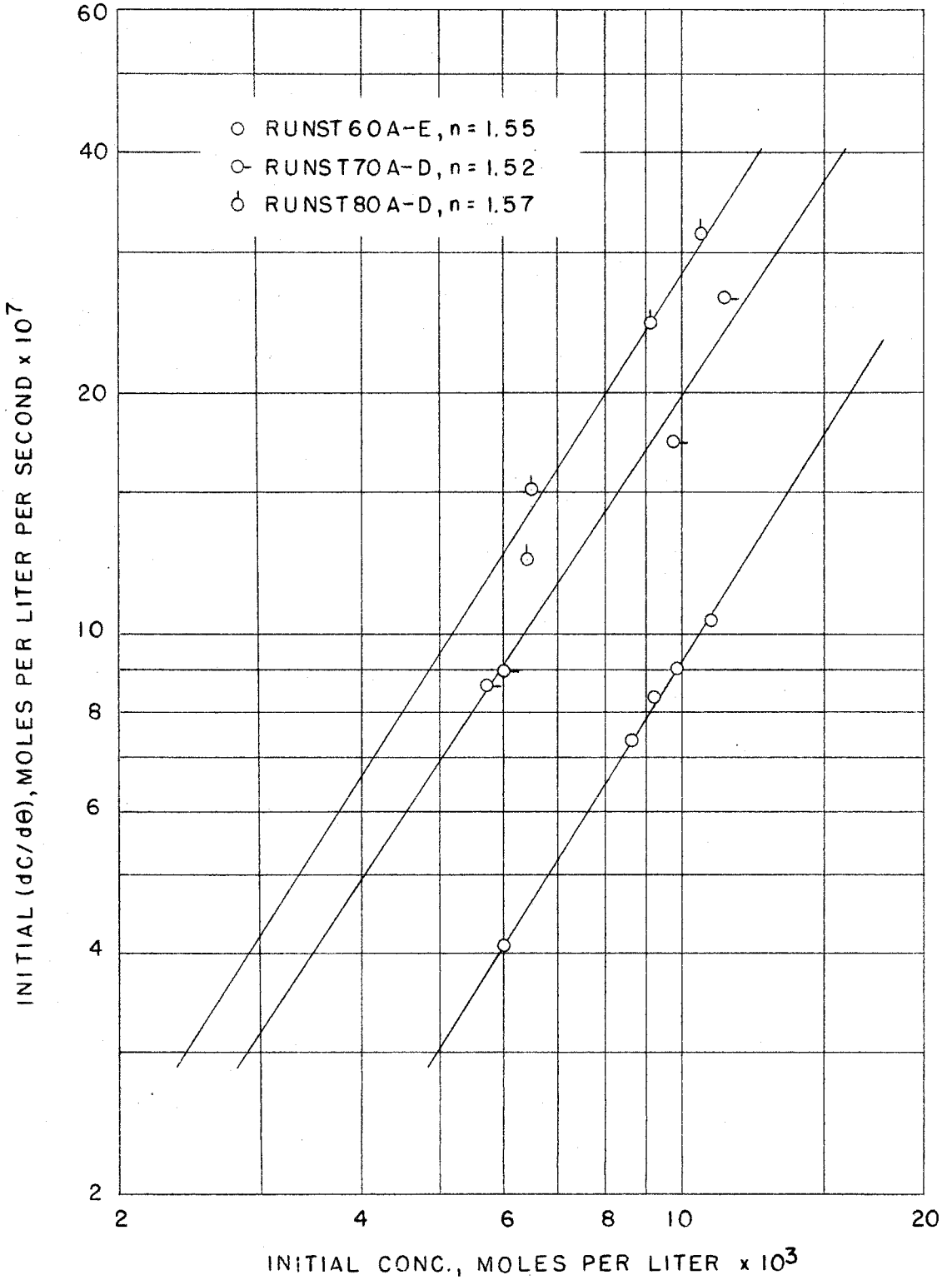

Figure 29--Thermal Decomposition Studies. Determination of n. Log $(dC/d\theta)_o$ vs log C_o at 60, 70, and 80°C

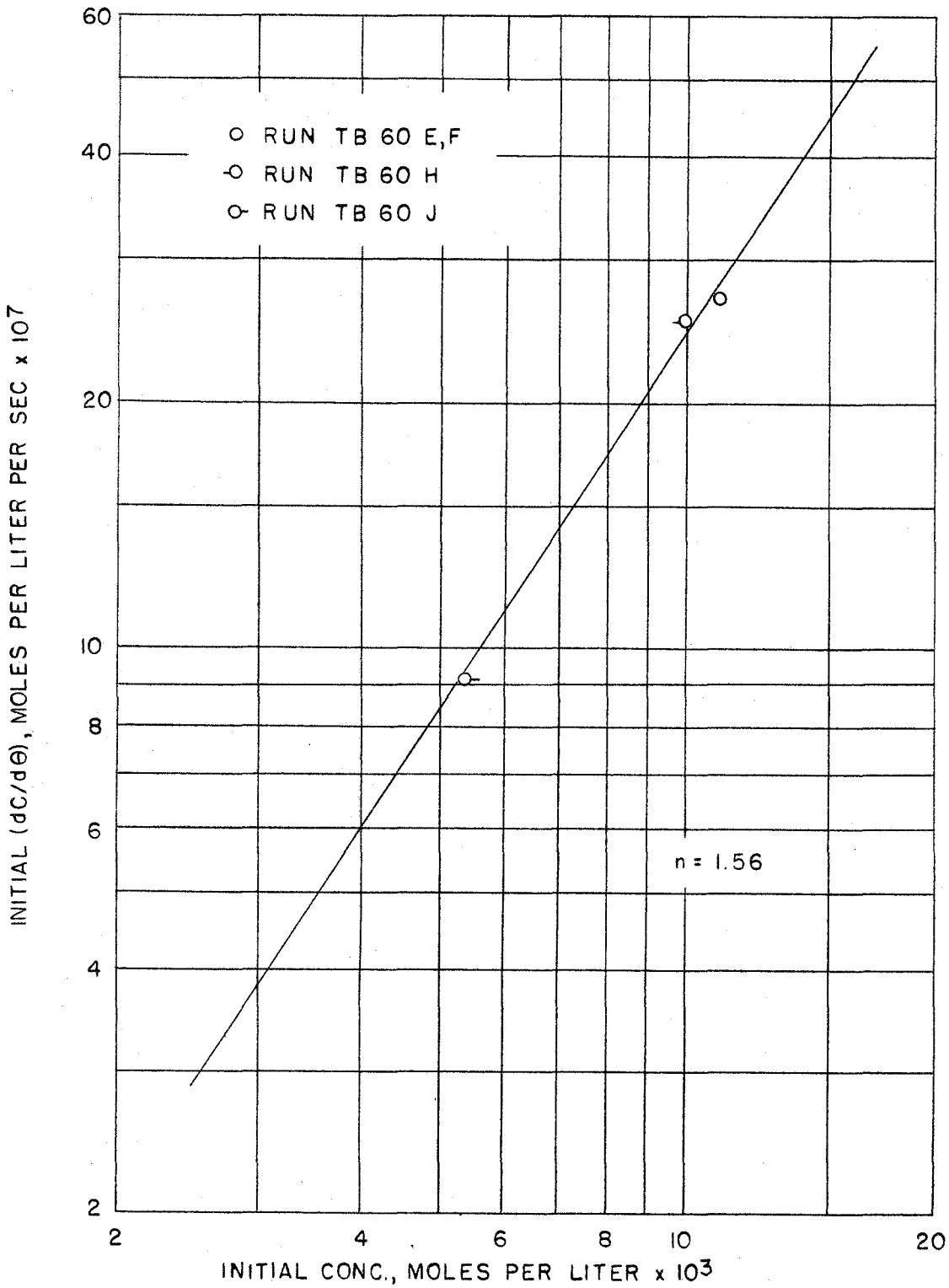

Figure 30--Thermal Decomposition Studies. Determination of n. Log $(dC/d\theta)_o$ vs log C_o at 60°C and pH 5.

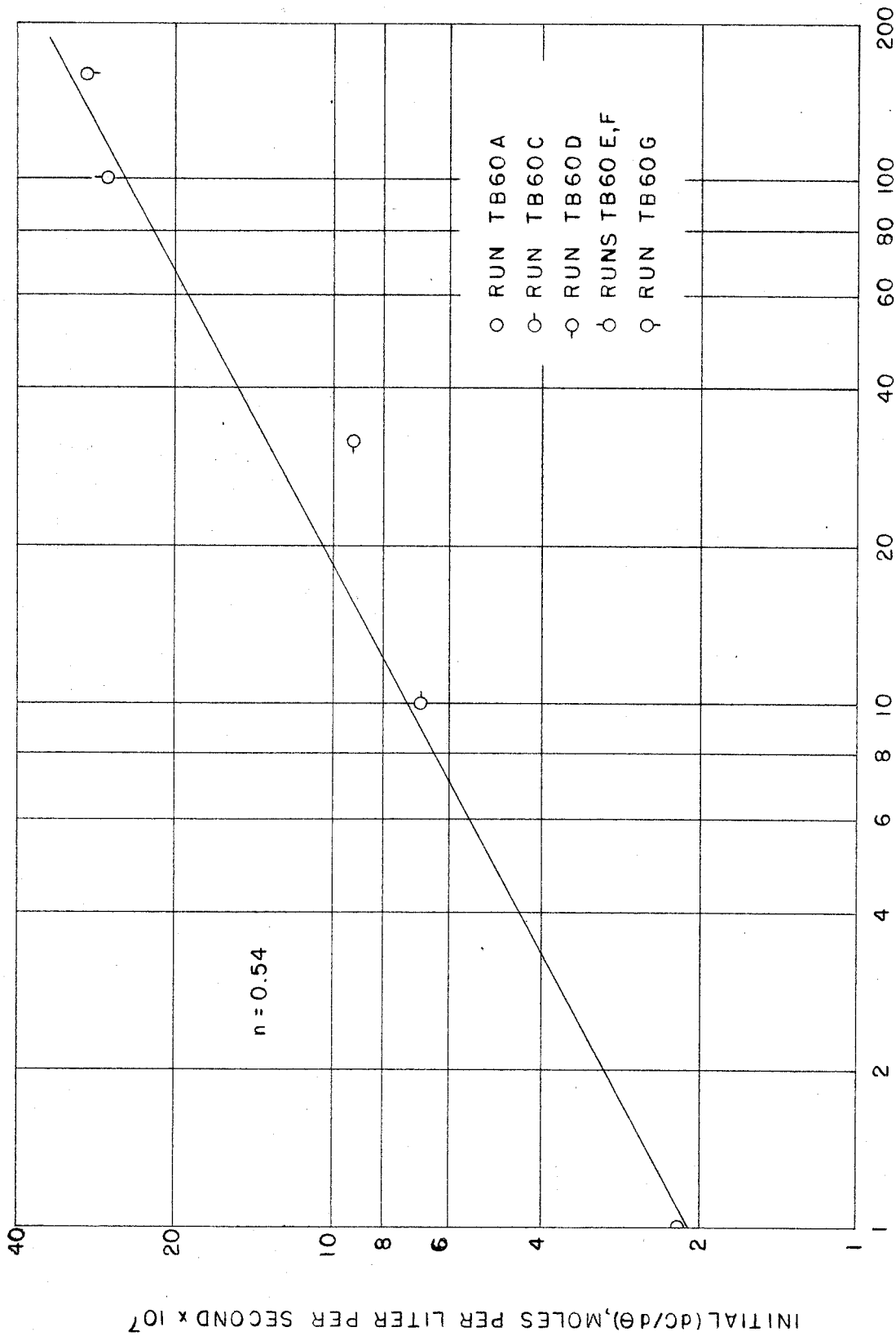

Figure 31--Thermal Decomposition Studies. Effect of H^+. Log $(dC/d\theta)_o$ vs log H^+ Concentration at 60°C for C_o = 11.00 x 10^{-3} Molar

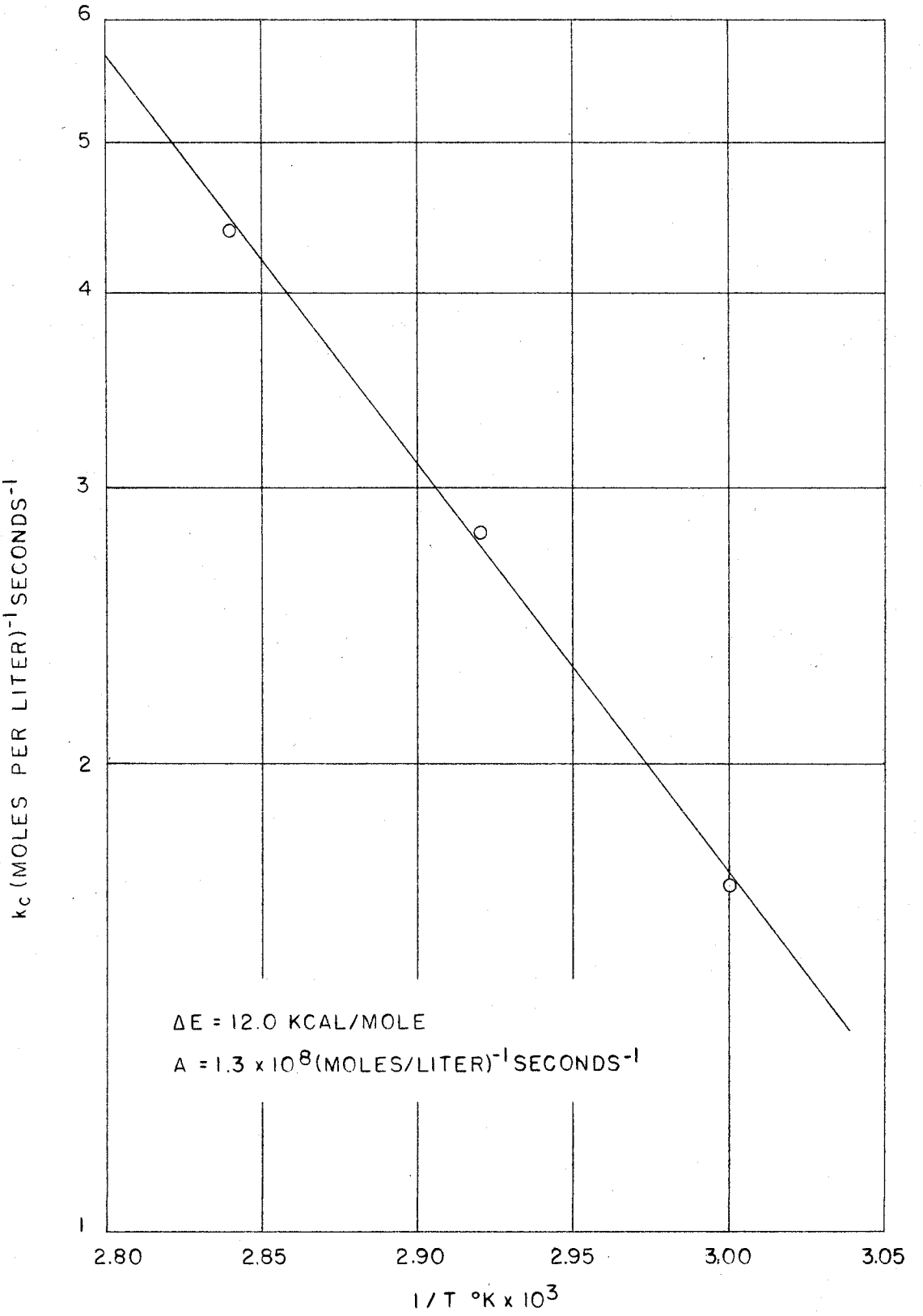

Figure 32--Thermal Decomposition Studies. Arrhenius Plot. Log k_c vs 1/T °K

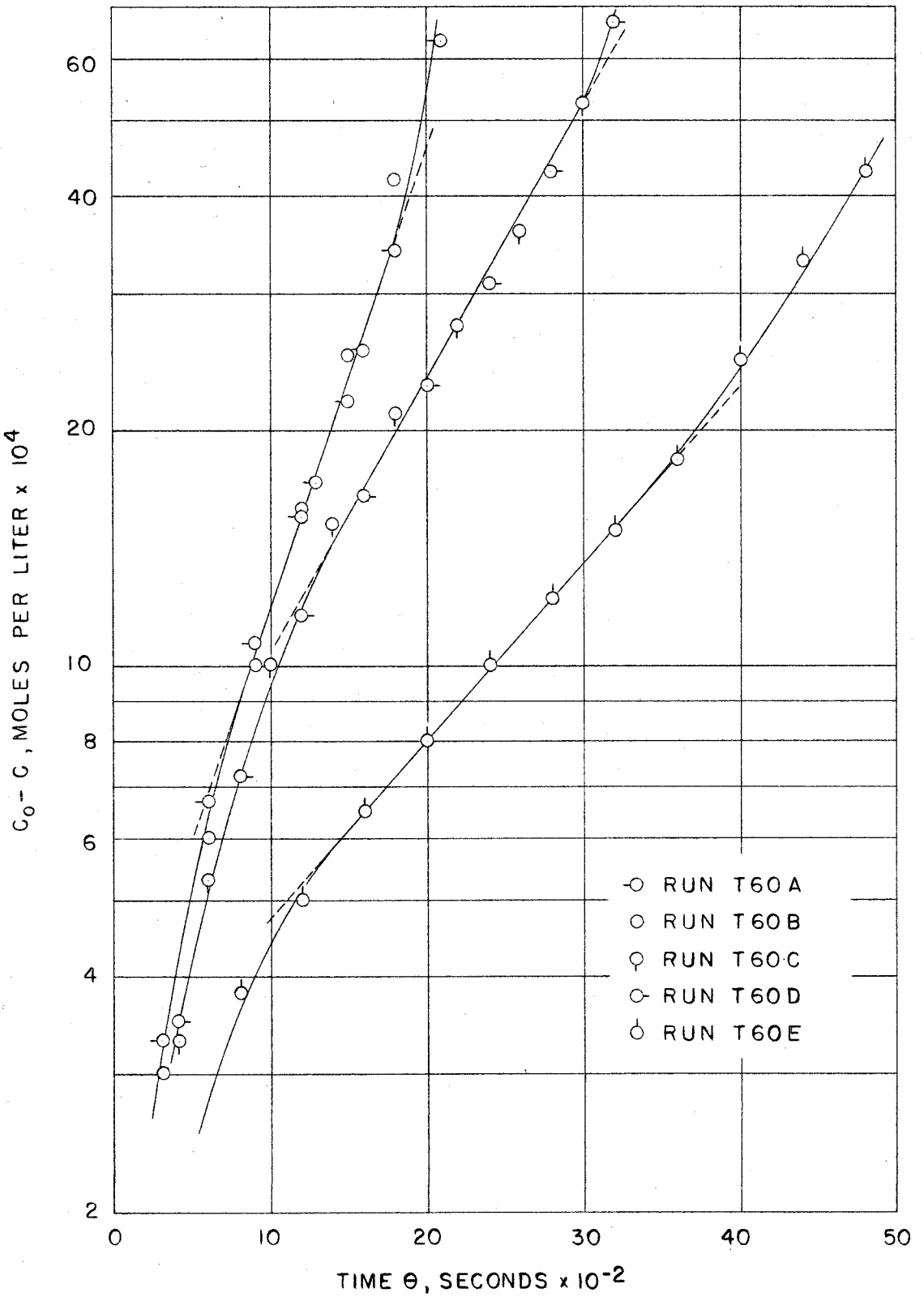

Figure 33--Thermal Decomposition Studies. Log (C_o - C) vs Time at 60°C

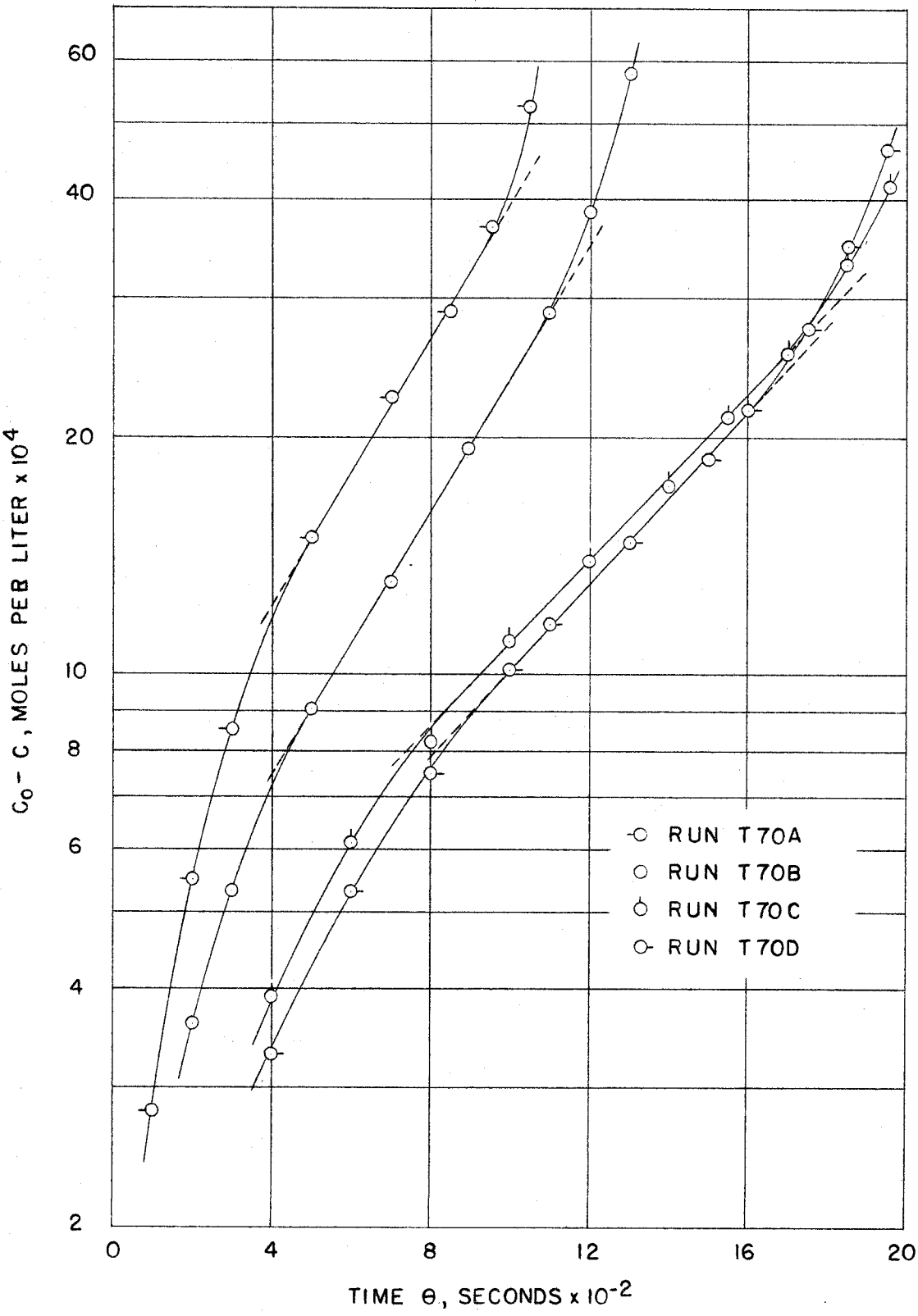

Figure 34--Thermal Decomposition Studies. Log (C_o - C) vs Time at 70°C

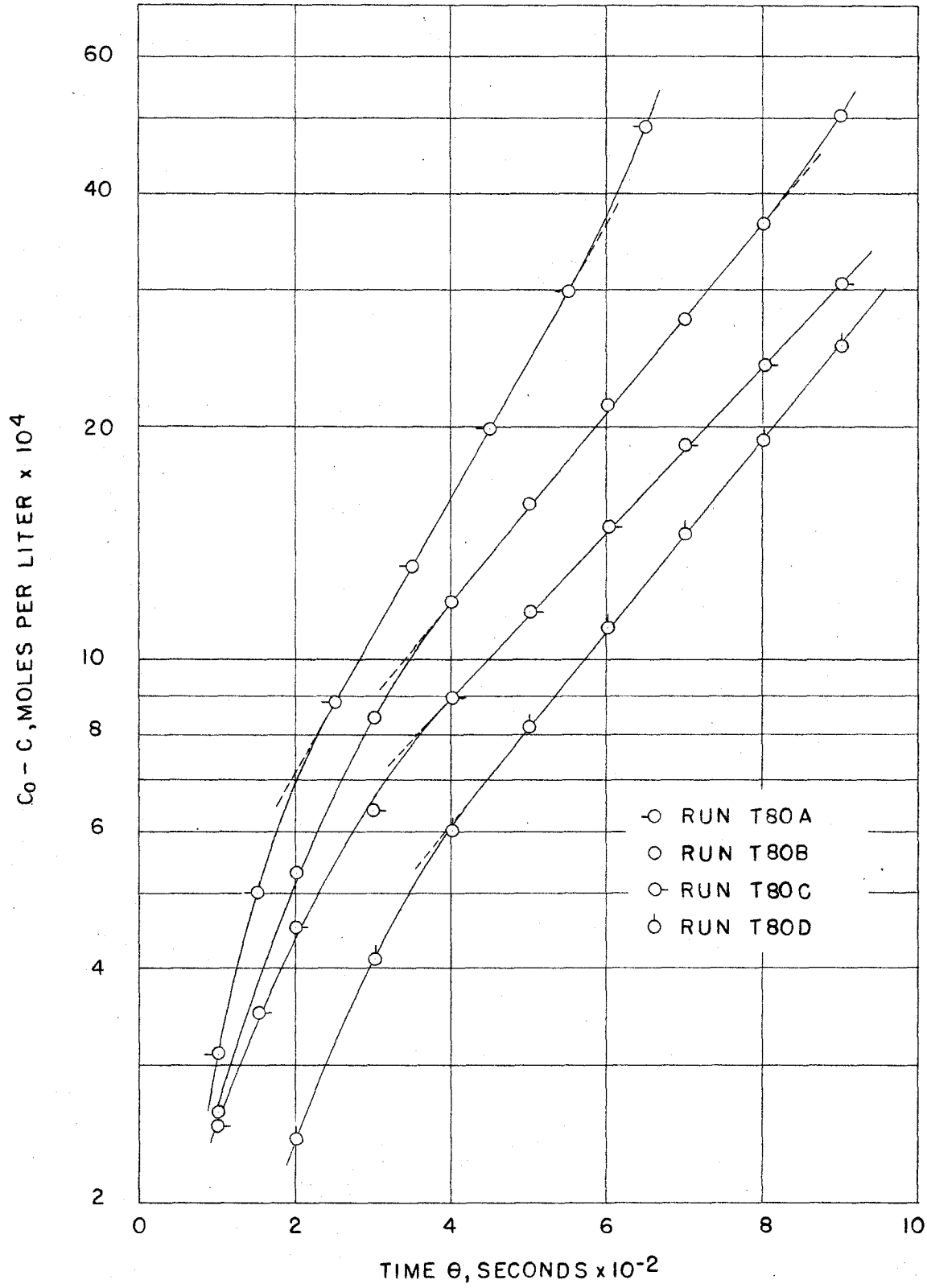

Figure 35--Thermal Decomposition Studies. Log (C_o - C) vs Time at 80°C

LIST OF TABLES

TABLE I

AIR OXIDATION STUDIES

DITHIONITE CONCENTRATION VS TIME AT 30°C

Run 30A

θ, Sec	$S_2O_4^=$ x 10^3 Moles/Liter
45	17.67
100	15.42
155	12.75
215	9.98
378	4.07
420	2.94
502	1.26
545	0.46
600	0.04

Run 30B

θ, Sec	$S_2O_4^=$ x 10^3 Moles/Liter
53	15.00
98	13.20
145	11.24
202	8.64
251	8.03
298	6.38
357	4.19
414	2.40
464	1.46
520	0.38
562	0.04

Run 30C

θ, Sec	$S_2O_4^=$ x 10^3 Moles/Liter
47	12.58
88	12.00
130	10.67
179	8.60
243	6.53
301	4.62
345	2.58
392	2.28
432	1.46
475	0.44
522	0.05

Run 30D

θ, Sec	$S_2O_4^=$ x 10^3 Moles/Liter
52	6.03
98	4.76
150	3.14
195	1.23
242	1.00
282	0.19
326	0.04

Run 30E

θ, Sec	$S_2O_4^=$ x 10^3 Moles/Liter
56	7.60
78	5.15
165	4.18
132	3.65
235	2.04
255	1.93
312	0.85
335	0.10

TABLE 2

AIR OXIDATION STUDIES

DITHIONITE CONCENTRATION VS TIME AT 40°C

Run 40A

θ, Sec	$S_2O_4^=$ x 10^3 Moles/Liter
20	6.02
66	4.86
115	3.27
159	1.94
203	0.91
247	0.15
280	0.03

Run 40B

θ, Sec	$S_2O_4^=$ x 10^3 Moles/Liter
28	8.58
77	6.72
130	4.73
199	2.42
238	1.53
273	0.95
314	0.29
352	0.04

Run 40C

θ, Sec	$S_2O_4^=$ x 10^3 Moles/Liter
44	11.03
100	8.06
175	4.20
220	2.44
265	1.28
310	0.43
350	0.03

Run 40D

θ, Sec	$S_2O_4^=$ x 10^3 Moles/Liter
52	16.42
122	12.00
172	9.81
225	6.02
300	3.63
350	2.12
395	1.16
437	0.07

Run 40E

θ, Sec	$S_2O_4^=$ x 10^3 Moles/Liter
41	18.18
91	15.50
130	12.33
198	8.60
264	5.64
313	3.77
362	2.25
406	0.81
448	0.05

TABLE 3

AIR OXIDATION STUDIES

DITHIONITE CONCENTRATION VS TIME AT 50°C

Run 50A

θ, Sec	$S_2O_4^=$ x 10^3 Moles/Liter
48	14.82
91	11.48
182	4.65
250	1.27
294	0.17
330	0.04

Run 50B

θ, Sec	$S_2O_4^=$ x 10^3 Moles/Liter
27	15.15
67	12.47
142	6.36
175	4.86
235	1.29
272	0.42
320	0.04

Run 50C

θ, Sec	$S_2O_4^=$ x 10^3 Moles/Liter
39	9.61
93	6.10
144	3.34
197	1.23
247	0.04

Run 50D

θ, Sec	$S_2O_4^=$ x 10^3 Moles/Liter
43	7.30
117	3.11
158	1.68
193	0.68
230	0.04

Run 50E

θ, Sec	$S_2O_4^=$ x 10^3 Moles/Liter
39	4.98
78	2.92
120	1.31
158	0.22
198	0.04

TABLE 4

AIR OXIDATION STUDIES
DITHIONITE CONCENTRATION VS TIME AT 60°C

Run 60A

θ, Sec	$S_2O_4^=$ x 10^3 Moles/Liter
60	11.94
102	8.54
137	5.10
181	2.37
218	0.67
289	0.02

Run 60B

θ, Sec	$S_2O_4^=$ x 10^3 Moles/Liter
38	16.59
108	8.90
185	2.76
233	0.68
272	0.04

Run 60C

θ, Sec	$S_2O_4^=$ x 10^3 Moles/Liter
47	10.69
84	6.98
122	3.97
181	0.19
196	0.04

Run 60D

θ, Sec	$S_2O_4^=$ x 10^3 Moles/Liter
48	5.35
83	2.94
124	1.20
158	0.23
192	0.05

Run 60E

θ, Sec	$S_2O_4^=$ x 10^3 Moles/Liter
39	3.92
85	1.64
124	0.18
160	0.04

Run 60F

θ, Sec	$S_2O_4^=$ x 10^3 Moles/Liter
38	3.52
77	1.70
120	0.21
156	0.02

TABLE 5

AIR OXIDATION STUDIES
DETERMINATION OF ORDER OF REACTION, n,
$(dC/d\theta)_o$ VS C_o AT 30, 40, 50, and 60°C

Run	Temperature °C	$(dC/d\theta)_o \times 10^5$ Moles/Liter, Sec	$C_o \times 10^3$ Moles/Liter, Sec
30A	30	5.06	20.20
30B	30	4.72	17.50
30C	30	4.43	15.85
30D	30	3.49	9.40
30E	30	3.25	7.72
40A	40	3.63	7.22
40B	40	4.01	9.73
40C	40	5.42	13.37
40D	40	6.11	19.37
40E	40	6.40	20.97
50A	50	9.24	19.25
50B	50	8.84	17.55
50C	50	7.29	12.40
50D	50	6.70	10.10
50E	50	6.30	7.30
60A	60	11.40	18.50
60B	60	12.07	20.77
60C	60	10.50	15.50
60D	60	7.70	9.00
60E	60	7.21	7.41
60F	60	6.20	5.80

TABLE 6

AIR OXIDATION STUDIES

k_c VS θ AT 30°C

Run 30A

θ, Sec	$k_c \times 10^4$ (Moles/Liter)$^{\frac{1}{2}}$Sec^{-1}
30	3.61
50	3.64
70	3.69
90	3.68
110	3.70
130	3.75
150	3.79
170	3.82
190	3.86

Run 30B

θ, Sec	$k_c \times 10^4$ (Moles/Liter)$^{\frac{1}{2}}$Sec^{-1}
30	3.59
50	3.60
70	3.66
90	3.64
110	3.68
130	3.72
150	3.74
170	3.80
190	3.82

Run 30C

θ, Sec	$k_c \times 10^4$ (Moles/Liter)$^{\frac{1}{2}}$Sec^{-1}
30	3.66
50	3.60
70	3.66
90	3.64
110	3.66
130	3.69
150	3.69
170	3.72
190	3.72

Run 30D

θ, Sec	$k_c \times 10^4$ (Moles/Liter)$^{\frac{1}{2}}$Sec^{-1}
30	3.73
50	3.84
70	3.92
90	3.98
110	4.08
130	4.14
150	4.24
170	4.32
190	4.40

Run 30E

θ, Sec	$k_c \times 10^4$ (Moles/Liter)$^{\frac{1}{2}}$Sec^{-1}
30	3.64
50	3.62
70	3.70
90	3.74
110	3.82
130	3.86
150	3.93
170	3.99
190	4.05

TABLE 6 (CONTINUED)

k_c VS θ AT 40°C

Run 40A

θ, Sec	$k_c \times 10^4$ $(\text{Moles/Liter})^{\frac{1}{2}}\text{Sec}^{-1}$
30	4.33
40	4.45
60	4.57
80	4.68
90	4.69
120	4.85
160	5.07

Run 40B

θ, Sec	$k_c \times 10^4$ $(\text{Moles/Liter})^{\frac{1}{2}}\text{Sec}^{-1}$
30	4.47
50	4.44
70	4.55
90	4.58
110	4.61
130	4.67
150	4.69
170	4.86
190	4.93

Run 40C

θ, Sec	$k_c \times 10^4$ $(\text{Moles/Liter})^{\frac{1}{2}}\text{Sec}^{-1}$
30	4.21
50	4.36
70	4.38
90	4.44
110	4.50
130	4.54
150	4.63
170	4.70
190	4.78

Run 40D

θ, Sec	$k_c \times 10^4$ $(\text{Moles/Liter})^{\frac{1}{2}}\text{Sec}^{-1}$
30	4.39
50	4.56
70	4.59
90	4.62
110	4.77
130	4.69
150	4.75
170	4.81
190	4.88

Run 40E

θ, Sec	$k_c \times 10^4$ $(\text{Moles/Liter})^{\frac{1}{2}}\text{Sec}^{-1}$
30	4.33
50	4.48
70	4.58
90	4.60
110	4.62
130	4.69
150	4.77
170	4.84
190	4.90

TABLE 6 (CONTINUED)

k_c VS θ AT 50°C

Run 50A

θ, Sec	$k_c \times 10^4$ $(\text{Moles/Liter})^{\frac{1}{2}}\text{Sec}^{-1}$
30	6.81
50	6.83
70	6.93
90	7.05
110	7.23
130	7.35
150	7.52
170	7.67
190	7.81
210	7.94

Run 50B

θ, Sec	$k_c \times 10^4$ $(\text{Moles/Liter})^{\frac{1}{2}}\text{Sec}^{-1}$
30	6.67
50	6.77
70	6.91
90	7.00
110	7.16
130	7.29
150	7.44
170	7.56
190	7.70
210	7.79

Run 50C

θ, Sec	$k_c \times 10^4$ $(\text{Moles/Liter})^{\frac{1}{2}}\text{Sec}^{-1}$
30	6.71
50	6.83
70	6.99
90	7.10
110	7.25
130	7.35
150	7.45
170	7.57
190	7.69
210	7.87

Run 50D

θ, Sec	$k_c \times 10^4$ $(\text{Moles/Liter})^{\frac{1}{2}}\text{Sec}^{-1}$
30	7.00
50	7.18
70	7.40
90	7.54
110	7.60
130	7.58
150	7.59
170	7.64
190	7.70

TABLE 6 (CONTINUED)

k_c VS θ AT 60°C

Run 60A

θ, Sec	$k_c \times 10^4$ (Moles/Liter)$^{\frac{1}{2}}$Sec^{-1}
30	8.72
50	8.88
70	9.01
90	9.11
110	9.25
130	9.28

Run 60B

θ, Sec	$k_c \times 10^4$ (Moles/Liter)$^{\frac{1}{2}}$Sec^{-1}
30	8.54
50	8.60
70	8.85
90	9.03
110	9.30
130	9.47
150	9.65

Run 60C

θ, Sec	$k_c \times 10^4$ (Moles/Liter)$^{\frac{1}{2}}$Sec^{-1}
30	8.76
50	8.96
70	9.07
90	9.40
110	9.70
130	9.90
150	10.20

Run 60D

θ, Sec	$k_c \times 10^4$ (Moles/Liter)$^{\frac{1}{2}}$Sec^{-1}
30	8.80
50	9.25
70	9.58
90	9.86
110	9.94

Run 60E

θ, Sec	$k_c \times 10^4$ (Moles/Liter)$^{\frac{1}{2}}$Sec^{-1}
30	8.80
50	9.04
70	9.18
90	9.45

Run 60F

θ, Sec	$k_c \times 10^4$ (Moles/Liter)$^{\frac{1}{2}}$Sec^{-1}
30	8.79
50	8.92
70	9.15
90	9.51

TABLE 7

AIR OXIDATION STUDIES
EFFECT OF STIRRING RATE AND AIR FLOW RATE.
DITHIONITE CONCENTRATION VS TIME AT 60°C

Run 60G

*Air Flow Rate = 295cc/min
Stirring Rate = 800 rpm

θ, Sec	$S_2O_4^=$ x 10^3 Moles/Liter
31	10.90
138	7.30
230	5.47
295	3.71
400	2.18
472	1.45
565	0.47
622	0.33
685	0.02

Run 60H

Air Flow Rate = 495cc/min
Stirring Rate = 800 rpm

θ, Sec	$S_2O_4^=$ x 10^3 Moles/Liter
38	9.67
113	6.55
206	2.98
260	1.81
310	0.85
355	0.34
401	0.02

Run 60J

Air Flow Rate = 720cc/min
Stirring Rate = 800 rpm

θ, Sec	$S_2O_4^=$ x 10^3 Moles/Liter
35	8.78
112	4.42
170	1.83
230	0.68
286	0.04

Run 60K

Air Flow Rate = 960cc/min
Stirring Rate = 800 rpm

θ, Sec	$S_2O_4^=$ x 10^3 Moles/Liter
27	8.92
102	4.27
162	1.63
208	0.57
252	0.02

Run 60L

Air Flow Rate = 1200cc/min
Stirring Rate = 800 rpm

θ, Sec	$S_2O_4^=$ x 10^3 Moles/Liter
33	7.65
100	3.40
160	1.41
210	0.20
250	0.03

Run 60M

Air Flow Rate = 2500cc/min
Stirring Rate = 1100 rpm

θ, Sec	$S_2O_4^=$ x 10^3 Moles/Liter
39	7.01
99	3.25
160	1.22
214	0.09
255	0.02

TABLE 8

AIR OXIDATION STUDIES
IONIC STRENGTH EFFECTS. DITHIONITE
CONCENTRATION VS TIME

Run 60N
μ = 0.50

θ, Sec	$S_2O_4^=$ x 10^3 Moles/Liter
36	9.42
127	3.00
200	0.27
265	0.04

Run 60P
μ = 0.30

θ, Sec	$S_2O_4^=$ x 10^3 Moles/Liter
42	7.95
135	1.94
187	0.35
222	0.04

Run 60Q
μ = 0.10

θ, Sec	$S_2O_4^=$ x 10^3 Moles/Liter
55	7.46
107	4.55
150	2.36
203	0.97
242	0.06

Run 60R
μ = 0.01 N

θ, Sec	$S_2O_4^=$ x 10^3 Moles/Liter
42	8.06
90	5.20
142	0.05

TABLE 9

AIR OXIDATION STUDIES
SULFITE AND THIOSULFATE CONCENTRATION VS TIME
AT 30° AND 60°C AND CONSTANT AIR RATE

Run 30A-A at 30°C

θ, Sec	$SO_3^=$ x 10^3 Moles/Liter
147	15.27
276	12.85
463	9.58
637	6.02

Run 30A-B at 30°C

θ, Sec	$SO_3^=$ x 10^3 Moles/Liter
33	20.50
153	19.54
255	17.64
355	17.13
472	15.03
578	13.84
648	13.03

Run 60A-A at 60°C

θ, Sec	$SO_3^=$ x 10^3 Moles/Liter
56	20.15
138	18.75
188	17.94
248	16.36
298	15.02

Run 60A-B at 60°C

θ, Sec	$SO_3^=$ x 10^3 Moles/Liter
48	20.37
93	19.66
161	18.77
237	17.44
293	16.22
370	15.03
427	14.02

Run 60A-C at 60°C

θ, Sec	$S_2O_3^=$ x 10^3 Moles/Liter
56	27.88
156	27.85
297	28.07
436	28.37
637	28.29

TABLE 10

AIR OXIDATION STUDIES

END PRODUCT ANALYSES

Run EP - A Diffusion controlled oxidation

Initial $[S_2O_4^{=}]$ = 10.30×10^{-3} moles/liter

Reaction time = 29 hrs

Average analyses:

$[SO_3^{=}]$ = 13.14×10^{-3} moles/liter

$[SO_4^{=}]$ = 5.72×10^{-3} moles/liter

$[S_2O_3^{=}]$ = 1.60×10^{-3} moles/liter

$$\frac{[SO_3^{=}]}{[SO_4^{=}]} = 2.3$$

Run EP - B Air oxidation

Initial $[S_2O_4^{=}]$ = 9.50×10^{-3} moles/liter

Analysis (corrected for 8.8% thermal decomposition):

$[SO_3^{=}]$ = 13.16×10^{-3} moles/liter

$[SO_4^{=}]$ = 4.16×10^{-3} moles/liter

$[S_2O_3^{=}]$ = 0.42×10^{-3} moles/liter

$$\frac{[SO_3^{=}]}{[SO_4^{=}]} = 3.16$$

Run EP - C Air oxidation

Initial $[S_2O_4^{=}]$ = 10.10×10^{-3} moles/liter

Analysis (corrected for 21% thermal decomposition):

$[SO_3^{=}]$ = 11.90×10^{-3} moles/liter

$[SO_4^{=}]$ = 4.26×10^{-3} moles/liter

$[S_2O_3^{=}]$ = 1.00×10^{-3} moles/liter

$$\frac{[SO_3^{=}]}{[SO_4^{=}]} = 2.78$$

Average: $\frac{[SO_3^{=}]}{[SO_4^{=}]} = 2.97$

TABLE 11

AIR OXIDATION STUDIES
SOLUBILITY OF SODIUM DITHIONITE AT 0°C

Run No.	Solubility in gms/100 ml H_2O at 0°C
S-A	14.39
S-B	14.38
S-C	14.35
S-D	13.85
S-E	13.69
S-F	12.51
S-6	11.63
S-H	11.68
S-I	13.15
S-J	13.52
S-K	12.00

Average = 13.20 σ = 1.08 or 8% of 13.20

TABLE 12

DITHIONITE STRUCTURE STUDIES. ELECTROLYTIC GENERATION OF DITHIONITE

Run 100A pH = 5.3 Temperature = 2.2°C Current = 100 ma

Time sec	Cathode Potential	Total Moles of $S_2O_4^=$ formed x 10^4	Moles of Electrons passed x 10^4
120	-0.67	0.35	1.244
420	-0.68	1.58	4.351
1020	-0.68	4.03	10.57
2100	-0.71	6.20	21.77
2700	-0.71	10.51	28.00
3300	-0.72	11.74	34.20
3900	-0.73	15.12	40.41
4500	-0.73	17.36	46.64

Average Current Efficiency = 75.0%

Run 150A pH = 5.0 Temperature = 2.8°C Current = 150 ma

300	-0.73	1.25	4.66
420	-0.74	2.49	6.53
900	-0.74	5.33	13.98
1020	-0.75	6.32	15.85
1500	-0.75	9.16	23.32
1620	-0.75	10.00	25.18
2280	-0.75	13.92	35.43
2400	-0.75	14.64	37.30
3180	-0.75	19.51	49.40
3360	-0.75	20.47	52.20
4200	-0.75	24.97	65.30
4320	-0.75	26.16	67.18

Average Current Efficiency = 78.5%

Run 200A pH = 5.1 Temperature = 2.8°C Current = 200 ma

300	-0.98	1.69	6.22
660	-0.97	5.00	13.68
1080	-0.96	8.40	22.38
1620	-0.97	12.87	33.58
2040	-0.96	16.44	42.30
2700	-0.96	21.46	55.92

Average Current Efficiency = 77.2%

TABLE 13

THERMAL DECOMPOSITION STUDIES. DITHIONITE CONCENTRATION VS TIME AT 60°C

T 60A		T 60B		T 60C	
θ, Sec	$S_2O_4^=$ x 10^3 Moles/Liter	θ, Sec	$S_2O_4^=$ x 10^3 Moles/Liter	θ, Sec	$S_2O_4^=$ x 10^3 Moles/Liter
105	10.75	68	10.14	89	9.23
258	10.33	145	9.52	220	8.80
375	10.63	265	9.74	267	9.20
573	9.89	390	9.44	343	8.85
708	9.49	488	9.45	480	9.18
993	9.45	582	9.45	567	7.92
1065	9.77	742	9.27	644	9.05
1218	9.83	870	9.23	757	8.50
1479	8.94	1036	8.50	823	8.60
1595	8.51	1164	8.62	882	8.20
1856	7.74	1368	7.11	1005	8.20
2040	4.37	1515	6.61	1058	8.03
2225	0.05	1716	6.73	1244	7.78
		1863	5.32	1317	7.93
		2036	1.53	1375	6.57
		2050	0.03	1433	6.36
				1496	7.27
				1551	7.86
				1610	8.20
				1669	7.61
				1727	6.50
				1915	8.32
				1971	7.02
				2139	6.29
				2383	6.50
				2438	5.71
				2487	5.27
				2624	5.90
				2788	4.93
				3019	3.78
				3233	2.18
				3340	0.03

TABLE 13 (CONTINUED)

T 60D		T 60E	
θ, Sec	$S_2O_4^=$ x 10^3 Moles/Liter	θ, Sec	$S_2O_4^=$ x 10^3 Moles/Liter
74	8.38	58	5.98
272	8.32	250	5.68
350	7.72	336	5.76
460	8.43	461	5.58
606	7.93	594	5.67
694	7.97	681	5.41
786	7.46	807	5.28
893	7.47	900	5.32
994	7.02	1150	5.35
1071	7.10	1365	5.35
1171	7.37	1512	4.46
1251	7.08	1700	5.05
1437	6.42	1983	5.17
1500	7.00	2155	5.21
1571	7.02	2324	5.51
1644	6.62	2572	4.52
1712	5.10	2665	4.92
1803	6.31	2810	5.04
1886	6.42	2947	4.74
1976	5.80	3400	4.36
2111	6.32	3480	4.27
2178	6.23	3585	4.24
2250	6.36	3685	4.07
2324	4.18	3950	3.43
2441	5.55	4059	3.20
2508	5.22	4255	2.74
2570	5.94	4587	2.17
2665	4.60	5025	1.13
2739	4.62		
2854	4.06		
2977	3.19		
3030	2.95		
3089	2.26		
3148	1.45		

TABLE 14

THERMAL DECOMPOSITION STUDIES. DITHIONITE CONCENTRATION VS TIME AT 70°C

T 70A

θ, Sec	$S_2O_4^=$ x 10^3 Moles/Liter
55	11.23
176	10.92
340	10.26
450	10.18
648	8.96
785	8.84
950	7.80
1057	6.10
1175	1.40
1240	-

T 70B

θ, Sec	$S_2O_4^=$ x 10^3 Moles/Liter
75	9.40
190	9.54
342	9.12
455	9.14
610	8.63
750	8.41
900	7.64
1040	7.21
1170	6.16
1285	4.42
1360	1.45
1445	-

T 70C

θ, Sec	$S_2O_4^=$ x 10^3 Moles/Liter
75	6.06
200	5.52
352	5.56
570	5.52
690	5.22
795	5.04
955	5.03
1085	4.71
1225	4.81
1350	4.36
1475	4.07
1620	3.22
1788	3.36
1835	2.85
1940	1.96
2125	-

T 70D

θ, Sec	$S_2O_4^=$ x 10^3 Moles/Liter
60	5.71
175	5.66
316	5.31
475	5.36
618	4.85
750	4.84
875	4.78
1030	4.70
1155	4.58
1235	4.41
1360	4.25
1525	3.83
1627	3.25
1732	3.08
1812	2.26
1892	1.33
1993	0.35
2025	-

TABLE 15

THERMAL DECOMPOSITION STUDIES. DITHIONITE CONCENTRATION VS TIME AT 80°C

Run T 80A

θ, Sec	$S_2O_4^=$ x 10^3 Moles/Liter
70	10.37
237	9.76
385	9.05
465	8.56
585	7.09
670	5.17
735	1.20
840	-

Run T 80B

θ, Sec	$S_2O_4^=$ x 10^3 Moles/Liter
45	9.05
120	8.82
265	8.48
345	8.17
465	7.55
540	7.37
660	6.71
740	6.05
828	5.45
935	3.39
1005	-

Run T 80C

θ, Sec	$S_2O_4^=$ x 10^3 Moles/Liter
65	6.35
230	5.95
375	5.78
452	5.44
560	5.07
738	4.42
882	3.55
975	2.67
1120	0.49
1195	-

Run T 80D

θ, Sec	$S_2O_4^=$ x 10^3 Moles/Liter
70	6.42
150	6.09
240	6.06
402	5.89
480	5.40
570	5.11
720	4.78
800	4.43
875	4.14
970	3.35
1100	1.60
1175	0.29
1240	-

TABLE 16

THERMAL DECOMPOSITION STUDIES. DITHIONITE CONCENTRATION VS TIME IN BUFFERED SYSTEMS AT 60°C

Run TB 60C pH = 6.00

θ, Sec	$S_2O_4^=$ x 10^3 Moles/Liter
88	11.35
215	11.45
554	11.00
1108	10.86
2095	9.32
2740	0.09

Run TB 60D pH = 5.50

θ, Sec	$S_2O_4^=$ x 10^3 Moles/Liter
70	10.96
164	11.18
350	10.60
532	10.52
728	10.53
1074	9.43
1230	8.39
1338	5.82
1456	0.03

Run TB 60E pH = 5.00

θ, Sec	$S_2O_4^=$ x 10^3 Moles/Liter
55	10.99
126	10.84
202	10.20
258	9.57
346	7.70
417	0.08

Run TB 60F pH = 5.00

θ, Sec	$S_2O_4^=$ x 10^3 Moles/Liter
50	10.90
117	10.62
187	10.59
318	8.70
378	4.76
400	0.04

Run TB 60G pH = 4.80

θ, Sec	$S_2O_4^=$ x 10^3 Moles/Liter
41	10.81
91	10.91
145	10.70
203	8.86
244	0.04

Run TB 60H pH = 5.00

θ, Sec	$S_2O_4^=$ x 10^3 Moles/Liter
68	9.47
142	9.55
218	8.75
304	7.97
401	6.81
493	0.09

TABLE 17

THERMAL DECOMPOSITION STUDIES. H^+ CONCENTRATION VS TIME AT 60° AND 70°C

Run T 60A		Run T 70C	
θ, Sec	$H^+ \times 10^7$ Moles/Liter	θ, Sec	$H^+ \times 10^7$ Moles/Liter
170	7.95	30	7.95
290	7.75	140	8.73
340	7.75	220	8.73
410	7.75	300	8.32
525	11.20	400	7.57
540	11.50	610	6.58
610	12.60	730	6.58
670	11.75	850	6.44
760	11.00	980	6.30
810	11.00	1140	5.87
890	17.75	1295	5.87
910	18.60	1410	5.74
930	19.10	1540	5.62
990	17.75	1685	5.74
1050	17.35	1755	6.00
1120	15.50	1855	6.30
1185	14.10	1950	6.90
1210	13.80	2140	10.50
1275	12.00	2210	12.90
1330	11.75	2325	12.90
1410	11.50		
1435	11.20		
1570	11.00		
1540	10.70		
1660	10.00		
1750	10.00		
1820	10.00		
1900	10.70		
1930	11.20		
1980	11.50		
2060	13.80		
2130	22.50		
2210	23.80		
2251	24.80		
2320	27.80		
2357	25.80		
2475	27.80		

TABLE 18

THERMAL DECOMPOSITION STUDIES. EFFECT OF O_2 ON H^+ IN UNBUFFERED SYSTEM AT 60°C

Run T 60F $C_o = 9.28 \times 10^{-3}$ Moles/Liter

θ, Sec	$H^+ \times 10^7$ Moles/Liter
150	4.80
300	4.90
550	4.90
750	5.15
950	5.15
1100	5.15
1300	5.25
1450	5.37
1650	5.37
1950	5.25
2050	5.25
2150	5.37
2550	5.37
2560	air injected (2cc)
2600	5.87
2650	6.90
2700	7.10
2750	7.40
2800	7.60
2900	7.60
2970	air injected (10cc)
2990	7.95
3000	11.20
3050	13.45
3100	14.10
3150	14.45

(Continued)

θ, Sec	$H^+ \times 10^7$ Moles/Liter
3200	14.75
3290	14.75
3300	air injected (10cc)
3320	21.45
3350	31.60
3360	37.22
3400	43.50
3450	42.55
3500	37.22
3550	31.60
3600	26.80
3650	24.65
3700	21.95
3750	20.90
3800	20.50
3850	21.95
3900	37.22
3950	48.90
4000	57.25
4050	66.20
4100	72.25
4150	77.50
4200	83.25
4250	87.30
4300	89.35
4350	93.70

TABLE 19

THERMAL DECOMPOSITION STUDIES. EFFECTS OF H^+ ON INDUCTION PERIOD TIME, AND $\left[\frac{dc}{d\theta}\right]_o$ VS H^+ AT 60^oC AND $C_o = 11.0 \times 10^{-3}$ MOLES/LITER

Run	$H^+ \times 10^7$ Moles/Liter	Time of Induction Period, Sec	$\left[\frac{dc}{d\theta}\right]_o \times 10^7 \frac{\text{Moles}}{\text{Liter}}\ \text{sec}^{-1}$
TB 60A	1	Not measured	2.2
TB 60C	10	2200	6.8
TB 60D	31.6	800	9.1
TB 60E & F	100	275	26.9
TB 60G	158.2	180	29.1

TABLE 20

THERMAL DECOMPOSITION STUDIES. EFFECTS OF ADDITIVES.
DITHIONITE CONCENTRATION VS TIME AT
60°C IN SYSTEM BUFFERED AT pH 7

Run TB 60A		Run TB 60B	
θ, Sec	$S_2O_4^{=}$ x 10^3 Moles/Liter	θ, Sec	$S_2O_4^{=}$ x 10^3 Moles/Liter
112	11.10	94	10.35
241	10.40	299	10.00
599	10.29	946	9.94
1044	10.64	1621	9.90
1694	9.90	2129	10.21
2781	9.85	2845	10.41
4281	10.32	4476	9.89
6178	9.52	6434	9.56
11297	8.41	7073	9.45
13754	8.24	8863	9.46
14965	8.21	9878	9.29
		13162	8.38

TABLE 21

THERMAL DECOMPOSITION STUDIES. EFFECTS OF END PRODUCTS. DITHIONITE CONCENTRATION VS TIME AT 60°C IN SYSTEM BUFFERED AT pH 5

Run TB 60Ja

θ, Sec	$S_2O_4^{=}$ x 10^3 Moles/Liter
42	5.16
97	5.10
155	4.86
209	4.64
271	4.95
337	4.76
392	3.50
469	4.41
565	3.72
682	-

Run TB 60Jb

θ, Sec	$S_2O_4^{=}$ x 10^3 Moles/Liter
39	5.45
115	4.97
216	2.66
293	-

Run TB 60Jc

θ, Sec	$S_2O_4^{=}$ x 10^3 Moles/Liter
40	5.60
95	3.49
167	3.75
224	-

Run TB 60Ka

θ, Sec	$S_2O_4^{=}$ x 10^3 Moles/Liter
44	5.51
91	5.30
148	4.80
202	4.58
256	4.90
306	4.43
365	3.46
419	4.61
481	4.32
538	3.79
601	3.14
671	-

Run TB 60Kb

θ, Sec	$S_2O_4^{=}$ x 10^3 Moles/Liter
38	5.71
89	3.94
147	4.81
193	4.54
262	1.53
334	-

Run TB 60Kc

θ, Sec	$S_2O_4^{=}$ x 10^3 Moles/Liter
40	5.86
89	5.51
145	4.51
197	2.06
256	-

TABLE 22

THERMAL DECOMPOSITION STUDIES. END PRODUCT ANALYSIS OF 30°C RUN

Initial Dithionite Concentration = 7.32×10^{-3} Moles/Liter

Final HSO_3^- Concentration = 7.32×10^{-3} Moles/Liter

Final $S_2O_3^=$ Concentration = 3.32×10^{-3} Moles/Liter

Ratio of $HSO_3^-/S_2O_3^=$ = 2.2

Sulfur Balance:

Sulfur in = 14.64×10^{-3} Moles/Liter

Sulfur out = 7.32×10^{-3}
$+6.64 \times 10^{-3}$
13.96×10^{-3} Moles/Liter

Sulfur unaccounted for = 0.68 Moles/Liter

Therefore, % of dithionite forming other products

$$= \frac{0.34 \times 10^{-3}}{7.32 \times 10^{-3}} \times 100 = 4.6\%$$

TABLE 23

THERMAL DECOMPOSITION STUDIES. DETERMINATION OF ORDER OF REACTION, n, IN UNBUFFERED SYSTEMS. $(dc/d\Theta)_o$ VS C_o AT 60, 70, AND 80°C

Run	Temperature °C	$C_o \times 10^3$ Moles/Liter	$(dc/d\Theta)_o \times 10^7$ Moles/Liter, Sec^{-1}
T 60A	60	10.85	10.32
T 60B	60	9.90	8.98
T 60C	60	9.25	8.28
T 60D	60	8.67	7.35
T 60E	60	6.00	4.05
T 70A	70	11.38	26.2
T 70B	70	9.78	17.3
T 70C	70	6.02	8.96
T 70D	70	5.72	8.58
T 80A	80	10.58	31.5
T 80B	80	9.17	24.4
T 80C	80	6.50	15.1
T 80D	80	6.42	12.3

TABLE 24

THERMAL DECOMPOSITION STUDIES. DETERMINATION OF ORDER OF REACTION, n , IN SYSTEM BUFFERED AT pH 5. $(dc/d\theta)_o$ VS C_o AT 60°C

Run	$C_o \times 10^3$ Moles/Liter	$(dc/d\theta)_o \times 10^7$ (Moles/Liter)(Sec^{-1})
TB 60 E & F	11.05	26.9
TB 60H	9.95	25.2
TB 60J	5.40	9.1

TABLE 25

THERMAL DECOMPOSITION STUDIES

k_c VS C_o AT 60, 70, AND 80°C

Run	Temperature °C	$C_o \times 10^3$ Moles/Liter	k_c $\frac{\text{Moles}}{\text{Liter}}^{-1}$ Sec^{-1}
T 60A	60	10.85	1.70
T 60B	60	9.90	1.70
T 60C	60	9.25	1.60
T 60D	60	8.67	1.70
T 60E	60	6.00	1.62
		$[H^+]_o^{\frac{1}{2}}$ (avg) = 5.38×10^{-4} Moles/Liter	$k_{c(avg)}$ = 1.67 $\frac{\text{Moles}}{\text{Liter}}^{-1}$ Sec^{-1}
T 70A	70	11.38	3.09
T 70B	70	9.78	2.56
T 70C	70	6.02	2.75
T 70D	70	5.72	2.84
		$[H^+]_o^{\frac{1}{2}}$ (avg) = 6.98×10^{-4} Moles/Liter	$k_{c(avg)}$ = 2.81 $\frac{\text{Moles}}{\text{Liter}}^{-1}$ Sec^{-1}
T 80A	80	10.58	4.67
T 80B	80	9.17	4.49
T 80C	80	6.50	4.65
T 80D	80	6.42	3.86
		$[H^+]_o^{\frac{1}{2}}$ (avg) = 6.20×10^{-4} Moles/Liter	$k_{c(avg)}$ = 4.38 $\frac{\text{Moles}}{\text{Liter}}^{-1}$ Sec^{-1}

TABLE 26

THERMAL DECOMPOSITION STUDIES. $(C_o - C)$ VS TIME AT 60, 70, AND 80°C

Run T 60A $C_o = 10.85 \times 10^{-3}$ moles/liter Run T 60B $C_o = 10.00 \times 10^{-3}$ moles/liter

Sec	$C_o - C$ $\times 10^3$	C $\times 10^3$	Sec	$C_o - C$ $\times 10^3$	C $\times 10^3$
0	0	10.85	0	0	10.00
100	0.10	10.75	100	0.11	9.89
200	0.22	10.63	200	0.21	9.79
300	0.33	10.52	300	0.30	9.70
400	0.44	10.41	400	0.40	9.60
500	0.55	10.30	500	0.50	9.50
600	0.67	10.18	600	0.60	9.40
700	0.80	10.05	700	0.70	9.30
800	0.93	9.92	800	0.84	9.16
900	1.07	9.78	900	1.00	9.00
1000	1.22	9.63	1000	1.16	8.84
1100	1.37	9.48	1100	1.35	8.65
1200	1.55	9.30	1200	1.58	8.42
1300	1.72	9.13	1300	1.84	8.16
1400	1.93	8.92	1400	2.14	7.86
1500	2.19	8.66	1500	2.50	7.50
1600	2.52	8.33	1600	2.94	7.06
1700	2.91	7.94	1700	3.48	6.52
1800	3.40	7.45	1800	4.20	5.80
1900	4.05	6.80	1900	5.25	4.75
2000	4.90	5.95	2000	7.15	2.85
2100	6.30	4.55	2100	10.00	0.00
2200	10.85	0.00			

TABLE 26 (CONTINUED)

$(C_o - C)$ VS TIME AT 60, 70, AND 80°C

Run T 60C

Sec	$C_o - C$ x 10^3	C x 10^3
0	0	9.20
200	0.19	9.01
400	0.35	8.85
600	0.54	8.66
800	0.72	8.48
1000	0.92	8.28
1200	1.16	8.04
1400	1.40	7.80
1600	1.65	7.55
1800	1.95	7.25
2000	2.28	6.92
2200	2.65	6.55
2400	3.09	6.11
2600	3.60	5.60
2800	4.30	4.90
3000	5.25	3.95
3200	6.68	2.52
3400	9.20	0.00

Run T 60D

Sec	$C_o - C$ x 10^3	C x 10^3
0	0	8.50
200	0.15	8.35
400	0.33	8.17
600	0.53	7.97
800	0.75	7.75
1000	1.00	7.50
1200	1.27	7.23
1400	1.52	6.98
1600	1.80	6.70
1800	2.10	6.40
2000	2.40	6.10
2200	2.72	5.78
2400	3.12	5.38
2600	3.60	4.90
2800	4.25	4.25
3000	5.25	3.25
3200	7.50	1.00
3400	8.50	0.00

Run T 60E

Sec	$C_o - C$ x 10^3	C x 10^3
0	0	6.00
200	0.10	5.90
400	0.20	5.80
600	0.29	5.71
800	0.38	5.62
1000	0.42	5.58
1200	0.50	5.50
1400	0.58	5.42
1600	0.65	5.35
1800	0.72	5.28
2000	0.80	5.20
2200	0.90	5.10
2400	1.00	5.00
2600	1.10	4.90
2800	1.22	4.78
3000	1.35	4.65
3200	1.49	4.51
3400	1.63	4.37
3600	1.83	4.17
3800	2.11	3.89
4000	2.48	3.52
4200	2.86	3.14
4400	3.30	2.70
4600	3.80	2.20
4800	4.30	1.70
5000	4.87	1.13

TABLE 26 (CONTINUED)

$(C_o - C)$ VS TIME AT 60, 70, AND 80°C

Run T 70A C_o=11.38 x 10^{-3} moles/liter

Sec	$C_o - C$ x 10^3	C x 10^3
0	0	11.38
100	0.28	11.10
200	0.55	10.83
300	0.85	10.53
400	1.17	10.21
500	1.49	9.89
600	1.86	9.52
700	2.24	9.14
800	2.62	8.76
850	2.88	8.50
900	3.23	8.15
950	3.80	7.68
1000	4.35	7.03
1050	5.23	6.15
1100	6.38	5.00
1150	8.28	3.10

Run T 70B C_o=9.78 x 10^{-3} moles/liter

Sec	$C_o - C$ x 10^3	C x 10^3
0	0	9.78
100	0.18	9.60
200	0.36	9.42
300	0.53	9.25
400	0.72	9.06
500	0.90	8.88
600	1.09	8.69
700	1.31	8.47
800	1.58	8.20
900	1.94	7.84
1000	2.36	7.42
1100	2.88	6.90
1150	3.29	6.49
1200	3.86	5.92
1250	4.66	5.12
1300	5.78	4.00
1350	7.78	5.00

Run T 70C C_o=6.02 x 10^{-3} moles/liter

Sec	$C_o - C$ x 10^3	C x 10^3
0	0	6.02
200	0.20	5.82
400	0.39	5.63
600	0.61	5.41
800	0.82	5.20
1000	1.10	4.92
1100	1.23	4.79
1200	1.39	4.63
1300	1.55	4.47
1400	1.74	4.28
1500	1.99	4.03
1550	2.11	3.91
1600	2.24	3.78
1650	2.41	3.61
1700	2.57	3.45
1750	2.77	3.25
1800	3.02	3.00
1850	3.32	2.70

Run T 70D C_o=5.72 x 10^{-3} moles/liter

Sec	$C_o - C$ x 10^3	C x 10^3
0	0	5.72
200	0.15	5.57
400	0.33	4.29
600	0.53	5.19
800	0.75	4.97
1000	1.02	4.70
1100	1.16	4.56
1200	1.32	4.40
1300	1.48	4.24
1400	1.65	4.07
1500	1.88	3.84
1550	2.02	3.70
1600	2.18	3.54
1650	2.37	3.35
1700	2.56	3.16
1750	2.82	2.90
1800	3.12	2.60
1850	3.50	2.22
1900	3.95	1.77
1950	4.64	1.98

TABLE 26 (CONTINUED)

$(C_o - C)$ VS TIME AT 60, 70, 80°C

Run T 80A $C_o = 10.58 \times 10^{-3}$ moles/liter Run T 80B $C_o = 9.17 \times 10^{-3}$ moles/liter

θ Sec	$C_o - C$ $\times 10^3$ moles/liter	C $\times 10^3$ moles/liter	θ Sec	$C_o - C$ $\times 10^3$ moles/liter	C $\times 10^3$ moles/liter
0	0	10.58	0	0	9.17
50	0.16	10.52	50	0.14	9.03
100	0.31	10.27	100	0.26	8.91
150	0.50	10.08	150	0.38	8.79
200	0.68	9.90	200	0.53	8.64
250	0.88	9.70	250	0.68	8.49
300	1.08	9.50	300	0.84	8.33
350	1.32	9.26	350	0.99	8.18
400	1.61	8.97	400	1.18	7.99
450	1.98	8.60	450	1.37	7.80
500	2.43	8.15	500	1.59	7.58
550	2.99	7.59	550	1.85	7.32
600	3.78	6.80	600	2.13	7.04
650	4.88	5.70	650	2.44	6.73
700	6.60	3.98	700	2.77	6.40
725	8.21	2.37	750	3.17	6.00
740	10.58	0	800	3.67	5.50
			850	4.26	4.91
			900	5.05	4.12
			950	6.18	2.99
			975	7.01	2.16
			1000	8.42	0.75

TABLE 26 (CONTINUED)

$(C_o - C)$ VS TIME AT 60, 70, 80°C

Run T 80C $C_o = 6.50 \times 10^{-3}$ moles/liter Run T 80D $C_o = 6.42 \times 10^{-3}$ moles/liter

Sec	$C_o - C$ $\times 10^3$	C $\times 10^3$	Sec	$C_o - C$ $\times 10^3$	C $\times 10^3$
0	0	6.50	0	0	6.42
50	0.15	6.35	50	0.04	6.38
100	0.25	6.25	100	0.12	6.30
150	0.35	6.15	150	0.18	6.24
200	0.45	6.05	200	0.24	6.18
250	0.53	5.97	250	0.32	6.10
300	0.64	5.86	300	0.41	6.01
350	0.76	5.74	350	0.50	5.92
400	0.89	5.61	400	0.60	5.82
450	1.01	5.49	450	0.70	5.72
500	1.15	5.35	500	0.82	5.60
550	1.30	5.20	550	0.94	5.48
600	1.48	5.02	600	1.10	5.32
650	1.67	4.83	650	1.26	5.16
700	1.89	4.61	700	1.45	4.97
750	2.11	4.39	750	1.67	4.75
800	2.40	4.10	800	1.92	4.50
850	2.71	3.79	850	2.22	4.20
900	3.07	3.43	900	2.54	3.88
950	3.50	3.00	950	2.94	3.48
1000	4.00	2.50	1000	3.42	3.00
1050	4.63	1.96	1050	4.04	2.38
1100	5.52	0.98	1100	4.82	1.60
			1150	5.67	0.75
			1190	6.42	0

SECTION I

APPENDIX I

TABLE 1A

COMPOSITION OF THE BUFFER SOLUTIONS

TOTAL VOLUME OF WATER SOLUTION = 1000 cc

Acid Salt	Weight of Acid-Salt grams	Weight of NaOH grams	pH
KH_2PO_4	6.800	1.190	7.0
KH_2PO_4	6.800	0.228	6.0
$KHC_8H_4O_4$	10.220	1.506	5.5
$KHC_8H_4O_4$	10.220	0.954	5.0
$KHC_8H_4O_4$	10.220	0.708	4.8
$KHC_8H_4O_4$	10.220	0.160	4.0

SECTION II

A pH STUDY OF THE α-CHYMOTRYPSIN CATALYSED HYDROLYSIS OF METHYL HIPPURATE

INTRODUCTION

The effects of pH changes on the velocity of enzyme catalysed reactions have been the object of a great many investigations. Since several authors (1,2) have recently reviewed the subject in detail, no effort will be made here to duplicate their efforts. A very brief summary of the theoretical papers pertinent to the study reported here, as well as a more detailed description of experimental investigations closely related to this study will, however, be helpful.

The fact that reactions catalysed by enzymes are sensitive to changes in pH has been recognized since enzyme systems were first investigated. Extremes of acidity or basicity cause denaturation of the protein substance in the enzymes, hence catalytic activity is irreversibly reduced under these conditions. However, within a rather broad band of pH values, frequently around neutrality, a large number of enzymes undergo apparently reversible changes that cause the observed rate of the enzyme catalysed reaction to pass through a maximum as pH is changed in one direction. This is the basis for the so-called "pH-optimum" of an enzyme catalysed reaction, namely that pH at which the rate of reaction is a maximum.

As early as 1911 Davidson and Michaelis (3) postulated that the presence of an acidic and a basic functional group on the enzyme both of which must be in a certain state of

protonation for the enzyme to be catalytically active would explain the observed pH-optimum of certain reactions. Since its first proposal this basic theory has been modified only slightly in principle, although important extensions and interpretations of the theory and its results have been made. Important to mention here are the modifications that acidic and basic groups on the enzyme-substrate complex (4) instead of on the enzyme, or on both the enzyme and the enzyme-substrate complex (5), would also explain the observed facts. Moreover, ionizations of the substrate itself (6) or competitive interaction of the substrate with hydronium ions for the functional group on the enzyme (7) further complicate any simple conclusions which one might draw from pH-optimum curves for an enzyme-substrate system. Since 1953 a number of important papers (2,6,8,9) have outlined the requirements for unambiguous interpretation of the effects of pH on enzyme-catalysed reactions. Application of the principles described by these authors will be made in this study of one esterase reaction of the enzyme α-chymotrypsin.

Although a large number of substrates have been reported for α-chymotrypsin (2,10,11), very little information is available concerning the effects of pH changes on the hydrolyses of these substrates. In some studies (12,13,14) a pH-optimum curve has been determined at one substrate and one enzyme concentration. This information is of limited value since one has no means of detecting whether or not the

substrate is interacting competitively with hydronium ions. A series of pH-optimum curves determined over a range of substrate concentrations large with respect to the Michaelis constant, K_s, would be most informative, although such information is rarely reported. An alternative method of evaluating the effects of pH changes is to determine the kinetic constants K_s, the Michaelis constant under conditions such that the free enzymes and the free substrate are essentially at equilibrium with the enzyme-substrate complex, and k_3, the velocity constant, which is equal to the maximum rate at high substrate concentration divided by the enzyme concentration, as a function of pH. To date, only four studies of hydrolysis reactions catalysed by α-chymotrypsin as a function of pH have been reported in sufficient detail to enable conclusions to be drawn with any degree of certainty.

In 1955 Hammond and Gutfreund (15) studied the α-chymotrypsin catalysed hydrolysis of acetyl l-phenylalanine ethyl ester as a function of pH. Values of K_s and k_3 were obtained in the pH range 6.5 to 9.0. Buffer systems of phosphate, diethylamine, glycine, and ethylenediamine tetracetic acid were used to hold the pH constant. All reaction systems were 0.1 M with respect to added sodium chloride. K_s was observed to be independent of pH in the range 6.5 to 8.0, but then increased in the interval 8.0 to 9.0. The constant k_3 increased from 6.5 to 7.0, and was independent of pH in the interval 7.0 to 9.0. Hammond and Gutfreund concluded

that the free enzyme and the enzyme-substrate complex both contain a functional group which has a pK_a 6.85.

In the same year Jennings (16) studied the α-chymotrypsin catalysed hydrolysis of acetyl l-tyrosine hydroxamide and l-tyrosine hydroxamide as a function of pH. Further, he studied the effects of pH on the inhibition constants of the competitive inhibitors l-tyrosinamide and acetyl l-tyrosine using the aforementioned compounds as substrates. The buffers trishydroxymethylamino-methane, imidazole, and cacodylic acid - NaOH were used to maintain constant pH during a given reaction. Although several of Jenning's results agree with those of other investigators described here, this study was complicated by a number of factors such as difficult experimental conditions, ionization of the substrate, and peculiar effects associated with the use of tyrosine-derived substrates (17), and hence much of this work should be repeated before any firm conclusions are justified.

In 1956 Cunningham and Brown (18) reported the study of the α-chymotrypsin catalysed hydrolysis of acetyl l-tryptophan ethyl ester and acetyl l-tyrosine ethyl ester as a function of pH. Buffers similar to those used by Jennings were employed to maintain constant pH. All reaction systems were adjusted to 0.1 M ionic strength with added calcium ion. (This was a particularly unhappy choice of metal ion with which to maintain constant ionic strength since calcium ion has subsequently been demonstrated (19) to have a specific

effect on reactions catalysed by α-chymotrypsin.) K_s was observed to be independent of pH in the interval 6.0 to 9.0, whereas k_3 rises to a maximum at about pH 7.0 and remains constant above this value. These authors concluded that the enzyme must have a weakly acidic group at the active site with pK_a 6.71, and that enzyme which is protonated at this acidic group is inactive. Furthermore, they found that K_I for the competitive inhibitor acetyl l-tyrosine increases with pH in the range 7 to 8.5. Similar increases in K_I values in this region for competitive anionic inhibitors had been obtained by Neurath and Schwert (10), and Foster and Niemann (20), and for acetyl 3,5 dibromotyrosine by Doherty and Vaslow (21). The consensus of these authors is that the increase in K_I, and hence decrease in the fraction of enzyme inhibited by the anionic inhibitor, results from repulsion of the anionic group on the inhibitor from a negative charge which develops at or near the active site in this pH region.

Laidler and Bernard (22) in 1956 reported a study of the α-chymotrypsin catalysed hydrolysis of methyl hydrocinnamate as a function of pH. The reaction systems studied were maintained 20% by volume in methanol, and of ionic strength 0.1 M with respect to univalent ions. Phosphate and borate buffers were used. K_s was determined over the range pH 7.0 to pH 8.4, and was found to be invariant. k_3 was determined over the range pH 5.75 to pH 8.7, and was reported to pass through a maximum at about pH 7.5. These authors concluded

that both the free enzyme and the enzyme-substrate-complex possess ionizing groups of pK_a 7.2 and 8.0. Since K_s was invariant with pH, the form of the velocity vs pH curve was independent of substrate concentration. Hence, competitive interaction of substrate with hydronium ions for functional groups at the active site was excluded.

It was evident on the basis of the incomplete, and in some cases inconsistent, nature of the work reported above that a careful study as a function of pH of one or more hydrolytic reactions catalysed by α-chymotrypsin would be of value. Since the simple hydrolysis reaction is evidently complicated by ionization of the substrate, added non-aqueous solvents, and specific effects of added buffer systems, the elimination of these complicating factors was desirable. Since the discovery (23) that methyl hippurate, or benzoyl glycine methyl ester, is a substrate for α-chymotrypsin, this compound has been used extensively in these laboratories as a typical "uncomplicated" substrate. Methyl hippurate is a neutral compound, sufficiently soluble in water, and its rate of hydrolysis when catalysed by enzyme concentrations of approximately 10^{-5} molar is in a range convenient to study. Since methyl hippurate is a bifunctional substrate, in the sense that the two hydrogen atoms bonded to the carbon atom alpha to the ester carbonyl carbon atom are unsubstituted, no specific steric interactions with the enzyme in the enzyme-substrate-complex have been anticipated. Martin and Niemann (24) showed that the addition of added sodium chloride

produced a profound effect on the unbuffered hydrolysis reaction catalysed by α-chymotrypsin at pH 7.90. A detailed discussion of their results will be presented in the RESULTS AND DISCUSSION section. It was evident on the basis of this work that the results of the study of the enzyme-catalysed hydrolysis of methyl hippurate as a function of pH might be influenced by ionic strength effects. A pH study over a range of added sodium chloride concentrations, therefore, was indicated. In a later paper (25), Martin and Niemann reported the effects of other added salts on the α-chymotrypsin catalysed hydrolysis of methyl hippurate in unbuffered systems. A further extension of our knowledge of this particular esterase reaction was the investigation by Applewhite, Martin, and Niemann (26) of the effects of added non-aqueous solvents, and the presence of the competitive inhibitor indole. Clearly, therefore, the wealth of information already accumulated about the enzyme catalysed hydrolysis of methyl hippurate, together with its simplicity and ready availability, recommended it for the pH study reported here.

SUMMARY

The base-catalysed and the α-chymotrypsin-catalysed hydrolysis of methyl hippurate were studied as a function of pH and added sodium chloride. Six values of pH in the range 7.5 to 8.6 and six values of added salt concentration in the range 0.02 to 1.00 molar were investigated in the base-catalysed case. An average of fourteen pH values in the range 6.10 to 9.40 and the three added salt concentrations 0.02, 0.20, and 1.00 molar were investigated in the enzyme-catalysed reaction.

The kinetic results of the enzyme-catalysed reaction are consistent with the postulation of ionizing groups at the active site of the enzyme with pK values 6.9 ± 0.1 and 8.6 ± 0.1. The group corresponding to the former value appears in both the free enzyme and the complex, and is involved in the breakdown of the complex to products. The pK value 8.6 ± 0.1 corresponds to a group involved in the substration of the enzyme.

Hippuric acid and L-tryptophan were observed to be competitive inhibitors. Their inhibition constants were determined over the pH range 6.5 to 8.7. Rapid increase in the inhibition constants above pH 8 is consistent with the postulation of the development of a negative charge at the active site of the enzyme in this pH region.

APPARATUS AND PROCEDURE

The pH-stat

All kinetic determinations reported here were made with a pH-stat. This apparatus has been described in detail in the literature (27,28), and hence only a brief description of its operational principles will be presented here. As used in this study, in which the rate of an aqueous chemical reaction at constant pH was desired, the pH was operated as follows: Since the ester hydrolysis reaction liberated hydrogen ions as the reaction proceeded, the pH-stat added sufficient standard base solution to maintain constant pH, and at the same time recorded the amount of base required as a function of time. The standard base was added through a microsyringe which was driven by a variable speed motor. Electrodes immersed in the reaction system sensed a decrease in pH, and, through a series of relays, transmitted this information to the syringe drive motor. Although base was added in discrete, discontinuous amounts, each addition was sufficiently small that the pH of the vigorously stirred reaction system did not vary by more than 0.02 pH unit under normal operating conditions. The recorder trace of the base addition appeared as a smooth curve or straight line, composed of minute steps.

Materials Used

The substrate studied, methyl hippurate, was prepared by a method described in the literature (26), employing hippuric

acid, methyl alcohol, and thionyl chloride. Recrystallization of the impure product from isopropyl ether and methanol yielded crystals with mp 81.5-82.5°C. Stock solutions containing approximately 10 mg per ml of CO_2-free distilled water were prepared in volumetric flasks on the day in which the kinetic determinations were made. The pH of these solutions was always below pH 7.0. It will be shown later in the RESULTS AND DISCUSSION section that the base-catalysed hydrolysis of methyl hippurate in stock solutions under these conditions was negligible.

The α-chymotrypsin used was bovine, salt-free chymotrypsin, Armour Lot No. 283. Repeated micro-Keldahl determinations indicated that the dry crystalline material contained 14.60 ± 0.05% nitrogen. Prior to use, the enzyme was stored in a desiccator at 0°C. A stock solution of enzyme containing almost exactly 10.0 mg per ml of CO_2-free distilled water was prepared in a volumetric flask immediately before use. Enzyme stock solution had a pH of 3.4, and did not appear to lose any activity when held at this pH, concentration, and at room temperature, for periods of one half day.

Hippuric acid was used in inhibition studies reported here. Matheson reagent grade acid was recrystallized from water to give crystals melting at 188-189°C.

L-Tryptophan was also used as an inhibitor. A Schwarz Laboratories preparation was used without further purification.

All other solutions, such as sodium chloride stock solution and standardized sodium hydroxide solution, were prepared by conventional procedures with utmost regard for purity.

Experimental Procedure

The operational procedure used in determining the rate of an enzyme catalysed reaction with a pH-stat has been described in detail in the literature (26). Briefly, 9.0 ml of the total 10.0 ml reaction mixture were prepared by pipetting appropriate volumes of substrate stock solution (and inhibitor stock solution in the case of inhibition studies), sodium chloride stock solution, and CO_2-free distilled water into a small reaction beaker. This beaker was positioned in the pH-stat, with electrodes, stirrer, and syringe needle tip immersed in the solution. The contents of the beaker were quickly equilibrated to 25° ± 0.2°C, the temperature at which all the kinetic determinations were made, by a circulating thermo-regulated water bath. A stream of CO_2-free nitrogen was passed over the solution, and standard base was added to bring the solution to the desired pH of the reaction. Simultaneously, a 1 ml portion of the enzyme stock solution was brought to the same pH by the addition of strong sodium hydroxide solution, using a separate pH meter and syringe. When both the diluted substrate and the enzyme solution were at the desired pH, exactly 1.00 ml of the enzyme solution was added by syringe to the substrate solution

in the pH-stat. Almost immediately, the pH-stat began titrating the acid liberated by the hydrolysis reaction.

An average of ten kinetic determinations were made at each pH and each added salt concentration studied. In each case, the initial concentration of methyl hippurate in the reaction mixture was varied over the range 3×10^{-3} to 30×10^{-3} molar.

In order to eliminate undesired effects such as retardation in rate by inhibition of enzyme by hydrolysis products, changes in methyl hippurate concentration as the reaction proceeds, and changes in the volume and ionic strength of the medium resulting from the necessary addition of sodium hydroxide solution, the initial rate of the hydrolysis reaction, v_o', was desired. Under most conditions studied, the recorded volume of standard base added as a function of time was linear for at least five minutes from time zero. Under these condition, simply the slope of the straight line was used to determine the initial rate. In some cases, however, particularly those at low substrate concentrations, marked curvature appeared in the indicated reaction velocity. In order to determine the initial velocity by an objective procedure, the method of Booman and Niemann (29) was used. In this method, a least squares fit of the experimental data to an orthogonal polynomial, and subsequent differentiation of the polynomial, followed by evaluation of the differential at time zero, provided an objectively determined value of the

initial velocity.

The observed initial reaction velocity, v_o', consisted not only of the velocity of the enzyme-catalysed hydrolysis of methyl hippurate but also of the base-catalysed hydrolysis of methyl hippurate and the so-called enzyme blank (30). Since the base-catalysed hydrolysis of methyl hippurate at higher pH values becomes very appreciable with respect to the total observed hydrolysis rate, and the enzyme blank could not, a priori, be neglected, careful investigation of these hydrolysis reactions as a function of pH and added salt concentration was undertaken. Experimental procedure was exactly as described above, except that in the former case, no enzyme was added to the 10.0 ml reaction system, and in the latter case, no substrate was present. It will be shown in the RESULTS AND DISCUSSION section that the enzyme blank could be neglected in the studies reported here. The initial substrate blank, however, evaluated at each set of experimental conditions, was subtracted from the observed initial reaction velocity, v_o', of the enzyme-catalysed hydrolysis reaction.

Knowledge of the initial substrate concentration, S_o, the initial enzyme concentration, E_o, and the corrected initial reaction velocity, v_o', permitted calculation of the kinetic parameters K_s and k_3 under each set of experimental conditions. Conventional linear plots of S_o/v_o vs S_o were used. The intercept of this plot is K_s/k_3E_o and the slope is $1/k_3E_o$. A least squares fit of the experimental data to the

straight line determining the kinetic constants was programmed on the Datatron digital computer for speed and accuracy of calculation.

RESULTS AND DISCUSSION

Base-Catalysed Hydrolysis of Methyl Hippurate

As indicated in the previous section, it was essential to know the initial velocity of the base-catalysed hydrolysis of methyl hippurate under those conditions of pH and added sodium chloride concentration that were used for the enzyme-catalysed hydrolysis of this substrate. Although the base-catalysed hydrolysis rate could have been evaluated experimentally under each set of conditions, this method would have been extremely tedious. For this reason, a systematic study was made of the effects of pH and added salt on the velocity of the base-catalysed hydrolysis reaction, and a general relationship relating this velocity to substrate concentration, pH, and added salt concentration was derived. Thereafter, this general relationship was used to calculate the base-catalysed hydrolysis of methyl hippurate under the desired conditions.

Although the rate of hydrolysis of organic esters, such as methyl hippurate, is assumed to be first order in ester concentration and also first order in hydroxide ion concentration, the evaluation of the exponents a and b in the general equation

$$\text{rate of hydrolysis} = k[\text{ester}]^{a}[OH^{-}]^{b} \qquad (1)$$

and the determination of the dependence of the rate constant k upon added sodium chloride concentration were undertaken. The method used was the familiar one of varying one parameter while holding the others constant. The ester concentration was varied over the range 5×10^{-3} to 25×10^{-3} molar, the pH varied over the range pH 7.5 to pH 8.60, and the sodium chloride concentration varied over the range 0.02 to 1.00 molar. Table 1 lists the experimental data.

Figure 1 shows that the base-catalysed hydrolysis reaction is, indeed, first order in ester concentration. The slope of the log-log plot of ester concentration as a function of initial rate of hydrolysis is unity, and furthermore is independent of added sodium chloride concentration.

Figure 2 indicates, on the basis of the same criterion of unity slope on a log-log plot, that the base-catalysed hydrolysis reaction is also first order in hydroxide ion concentration. Furthermore, the unity exponent of the hydroxide ion concentration in equation 1 is apparently also independent of added sodium chloride concentration.

Figure 3 shows one of the plots used to determine the rate constant, k, at constant pH and different added salt concentrations. The slopes of the lines on these $v_{o(s)}$ vs S_o plots, as determined by least squares fit of the experimental data, were divided by the hydroxide ion concentration to determine k at each added salt concentration. The fact that the lines pass through the origin confirms the purity of the methyl

hippurate sample used. The values of k determined as a function of added salt are as follows: $k = 198 \pm 8$, 211 ± 9, 225 ± 7, 261 ± 11, and 279 ± 12 $(\text{moles/liter})^{-1}\text{min}^{-1}$ at 0.02, 0.05, 0.10, 0.50, and 1.00 molar sodium chloride, respectively. Figure 4 indicates that, within the limits of experimental error, k is a linear function of the logarithm of the added sodium chloride concentration. This result is unchanged when mean ion activities of the sodium chloride are used instead of molarities. The logarithmic relationship between the rate constant, k, and the added salt concentration can be described by the equation

$$k = 279 + 49 \log M \qquad (2)$$

where M is the molarity of the added sodium chloride.

The general relationship, therefore, describing the base-catalysed hydrolysis of methyl hippurate as a function of ester concentration, pH, and added sodium chloride is

$$\text{rate of hydrolysis} = (279 + 49 \log M)[\text{ester}][OH^-] \qquad (3)$$

The accuracy of this relationship is within $\pm$ 5% in the range investigated. Its use in the calculation of initial rates of the base-catalysed hydrolysis reaction for subtraction as substrate blanks was restricted to the range in which the relationship was derived, with the exception that base

concentrations as high as that corresponding to pH 9.4 were used. Since the hydrolysis reaction is almost certainly first order in hydroxide ion in this range as well, most likely no additional error was incurred.

The Enzyme Blank

When crystalline α-chymotrypsin is dissolved in CO_2-free distilled water to prepare a solution which is approximately 10^{-4} molar, the pH of the resulting solution is 3.4. This liberation of acid corresponds to approximately ten moles of hydrogen ion liberated per mole of enzyme. When this acidic solution is adjusted to pH 7.5 or higher, and then diluted ten-fold, the resulting solution releases hydrogen ion as a function of time at constant pH. This release of acid at constant pH is called the enzyme blank. Increasing the pH at which the solution is maintained causes an increase in the rate of liberation of acid. Increasing concentrations of sodium chloride, however, cause a decrease in the acid liberated as a function of time. In all cases, the rate of liberation of acid decreases with time, thus producing a plot of marked curvature.

Martin and Niemann (30) have suggested that this release of acid might be associated with the enzyme-catalysed hydrolysis of an unknown substrate contained in the enzyme preparation. The fact that a competitive inhibitor such as indole decreases the enzyme blank suggested to these authors

that only free enzyme, i.e. enzyme not complexed at the active site by either added substrate or added inhibitor, is capable of catalysing the hydrolysis of the contained substrate. These authors suggested a procedure for subtracting the blank resulting from free enzyme catalysed hydrolysis of the contained substrate when one knows the enzyme blank velocity determined experimentally for the total enzyme concentration, E_o, and the K_s and k_3 values of the added substrate.

Although not reported here in detail, enzyme blank velocities were estimated throughout the pH range 6.10 to 9.40 from the curved experimental velocities obtained in the absence of added substrate or inhibitor. At the highest pH and lowest added salt concentration investigated, blank velocities were of the order of 10% of the corresponding velocity of the enzyme-catalysed hydrolysis of methyl hippurate. In an experiment designed to check the applicability of the Martin and Niemann treatment to the system investigated here, the enzyme blank was determined in the presence of hippuric acid, which will be shown later to be an inhibitor competitive with methyl hippurate. When hippuric acid was used in sufficient concentration to reduce the concentration of free enzyme to one tenth its original value, the observed enzyme blank was also reduced by almost exactly this fraction. This result, therefore, is in excellent agreement with the Martin and Niemann hypothesis. Furthermore, this diminution in the enzyme blank in the presence of competitive inhibitor, and

hence substrate, concentrations large with respect to K_I or K_S in the case of a substrate, reduces the velocity of the enzyme blank to such a value that it becomes insignificant with respect to the velocity of the enzyme-catalysed hydrolysis of methyl hippurate.

Recent work (31) in these laboratories suggest that the enzyme blank may, in fact, be zero in the presence of added substrate. In any event, the substrate blank may be neglected in the work reported here.

Enzyme-Catalysed Velocity of Methyl Hippurate

As mentioned in the INTRODUCTION, Martin and Niemann (24) reported that the concentration of added sodium chloride present in the enzyme-catalysed hydrolysis of methyl hippurate exerts a profound influence upon the kinetic parameters K_S and k_3 at pH 7.90. K_S was observed to decrease sharply from an arbitrarily high value as very small concentrations of salt were added. At added sodium chloride concentrations equal to or greater than 0.50 molar, K_S remained constant at 2.7×10^{-3} moles per liter. One inference that might be drawn from this result is that salt is necessary to stabilize the enzyme-substrate-complex. On the other hand, k_3 increased very rapidly from an arbitrarily low value as salt was introduced, and continued to increase thereafter at a slower rate throughout the added salt concentration range investigated. One might conclude that the presence of salt is necessary in the promotion of the enzyme-substrate-

complex to products. Increasing salt concentration apparently facilitates this reaction.

In order to determine any interaction of added salt effects, as described above, with effects of changing pH, K_s and k_3 for methyl hippurate were determined over a range of pH values at three different added salt concentrations. The added salt concentrations were selected to investigate the different regions described by the Martin and Niemann work, i.e., a low salt concentration of 0.02 molar, a transition region concentration of 0.20 molar, and a high concentration of 1.00 molar sodium chloride. The pH ranges investigated were 6.00 to 9.40 at 0.02 molar salt, 6.10 to 9.40 at 0.20 molar salt, and 6.20 to 9.40 at 1.00 molar salt. In Table 2 are listed the initial velocities and the initial substrate concentrations at each value of pH and added salt concentration. In all systems, the enzyme concentration was 0.146 mg of protein-nitrogen per ml of reaction mixture.

Figure 5 illustrates the plot of S_o/v_o vs S_o that was used to determine the kinetic parameters K_s and k_3 at one pH and one added salt concentration. In this instance, thirteen sets of S_o and v_o data were obtained at pH 7.00 and 1.00 molar sodium chloride. The error limits indicated by the standard deviation of the derived kinetic parameters, i.e., $K_s = 2.76 \pm 0.25 \times 10^{-3}$ and $k_3 = 2.62 \pm 0.05 \times 10^{-3}$, are typical of those obtained throughout. Table 3 lists all the values of K_s and k_3 obtained for methyl hippurate as a function of pH and added sodium chloride.

Figures 6 and 7 show the familiar pH-optimum curves for the lowest and highest added salt concentrations and an arbitrarily selected substrate concentration of 10×10^{-3} molar. The 0.20 molar salt concentration data is very similar, particularly to the 1.00 molar data, and need not be considered separately. The velocities plotted were obtained by calculation from the equation

$$v_o = \frac{k_3 E_o S_o}{K_s + S_o} \qquad (4)$$

This equation can be derived from the postulates of the Michaelis-Menton theory assuming that the enzyme-substrate-complex is in equilibrium with free enzyme and free substrate in solution. The fact that bell-shaped pH-optimum curves are obtained agrees with previous work described in the INTRODUCTION for systems of α-chymotrypsin and ester-type substrates. The generalized postulate of two ionizing groups on the enzyme, and on the enzyme-substrate-complex, at the active site again seems reasonable. Thus, the following set of equilibria can be described:

$$
\begin{array}{ccccccccc}
E & + & S & \rightleftharpoons & ES & \xrightarrow{k_3} & E & + & P \\
+ & & & & + & & & & \\
H^+ & & & & H^+ & & & & \\
\uparrow\downarrow & & & & \uparrow\downarrow & & & & \\
EH & + & S & \rightleftharpoons & EHS & \xrightarrow{k_3'} & EH & + & P \\
+ & & & & + & & & & \\
H^+ & & & & H^+ & & & & \\
\uparrow\downarrow & & & & \uparrow\downarrow & & & & \\
EH_2 & + & S & \rightleftharpoons & EH_2S & \xrightarrow{k_3''} & EH_2 & + & P
\end{array}
\qquad (5)
$$

where

$$K_{ea} = \frac{(E)(H^+)}{(EH)} \qquad K_s = \frac{(E)(S)}{(ES)}$$

$$K_{eb} = \frac{(EH)(H^+)}{(EH_2)} \qquad K_s' = \frac{(EH)(S)}{(EHS)}$$

$$K_{esa} = \frac{(ES)(H^+)}{(EHS)} \qquad K_s'' = \frac{(EH_2)(S)}{(EH_2S)}$$

$$K_{esb} = \frac{(EHS)(H^+)}{(EH_2S)}$$

No attempt has been made to describe the net charge of enzyme-containing species in this description. Furthermore, ionizations of the substrate have not been included since none occur in the work reported here.

In order to account for the decrease in rate of reaction at high and low pH, one assumes in this treatment that only the complex EHS can decompose to products, i.e., $k_3' \gg k_3$ and k_3''. Accordingly, the rate of expression, equation 4, becomes

$$v_o = \frac{k_3' E_o S_o}{K_s\left[1 + \frac{K_{ae}}{(H^+)} + \frac{(H^+)}{K_{be}}\right] + S_o\left[1 + \frac{K_{aes}}{(H^+)} + \frac{(H^+)}{K_{bes}}\right]} \tag{6}$$

The experimentally determined kinetic parameters k_3 and K_s are found to be related to the new parameters k_3' and K_s' by the following relationships:

$$k_3 = \frac{k_3'}{1 + \frac{K_{aes}}{(H^+)} + \frac{(H^+)}{K_{bes}}} \tag{7}$$

$$K_s = K_s' \frac{1 + \frac{K_{ae}}{(H^+)} + \frac{(H^+)}{K_{be}}}{1 + \frac{K_{aes}}{(H^+)} + \frac{(H^+)}{K_{bes}}} \tag{8}$$

Another derived relationship which will be shown to be useful is

$$\frac{k_3}{K_s} = \frac{k_3'}{K_s'} \frac{1}{1 + \frac{K_{ae}}{(H^+)} + \frac{(H^+)}{K_{be}}} \tag{9}$$

Equations 7, 8, and 9 indicate that the observed kinetic parameters k_3 and K_s should be sensitive to changes in hydrogen ion concentration, and hence pH, if the ionizing groups represented by K_{ae}, K_{be}, K_{aes}, and K_{bes} possess pK values within

or near the pH range investigated. The marked changes in k_3 and K_s as a function of pH shown in Table 3 suggest that this is, in fact, the case. Inspection of equation 7 suggests that a plot of log k_3 vs pH should consist of straight line segments of slope +1, 0, or -1. The points of intersection of the straight line segments define the pK values of the ionizing groups. Since only K_{aes} and K_{bes} are found in this equation, this plot will reveal information about ionization at the active site of the enzyme-substrate-complex only. Furthermore, the experimental data should define a smooth curve which is 0.30 log units below points of intersection at the determined pK values. A similar analysis of equation 9 reveals that this equation, when plotted as log k_3/K_s vs pH should also consist of straight line segments, and that the points of intersection of these segments define pK values of ionizing groups at the active site of the free enzyme. The analysis of a plot of log K_s vs pH, as suggested by equation 8, is somewhat more complex in that points of intersection of the straight line segments correspond to pK values either in the free enzyme or in the enzyme-substrate-complex. One useful conclusion that can be drawn from this plot is that any change in K_s with pH indicates competitive interaction of the substrate with hydrogen ions with respect to an ionizing group at the active site of the enzyme.

Figure 8 shows a plot of log k_3 vs pH for the data at 0.02 molar sodium chloride. Evidently the experimental data

define straight line segments with unity and zero slopes. The point of intersection of the straight line segments is 6.9 ± 0.1. This value corresponds to pK_{bes}, the pK value of an ionizing group at the active site of the enzyme in the enzyme-substrate-complex. Apparently, protonation of this ionizing group in the complex prevents the hydrolysis reaction from occurring. One may conclude, therefore, that the functional group at the active site of the enzyme with pK 6.9 ± 0.1 is involved in the promotion of the enzyme-substrate-complex to products.

Figure 9 indicates that K_s is relatively insensitive to pH changes throughout the lower pH range, but appears to increase rather sharply at the highest pH values investigated. This increase defines rather poorly a pK value (which must be associated with an ionizing group in the free enzyme since k_3 is constant in this region) at about 8.9. The scatter of experimental data on this plot, and on others involving K_s values, indicates the magnitude of the uncertainties involved in these constants. There is no doubt that the standard deviation values of 10%, on the average, do not adequately describe this uncertainty.

Figure 10 shows a plot of log k_3/K_s vs pH for the same 0.02 molar sodium chloride data. The points of intersection of the straight line segments define pK values of ionizing groups at the active site of the free enzyme. Again, we see a point of intersection at pH 6.9 ± 0.1, suggesting that pK_{be}

is 6.9 ± 0.1. Thus, both the free enzyme and the enzyme-substrate-complex have an ionizing group with the same pK value at the active site. One may conclude that this ionizing group, which has been shown before to be involved in the breakdown of enzyme-substrate-complex to products, is not involved in the formation of the complex. If substration of the enzyme occurred at or very near this ionizing group, the pK_{be} value would almost certainly be displaced or reduced to zero. Figure 10 further suggests that the free enzyme does, in fact, possess an ionizing group at the active site with pK_{ae} of about 8.9. This ionizing group does not appear in the enzyme-substrate-complex, and hence is presumably involved in the substration of the enzyme at its active site. Loss of a proton from this ionizing group prevents the formation of the complex (or renders the complex unstable with respect to the reactants). In this sense there is a competitive, or in this case concerted, interaction of hydrogen ions and substrate with respect to this ionizing group.

Figures 11, 12, and 13, for the data at 0.20 molar salt, and Figures 14, 15, and 16 for the data at 1.00 molar salt, are similar to Figures 8, 9, and 10 discussed above. Since experimental conditions were more favorable in the case of the higher added salt concentrations, i.e., greater electrode stability and insensitivity of rate to small changes in ionic strength, the data obtained and plotted on these figures show less random error. pK_{be} and pK_{bes} remain remarkably constant

at 6.9 ± 0.1 as added salt concentration is increased from 0.02 molar to 1.00 molar. pK_{ae}, however, which corresponds to the ionizing group involved in substration of the enzyme, apparently decreases somewhat as added salt is increased, and becomes rather well defined at 8.6 ± 0.1 in 1.00 molar salt. This small shift in pK value presumably results from an ionic strength effect. Evidently gross interaction of added sodium chloride with pH effects is absent in the experiments reported here.

Inhibition by Hippuric Acid

The pronounced decrease in rate of the enzyme-catalysed hydrolysis of methyl hippurate observed under conditions of extended periods of reaction suggested that competitive inhibition of the enzyme by one of the hydrolysis products, namely, hippuric acid, might be occurring. The phenomenon of competitive inhibition of α-chymotrypsin by acylated α-amino acids liberated from their esters is well known (32). Furthermore, Applewhite, Martin, and Niemann (26) reported preliminary experiments which indicated that hippuric acid is, indeed, a competitive inhibitor with $K_I \sim 16 \times 10^{-3}$ molar at 0.02 molar sodium chloride and pH 7.90. In order to confirm this reported result, a series of experiments were conducted with the system methyl hippurate-hippuric acid-α-chymotrypsin at pH 7.00 and two added salt concentrations, 0.02 and 1.00 molar. Table 4 lists the experimental results.

In the presence of an added competitive inhibitor the Michaelis-Menton rate law described above in equation 4 becomes modified in the following way

$$v_o = \frac{k_3 E_o S_o}{K_s\left[1 + \frac{I_o}{K_I}\right] + S_o} \qquad (10)$$

where I_o is the concentration of added inhibitor and K_I is the equilibrium constant defined by $K_I = (E)(I)/(EI)$. Equation 10 indicates that a plot of S_o/v_o vs S_o for different concentrations of added inhibitor should produce a family of parallel lines with identical slopes and different intercepts. The different intercepts correspond to different inhibitor concentrations used. These intercepts define K_s' values, apparent Michaelis constants, which are related to K_s by the relationship $K_s' = K_s(1 + I_o/K_I)$. Figures 17 and 18 have been plotted from the experimental data listed in Table 4. These figures do not show all the data since crowding would obscure the results. They are typical, however, and indicate that hippuric acid fulfills the requirements for competitive inhibition implicit in equation 10. The values of K_I calculated from experiments at three different concentrations of added hippuric acid and at 0.02 molar sodium chloride were 13.0×10^{-3}, 13.0×10^{-3}, and 13.6×10^{-3} molar. At 1.00 molar sodium chloride four different concentrations of hippuric acid were used, and the values of K_I obtained were 5.8×10^{-3},

5.9×10^{-3}, 5.9×10^{-3}, and 6.2×10^{-3} molar. The accuracy of these K_I values is no better than approximately $\pm$ 20% since errors in K_s are necessarily also included in K_I. Apparently K_I for hippuric acid decreases with increasing salt at constant pH in a manner similar to the decrease in K_s for methyl hippurate under the same conditions.

Since hippuric acid had been confirmed as a competitive inhibitor for the system methyl hippurate-α-chymotrypsin, the method of Foster and Niemann (33) could be used to evaluate the product inhibition constant, K_p, as a function of pH from the same data used to evaluate K_s and k_3. Foster and Niemann showed that for a system described by the following equations

$$E + S \underset{k_2}{\overset{k_1}{\rightleftharpoons}} ES \xrightarrow{k_3} E + P \qquad (11)$$

$$E + P \underset{k_5}{\overset{k_4}{\rightleftharpoons}} EP \qquad (12)$$

and where K_p is defined by $K_p = (E)(P)/(EP)$ (and hence is identical with K_I discussed above) the course of reaction is described by the integrated equation

$$\left[1 - \frac{K_s}{K_p}\right]\left[S_o - S\right] + K_s\left[1 + \frac{S_o}{K_p}\right] \ln \frac{S_o}{S} = k_3 E_o t \qquad (13)$$

Rearrangement of equation 13 in the following way

$$\frac{S_o - S}{t} + K_s \left[\frac{K_p + S_o}{K_p - K_s}\right]\frac{\ln S_o/S}{t} = \frac{k_3 E_o}{1 - K_s/K_p} \qquad (14)$$

gives an expression which may be used to calculate K_s, k_3, and K_p from a knowledge of S_o and the substrate concentration as a function of time. In the case that K_s has been previously evaluated by other means, which is the case here, K_p may be evaluated from the slope of a plot of $(S_o - S)/t$ vs $(\ln S_o/S)/t$. This plot gives a straight line for each value of S_o with slope equal to $-K_s((K_p + S_o)/(K_p - K_s))$.

It is important to note that the system described by equations 11 and 12 is not unique in its ability to describe the experimental data. Alberty and co-workers (34,35) have proposed the following system

$$E + S \underset{k_2}{\overset{k_1}{\rightleftharpoons}} X_1 \rightleftharpoons X_2 \rightleftharpoons \cdots \underset{k_4}{\overset{k_3}{\rightleftharpoons}} E + P \qquad (15)$$

where there may be, formally, an indefinite number of intermediates in equilibrium with the free enzyme, substrate, and product(s). Perhaps the most significant feature of this proposal is that the enzyme-substrate-complex is in equilibrium with the liberated product(s). The steady state rate equation for this system, under the condition that $S_o \gg E_o$, is

$$\frac{-ds}{dt} = \frac{k_3 E_o\left(\frac{(S)}{K_s}\right) + k_2 E_o\left(\frac{(P)}{K_p}\right)}{1 + \frac{(S)}{K_s} + \frac{(P)}{K_p}} \qquad (16)$$

where K_s is defined by $K_s = (k_2 + k_3)/k_1$, and K_p is defined by $K_p = (k_2 + k_3)/k_4$. If k_3 is much larger than k_2, equation 16 simplifies to equation 4 when used to describe the initial reaction velocity in the absence of added inhibitor. Moreover, integration of equation 16, subject to the condition $k_3 \gg k_2$, gives an equation identical with equation 13, and hence describes the experimental data with respect to product inhibition.

The system described by Foster and Niemann contains the implicit assumption that $k_2 \gg k_3$. The system described by Alberty and co-workers, on the other hand, requires, in the present case, that $k_3 \gg k_2$. Both systems lead to the same equations which apparently describe adequately the observed experimental facts. The decision as to which of these two systems is preferred awaits the independent evaluation of the relative magnitudes of k_2 and k_3.

In spite of the existence of the theoretical difficulty mentioned above in the interpretation of the relationship of the enzyme-product-complex to the enzyme-substrate-complex, knowledge of K_p as a function of pH is still of considerable value. Prior to the calculation of K_p under all conditions of pH and added salt for which experimental data were available, inspection of the reaction conditions was undertaken, in accordance with a suggestion of Kerr (36), to determine what extents of hydrolysis would be required for product inhibition to be clearly discernible. The method suggested

by Kerr was based upon earlier work of Jennings and Niemann (37) and Lands and Niemann (38). The method involves calculation of the ratio $t_{o(p)}/t_o$ as a function of percent hydrolysis. The meaning of this ratio, in common sense terms, is the time required for the reaction to reach a certain percent hydrolysis with product inhibition occurring divided by the time required to reach the same percent hydrolysis in the absence of product inhibition. If one anticipates a 5 percent random error in the experimental data, clearly the above ratio must be greater than 1.05 in order to obtain meaningful results. The parameters $t_{o(p)}$ and t_o can be calculated when one knows (or assumes) values of K_s, S_o, and K_p. In this particular case all three were previously known at one pH and two different added salt concentrations from the competitive inhibitor studies. Table 5 lists the values of K_s, S_o, and K_p which were used in the calculation, together with the equations used, and the resulting values of the ratio as a function of percent hydrolysis. Figure 19 shows the calculated ratio and percent hydrolysis in graphical form for the 1.00 molar sodium chloride data. Evidently the phenomenon of product inhibition becomes clearly discernible only at 30 percent hydrolysis and greater if one assumes a random error of 5 percent in the experimental data. At 0.02 molar sodium chloride, however, the reaction must reach 45 percent completion, as shown in Figure 20, before product inhibition becomes clearly discernible. In order to evaluate K_p as a

function of pH from the integrated rate equation at 0.02 molar salt, reactions would have to be carried well beyond 50 percent completion. This result is unfortunate since Martin and Niemann (24) showed that small changes in ionic strength cause significant changes in K_s and k_3 in solutions of such low ionic strength as 0.02 molar. Addition of the requisite amount of sodium hydroxide to maintain constant pH would cause appreciable changes in ionic strength, and hence would render meaningless the results obtained. This unfortunate situation, together with the fact that the 0.20 molar data is extremely similar to the 1.00 molar data, restricted the calculation of K_p as a function of pH to the data at 1.00 molar added sodium chloride.

The use of the integrated rate equation to calculate K_p for the system represented by equations 11 and 12 implicitly neglects the substrate blank reaction. If we add the reaction

$$S \xrightarrow{k_6} P \qquad (17)$$

to the system described by equations 11 and 12, integration of the resulting rate equation leads to an expression of great complexity. Although k_6 at any pH is known accurately in the case of methyl hippurate, the complex integrated rate equation still cannot be used in a straightforward manner to determine K_p from a knowledge of the kinetic constants and the substrate concentrations as a function of time. Fortunately the use of the complex integrated equation is not necessary in the case

of methyl hippurate in the pH range investigated. Inspection of the complete rate equation prior to integration

$$-\left[1+\frac{K_s}{(S)}+\frac{K_s}{K_p}\cdot\frac{S_o-(S)}{(S)}\right]dS=\left[k_3E_o+K_sk_6+\frac{K_s}{K_p}k_6S_o+k_6\left(1-\frac{K_s}{K_p}\right)(S)\right]dt \quad (18)$$

reveals that addition of equation 17 affects only the right side of equation 18 and by the simple addition of three terms containing k_6. It is fortunate that these three terms are negligible with respect to k_3E_o throughout the pH range in which K_p was evaluated. Neglecting these three terms reduces equation 18 to an expression which, when integrated, is identical with equation 13.

Table 6 lists the 19 different kinetic determinations whose values of substrate concentration as a function of time were used to determine K_p values over the pH range 6.20 to 8.70. Also listed in Table 6 are the calculated values of $(S_o-S)/t$ and $(\log S_o/S)/t$ which were plotted to determine the slopes $-K_s((K_p+S_o)/(K_p-K_s))$, from which the K_p values were calculated. Figure 21 shows such a plot for two initial substrate concentrations at pH 7.50. Table 8 lists the values of K_p obtained. A plot of K_p as a function of pH is shown in Figure 22.

The observed rapid increase in K_p as the pH of the reaction medium is increased above pH 8 suggests that the enzyme-inhibitor complex either does not form or is unstable

at higher pH values. It is important to note that the increase in K_p is much greater than the increase in K_s in this pH range. Evidently a repulsion of the anionic inhibitor is occurring which is superimposed upon the decrease in concentration of complexed enzyme resulting from the ionization of the enzyme at the functional group with pK_{be} 8.6. Thus the data reported here provide quantitative support for the proposal of other investigators (10,20,21,39) that α-chymotrypsin develops a negative charge at its active site in this pH region.

Inhibition by L-Tryptophan

The demonstration that hippuric acid is a competitive inhibitor whose K_p value increases rapidly when the functional group on the enzyme with pK_{ae} 8.6 becomes appreciably ionized stimulated interest in the absence of a significant change in K_p when the pH of the reaction medium was decreased below 6.9. As discussed earlier, this pH corresponds to the pK value of the second ionizing group at the active site of the enzyme. Apparently there is little or no interaction between the inhibitor hippuric acid and this ionizing group. This result is not surprising since there are no other charges on the hippuric acid molecule except the negatively charged carboxyl group, which is presumably anchored at the group on the enzyme with pK_{ae} 8.6. In an attempt to investigate the proximity of the functional groups on the enzyme corresponding to pK_{ae} and pK_{be}, a study as a function of pH was made of the doubly

charged inhibitor L-tryptophan. L-Tryptophan is a free amino acid and hence has a carboxyl group which should be repelled by the enzyme above pH 8. Furthermore, it has a free amino group which is completely protonated below pH 8.5 and which could, under favorable circumstances, be repelled by the enzyme below pH 7. Repulsion of the protonated amino group by the ionizing group on the enzyme would be contingent upon the following circumstances. The spatial geometry of the enzyme-inhibitor-complex would have to be such that this repulsion would occur. In addition, the group on the enzyme with pK_{be} 6.9 would have to be positively charged below pH 6.9. Of course, absence of a rapid increase in K_I above pH 8 would indicate that the enzyme-inhibitor-complex of α-chymotrypsin with L-tryptophan is dissimilar to that with hippuric acid.

L-Tryptophan was selected for this study since all other free α-amino acids are either insufficiently soluble in water or are poor inhibitors. Among those acids sufficiently soluble glycine, L-phenylalanine, and L-tryptophan were subjected to preliminary investigation. Glycine possesses no detectable inhibitory power. Its K_I value is greater than 4000×10^{-3} molar at pH 7.00. L-Phenylalanine is an inhibitor, although a weak one, with $K_I \sim 100 \times 10^{-3}$ molar at pH 7.00. L-Tryptophan was found to be a surprisingly good inhibitor which is competitive with the substrate methyl hippurate and has $K_I = 14.5 \times 10^{-3}$ molar at pH 7.00.

Table 7 lists the values of S_o, I_o, and pH used in the experiments with L-tryptophan. The resulting initial velocities are also listed in this table. Plots of S_o/v_o vs I_o, which define straight lines with slopes equal to $K_s/K_I k_3 E_o$, were used to obtain the value of K_I at each pH. Figure 23 shows the data at pH 7.00 plotted in this manner. The values of K_I obtained over the pH range 6.20 to 8.60 are listed in Table 8. Figure 24 shows the results in graphical form.

The similarity of Figure 24, showing K_I as a function of pH for L-tryptophan, to Figure 22, showing K_I for hippuric acid as a function of pH, suggests that these two inhibitors form structually similar enzyme-inhibitor-complexes. The absence of a sharp increase in K_I for L-tryptophan below pH 7 suggests the following possibilities. Either the enzyme does not acquire a positive charge at its active site as the pH is decreased below pH 7, or, in the event that it does, the spatial geometry of the enzyme-inhibitor-complex is such that repulsion of like positive charges does not occur. These suggestions by no means exhaust the possibilities. They do indicate, however, the usefulness of the negative result obtained in this experiment.

CONCLUSIONS

A detailed study of the α-chymotrypsin catalysed hydrolysis of methyl hippurate as a function of pH indicates that the kinetic parameters K_s and k_3 are affected by changes in pH in a manner consistent with the hypothesis that the active site of the enzyme possesses two ionizing functional groups. One of the two ionizing groups, which has a pK value of 6.9 ± 0.1, also appears to be present in the enzyme-substrate-complex. Protonation of this group on the enzyme-substrate-complex inhibits the hydrolysis reaction. For this reason this ionizing group is believed to be involved in the breakdown of the complex to products. Since the pK value of this ionizing group on the free enzyme is unchanged in the enzyme-substrate-complex, one may conclude that this group is not bound to the substrate in the enzyme-substrate-complex.

The second ionizing group at the active site of α-chymotrypsin has a pK value of 8.6 ± 0.1. Decreasing salt apparently increases this pK value slightly, whereas the ionizing group with pK 6.9 ± 0.1 is unaffected by changes in added sodium chloride concentration. The ionizing group with pK 8.6 is involved in the formation of the enzyme-substrate-complex since this ionizing group is absent in the complex.

Hippuric acid is an inhibitor competitive with methyl hippurate. The inhibition constant of hippuric acid increases rapidly as the pH of the reaction medium is increased above pH 8, thus supporting the suggestion that a negative charge

develops at the active site of the enzyme in this pH range.

L-Tryptophan is also an inhibitor competitive with methyl hippurate. The pH behavior of the inhibition constant of L-tryptophan is identical with that of hippuric acid, thus suggesting that the two inhibitors form structurally similar enzyme-inhibitor-complexes. The absence of an increase in K_I for L-tryptophan below pH 7 indicates no interaction between the positive charge on the protonated α-amino group of the inhibitor and the ionizing group with pK 6.9 on the enzyme.

REFERENCES

1. Alberty, R. A., J. Cell. and Comp. Physiol., 47, 245 (1956).

2. Laidler, K. J., "The Chemical Kinetics of Enzyme Action," Oxford Clarendon Press, 1958.

3. Michaelis, L., and Davidson, H., Biochem. Z., 35, 386 (1911).

4. Michaelis, L., and Rothstein, M., Biochem. Z., 110, 217 (1920).

5. von Euler, H., Josephson, K., and Myrbäch, K., Z. physiol. Chem., 134, 39 (1924).

6. Dixon, M., Biochem. J., 55, 161 (1953).

7. Laidler, K. J., Tr. Faraday Soc., 51, 528 (1955).

8. Waley, S. G., Biochim. Biophys. Acta, 10, 27 (1953).

9. Botts, J., and Morales, M., Tr. Faraday Soc., 11, 615 (1953).

10. Neurath, H., and Schwert, G. W., Chem. Revs., 46, 69 (1950).

11. Foster, R. J., and Niemann, C., J. Am. Chem. Soc., 77, 1886 (1955).

12. Huang, H. T., and Niemann, C., J. Am. Chem. Soc., 73, 1541 (1951).

13. Huang, H. T., MacAllister, R. V., Thomas, D. W., and Niemann, C., J. Am. Chem. Soc., 73, 3231 (1951).

14. Lutwack, R., Mower, H. F., and Niemann, C., J. Am. Chem. Soc., 79, 2179 (1957).

15. Hammond, B. R., and Gutfreund, H., Biochem. J., 61, 187 (1955).

16. Jennings, R. B., Ph.D. Thesis, California Institute of Technology 1955.

17. Kurtz, A. N., unpublished investigations.

18. Cunningham, L. W., and Brown, C. S., J. Biol. Chem., 221, 287 (1956).

19. Jennings, R. B., Kerr, R. J., and Niemann, C., Biochem. Biophys. Acta, 28, 144 (1958).

20. Foster, R. J., and Niemann, C., J. Am. Chem. Soc., 77, 3365 (1955).

21. Doherty, D. G., and Vaslow, F., J. Am. Chem. Soc., 74, 931 (1952).

22. Laidler, K. J., and Bernard, M. L., Tr. Faraday Soc., 52, 497 (1956).

23. Huang, H. T., and Niemann, C., J. Am. Chem. Soc., 74, 4634 (1952).

24. Martin, R. B., and Niemann, C., J. Am. Chem. Soc., 79, 4814 (1957).

25. Martin, R. B., and Niemann, C., J. Am. Chem. Soc., 80, 1481 (1958).

26. Applewhite, T. H., Martin, R. B., and Niemann, C., J. Am. Chem. Soc., 80, 1457 (1958).

27. Jacobsen, C. F., and Leonis, L., Compt. rend. trav. lab. Carlsberg, Ser. Chim., 27, 333 (1951).

28. Nielands, J. B., and Cannon, M. D., Anal. Chem., 27, 29 (1955).

29. Booman, K. A., and Niemann, C., J. Am. Chem. Soc., 78, 3642 (1956).

30. Martin, R. B., and Niemann, C., Biochim. Biophys. Acta, 26, 634 (1957).

31. Wolff, J. P. III, Ph.D. Thesis, California Institute of Technology 1959.

32. Foster, R. J., and Niemann, C., J. Am. Chem. Soc., 77, 3370 (1955).

33. Foster, R. J., and Niemann, C., Proc. Nat. Acad. Sci., 39, 999 (1953).

34. Alberty, R. A., and Koerber, B. M., J. Am. Chem. Soc., 79, 6379 (1957).

35. Miller, W. G., and Alberty, R. A., J. Am. Chem. Soc., 80, 5146 (1958).

36. Kerr, R. J., Ph.D. Thesis, California Institute of Technology 1957.

37. Jennings, R R., and Niemann, C., J. Am. Chem. Soc., 75, 4687 (1953).

38. Lands, W. E. M., and Niemann, C., J. Am. Chem. Soc., 77, 6508 (1955).

39. Canaday, W. J., and Laidler, K. J., Can. J. Chem., 36, 1289 (1958).

LIST OF FIGURES

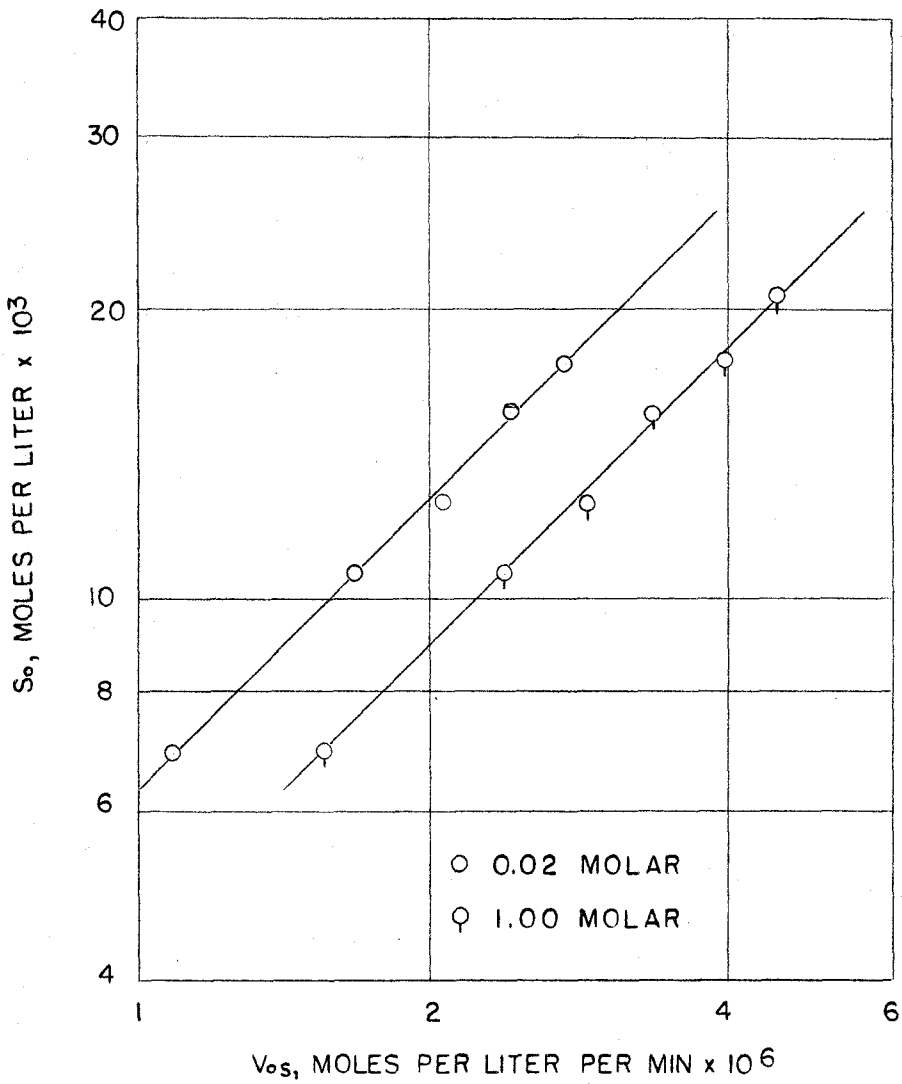

Figure 1--Methyl Hippurate Blank. Log S_o vs log $v_{o(s)}$

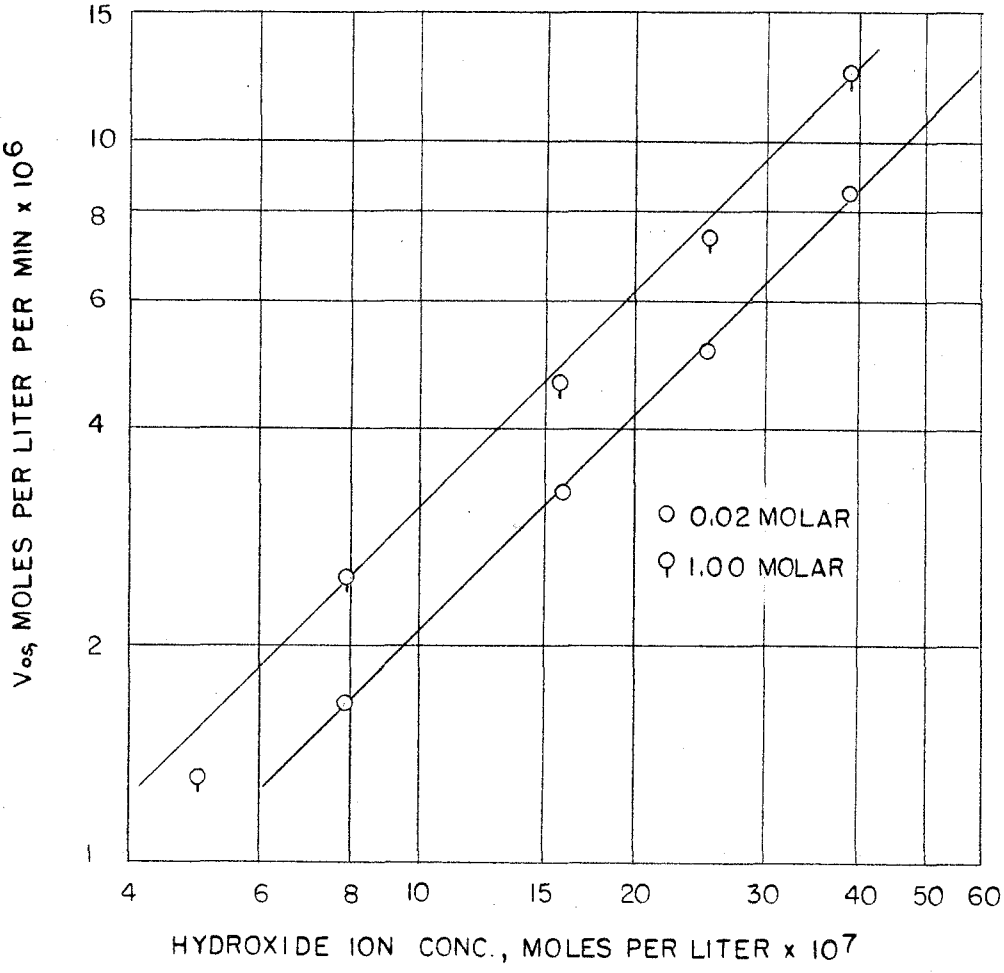

Figure 2--Methyl Hippurate Blank. Log $[OH^-]$ vs log $v_{o(s)}$

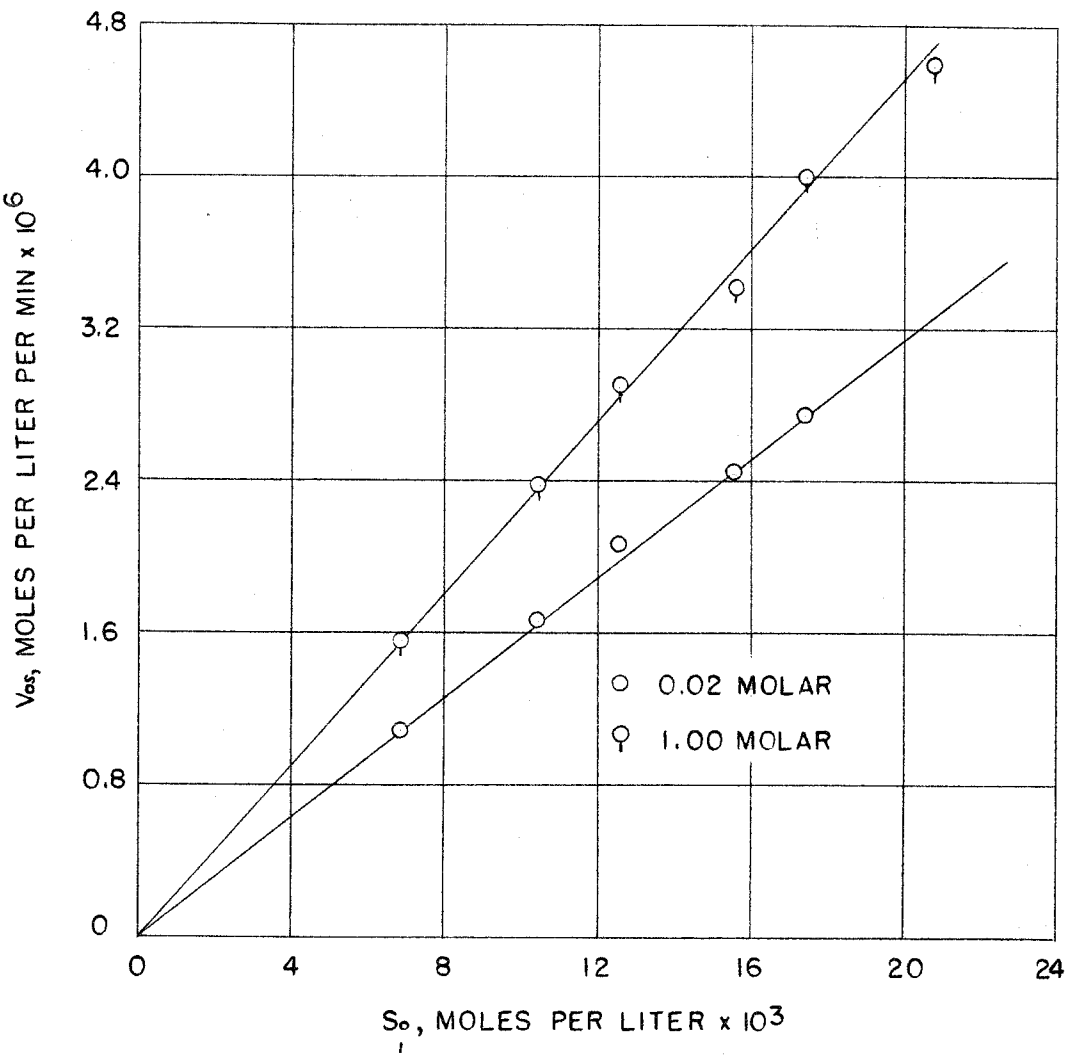

Figure 3--Methyl Hippurate Blank. S_o vs $v_{o(s)}$ at 0.02 and 1.00 molar NaCl

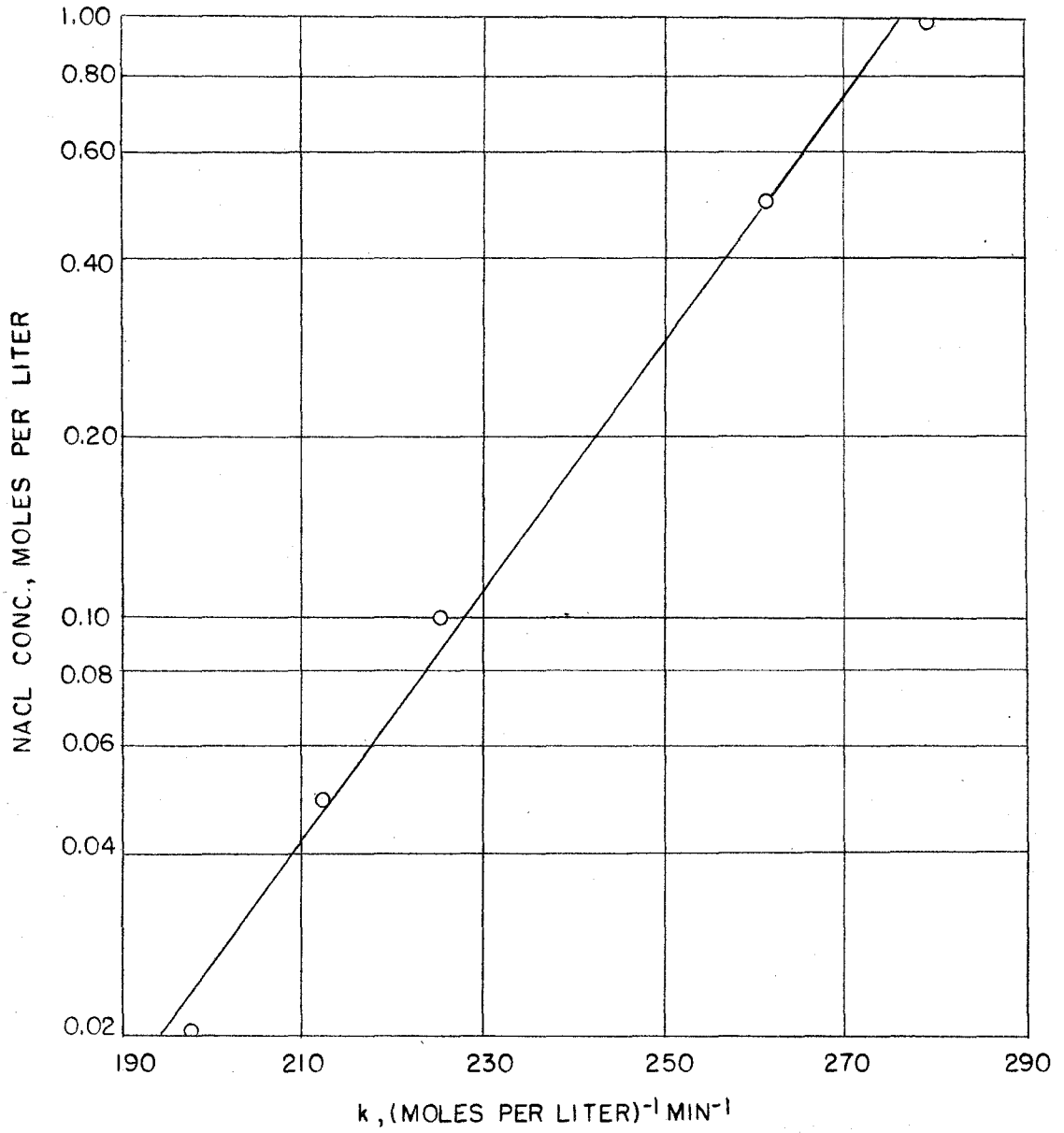

Figure 4--Methyl Hippurate Blank. k vs NaCl concentration

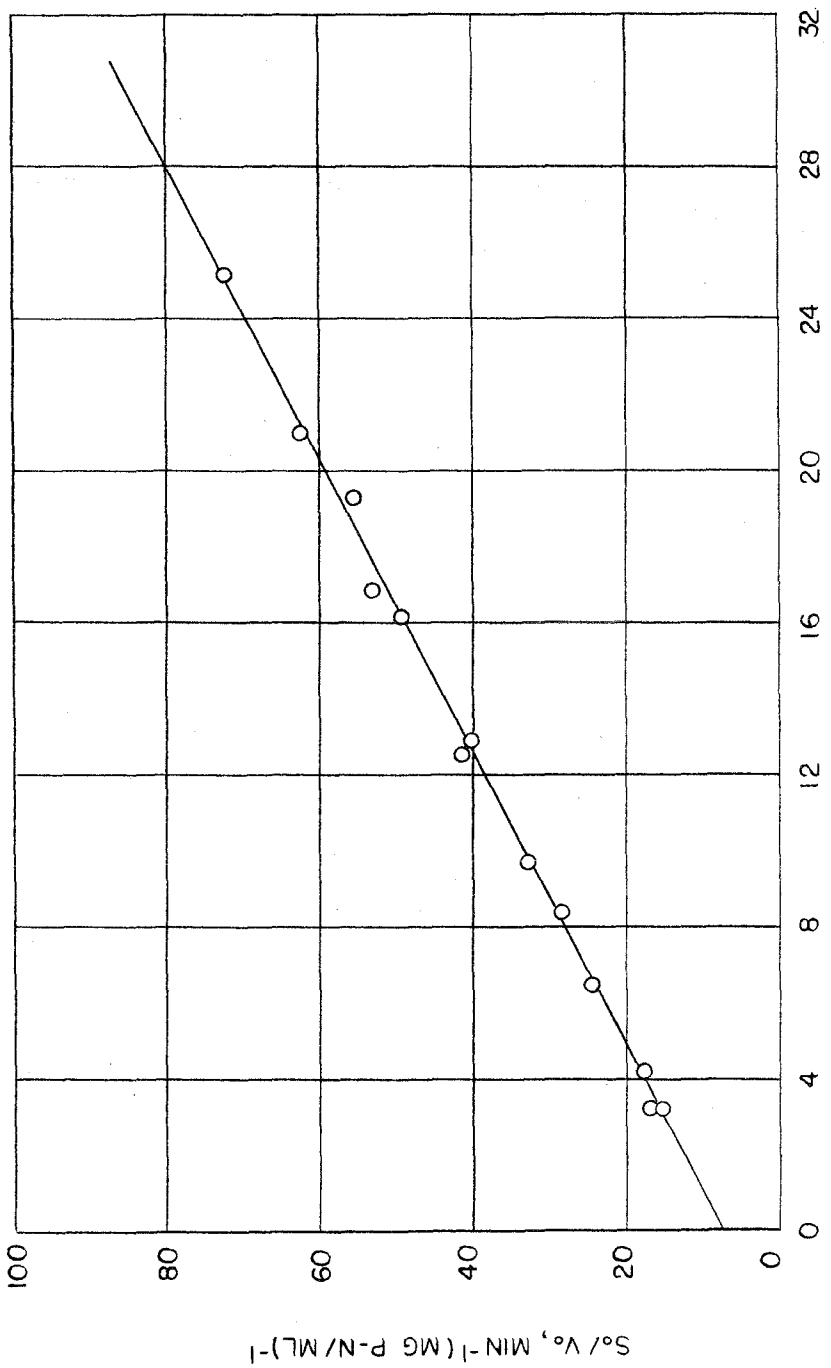

Figure 5--Enzyme-Catalysed Hydrolysis. S_o/v_o vs S_o at pH 7.00 and 1.00 molar NaCl

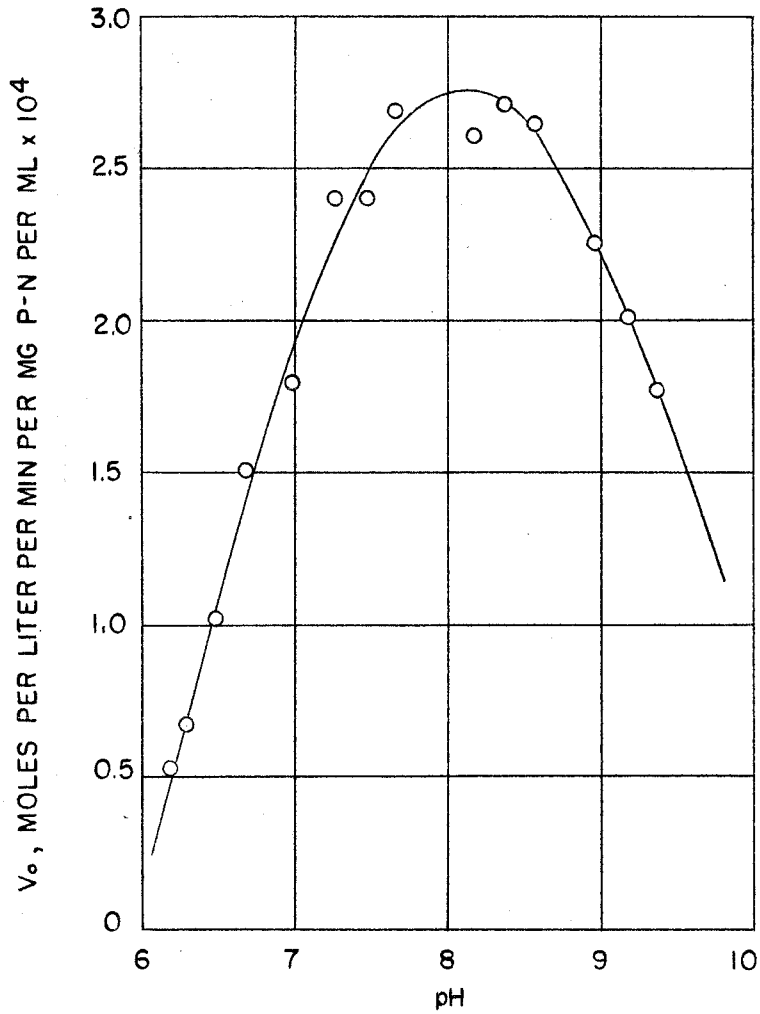

Figure 6--Enzyme-Catalysed Hydrolysis. v_o vs pH at S_o = 10 x 10^{-3} molar and 0.02 molar NaCl

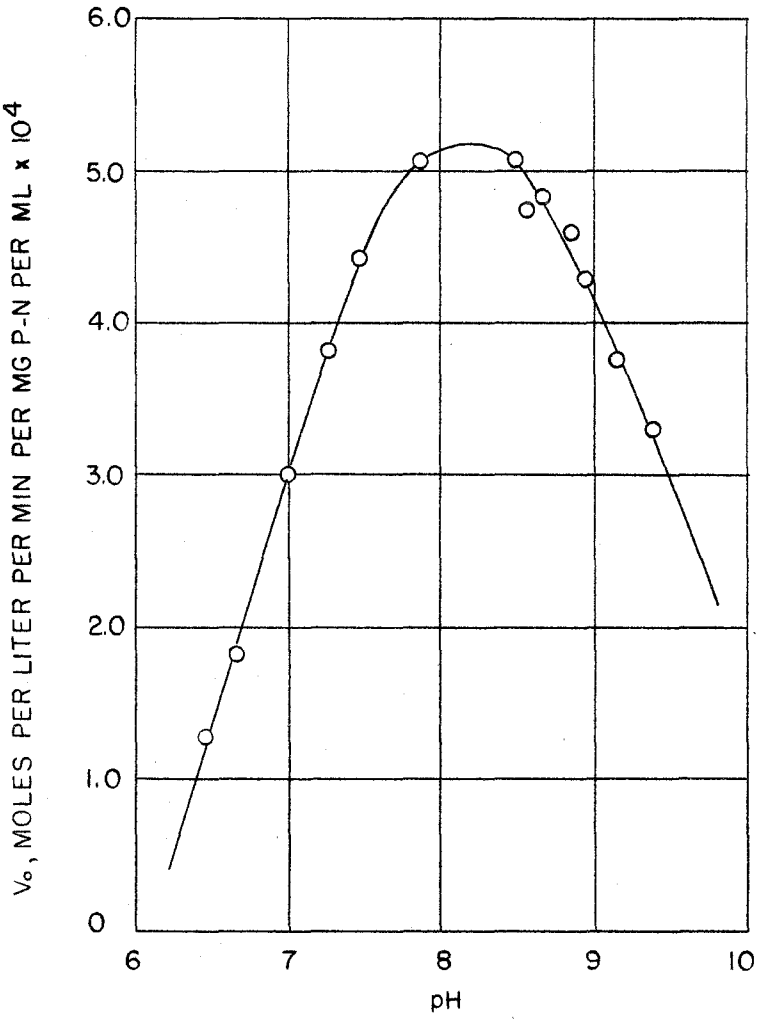

Figure 7--Enzyme-Catalysed Hydrolysis. v_o vs pH at $S_o = 10 \times 10^{-3}$ molar and 1.00 molar NaCl

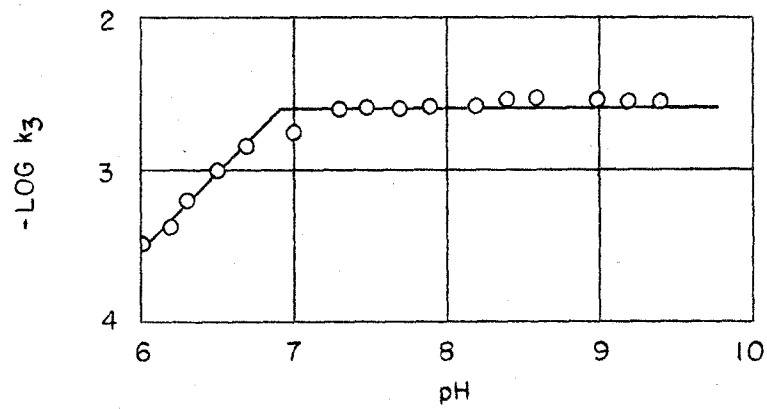

Figure 8--Enzyme-Catalysed Hydrolysis. Log k_3 vs pH at 0.02 molar NaCl

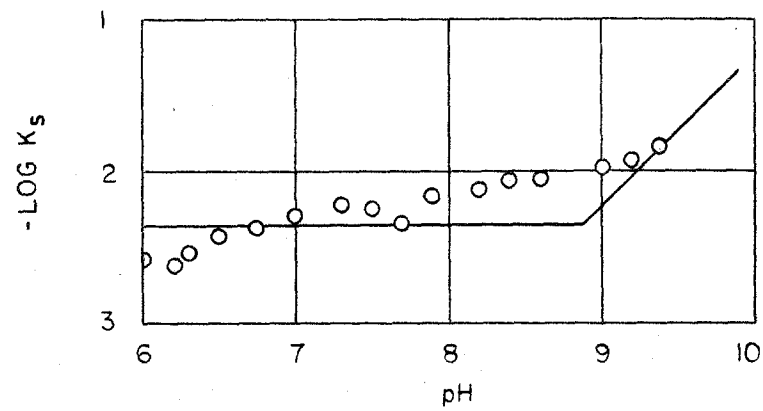

Figure 9--Enzyme-Catalysed Hydrolysis. Log K_s vs pH at 0.02 molar NaCl

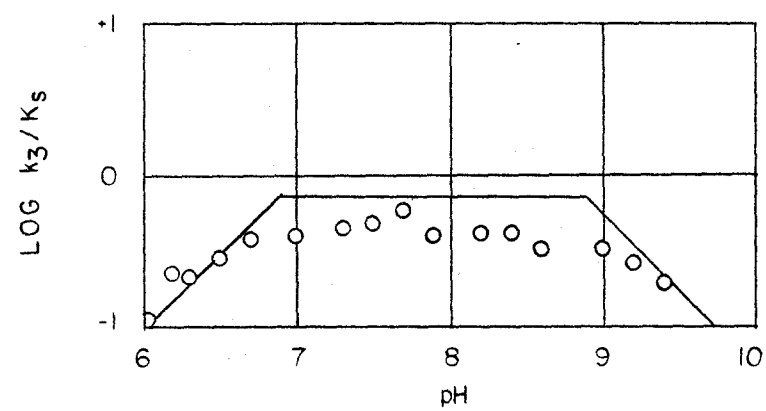

Figure 10--Enzyme-Catalysed Hydrolysis. Log k_3/K_s vs pH at 0.02 molar NaCl

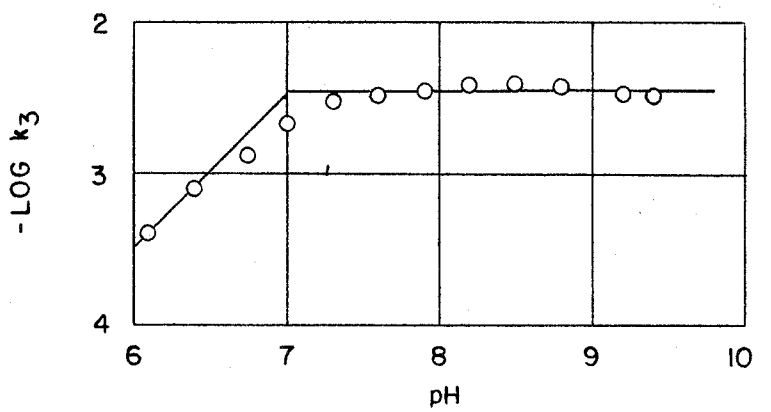

Figure 11--Enzyme-Catalysed Hydrolysis. Log k_3 vs pH at 0.20 molar NaCl

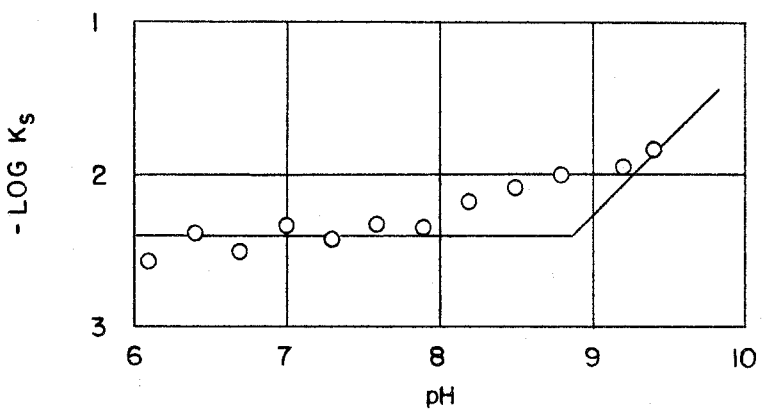

Figure 12--Enzyme-Catalysed Hydrolysis. Log K_s vs pH at 0.20 molar NaCl

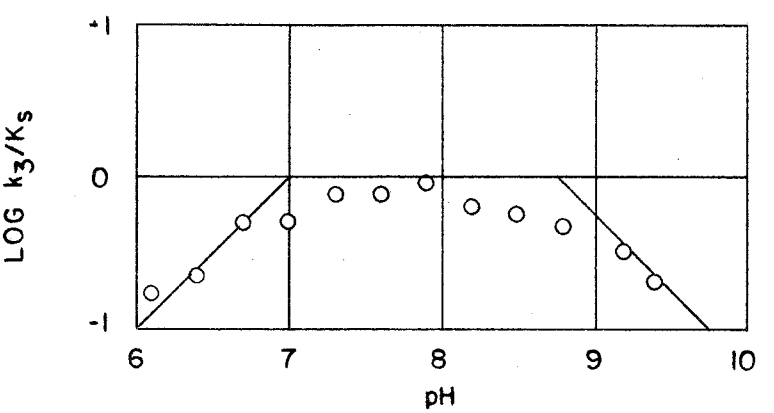

Figure 13--Enzyme-Catalysed Hydrolysis. Log k_3/K_s vs pH at 0.20 molar NaCl

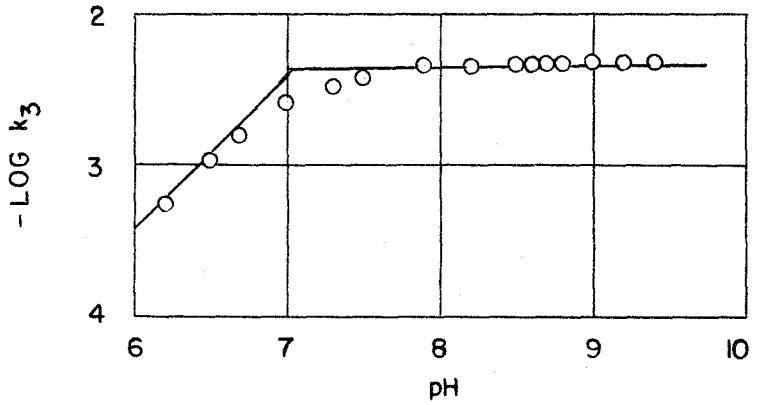

Figure 14--Enzyme-Catalysed Hydrolysis. Log k_3 vs pH at 1.00 molar NaCl

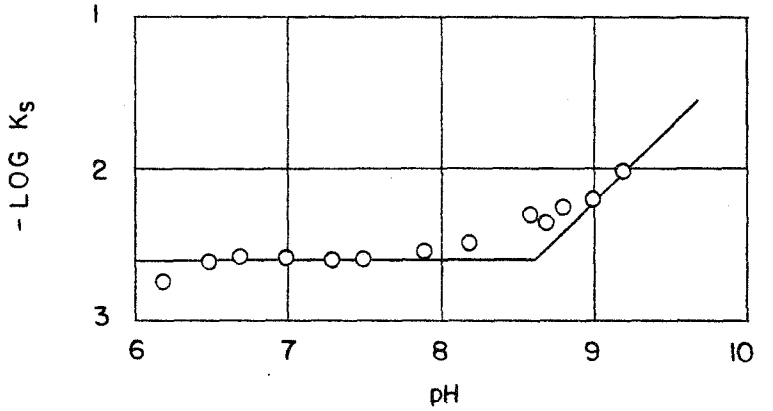

Figure 15--Enzyme-Catalysed Hydrolysis. Log K_s vs pH at 1.00 molar NaCl

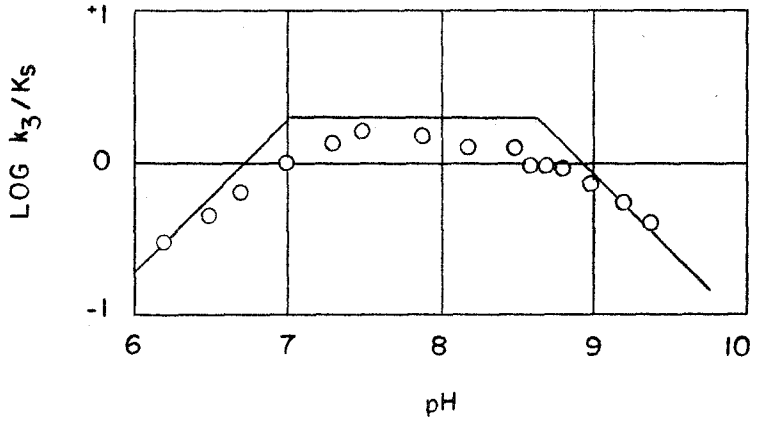

Figure 16--Enzyme-Catalysed Hydrolysis. Log k_3/K_s vs pH at 1.00 molar NaCl

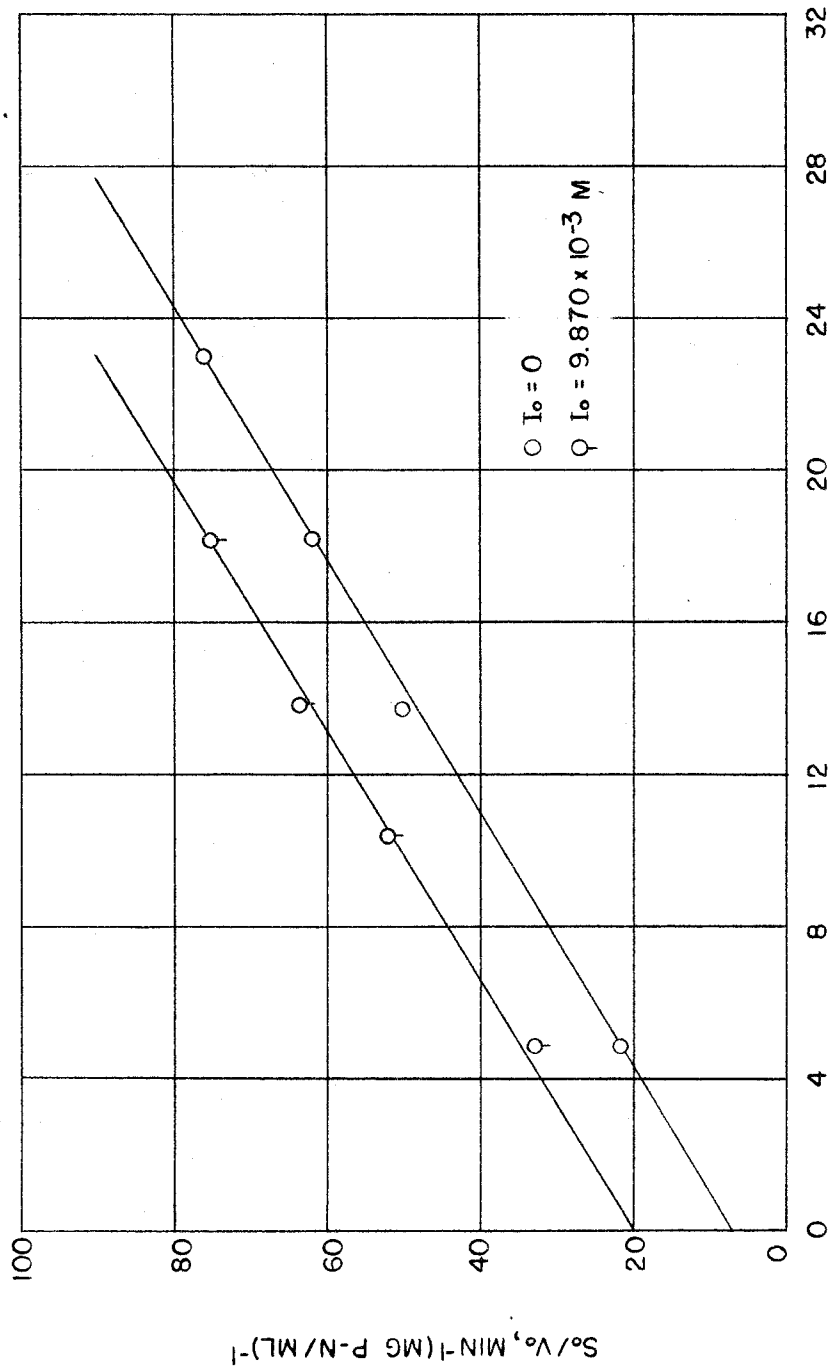

Figure 17--Inhibition by Hippuric Acid. S_o/v_o vs S_o at I_o = 0 and 9.870×10^{-3} molar and 1.00 molar NaCl

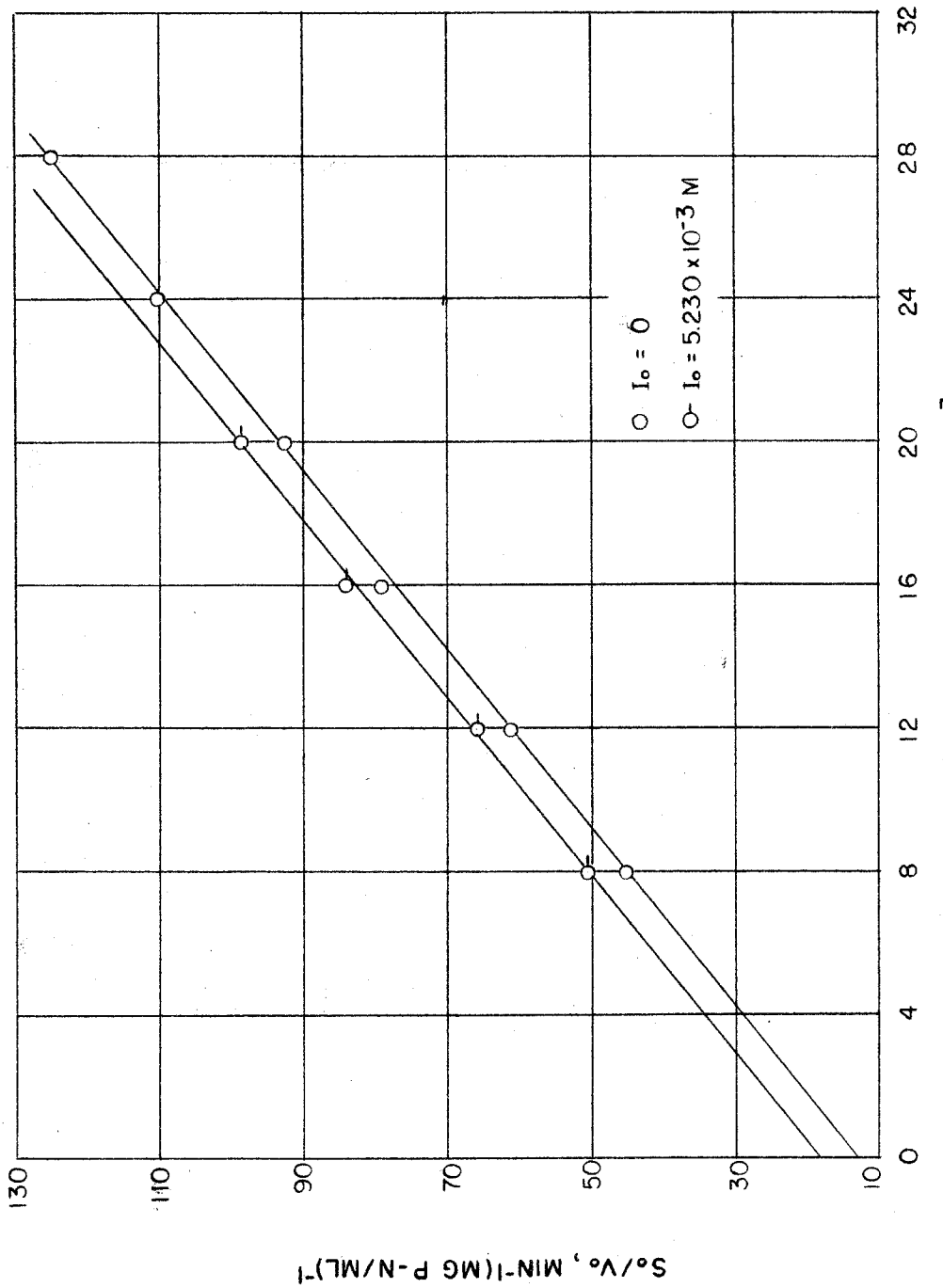

Figure 18--Inhibition by Hippuric Acid. S_o/v_o vs S_o at I_o = 0 and 5.230 x 10-3 molar and 0.02 molar NaCl

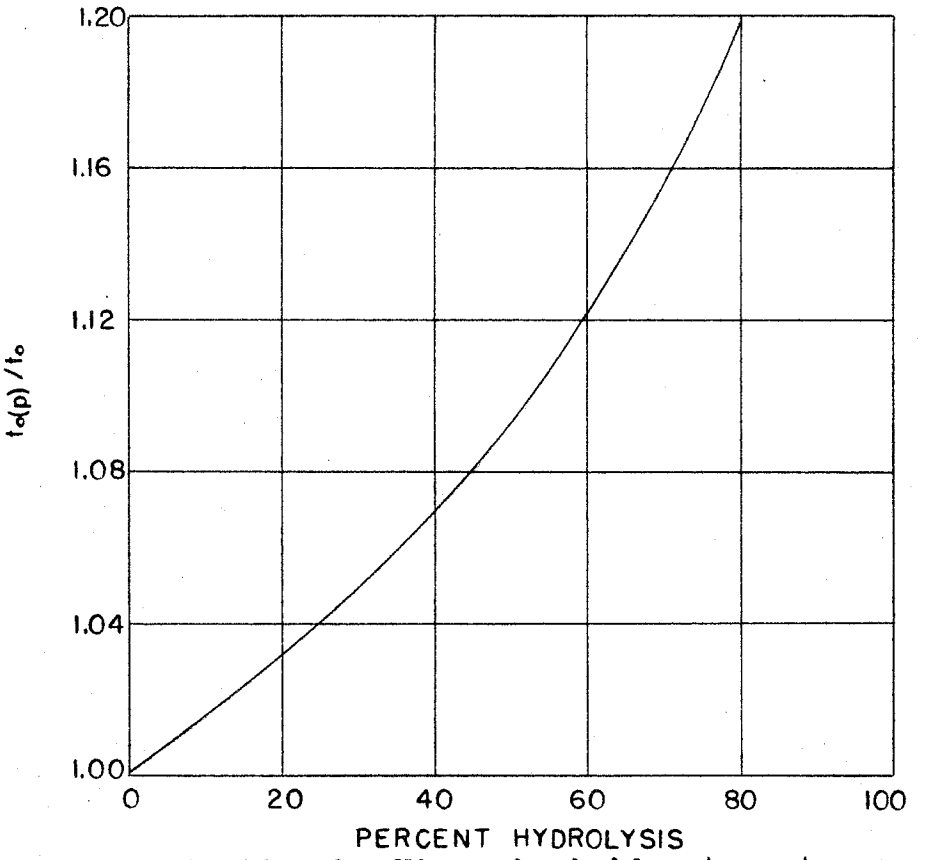

Figure 19--Inhibition by Hippuric Acid. $t_{o(p)}t_o$ vs percent hydrolysis at 1.00 molar NaCl

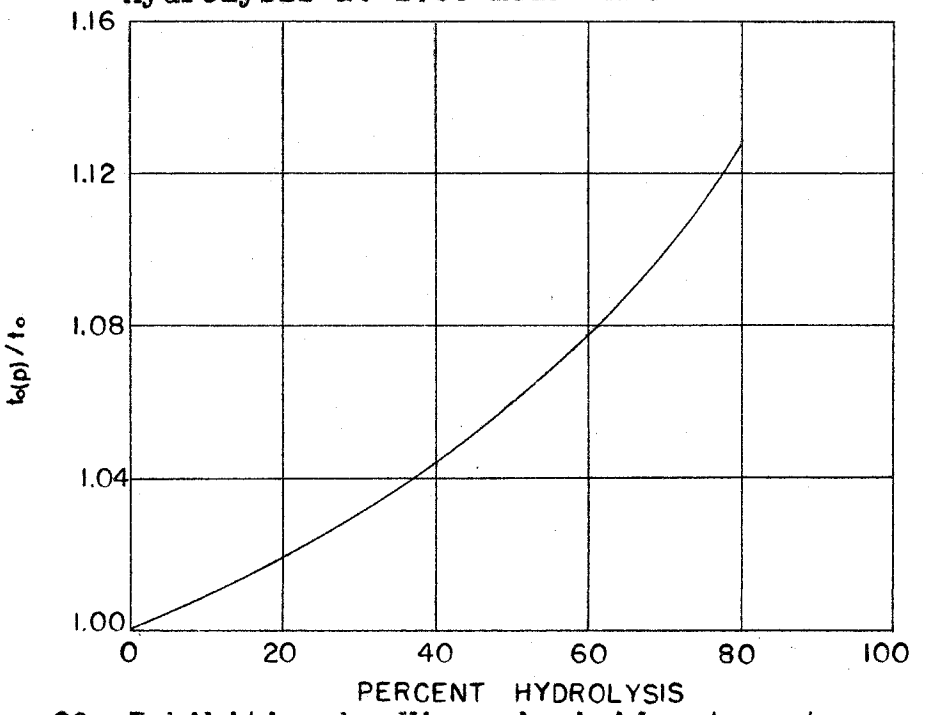

Figure 20--Inhibition by Hippuric Acid. $t_{o(p)}t_o$ vs percent hydrolysis at 0.02 molar NaCl

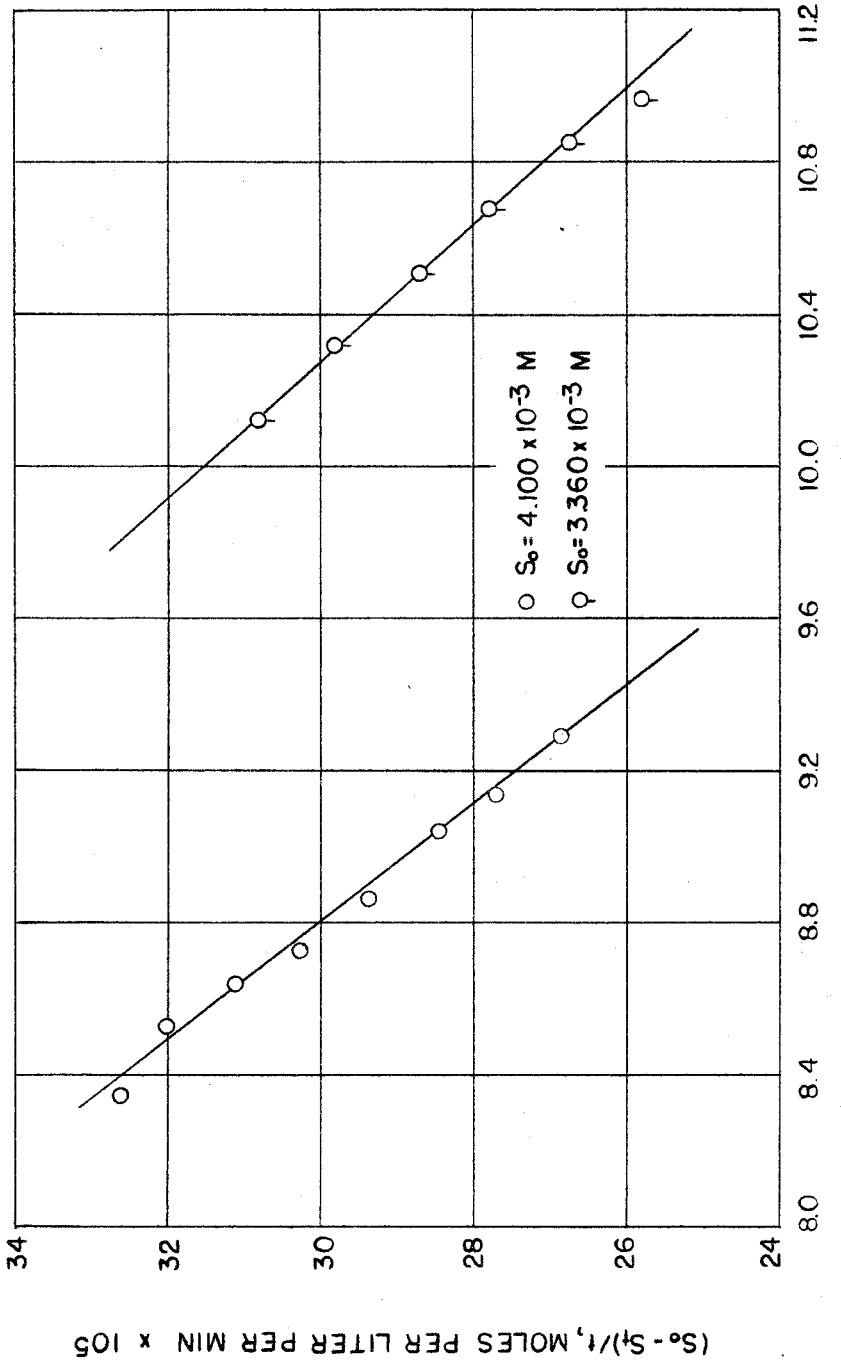

Figure 21--Inhibition by Hippuric Acid. $(S_o - S)/t$ vs $(\log S_o/S)/t$ at pH 7.50 and 1.00 molar NaCl

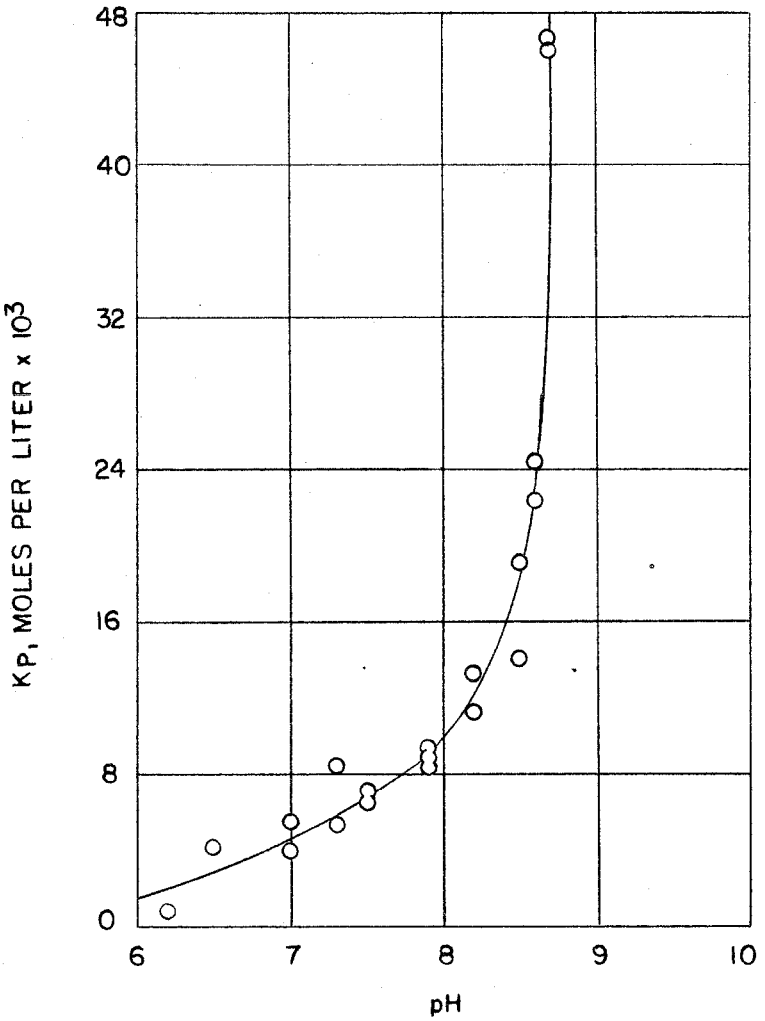

Figure 22--Inhibition by Hippuric Acid. K_p vs pH at 1.00 molar NaCl

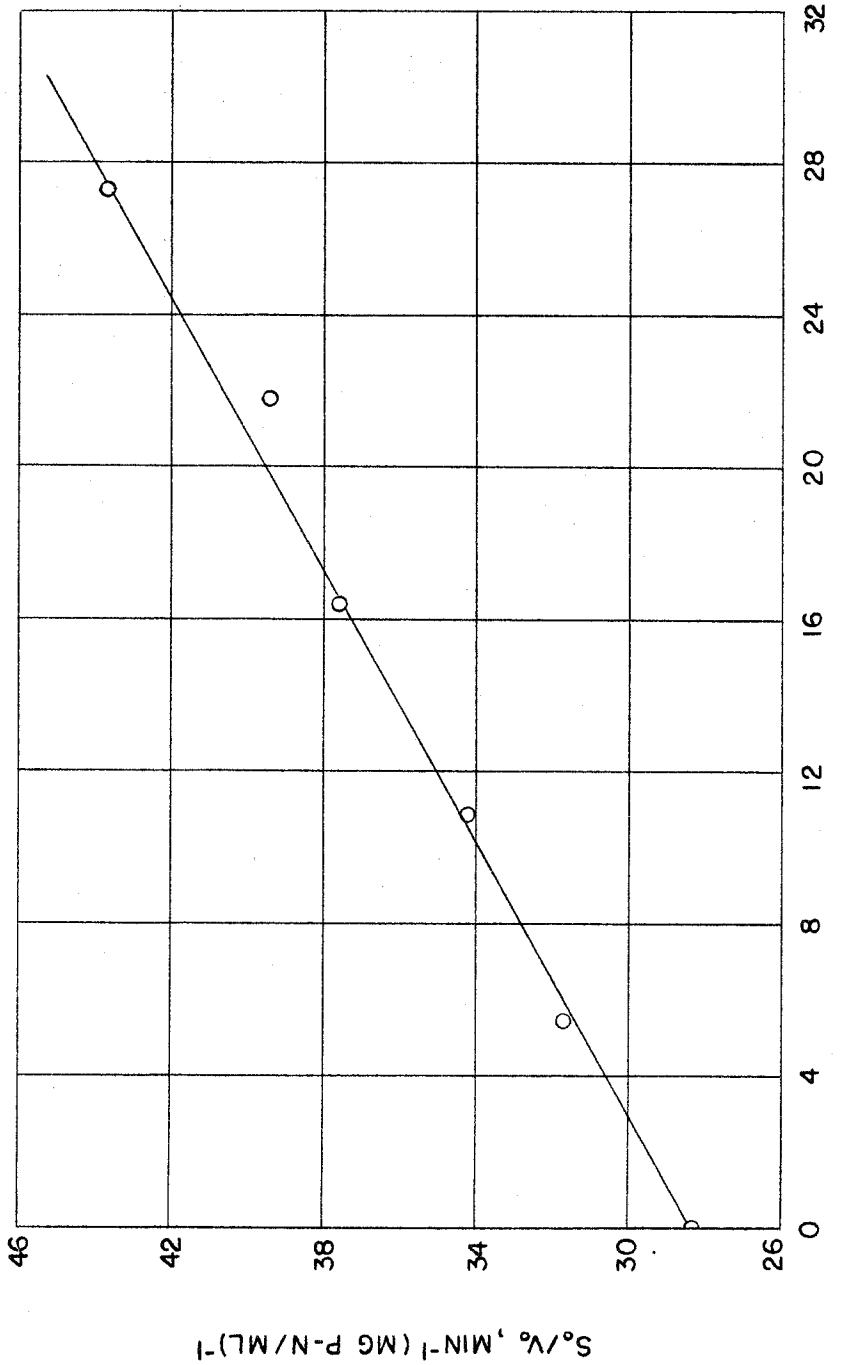

Figure 23--Inhibition by L-Tryptophan. S_o/v_o vs I_o at pH 7.00 and 1.00 molar NaCl

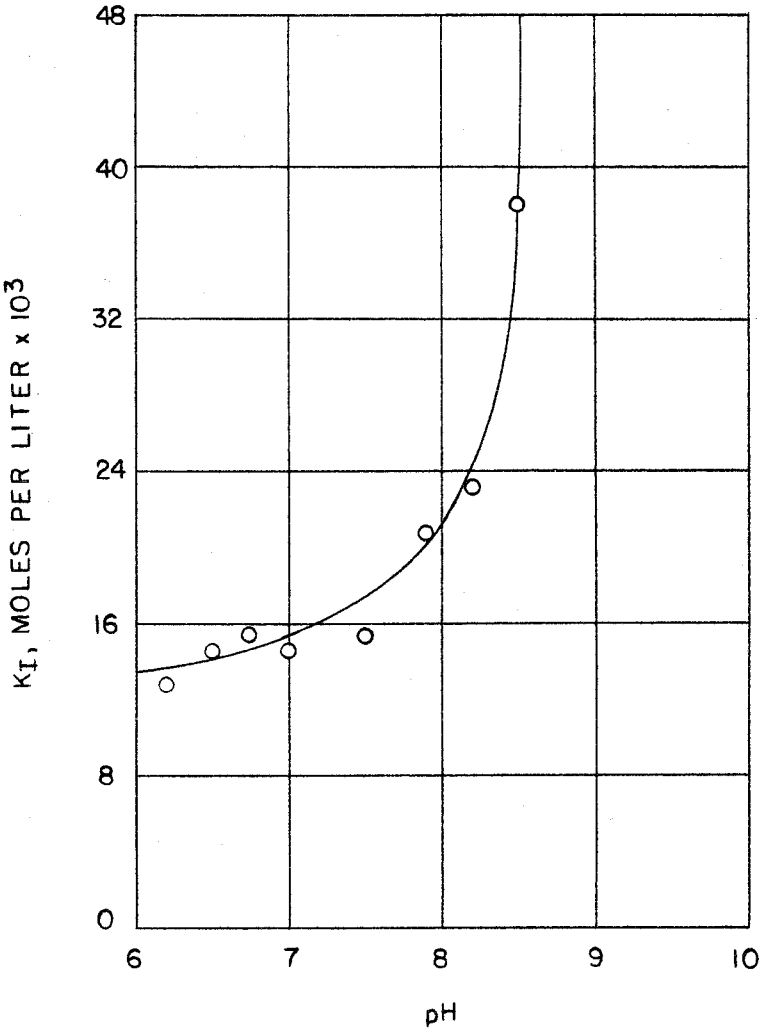

Figure 24--Inhibition by L-Tryptophan. K_I vs pH at 1.00 molar NaCl

LIST OF TABLES

Table 1

METHYL HIPPURATE BLANK

S_o and $v_{o(s)}$ as a function of pH and NaCl concentration

NaCl moles/liter	pH	S_o moles/liter x 10^3	$v_{o(s)}$ moles/liter/min x 10^6
0.02	7.90	10.54	1.674
		17.57	2.753
		12.61	2.075
		15.77	2.429
		6.95	1.085
		0.00	0.000
0.05	7.90	10.54	1.859
		17.57	2.890
		12.61	2.205
		15.77	2.579
		6.95	1.170
		20.85	3.528
		0.00	0.000
0.10	7.90	10.54	1.845
		17.57	3.132
		12.61	2.265
		15.77	2.820
		6.95	1.288
		0.00	0.000
0.50	7.90	10.54	2.380
		17.57	3.750
		12.61	2.490
		15.77	3.153
		20.85	4.340
		24.38	4.985
		20.32	4.190
		16.25	3.567
		8.12	1.776
		0.00	0.000
1.00	7.90	10.54	2.374
		17.57	4.002
		12.61	2.903
		15.77	3.390

Table 1 (Continued)

NaCl moles/liter	pH	S_o moles/liter x 10^3	$v_{o(s)}$ moles/liter/min x 10^6
1.00	7.90	6.95	1.555
		20.85	4.560
		0.00	0.000
0.02	7.70	10.40	0.809
	7.90	10.40	1.676
	8.20	10.40	3.264
	8.40	10.40	5.139
	8.60	10.40	8.524
1.00	7.70	10.40	1.301
	7.90	10.40	2.477
	8.20	10.40	4.606
	8.40	10.40	7.304
	8.60	10.40	12.26

Table 2

ENZYME-CATALYSED HYDROLYSIS

S_o and v_o as a function of pH and NaCl concentration

pH	NaCl moles/liter	S_o moles/liter x 10^3	v_o moles/liter/min/mg P-N/ml x 10^4
6.00	0.02	3.530	0.2499
		5.295	0.2941
		8.028	0.3583
		12.04	0.3934
		16.06	0.4218
		5.311	0.3338
		7.966	0.3702
		10.62	0.3977
		14.08	0.4222
		18.77	0.4095
		3.530	0.2595
6.20	0.02	4.710	0.4990
		6.775	0.4908
		10.16	0.5299
		13.55	0.5628
		4.710	0.4944
		15.92	0.5789
		11.94	0.5505
		7.961	0.4758
		8.965	0.5192
		13.45	0.5672
		13.57	0.5585
		9.048	0.5061
6.30	0.02	3.499	0.4927
		5.248	0.5757
		7.231	0.6473
		10.85	0.6869
		14.46	0.7115
		5.487	0.5799
		8.230	0.6648
		10.97	0.7307
		19.48	0.7894
		14.61	0.8050

Table 2 (Continued)

pH	NaCl moles/liter	S_o moles/liter x 10^3	V_o moles/liter/min/mg P-N/ml x 10^4
6.50	0.02	4.961	0.8204
		4.961	0.8513
		7.441	1.014
		10.65	1.101
		15.98	1.188
		23.25	1.282
		17.44	1.215
		11.62	1.076
		9.017	1.020
		13.53	1.185
670	0.02	4.205	1.130
		5.636	1.245
		5.863	1.312
		9.003	1.404
		5.919	1.191
		4.820	1.120
		17.64	1.798
		14.13	1.674
		11.05	1.629
		17.81	1.774
		13.40	1.670
7.00	0.02	4.727	1.368
		7.317	1.555
		19.70	2.205
		24.58	2.273
		6.917	1.742
		19.43	2.101
		7.460	1.615
		5.136	1.343
		11.18	1.780
		10.82	1.770
		5.642	1.514
		5.176	1.423
		15.45	1.971
7.30	0.02	9.146	2.372

Table 2 (Continued)

pH	NaCl moles/liter	S_o moles/liter x 10^3	v_o moles/liter/min/mg P-N/ml x 10^4
7.30	0.02	4.555	1.692
		4.555	1.692
		11.32	2.597
		11.09	2.476
		22.63	3.093
		16.97	2.738
		23.69	3.093
		24.74	3.127
		18.56	2.890
		13.72	2.661
7.50	0.02	3.561	1.573
		3.561	1.526
		5.774	1.858
		8.137	2.244
		8.605	2.397
		12.74	2.555
		14.68	2.867
		19.90	2.911
		7.385	2.259
		11.37	2.584
		15.45	2.776
		20.12	3.013
		23.89	3.093
7.70	0.02	9.607	2.539
		9.058	2.444
		6.775	2.288
		6.869	2.187
		4.803	1.695
		7.205	2.152
		14.56	2.968
		11.57	2.697
		17.36	3.134
		23.15	3.400
		19.41	3.331
		13.55	2.945
		13.59	2.923

Table 2 (Continued)

pH	NaCl moles/liter	S_o moles/liter x 10^3	v_o moles/liter/min/mg P-N/ml x 10^4
7.70	0.02	13.74	2.909
		10.30	2.547
7.90	0.02	4.000	1.487
		4.000	1.459
		12.00	2.595
		12.00	2.489
		4.00	1.454
		12.00	2.594
		16.00	2.884
		20.42	2.982
		21.49	3.021
8.20	0.02	7.973	2.347
		7.973	2.278
		6.698	2.268
		10.05	2.617
		7.057	1.998
		13.40	3.025
		17.21	3.361
		12.90	2.802
		4.705	1.898
		20.13	3.371
		15.10	3.017
		8.292	2.414
		11.06	2.722
		5.528	2.010
		4.705	1.809
8.40	0.02	5.502	1.891
		8.106	2.753
		4.053	1.787
		4.695	1.893
		9.389	2.673
		11.00	2.917
		14.43	3.221
		6.079	2.254
		7.042	2.261

Table 2 (Continued)

pH	NaCl moles/liter	S_o moles/liter x 10^3	v_o moles/liter/min/mg P-N/ml x 10^4
8.40	0.02	8.253	2.468
		9.617	2.738
		14.43	3.255
		16.17	3.328
		16.17	3.419
8.60	0.02	5.900	1.718
		8.855	2.322
		6.378	1.879
		9.907	2.379
		17.72	3.193
		14.77	2.896
		12.76	2.726
		13.98	2.828
		10.15	2.589
		11.91	2.684
		5.952	1.883
		6.765	2.224
		9.317	2.580
		8.929	2.508
9.00	0.02	10.73	2.228
		10.97	2.333
		16.37	2.708
		18.79	2.978
		19.03	2.956
		23.75	3.182
		25.10	3.224
9.20	0.02	7.880	1.758
		11.83	2.144
		11.83	2.144
		15.77	2.502
		19.71	2.688
		19.71	2.763
		23.65	2.889
		27.59	2.990

Table 2 (Continued)

pH	NaCl moles/liter	S_o moles/liter x 10^3	v_o moles/liter/min/mg P-N/ml x 10^4
9.40	0.02	4.060	0.959
		8.120	1.546
		12.18	1.998
		12.18	2.007
		16.24	2.332
		20.30	2.560
		24.36	2.649
		24.36	2.698
		28.42	2.751
6.10	0.20	4.935	0.4111
		9.970	0.4980
		9.970	0.4930
		14.97	0.5352
		14.97	0.5412
		19.95	0.5508
		19.95	0.5580
		24.93	0.5602
		24.93	0.5772
		29.91	0.5722
		29.91	0.5798
6.40	0.20	9.970	0.9042
		9.970	0.9190
		14.97	0.9762
		14.97	0.9860
		19.95	1.030
		19.95	1.058
		24.93	1.073
		24.93	1.080
		29.91	1.124
		29.91	1.123
6.70	0.20	5.013	1.336
		10.02	1.611
		10.02	1.573
		15.04	1.713
		15.04	1.693

Table 2 (Continued)

pH	NaCl moles/liter	S_o moles/liter x 10^3	V_o moles/liter/min/mg P-N/ml x 10^4
6.70	0.20	20.05	1.833
		20.05	1.780
		25.07	1.857
		25.07	1.843
		30.08	1.905
		30.08	1.841
7.00	0.20	5.013	1.644
		10.02	2.218
		10.02	2.252
		15.04	2.479
		15.04	2.469
		20.05	2.700
		20.05	2.690
		25.07	2.762
		25.07	2.792
		30.08	2.830
		30.08	2.815
7.30	0.20	4.930	2.438
		9.864	2.083
		9.864	3.015
		14.81	3.457
		14.81	3.448
		19.74	3.649
		19.74	3.639
		24.68	3.762
		24.68	3.704
		29.60	3.760
		29.60	3.886
7.60	0.20	4.932	2.773
		9.864	3.541
		9.864	3.542
		14.81	3.955
		14.81	4.014
		19.74	4.141
		19.74	4.288

Table 2 (Continued)

pH	NaCl moles/liter	S_o moles/liter x 10^3	V_o moles/liter/min/mg P-N/ml x 10^4
7.60	0.20	24.68	4.426
		24.68	4.389
		29.60	4.568
		29.60	4.557
7.90	0.20	4.965	2.822
		9.930	3.753
		9.930	3.679
		14.90	4.253
		14.90	4.175
		19.87	4.328
		19.87	4.462
		24.82	4.552
		24.82	4.627
		29.79	4.541
		29.79	4.781
8.20	0.20	3.873	2.145
		7.746	2.234
		9.660	3.673
		11.63	3.855
		14.48	4.222
		15.50	4.221
		19.32	4.536
		19.38	4.465
		24.14	4.714
		23.25	4.642
		28.97	4.867
8.50	0.20	4.830	2.395
		9.660	3.535
		9.660	3.593
		14.48	4.138
		14.48	4.240
		19.32	4.468
		19.32	4.658
		24.14	4.662
		24.14	4.901

Table 2 (Continued)

pH	NaCl moles/liter	S_o moles/liter x 10^3	V_o moles/liter/min/mg P-N/ml x 10^4
8.50	0.20	28.97	5.000
		28.97	4.974
8.80	0.20	4.830	2.093
		9.660	3.171
		9.250	3.128
		14.48	3.801
		24.14	4.319
		28.97	4.682
		18.50	4.117
		18.50	4.224
		23.13	4.452
		27.75	4.606
		13.88	3.763
9.20	0.20	4.630	1.562
		9.250	2.429
		9.250	2.381
		13.87	2.889
		13.87	2.869
		18.50	3.273
		18.50	3.309
		23.13	3.534
		23.13	3.544
		27.75	3.723
		27.75	3.723
9.40	0.20	5.140	1.181
		9.250	1.813
		10.28	1.950
		15.42	2.403
		20.57	2.768
		25.70	2.859
		30.83	3.344
		30.83	3.174
		15.42	2.494
		18.50	2.714
		27.75	2.986

Table 2 (Continued)

pH	NaCl moles/liter	S_o moles/liter x 10^3	v_o moles/liter/min/mg P-N/ml x 10^4
9.40	0.20	23.13	2.847
		13.88	2.312
6.20	1.00	3.673	0.6260
		3.673	0.5900
		7.346	0.6650
		3.836	0.5570
		7.672	0.6525
		11.03	0.6975
		11.52	0.7080
		14.70	0.7280
		18.37	0.7455
		25.27	0.7510
		21.07	0.7072
		12.64	0.6800
6.50	1.00	3.380	0.9650
		6.760	1.160
		10.14	1.293
		13.53	1.303
		16.90	1.457
		20.29	1.440
6.70	1.00	3.525	1.535
		7.050	1.816
		3.870	1.444
		7.740	1.714
		11.62	1.835
		10.58	1.844
		15.48	2.031
		14.12	1.893
		19.36	2.093
		23.22	2.056
		24.69	2.062
7.00	1.00	3.223	2.014
		3.223	2.081
		6.446	2.648

Table 2 (Continued)

pH	NaCl moles/liter	S_o moles/liter x 10^3	v_o moles/liter/min/mg P-N/ml x 10^4
7.00	1.00	9.670	2.942
		12.90	3.231
		16.12	3.240
		19.35	3.486
		4.200	2.424
		8.400	2.968
		12.60	3.041
		16.80	3.164
		21.00	3.370
		25.20	3.462
7.30	1.00	4.050	2.975
		8.100	3.715
		12.15	4.041
		16.20	4.231
		20.25	4.340
		24.30	4.430
		4.287	2.930
		8.574	3.631
		12.87	3.939
		17.15	4.155
		21.43	4.230
		25.72	4.270
7.50	1.00	6.720	4.121
		4.100	3.218
		8.200	4.245
		4.100	3.370
		24.60	4.929
		20.50	4.823
		16.40	4.633
		12.30	4.617
		10.08	4.572
		13.44	4.760
		16.81	4.858
		20.18	4.996
		3.360	3.193

Table 2 (Continued)

pH	NaCl moles/liter	S_o moles/liter x 10^3	V_o moles/liter/min/mg P-N/ml x 10^4
7.90	1.00	3.700	3.414
		7.400	4.859
		3.960	3.457
		7.920	4.576
		11.10	5.280
		14.80	5.660
		18.50	5.788
		22.20	6.099
		11.88	5.101
		15.84	5.436
		19.21	5.610
		23.76	5.735
8.20	1.00	3.947	3.439
		3.443	3.011
		3.443	3.026
		6.886	4.124
		7.894	4.799
		10.33	4.799
		13.78	5.112
		17.22	5.339
		11.85	5.234
		15.80	5.501
		19.75	5.939
		23.70	6.084
8.50	1.00	3.875	3.522
		7.750	4.623
		3.540	3.287
		7.080	4.473
		11.63	5.253
		15.50	5.705
		19.38	5.700
		23.25	5.958
		10.63	5.139
		14.17	5.495
		17.70	5.639
		21.25	5.752

Table 2 (Continued)

pH	NaCl moles/liter	S_o moles/liter x 10^3	v_o moles/liter/min/mg P-N/ml x 10^4
8.60	1.00	3.545	2.987
		2.995	2.646
		3.293	2.658
		9.879	4.592
		6.586	3.969
		5.990	3.904
		7.090	4.029
		10.64	5.092
		14.18	5.487
		21.27	5.860
		17.73	5.504
		14.98	5.500
		19.77	5.476
		16.47	5.325
		13.17	5.044
8.70	1.00	3.825	3.208
		3.900	3.105
		7.650	4.494
		7.800	4.373
		11.48	5.184
		11.70	5.146
		15.31	5.554
		15.60	5.462
		19.14	5.856
		19.50	5.759
		22.97	5.934
		23.40	5.872
8.80	1.00	4.141	2.903
		8.282	4.284
		3.940	2.964
		7.880	4.181
		12.43	4.974
		16.57	5.293
		20.71	5.700
		24.85	5.784
		11.83	4.992

Table 2 (Continued)

pH	NaCl moles/liter	S_o moles/liter x 10^3	v_o moles/liter/min/mg P-N/ml x 10^4
8.80	1.00	15.77	5.367
		19.70	5.572
		23.65	5.882
9.00	1.00	3.775	2.614
		7.550	3.917
		3.605	2.505
		7.210	3.802
		11.33	4.603
		10.82	4.460
		15.10	5.255
		14.42	4.813
		18.86	5.522
		18.03	5.160
		22.66	5.576
		21.63	5.306
9.20	1.00	3.671	2.068
		7.342	3.193
		7.342	3.163
		11.01	4.011
		14.68	4.503
		14.68	4.418
		18.37	4.694
		22.03	4.844
		22.03	4.841
9.40	1.00	3.671	1.673
		7.342	2.688
		7.342	2.686
		11.01	3.313
		14.68	3.780
		14.68	3.737
		18.37	4.042

Table 3

ENZYME-CATALYSED HYDROLYSIS

K_s and k_3 as a function of pH and NaCl concentration

pH	NaCl moles/liter	K_s moles/liter x 10^3	k_3 moles/liter/min/mg P-N/ml x 10^3
6.00	0.02	3.04 ± 0.34	0.34 ± 0.01
6.20	0.02	1.85 ± 0.36	0.42 ± 0.14
6.30	0.02	2.99 ± 0.40	0.62 ± 0.02
6.50	0.02	3.88 ± 0.26	0.99 ± 0.02
6.70	0.02	4.14 ± 0.48	1.46 ± 0.06
7.00	0.02	4.76 ± 0.33	1.78 ± 0.04
7.30	0.02	6.15 ± 0.30	2.66 ± 0.05
7.50	0.02	5.49 ± 0.30	2.53 ± 0.05
7.70	0.02	4.78 ± 0.89	2.74 ± 0.18
7.90	0.02	6.90 ± 0.30	2.68 ± 0.05
8.20	0.02	7.67 ± 0.47	3.10 ± 0.10
8.40	0.02	8.23 ± 0.40	3.37 ± 0.10
8.60	0.02	8.82 ± 0.50	3.38 ± 0.10
9.00	0.02	10.18 ± 0.52	3.10 ± 0.12
9.20	0.02	11.05 ± 0.50	2.91 ± 0.10
9.40	0.02	13.93 ± 0.60	2.89 ± 0.13
6.10	0.20	2.57 ± 0.19	0.43 ± 0.00
6.40	0.20	4.19 ± 0.32	0.87 ± 0.01
6.70	0.20	3.12 ± 0.21	1.43 ± 0.01
7.00	0.20	4.84 ± 0.20	2.26 ± 0.02
7.30	0.20	3.98 ± 0.26	2.98 ± 0.04
7.60	0.20	4.78 ± 0.22	3.62 ± 0.04
7.90	0.20	4.33 ± 0.40	3.68 ± 0.07
8.20	0.20	6.54 ± 0.24	4.11 ± 0.05
8.50	0.20	7.53 ± 0.43	4.32 ± 0.09
8.80	0.20	8.99 ± 0.40	4.19 ± 0.08
9.20	0.20	11.09 ± 0.20	3.58 ± 0.32
9.40	0.20	15.20 ± 1.00	3.27 ± 0.13
6.20	1.00	1.87 ± 0.24	0.55 ± 0.01
6.50	1.00	2.60 ± 0.49	1.11 ± 0.04
6.70	1.00	2.70 ± 0.28	1.58 ± 0.03
7.00	1.00	2.76 ± 0.25	2.62 ± 0.05

Table 3 (Continued)

pH	NaCl	K_s	k_3
	moles/liter	moles/liter x 10^3	moles/liter/min/mg P-N/ml x 10^3
7.30	1.00	2.52 ± 0.25	3.28 ± 0.05
7.50	1.00	2.39 ± 0.22	3.75 ± 0.06
7.90	1.00	2.99 ± 0.41	4.48 ± 0.12
8.20	1.00	3.33 ± 0.40	4.43 ± 0.01
8.50	1.00	3.70 ± 0.18	4.71 ± 0.06
8.60	1.00	5.22 ± 0.33	4.92 ± 0.01
8.70	1.00	4.81 ± 0.21	4.93 ± 0.06
8.80	1.00	5.84 ± 0.22	4.98 ± 0.07
9.00	1.00	6.44 ± 0.44	4.89 ± 0.14
9.20	1.00	9.10 ± 0.46	4.89 ± 0.15
9.40	1.00	11.25 ± 0.22	4.85 ± 0.06

Table 4

INHIBITION BY HIPPURIC ACID

S_o, I_o, and v_o at pH 7.00 and 0.02 and 1.00 molar NaCl

NaCl moles/liter	S_o moles/liter x 10^3	I_o moles/liter x 10^3	v_o moles/liter/min/mg P-N/ml x 10^4
0.02	8.040	0.000	1.780
		3.488	1.625
		5.230	1.601
		6.978	1.490
	12.06	0.000	2.031
		3.488	1.916
		5.230	1.892
		6.978	1.730
	16.08	0.000	2.018
		3.488	2.000
		5.230	1.898
		6.978	1.816
	20.10	0.000	2.212
		1.744	2.130
		3.488	2.100
		5.230	2.070
	24.12	0.000	2.198
		1.744	2.148
		3.488	2.105
	28.14	0.000	2.279
		1.744	2.195
1.00	4.585	0.000	2.140
		3.290	1.840
		6.580	1.654
		9.870	1.421
		13.16	1.323
	9.170	3.290	2.608
		6.580	2.160
		9.870	1.921

Table 4 (Continued)

NaCl moles/liter	S_o moles/liter x 10^3	I_o moles/liter x 10^3	v_o moles/liter/min/mg P-N/ml x 10^4
1.00	9.170	13.16	1.761
	13.75	0.000	2.724
		3.290	2.631
		6.580	2.355
		9.870	2.140
		13.16	2.117
	18.34	0.000	3.045
		3.290	2.840
		6.580	2.580
		9.870	2.409
	22.93	0.000	3.041
		6.58	2.850
	27.50	0.000	3.017
		3.290	2.890

Table 5

INHIBITION BY HIPPURIC ACID

$t_{o(p)}/t_o$ as a function of percent hydrolysis

Equations and calculated values

1.00 molar NaCl	0.02 molar NaCl
K_s = 2.5×10^{-3} moles/liter	K_s = 5.0×10^{-3} moles/liter
S_o = 5.0×10^{-3} moles/liter	S_o = 5.0×10^{-3} moles/liter
K_p = 6.0×10^{-3} moles/liter	K_p = 13.0×10^{-3} moles/liter

% Hydrolysis	t_o	$t_{o(p)}$	$t_{o(p)}/t_o$	t_o	$t_{o(p)}$	$t_{o(p)}/t_o$
0						
10	.985	.974	1.012	.978	.972	1.007
20	.963	.934	1.032	.945	.927	1.020
30	.941	.897	1.049	.914	.885	1.046
40	.915	.855	1.070	.879	.840	1.047
50	.886	.811	1.093	.838	.791	1.060
60	.850	.755	1.127	.791	.733	1.079
70	.806	.694	1.162	.734	.667	1.100
80	.748	.617	1.213	.664	.588	1.129

$$f_o = \frac{\frac{K_s}{S_o} + 1}{P \cdot \frac{K_s}{S_o} + 1}$$

where $P = \left[\frac{S_o}{S_o - S_t}\right] \ln \frac{S_o}{S_t}$

$$f_{o(p)} = \frac{\left[\frac{K_s}{S_o} + 1\right]\left[1 - \frac{K_s}{K_p}\right]^{-1}}{P\left[\frac{K_s}{S_o} + \frac{K_s}{K_p}\right]\left[1 - \frac{K_s}{K_p}\right]^{-1} + 1}$$

$$f_o = \frac{t_o}{t}$$

$$f_{o(p)} = \frac{t_{o(p)}}{t}$$

$$\frac{f}{f_{o(p)}} = \frac{t_{o(p)}}{t_o}$$

Table 6

INHIBITION BY HIPPURIC ACID

$(S_o - S)/t$ as a function of $(\log S_o/S)/t$ at 1.00 molar NaCl and different pH values

pH	S_o moles/liter x 10^3	$\frac{S_o - S_t}{t}$ moles/liter/min x 10^5	$\frac{\ln S_o/S_t}{t}$ min^{-1} x 10^2
6.20	3.673	6.240	1.735
		6.155	1.721
		5.980	1.692
		5.950	1.693
		5.870	1.678
		5.810	1.620
		5.740	1.652
		5.700	1.667
6.50	6.760	11.12	1.685
		11.39	1.671
		11.11	1.690
		11.30	1.737
		11.24	1.742
		11.20	1.741
		11.10	1.748
		11.06	1.759
7.00	3.223	20.09	6.483
		19.68	6.510
		19.17	6.570
		18.73	6.615
		18.18	6.630
		17.87	6.740
		17.35	6.770
		16.97	6.840
7.00	4.200	24.42	6.020
		23.85	6.030
		23.17	6.020
		22.38	5.990
		21.80	6.000

Table 6 (Continued)

pH	S_o moles/liter x 10^3	$\frac{S_o - S_t}{t}$ moles/liter/min x 10^5	$\frac{\ln S_o/S_t}{t}$ min^{-1} x 10^2
7.00	4.200	21.25	6.030
		20.76	6.080
		20.23	6.090
7.30	4.050	29.83	7.560
		29.04	7.750
		28.23	7.810
		27.45	7.910
		26.70	8.010
		25.95	8.080
		25.11	8.123
		24.50	8.275
7.30	4.287	29.30	6.110
		28.90	7.250
		28.66	7.465
		28.08	7.595
		27.35	7.670
		26.73	7.805
		26.13	7.950
		25.45	8.045
7.50	3.360	32.30	10.08
		30.80	10.12
		29.85	10.33
		28.78	10.51
		27.80	10.68
		26.78	10.86
		25.71	10.97
		24.70	11.09
7.50	4.100	32.58	8.350
		32.03	8.530
		31.11	8.620
		30.25	8.734
		29.33	8.861
		28.58	9.032
		27.68	9.142
		26.87	9.295

Table 6 (Continued)

pH	S_o moles/liter x 10^3	$\frac{S_o - S_t}{t}$ moles/liter/min x 10^5	$\frac{\ln S_o/S_t}{t}$ min^{-1} x 10^2
7.90	3.700	34.18	9.750
		32.82	9.780
		32.10	10.07
		30.84	10.16
		29.95	10.38
		28.75	10.48
		27.76	10.65
		26.65	10.74
7.90	3.960	36.08	9.620
		34.45	9.538
		33.72	9.855
		32.55	9.970
		31.45	10.14
		30.48	10.33
		29.37	10.48
		28.35	10.64
7.90	7.400	49.36	6.945
		48.15	6.990
		46.70	7.010
		45.30	7.000
		44.18	7.095
		43.22	7.190
		42.22	7.275
		41.37	7.410
8.20	3.443	30.92	9.350
		29.85	9.535
		28.76	9.635
		27.82	9.770
		26.92	9.930
		26.10	10.12
		25.70	10.28
		24.65	10.65
8.20	3.947	34.72	9.170
		32.83	9.080
		32.08	9.310

Table 6 (Continued)

pH	S_o moles/liter x 10^3	$\frac{S_o - S_t}{t}$ moles/liter/min x 10^5	$\frac{\ln S_o/S_t}{t}$ min^{-1} x 10^2
8.20	3.947	31.13	9.470
		30.07	9.580
		29.27	9.800
		28.37	9.990
		27.27	10.06
8.50	3.540	33.63	9.900
		32.57	10.20
		31.45	10.35
		30.85	10.73
		29.67	10.88
		28.69	11.12
		27.53	11.24
8.50	3.875	35.27	9.540
		34.20	9.700
		33.20	9.920
		32.20	10.12
		31.25	10.33
		30.10	10.48
8.60	3.293	26.05	8.340
		26.05	8.610
		25.60	8.850
		24.95	9.020
		24.30	9.210
		23.60	9.380
		22.80	9.490
		22.05	9.600
8.60	3.545	29.03	8.525
		29.37	8.805
		28.40	9.175
		27.40	9.240
		26.46	9.330
		25.79	9.560
		24.80	9.630
		23.95	9.720

Table 6 (Continued)

pH	S_o moles/liter x 10^3	$\frac{S_o - S_t}{t}$ moles/liter/min x 10^5	$\frac{\ln S_o/S_t}{t}$ min^{-1} x 10^2
8.70	3.825	32.56	8.895
		32.14	9.200
		31.46	9.450
		30.75	9.695
		29.67	9.810
		28.80	10.03
	3.900	32.56	8.720
		31.49	8.575
		31.30	9.180
		30.25	9.295
		29.38	9.470
		28.49	9.620

Table 7

INHIBITION BY L-TRYPTOPHAN

S_o, I_o, and v_o as a function of pH at 1.00 molar NaCl

pH	S_o moles/liter x 10^3	I_o moles/liter x 10^3	v_o moles/liter/min/mg P-N/ml x 10^4
6.20	8.250	0.000	0.633
		5.650	0.560
		11.29	0.526
		16.95	0.497
		22.60	0.467
		28.23	0.426
6.50	8.250	0.000	1.189
		5.650	1.082
		11.29	1.004
		16.95	0.944
		22.60	0.874
		28.23	0.823
6.70	8.250	0.000	1.579
		5.650	1.495
		11.29	1.456
		16.95	1.360
		22.60	1.286
		28.23	1.184
7.00	7.850	0.000	2.771
		5.450	2.473
		10.90	2.300
		16.35	2.009
		21.80	1.994
		27.25	1.797
7.50	8.250	0.000	3.898
		5.650	3.525
		11.29	3.323
		16.95	3.110
		22.60	2.948
		28.23	2.826
7.90	8.250	0.000	4.412

Table 7 (Continued)

pH	S_o moles/liter x 10^3	I_o moles/liter x 10^3	v_o moles/liter/min/mg P-N/ml x 10^4
7.90	8.250	5.650	4.042
		11.29	3.782
		16.95	3.583
		22.60	3.429
		28.23	3.292
8.20	8.250	0.000	4.531
		5.650	4.209
		11.29	4.119
		16.95	3.664
		22.60	3.634
8.60	8.250	0.000	4.240
		5.650	3.898
		11.29	3.821
		16.95	3.533
		21.81	3.487

Table 8

Summary of K_I values of Hippuric Acid and L-Tryptophan as a function of pH and added NaCl concentration

pH	NaCl moles/liter	Hippuric Acid moles/liter x 10^3	L-Tryptophan moles/liter x 10^3
6.20	1.00	0.6	12.4
6.50	1.00	4.2	14.6
6.70	1.00		15.6
7.00	1.00	4.0	14.5
		5.7	
		5.8	
		5.9	
		5.9	
		6.2	
7.00	0.02	13.0	
		13.0	
		13.6	
7.30	1.00	5.3	
		8.3	
7.50	1.00	6.3	15.5
		6.4	
7.90	1.00	8.1	20.8
		8.6	
		9.3	
8.20	1.00	11.2	23.1
		13.0	
8.50	1.00	14.1	
		19.3	
8.60	1.00	22.2	38.0
		22.6	
8.70	1.00	46.3	
		46.6	

PROPOSITIONS

1. Westheimer (1) has proposed a hypothesis for the mechanism of the enzymic action of chymotrypsin. Among the observed facts which this hypothesis is reported to explain is the pH dependence of chymotrypsin activity. The data of Gutfreund et al. (2,3) is cited as evidence. Gutfreund's data, however, is not consistent with Westheimer's hypothesis. The hypothesis describes an acylated imidazole ring in the enzyme-substrate-complex, whereas Gutfruend's data indicates that the pK_a of the imidazole is unchanged upon conversion of the free enzyme to the complex.

2. A. An extension of the method of Fritz and Freeland (4) permits the rapid volumetric determination of sulfite, thiosulfate, and sulfate ions in a mixture of the three. Two titrations samples are required. Titration with standard iodine determines the sum of the sulfite and thiosulfate concentrations. The second sample is adjusted to pH 4-5 with acetic acid, formaldehyde is added to complex the sulfite, and the thiosulfate alone is then titrated with standard iodine. At the end point, methanol is added to the solution, as are a few drops of Alizarin adsorption indicator. The yellow solution is then titrated with standard barium chloride to a pink end point, which occurs when the indicator is adsorbed on the positively charged precipitate. Using this method,

a mixture may be analyzed in two or three minutes time with an accuracy of a few tenths of a percent under ideal conditions.

B. A further extension of the method of Fritz and Freeland, in which a fine suspension of precipitated barium sulfate in methanol is added to the titration flask, permits a greater than ten-fold increase in the sensitivity of this method for the volumetric determination of sulfate.

3. The electron microscope has been used extensively in recent years to investigate the fiber structure of soaps and soap-base lubricating greases. In some cases (5,6) the gross physical properties of a lubricating grease can be correlated with microstructural features of its soap fibers, as revealed by the electron microscope. Another area of investigation in which the electron microscope has proved valuable is in the examination of surface friction of metals. An extension of the oxide film technique (7), in which a thin film of alumina is used to support the sample, suggests that a study of friction of aluminum surfaces with and without lubricants present would be feasible. A thin film of lubricant would be spread over the polished aluminum surface prior to a given friction experiment. After the experiment, the surface could be oxidized electrolytically, shadowed with evaporated chromium to reveal the presence of organic

matter if any remained, and examined under the electron microscope.

4. The apparent anomaly in K_I values for several anionic inhibitors of chymotrypsin determined in 0.02 M THAM and 0.1 M phosphate buffers, as discussed by Foster and Niemann (8), may be explained on the basis of an added sodium ion effect. As shown in this thesis, increasing added salt concentration causes a decrease in the value of K_I. Since the added salt concentration in the case of the THAM buffer experiments was ~ 0.02 M, and in the case of the phosphate buffer experiments ~ 0.1 M, the observed change in K_I values determined in the different media is not unexpected.

5. The demonstration that L-tryptophan is a competitive inhibitor of chymotrypsin suggests the following experiments:

   A. The use of O^{18}-labeled L-tryptophan to determine whether O^{18} exchange occurs in the presence of enzyme. The result would almost certainly be positive.

   B. Repetition of part A with enzyme which has been inactivated by diisopropyl fluorophosphate.

   If L-tryptophan exchanges O^{18} in the presence of inactivated enzyme, one may conclude that the inactive enzyme is still capable of forming an enzyme-substrate-complex. This information concerning the nature of the inactivation process would be of value.

6. The problem of whether reduction of sulfurous acid at constant potential involves the transfer of one or two electrons could be solved by quantitative measurement of the current passed in the reduction of a known amount of sulfurous acid.

7. A. Cymerman and Willis (9) reported the infra-red spectra of diphenyl disulfone and an extended series of disulfides and thiosulfonates. All of those compounds investigated, with the exception of diphenyl disulfone, showed an adsorption corresponding to the S-S stretching frequency in the range 430-490 cm^{-1}. These authors tentatively attributed the anomalous spectrum of diphenyl disulfone to the symmetrical character of the molecule. An alternative explanation, I believe, is the existence of an elongated S-S bond, by analogy with the inorganic salt sodium dithionite. Preparation and infra-red investigation of an unsymmetrical diphenyl disulfone is suggested.
B. Increasing substitution of the aromatic nuclei in diphenyl disulfone with electron-withdrawing groups should weaken the S-S bond and increase the free radical character of the compound. One (or more) compounds in such a series, which has not been prepared, could be a stable free radical.

8. The use of the pH-stat in these laboratories has been confined to the measurement of the hydrolysis rates of substituted α-amino acid derivatives and related compounds.

I propose the following additional uses of the pH-stat:

A. Schuller and Niemann (10) examined the α-chymotrypsin catalysed synthesis of the phenylhydrazides of certain acylated α-amino acids. The pH-optima for the synthesis reactions were observed to be sensitive to the buffer systems used. I propose that the rates of these synthesis reactions could be measured as before, while using the pH-stat to maintain constant pH and hence eliminate undesired buffer effects.

B. Furthermore, the pH-stat could be used to measure directly the rates of α-chymotrypsin catalysed synthesis reactions of acylated α-amino esters from their corresponding acids and alcohols.

C. Sorum et al. (11) have shown that a number of inorganic reactions such as iodate-iodide, iodate-thiosulfate, bromate-thiosulfate, bromate-sulfite, iodate-sulfite, and permanganate-sulfite proceed at measurable rates and take up or release hydrogen ions as the reaction proceeds. I propose that the pH-stat could be used to study the kinetics of these reactions.

9. The metal alkyls of boron and aluminum are highly reactive chemically and are used at the present time in jet fuels. These compounds are strong Lewis acids and form addition compounds, which are stable at room temperature but dissociate at high temperatures, with Lewis bases such as ammonia and the amines. I propose that such

addition compounds prepared from the metal alkyls and polyamides or polyamines would be of interest as solid propellants for missile propulsion systems.

10. Brown (12) has observed that the trialkoxyborohydrides are extremely powerful reducing agents. He has postulated that the higher reactivity of the trialkoxyborohydrides compared to unsubstituted borohydrides can be attributed to the greater ease in removing a hydride ion from a weak Lewis acid, alkyl borate, than from a stronger Lewis acid, borane. Investigation of the reducing properties of the adduct of sodium hydride and the extremely weak Lewis acid, triethanolamine borate (13), is suggested to test this postulate.

11. The Gourmet Cookbook (14) describes the preparation of Coquille St. Jacques in the following way: Fresh scallops, which have been cooked in wine, are added to mushrooms and onions in a white sauce enriched with egg yolks and heavy cream. The mixture is placed in individual large oyster shells and browned in the broiler before serving. I propose that the addition of shrimp and King crab meat to the scallops, and the sprinkling with freshly grated cheese before browning produces a shellfish delicacy of exceptional quality.

REFERENCES

1. Westheimer, F. H., Proc. Nat. Acad. Sci., 43, 969 (1957).

2. Hammond, R. B., and Gutfreund, H., J. Biochem., 61, 187 (1955).

3. Gutfreund, H., and Sturdivant, J. M., J. Biochem., 63, 656 (1956).

4. Fritz, J. S., and Freeland, M. Q., Anal. Chem., 26, 1593 (1954).

5. Brown, J. A., Hudson, C. N., and Loring, L. W., Institute Spokesman, 15, Vol. 1, 8 (1952).

6. Evans, D., Hutton, J. F., Mathews, J. B., J. Applied Chem. (London), 2, 252 (1952).

7. Keller, F., and Geisler, A. H., A.I.M.M.E. Tech. Pub. No. 1700 (1944).

8. Foster, R. J., and Niemann, C., J. Am. Chem. Soc., 77, 3365 (1955).

9. Cymerman, J., and Willis, J. B., J. Chem. Soc., Vol. 2, 1332 (1951).

10. Schuller, W. H., and Niemann, C., J. Am. Chem. Soc., 74, 4630 (1952).

11. Sorum, C. H., Charlton, F. S., Neptune, J. A., and Edwards, J. O., J. Am. Chem. Soc., 74, 219 (1952).

12. Brown, H. C., Mead, E. J., and Shoaf, C. J., J. Am. Chem. Soc., 78, 3613 (1956).

13. Brown, H. C., and Fletcher, E. A., J. Am. Chem. Soc., 73, 2808 (1951).

14. "The Gourmet Cookbook," Gourmet Distributing Corp., N.Y., N.Y. (1950).